AFFDL-TR-78-167

LEVEL II

INVESTIGATION OF STRESS-STRAIN HISTORY MODELING AT STRESS RISERS

PHASE II

LOCKHEED-GEORGIA COMPANY
MARIETTA, GEORGIA 30063

December 1978

TECHNICAL REPORT AFFDL-TR-78-167
FINAL TECHNICAL REPORT FOR PERIOD FEBRUARY 1977-OCTOBER 1978

AIR FORCE FLIGHT DYNAMICS LABORATORY
AIR FORCE WRIGHT AERONAUTICAL LABORATORIES
AIR FORCE SYSTEMS COMMAND
WRIGHT-PATTERSON AIR FORCE BASE, OHIO 45433

NOTICE

When Government drawings, specifications, or other data are used for any purpose other than in connection with a definitely related Government procurement operation, the United States Government thereby incurs no responsibility nor any obligation whatsoever; and the fact that the government may have formulated, furnished, or in any way supplied the said drawings, specifications, or other data, is not to be regarded by implication or otherwise as in any manner licensing the holder or any other person or corporation, or conveying any rights or permission to manufacture, use, or sell any patented invention that may in any way be related thereto.

This report has been reviewed by the Information Office (OI) and is releasable to the National Technical Information Service (NTIS). At NTIS, it will be available to the general public, including foreign nations.

This technical report has been reviewed and is approved for publication.

ROBERT M. ENGLE
Project Engineer

NELSON D. WOLF, Acting Chief
Structural Integrity Branch

FOR THE COMMANDER

RALPH L. KUSTER, JR., Col, USAF
Chief, Structures & Dynamics Division

If your address has changed, if you wish to be removed from our mailing list, or if the addressee is no longer employed by your organization please notify AFFDL/FBE ,W-PAFB, OH 45433 to help us maintain a current mailing list .

Copies of this report should not be returned unless return is required by security considerations, contractual obligations, or notice on a specific document.

AIR FORCE/56780/11 May 1979 -- 475

UNCLASSIFIED

SECURITY CLASSIFICATION OF THIS PAGE (When Data Entered)

REPORT DOCUMENTATION PAGE

READ INSTRUCTIONS BEFORE COMPLETING FORM

(18) 1. REPORT NUMBER: AFFDL-TR-78-167 (19) TR-78-167

2. GOVT ACCESSION NO.

3. RECIPIENT'S CATALOG NUMBER

(6) 4. TITLE (and Subtitle): INVESTIGATION OF STRESS-STRAIN HISTORY MODELING AT STRESS RISERS, PHASE II. AD A062633

5. TYPE OF REPORT & PERIOD COVERED: Final Report - Phase II, 15 Feb. 1977 to 30 Sept. 1978

(14) 6. PERFORMING ORG. REPORT NUMBER: LG78ER240

(10) 7. AUTHOR(s): James R. Carroll, R. L. Brugh, R. W. Wilkinson

(15) 8. CONTRACT OR GRANT NUMBER(s): F33615-75-C-3078

9. PERFORMING ORGANIZATION NAME AND ADDRESS: Lockheed-Georgia Company, A Division of Lockheed Corporation, Marietta, Georgia 30063 2.10 065

(16) 10. PROGRAM ELEMENT, PROJECT, TASK AREA & WORK UNIT NUMBERS: [redacted]1367, Task Number 03, Work Unit Number 11 (17) 03

11. CONTROLLING OFFICE NAME AND ADDRESS: Air Force Flight Dynamics Laboratory (AFFDL/FBE), Wright-Patterson AFB, Ohio 45433

(11) 12. REPORT DATE: December 1978

13. NUMBER OF PAGES: 248

14. MONITORING AGENCY NAME & ADDRESS (if different from Controlling Office): (12) 2.64 p.

15. SECURITY CLASS. (of this report): Unclassified

15a. DECLASSIFICATION/DOWNGRADING SCHEDULE

16. DISTRIBUTION STATEMENT (of this Report)

Approved for public release; distribution unlimited.

17. DISTRIBUTION STATEMENT (of the abstract entered in Block 20, if different from Report)

(9) Final rept. 15 Feb 77-30 Sep 78 on Phase 2,

18. SUPPLEMENTARY NOTES

19. KEY WORDS (Continue on reverse side if necessary and identify by block number)

Stress-strain history, fatigue life, residual stress, creep and stress relaxation, finite-element analysis, hysteresis analysis

20. ABSTRACT (Continue on reverse side if necessary and identify by block number)

An analytical and experimental study of the stress and strain history at stress risers was conducted to evaluate the effects of time- and cycle-dependent changes on the fatigue life of aluminum alloy structures. This report covers Phase II of a two-phase program. Both creep and stress relaxation were modeled and measured. An elastic-plastic finite element code simulation was utilized to model the nonlinear stress-strain field around the stress riser and to model creep during sustained load hold periods. →

DD FORM 1 JAN 73 1473 EDITION OF 1 NOV 65 IS OBSOLETE

UNCLASSIFIED

SECURITY CLASSIFICATION OF THIS PAGE (When Data Entered)

2.10 065

20. ABSTRACT (Continued)

A four-part experimental program was conducted to generate constitutive data necessary for the formulation of a hysteresis analysis model. The experimental program included simple coupon specimens, a unique simplified stress concentration specimen, center circularly notched super-scale specimens, and notched fatigue specimens. Complex, load time test sequences and flight-by-flight spectrum loadings representative of transport aircraft loads were used in the program.

Significant creep and stress relaxation was measured during the experimental program. These data were used in the development of creep/stress relaxation module for the hysteresis analysis. The automated hysteresis analysis developed during this program includes a material hardening/softening module, a creep/stress relaxation module, locus and branch curve definition for the stable material response, and a damage accumulation module. Correlation studies have been conducted using this analysis as well as a linear damage analysis method to compare predicted versus actual specimen life.

FOREWORD

The research and development reported herein was conducted under Air Force Contract F33615-75-C-3078 by the Lockheed-Georgia Company, a Division of Lockheed Corporation. The work was sponsored by the Air Force Flight Dynamics Laboratory, Air Force Systems Command, Wright-Patterson Air Force Base, Ohio. This report covers the work conducted during the period of February, 1977, through October, 1978. This research was initiated under the direction of Dr. Robert L. Neulieb of the Fatigue, Fracture, and Reliability Group, Structural Integrity Branch, (FBE), Structural Mechanics Division as the Project Engineer. The program was completed under the direction of Mr. Robert M. Engle of the AFFDL/FBE as the Project Engineer. This report covers Phase II of the program conducted during the period of 15 February 1977 to 30 September 1978. The work was performed under Project 1367, Task 03, Work Unit 11.

This report was submitted for publication in December, 1978. Mr. James R. Carroll was the Lockheed-Georgia Company Program Manager. Finite element analysis was conducted by Dr. R. L. Brugh and Dr. L. S. Long. Mr. R. W. Wilkinson and Mr. L. W. Liu were responsible for the hysteresis analysis development, and Mr. J. F. Holliday conducted the computer programming. The experimental program was conducted by Mr. G. J. Gilbert and Mr. F. L. Amend.

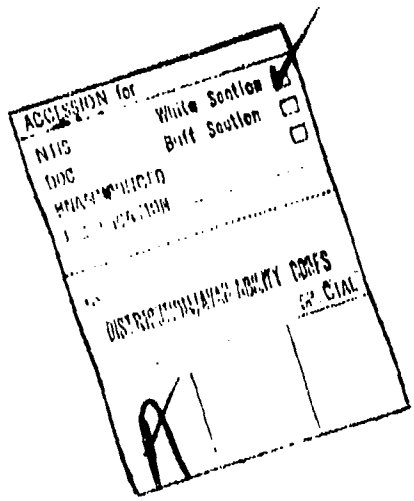

TABLE OF CONTENTS

TABLE OF CONTENTS (Continued)

LIST OF ILLUSTRATIONS

LIST OF ILLUSTRATIONS (Continued)

LIST OF ILLUSTRATIONS (Continued)

LIST OF ILLUSTRATIONS (Continued)

LIST OF ILLUSTRATIONS (Continued)

LIST OF TABLES

SECTION I
INTRODUCTION

Structural cracking is a major factor in assessing the useful life of aircraft structures. The potential crack initiation sites must be accurately identified and assessed, usually at or near stress concentrations such as fastener holes. Numerous analysis methods are available to predict crack initiation; however, few of these techniques consider the complete stress-strain history and the effects of plasticity on this history. Recent studies, including those in Phase I of this program and reported in Reference 1, have shown that plasticity induced by overloads produces a life-lengthening effect in the structures, but this plastic zone also undergoes time-dependent changes under sustained loading conditions. These time-dependent creep and stress relaxation changes can be a predominant factor in predicting time to initial cracking, crack growth, and in establishing test requirements and procedures.

The research reported here is an extension of the Phase I program that includes an analytical and experimental effort to develop an empirical analysis for stress-strain history accountability. An elastic-plastic finite element code simulation was used to model the stress-strain history and creep at the stress concentration. A four-part experimental program was conducted to collect material constitutive data necessary for the formulation of a hysteresis stress-strain analysis. This analysis method includes: an algorithm for the basic material response, a cyclic hardening or softening module, creep and stress relaxation, and a damage accumulation model. It is a very useful tool for the analyst in defining the stress-strain history and for predicting time to initial cracking.

SECTION II
PROGRAM OBJECTIVES AND SUMMARY

This program had as its main objective the development of an empirical analysis to model the stress-strain history at stress risers. It includes a study of the effects of load and mechanically induced plastic yielding at the stress riser; variations in the plastically induced stress-strain field resulting from sustained loading, constant amplitude cycles, and temperatures; and the effects of loading history on the stress-strain curve. A two phase analytical and experimental program was conducted to develop data necessary to formulate a hysteresis type stress-strain analysis method.

In Phase I, it was demonstrated that complex loading histories which include sufficiently high loads to induce plasticity and sustained loadings do, in fact, significantly affect the stress-strain history and the time to initial cracking of the structure. Experiments were conducted to measure creep at the stress riser. Based on these experimental data, it was hypothesized that the stress-strain history modeling is a complex function of both stress (relaxation) and creep (strain). Phase II included finite-element code simulation of the observed phase I results as well as an experimental program to develop constitutive data necessary to the formulation of the hysteresis analysis.

The results of the Phase I program are published in AFFDL-TR-76-150, Reference 1. This report documents the results of Phase II. For completeness, however, a brief summary of Phase I is included in this section.

2.1 PHASE I - SUMMARY

An extensive experimental program was conducted during this phase to evaluate the effects of overloads, sustained load hold periods, constant amplitude cycle block size, and temperature on the time to initial cracking of centrally notched, open hole test specimens. These data were then used in the formulation of a hysteresis type of analysis which includes modules for both the transient and stable stress-strain state.

Typical results from the complex load, time, temperature testing which was conducted are illustrated in Tables 1 and 2. Thirty-two different sequences were included. These

can be grouped into similar sequences as illustrated by A,B,C, and D in Table 1. Sequence A is the baseline constant amplitude test. Sequences B,C, and D include tensile overloads, compression underloads, 24-hour and 1-hour hold periods, and 15 thousand and one thousand cycle block size between overloads. The table illustrates the effect of these variables on time to crack initiation. The baseline constant amplitude cycling demonstrated, for example, 48,000 cycles to crack initiation. Tensile overloads as applied in Sequence B greatly extend the specimen life. However, a compression load immediately following the tensile overload (Sequence C) reduces the impact of the overload. An even more significant effect is demonstrated in the Sequence D results. Here time-dependent effects become important. For example, a tensile overload in B resulted in a life greater than two-million cycles; the underload when added reduced this to 715,000 cycles, but, when the compression load was held the life was red to 141,000 cycles. Similar data for increased underloads are included in Table 2.

The tension overloads were sufficient to induce a plastic zone around the stress riser. A super-scale test specimen (with a 2.0-inch diameter center hole) and a unique strain transducer were used to measure strain changes (creep) in this plastic zone during these hold periods. These measured changes, although not large, are sufficient to affect the specimen life. The effect of the measured strain changes can be illustrated by the data shown in Figure 1. These data are from tests which do not include hold periods (they are of the Sequence C grouping in Table 1) but the cyclic limits and times to failure tend to illustrate the time-dependent changes in the plastic zone. For example, cycling between the limits A-A is similar to a sequence with no underload. Cycling between B-B is typical of Sequence B and limits C-C tend to show the effect of the hold time or Sequence D. Note that as the cyclic limits change from A to C there is both a change in stress and strain. From this observation of measured test data, it was hypothesized that there is a complex, time dependent relationship between stress and strain which tend to significantly affect time to crack initiation.

This hypothesis is illustrated in Figure 2. In this figure both a time dependent creep, $\Delta\epsilon$, and a time dependent stress relaxation, $\Delta\sigma$, are shown.

These results and the hypothesis proposed (Figure 2) led to the development of the program scope for Phase II. Additional analyses and tests were conducted in this phase to model the observed Phase I results as well as to develop constitutive data for the hysteresis analysis model.

2.2 PHASE II - SUMMARY

Phase II in itself was a two-part program. The first part of the program involved a finite-element code simulation of the elastic-plastic stress-strain history from the Phase I experimental data. Part B was both an analytical and experimental effort, again using finite-element simulations in the analysis. The experimental program included development of constitutive data for the creep and stress relaxation modeling, super-scale specimen testing, and spectrum fatigue tests of notched coupons.

Several available elastic-plastic finite element analysis programs were evaluated to determine the one most applicable for the stress-strain model. The MARC General Purpose Program was selected primarily because of its flexibility in user subroutines and its available creep module. This finite-element program was used to model simple plates, the super-scale specimen used for the complex sequence tests, and the three bar, simplified stress concentration (SSC) specimen. The analysis, using this finite element code, demonstrated that the Phase I elastic-plastic stress-strain history and the creep could be modeled.

Following the analysis demonstration, a four part experimental program was initiated. Simple unnotched coupons were tested to obtain creep and stress relaxation data. The simplified stress-concentration (SSC) specimen was used in complex loading sequences to evaluate creep and the associate plastic stress and stress relaxation. Additional super-scale specimens were then tested to expand the data base developed in Phase I. Finally, notched coupon specimens were tested using flight-by-flight spectrum fatigue loadings. The finite-element code was used to model the SSC specimen and super-scale specimens to compare the predicted and experimental results.

The experimental data have been used in formulating a hysteresis type of an analysis for predicting the stress-strain history at stress concentrations.

SECTION III

FINITE ELEMENT ANALYSIS

A finite-element analysis technique was used for modeling the creep/relaxation behavior for this contract. The first task of this phase was to select an acceptable existing finite-element computer program. A computer program developed by Lockheed Missiles and Space Company entitled "Non-Linear Elastic Plastic Structural Analysis Program (NEPSAP)" was first examined. It was determined that this program had several deficiencies which prohibited proper modeling of the creep/relaxation phenomena. The second program examined was the MARC General-Purpose Program. The results obtained from MARC are discussed in the following paragraphs.

3.1 MARC - GENERAL PURPOSE PROGRAM

The MARC general purpose finite-element program is designed to cover a wide spectrum of linear and/or nonlinear problems encountered in structural analysis. MARC has a large library of elements which can be used to model virtually any geometry that may be encountered. To provide additional flexibility, user subroutines are available in this program so that modifications may be made by the user. The user subroutines utilized in this study allowed user-specified input for both a particular creep law and work-hardening behavior.

3.1.1 Creep Formulation

An evaluation of various creep laws was made to determine the best mathematical representation for creep of the material in this study. A summary of the various creep formulations which were considered and the limitations of each is shown in Table 3. The Nutting, Hoff, Scott-Blair formulation was considered the most applicable for the program. A user subroutine, WKSLP, was written to represent this formulation and incorporated into the run stream of MARC. Constants for this subroutine were obtained from experimental tests. Figure 3 shows a comparison between the results obtained from this subroutine and those obtained from coupon tests for an axially loaded square plate.

3.1.2 MARC Program Modifications

A simple unnotched flat plate (Figure 4) which is fixed at one edge and loaded axially at the opposite edge was used initially to gain an understanding of the nonlinear capability in MARC. The standard version of MARC allows only a bilinear representation of the stress-strain curve. Figure 5 illustrates a typical stress-strain curve obtained from loading the simple plate for 1 1/2 cycles. The open symbols are computed stress-strain data points. A comparison between the finite element analysis results and a typical coupon tested during Phase I is illustrated in Figure 6. Correlation between the two is within acceptable limits for the initial tension loading; however, it is rather poor on unloading. The area where the correlation is the poorest possibly corresponds to values of notch stress and notch strain in elements immediately adjacent to a hole when the specimen is loaded in compression during a hold period. In order to better represent this phenomena, in-house IRAD funds were used to develop a capability in MARC to allow the user to define multi-linear representation of the tension and compression yield surfaces. In addition, the capability of defining a different yield point in tension and compression was added. This involved modifying twelve subroutines in MARC. Figure 7 is a typical example of the stress-strain curve obtained from MARC after this feature was added.

3.2 PLATE/LAYERED MODEL ANALYSIS

A layered model was developed to evaluate through the thickness variances in stress and strain. Figure 8 illustrates the simple model utilized for this evaluation. Edge A of this model is restrained in the Y-direction and Edge B is restrained in the X-direction. Also, the model is restrained along the bottom so that no vertical displacements (Z-axis) are possible. This model as restrained represents a four-layered plate with a rectangular hole in the center. The plate was loaded in the X-direction as shown in Figure 8.

The evaluation of a finite-element analysis obtained for this model indicated that through-the-thickness variances in stress and strain cannot be detected. At the region of highest stress concentration both the stress and strain varied through the thickness by less than 0.5 percent. For this evaluation, the loading was simple tension until the first element went plastic. In addition, the effects of creep were examined. The data obtained for Elements 1-2, 3-4 and 7-8 are shown in Table 4. In Figure 8, Element 1 is directly below Element 2. The same holds true for element pairs 3-4 and 7-8. In Table 4, Increment 0 is the maximum tension

load (or the start of the creep time) and increment 6 corresponds to the end of the 30-hour creep time. The stresses and strains are listed for the Gaussian integration point in each element. Elements 1 and 2, for example, show that there is essentially no difference in stress or strain at either increment 0 or 6; i.e., before or after the hold period. The same is true for the other element pairs.

3.3 SUPER-SCALE SPECIMEN

Two finite element models were constructed of the super-scale specimen. Both models have the same geometry. The first utilized solid elements and the second used plate elements. These are illustrated in Figures 9 and 10. Since the structure had two axes of symmetry, only one-fourth of the structure was modeled with the proper boundary conditions. The grid points along Edge A were fixed in the X-direction and similarly those along Edge B in the Y-direction. The results obtained from these models are discussed in Section 6.1.2.

3.4 SIMPLIFIED STRESS CONCENTRATION MODEL

A finite element model was made of the simplified stress concentration specimen shown in Figure 11. The shaded area was modeled as shown in Figure 12. This could be accomplished since there are two axes of symmetry and the nodes along the grip line move uniformly. The boundary conditions consist of the nodes along Axis A fixed in the X-direction, the nodes along Axis B fixed in the Y-direction, and the nodes along the grip line are fixed in the Y-direction. In addition, the X displacements along the grip line were uniformly imposed. The results of this model are discussed in Section 6.1.2.

SECTION IV
EXPERIMENTAL PROGRAM

The experimental program conducted here was to develop a sufficient understanding of the time dependent changes in the stress-strain field around central notches such that a creep and stress relaxation module could be developed for the hysteresis analysis. Testing was directed primarily to collecting constitutive data and to verify analytical predictions, both the finite element code simulations and the hysteresis analysis results. Four types of test specimens were used in the program. These include:

- Simple Bar Coupon Specimens

  Coupon specimens were used to obtain constitutive data for creep and stress relaxation during sustained hold periods following tensile overloads.

- Simplified Stress Concentration Specimens (SSC)

  Unique 3-bar, simplified stress concentration specimens were used to simulate the stress concentration of the center-notched super-scale specimen to evaluate creep, stress relaxation. and load shedding.

- Super-Scale Specimens

  Center-notched super-scale specimens were used to verify finite-element code predictions of time-dependent strain variations.

- Center-Notched Coupon Specimens

  Circular-notched coupon specimens were flight-by-flight spectrum fatigue tested using loading conditions representative of a transport/bomber wing lower surface. The tests were conducted to verify the predictions from the hysteresis analysis.

Each test series involved complex load-time test sequences representative of typical flight loadings for transport/bomber wing structures. The complexity of the test sequences varied from initial tensile overloads followed by step hold periods for the

simple bar specimens to the spectrum loadings, including hold periods, for the notched coupon specimens. Continuous recordings of load and strain were made during the first three test series. These data were used to determine material constants for the creep formulation and to verify analytical predictions.

Specific details of the four test series are discussed in paragraphs 4.1 through 4.4. The analytical model formulation is discussed in Section V. Data analysis and correlation studies are in Section VI.

4.1 COUPON CREEP TESTS

During the Phase I program it became evident that constitutive data would be necessary in the formulation of a creep-stress relaxation module for the hysteresis analysis model. Consequently, the initial experimental work in Phase II involved testing simple unnotched coupons and continuously measuring strain and/or stress changes during sustained load hold periods.

The specimen used in these tests is illustrated in Figure 13. These specimens and all specimens for subsequent tests in Phase II were made from the same 7075-T651 plates used to fabricate all the Phase I specimens. This was done in order to minimize plate-to-plate material properties variations that might exist. Since the magnitude of the strains being measured is small, care was taken to assure a minimum variation in material.

Twelve coupon specimens were tested. The loading conditions are identified in Table 5. Two replicates were tested for each of the six tests listed in the table for the total of twelve. A schematic of the loading conditions is illustrated in the sketch in the table. Tests 1 through 4 were run under automatic load control and strain data were recorded from extensometers attached to the specimen. Tests 5 and 6 were run in a strain control mode using feedback from the extensometer to automatically control the tests. All tests were run at laboratory ambient conditions.

Each specimen was initially loaded to a positive strain of 0.016 in/in (sufficient to produce plastic deformation) and then unloaded, and reloaded into compression for

three periods of sustained loading. The first sustained load hold was 24-hours. This was followed by two, one-hour periods; the first at a different stress/strain and the second at the initial stress/strain loading. The variation in load in each sequence was to evaluate the "memory" of prior loadings and any subsequent effects. Results from the finite-element analysis of the super-scale specimen were used to establish the test loading conditions. For example, the -50 ksi and -66 ksi are typical of the resultant stress in the most highly loaded element at the hole edge for the -7.9 and -15.8 ksi sustained compression loads.

Table 6 is a summary of the strain creep and stress relaxation data measured during the hold periods for each specimen. The data shown are the total strain or stress measured for each test loading condition. Stress-strain curves and creep/relaxation curves are illustrated in Figures 14 through 37 for these twelve tests. Figure 14, for example, is the stress-strain curve for test 1A and depicts the tensile loading to approximately 0.016 in/in followed by the sustained load hold periods at -50 ksi and -66 ksi. The stress here is calculated based on the specimen net section. During the initial 24-hour hold period at -50 ksi, 1100 μin/in strain was measured. The stress was then changed to -66 ksi and held for one hour, then returned to -50 ksi for one hour. Approximately 540 μ in/in strain change was measured during the second hold period and zero change was measured during the final hold period at -50 ksi. The creep curves for this test specimen are shown in Figure 15.

Some of the observations that have been made from the data in Table 6 and the accompanying figures are listed below.

1. A significant amount of creep and stress relaxation was measured during these tests.

2. In each case the "primary" creep accounts for the largest percentage of the total measured. Seventy to eighty percent of the total strain or stress change occurs during the first hour of the sustained load hold period.

3. There appears to be a limiting value of creep which occurs, at least at stress levels above -40 ksi. For example, in Sequences 1 through 3, the maximum strain change averages 2000 μin/in. There is some variation from test to test which may be attributed to basic differences in specimen and material. The sequence of applied stress does not effect the total strain change measured. In Sequence 2, for example, slightly over 2000 μin/in was measured at the initial -66 ksi hold period, while approximately the same total was measured in Sequence 3 at two stress levels. A similar trend is shown in Sequence 1, although the totals are somewhat less.

4. The creep and stress relaxation seen in these tests does not appear to be sequence dependent. That is, by increasing load, strain and stress changes continue to increase in the classical "primary-secondary" sense. On returning to a lower loading there is little or no change in the measured data.

The creep data from these coupon tests were used to determine the material constants β, p, and n for the creep formulation used in the finite-element analysis. Hoff's creep formulation was used in the MARC analysis; i.e.,

$$\epsilon^c = \beta \sigma^p t^n$$

where:

ϵ^c = creep strain

σ = stress

t = time

$\beta = 1.120 \times 10^{-13}$

p = 2.11

n = 0.065

} material constants for 7075-T6511 plate

A comparison between predicted and measured creep strain is illustrated in Figures 38 through 40. The analytical curves use Hoff's formulation with the material constants listed above. The experimental data in these figures is the average of the two specimens

tested at each stress level. Agreement between the predictions and the experimental results are considered quite good, especially in the primary creep regime.

The significance of these creep and stress relaxation data is of course, in the formulation of a hysteresis analysis model. The data here do substantiate the hypothesis of the complex, time-dependent relationship between stress and strain and the effect on time to crack initiation which was illustrated previously in Figure 2. Use of these data in the formulation of a creep/stress relaxation module is discussed in Section 5.3.

4.2 SIMPLIFIED STRESS CONCENTRATION SPECIMEN

In all tests during the Phase I program and the coupon and super-scale testing conducted here, strain data could be collected with reasonable ease. However, plastic stress could not be measured directly. Since it has been hypothesized that the time-dependent effects on life are a complex function of both stress and strain, an experiment was necessary to measure stress and stress change. Burski and Hayes, Reference 2, had previously used a unique, three-member specimen to evaluate residual stress relaxation as a function of cyclic loading. This specimen was used here to evaluate the time-dependent changes in plastic stress.

This simplified stress concentration (SSC) specimen is illustrated in Figure 41. The specimen behaves like a notched coupon in that it will have plastic and elastic regions existing simultaneously when loaded axially. It is designed so that the center bar will yield while the two outer bars remain elastic. For this experiment, the specimen geometry is such that the elastic stress concentration is the same as the center notched super-scale specimens tested previously; i.e., approximately 2.43.

4.2.1 Theoretical Analysis

In the analysis of this specimen, it is assumed that the elongation is the same in all three bars when an external load is applied. This allows for the calculation of the plastic stresses in the center bar when only the elastic stresses in the two outer bars and the applied load are known. A schematic representation of the specimen, including a definition of terms used here, is illustrated in Figure 42. The basic assumption here is

$$\delta_1 = \delta_2 = \delta_3 \tag{1}$$

where,

$$\delta_1 = \frac{P_1 \ell_1}{A_1 E} \tag{2}$$

$$\delta_2 = \frac{P_2 \ell_2}{A_2 E} \tag{3}$$

$$\delta_a = \frac{P_3 \ell_a}{A_a E} \tag{4}$$

$$\delta_b = \frac{P_3 \ell_b}{A_b E} \tag{5}$$

$$\delta_c = \frac{P_3 \ell_c}{A_c E} \tag{6}$$

Also,

$$P_T = P_1 + P_2 + P_3 \tag{7}$$

or

$$P_3 = P_T - (P_1 + P_2) = P_T - 2P_1 \tag{8}$$

The elongation of the center bar can be written as,

$$\delta_3 = \delta_a + \delta_b + \delta_c \tag{9}$$

and by combining Equations 4, 5, and 9 and assuming $\ell_a = \ell_c$ and $A_a = A_c$, then,

$$\delta_3 = \frac{P_3}{E}\left(\frac{2\ell_a}{A_a} + \frac{\ell_b}{A_b}\right) \tag{10}$$

Since $P_1 = P_2$, and δ_1 and $\delta_2 = \delta_3$, Equation 10 can be written as,

$$\frac{P_1 \ell_1}{A_1} = P_T - 2P_1\left(\frac{2\ell_a}{A_a} + \frac{\ell_b}{A_b}\right) \tag{11}$$

also,

$$\frac{P_1}{P_T} = \frac{P_2}{P_T} = \left(\frac{2\ell_a}{A_a} + \frac{\ell_b}{A_b}\right)\left(\frac{\ell_1}{A_1} + \frac{4\ell_a}{A_a} + \frac{2\ell_b}{A_b}\right) \tag{12}$$

And then,

$$\frac{P_3}{P_T} = \frac{\ell_1/A_1}{\left(\ell_1/A_1 + \frac{4\ell_a}{A_a} + \frac{2\ell_b}{A_b}\right)} \qquad (13)$$

Using the specimen geometry in Figure 41 and the following segment lengths for the center bar,

$$\ell_a = \ell_c = 2.09 \text{ in.}$$

$$\ell_b = 1.82 \text{ in.}$$

results in,

$$\frac{P_3}{P_T} = 0.380 \qquad \frac{P_1}{P_T} = \frac{P_2}{P_T} = 0.31 \qquad \frac{P_3}{P_1} = 1.23$$

The test sequences utilized in this program were such that the outer two bars did remain elastic and it was possible to calculate the center bar plastic stress from the recorded data. Strain gages and extensometers were used to measure strain in all three bars and the plastic stress calculated using the above relationships.

Stresses σ_1 and σ_2 were calculated directly from the measured elastic strain data. Where multiple measurements were made on any single bar, the average values were used. These outer bar stresses were then converted to loads (P_1 and P_2) and the center bar load calculated from Equation 8; i.e.,

$$P_3 = P_T - (P_1 + P_2)$$

This load was then converted to stress in the center bar by dividing by the center bar area, A_3. The calculated center bar stress and changes in this stress during hold periods are then plotted versus strain and strain changes measured during the load sequences. A discussion of the loading sequences, instrumentation used, and data collected is in the following section.

4.2.2 Experimental Program

Test sequences for these SSC specimens are illustrated in Figure 43. Four sequences were developed to simulate in part some of the more typical super-scale tests conducted in Phase I. Initially, only creep and stress relaxation data were to be collected; however, the program was modified to also attempt to fatigue test two specimens. In general, the specimen does not lend itself to the magnitude of fatigue loads applied, but the creep and stress relaxation measurements were considered to be very successful.

Sequences 1 and 2 consisted of an initial overload followed by 24-hours of sustained compression loading. This was repeated in each sequence for a total of 48-hours of sustained loading as shown in the figure. Loading conditions for each sequence are included in Figure 43. The loads defined are the total applied loads, P_T discussed in 4.2.1. Sequences 1 and 2 are identical except for the magnitude of the compression load, P_{MIN}. Sequence 3, a fatigue test, consisted of the initial overload followed by a compression underload and then constant-amplitude cycling. The period between tension overloads, N_{OL}, was 1000 cycles of constant amplitude loading. The last sequence, Sequence 4, was identical except that the compression underload was sustained for one hour. Strain data listed in Figure 43 under Loading Conditions are measured center bar data. The variable strains listed for Sequences 3 and 4 illustrate the apparent cyclic strain changes measured during the fatigue cycling. This is discussed in subsequent sections.

Each SSC specimen was instrumented with seven strain gages and two extensometers and tested in a computer-controlled, closed-loop test machine. Instrumentation locations are shown in Figure 44. Specific test procedures and equipment systems are discussed in 4.5.

Two of the SSC specimens were tested under the Sequence 1 loading conditions. Some difficulties were encountered during the first test and, although this was not sufficient to negate the test, it was decided to test a second specimen. Data was recorded from the strain gages on the outer bar as well as the two extensometers shown in Figure 44. A sample of the stress-strain data print-out for the initial ramp to load and the 24-hour

hold period is shown in Table 7. This data is typical of that collected automatically during each SSC test and was used to calculate the center bar plastic stress and stress relaxation. The stress column in the table is the total net section stress across the center of the SSC specimen. These tests were load control and the stress shown is simply the total applied load divided by this total net area ($A_1 + A_3 + A_2$).

The specimen was loaded to the tension peak and unloaded to a predetermined compression stress for the sustained load hold period. Only segments of the data recorded during the hold period are included in the example. However, the time intervals selected were such that the "primary" changes in both strain and stress were documented. These data were then used along with the analysis method outline in 4.2.1 to calculate center bar stress. An average of the two gages, front and rear, was used in the data analysis. For the other two bars, the extensometer data was used directly.

The data from the two Sequence 1 tests are shown in Figures 45 through 48. A stress-strain curve for the elastic-plastic loading on the center bar is illustrated in Figures 45 and 47. Both the first and second load cycle, see Figure 43, and the two sustained load hold periods are shown in these figures. As noted earlier, these tests were considered to be very successful in regard to better defining the relationship between strain creep and stress relaxation. These changes, as measured and as calculated from the measured data, are illustrated in Figures 46 and 48 for these two specimens.

Calculated center bar stress relaxation is plotted versus measured center-bar strain creep in these two figures. Data for both the first and second loading cycles are presented. The initial stress-strain conditions at the start of each hold period (time = 0) are somewhat different for the two specimens. This may be attributed to material or specimen geometry variations, or uniformity in loading through the end grips. The second hold period on the repeat test was only 40-minutes due to a system malfunction; but overall sufficient data was collected to establish trends for the creep/relaxation analysis module development. Additional data was collected from Sequences 2 and 4.

Sequence 2 is a repeat of the first sequence; but the compression stress was less than that used on those tests. Similar data and trends were seen in this loading sequence.

Figure 49 is the stress-strain curve for this specimen. Again, two loading cycles were applied and creep and relaxation data were obtained during the two 24-hour hold periods. The center bar stress relaxation and creep are shown in Figure 50. Less creep was seen in this test than was measured from the Sequence 1 specimens. This follows the trend seen in the simple coupon tests which were discussed in 4.1.; that is, the lower the stress levels the less creep change measured.

Sequences 3 and 4 were intended to be primarily fatigue tests, but, as mentioned earlier, the specimen size, thickness, etc. did not lend itself to fatigue testing at the stress levels used here. This is not to say that the basic specimen should not be used for fatigue testing in general. A considerable amount of useful data was collected from these test sequences, however. Both sequences are defined in Figure 43.

Two test specimens were tested for Sequence 3. It was originally planned to apply 10,000 cycles, N_{OL}, between the tension-compression overloads; however, the first specimen tested failed after 5990 cycles. Only the initial overload cycles were applied. After this test, N_{OL} was reduced to 1000 cycles, primarily to allow for more overloads and subsequent hold periods which were to be applied in Sequence 4. The second specimen was then tested as shown in Figure 43 with 1000 cycles between overloads and failed in the center bar after 10,278 cycles.

The center bar stress-strain curve for the initial load cycles applied on the first Sequence 3 specimen is shown in Figure 51. No hold period was included to measure creep or relaxation,but this figure illustrates the specimen response from the minimum compression stress back to the positive mean stress prior to constant amplitude cycling. Typical data for the first, second, and tenth overload cycles applied on the second specimen are illustrated in Figure 52. These are plots of specimen net section stress versus center bar strain directly from the computer controlled test equipment.

These data plots are included here to illustrate an apparent cyclic creep which was observed during this test (also observed during the Sequence 4 testing). A time history of the center bar strain is illustrated in Figure 53. Both the mean strain and the

minimum strain are plotted versus the N_F/N_{OL} ratio in this figure. The mean strain is the mean value of the constant amplitude loading and the minimum strain is the strain measured during the application of each compression underload. N_F is the total number of applied cycles and N_{OL} is the number of cycles between overloads. The data shown are for the second specimen tested for Sequence 3. These same trends were observed during the super-scale specimen tests in Phase I and are reported in Reference 1. Several investigators have previously reported on cyclic creep and its impact on time to crack initiation. The data here are simply presented as trends, in that there is insufficient data to incorporate a cyclic creep module in the hysteresis analysis program.

The final SSC test sequence was Sequence 4 (Figure 43). This was also a fatigue test and was similar to Sequence 3 except that one-hour hold periods were included. One specimen was tested and failed after 9000 cycles of constant amplitude loading during the application of the tenth tensile overload. Figure 54 is an illustration of the center bar strain data for loading cycles 1, 5, and 9. These are typical data plots obtained during the conduct of the test.

Stress relaxation and creep were measured during each sustained load hold period. Figure 55 shows this data for the first, fifth, and ninth hold periods. The trends toward a creep and relaxation saturation limit that was discussed in 4.1 for the coupon tests is also evident here. These data indicate a continuing decrease in both stress and strain change with cumulative time. The stress and strain changes shown in all these SSC specimen tests are sufficient to significantly influence subsequent loadings and the time to crack initiation. The development of the creep and stress relaxation model for the hysteresis analysis is discussed in 5.3.

One final set of data from the Sequence 4 test is illustrated in Figure 56. This is the history of the center bar strain changes which were recorded during the test. Again the mean strain and minimum strain changes are plotted versus the N_F/N_{OL} ratio. The "sawtooth" effect on the minimum strain curve reflects the creep which occurred during each sustained load hold period. This data also illustrates the decrease in the amount of creep per hold period with cumulative time. The discontinuities in the mean strain curve reflect measurements before and after each block of constant amplitude cycles.

4.3 SUPER-SCALE SPECIMEN TESTS

The center circularly notched super-scale test specimen used in Phase I for complex sequence testing was again utilized as a part of the experimental effort in this program phase. This specimen and the instrumentation used for strain measurement (strain gages and strain transducer) are illustrated in Figure 57. Ten loading sequences were included in this program. Tests were conducted to collect strain data in and around the center notch to evaluate the finite-element code predictions and update the constitutive data.

The specimen, as illustrated, is 8.0 inches wide with a 2.0-inch diameter hole in the center. It has a geometric stress concentration factor of 2.43. This scaled-up specimen is used in order to insert the Lockheed-developed strain transducer inside the hole for notch strain measurements. Specific details of the transducer design and function are reported in the Phase I final report, Reference 1. This transducer has a gage length of approximately 0.080-inch and provides a reliable means to continuously monitor notch strain. Four strain gages, as shown, were also installed on each specimen to measure strain immediately adjacent to the hole on the specimen surface.

The ten test sequences, loading conditions and cycles-to-failure are shown in Figure 58. Basically, this group of tests is a continuation of the Phase I super-scale test program and is intended to supplement and expand those data. All test sequences include an initial tensile overload equivalent to a specimen net section stress of 47.3 ksi. All constant amplitude cycling was conducted at a mean stress of 15 ksi and a variable stress of 10 ksi. Both compression underloads and compression underloads with sustained load hold periods follow the initial tensile overloads. Most of the test sequences included underloads at either -7.9 ksi or -4.0 ksi net section stress. The -7.9 ksi was the baseline in Phase I and was carried over here for additional tests. This stress level is typical for transport aircraft wing lower surfaces during on-ground operations as is the -4.0 ksi, which was added to the Phase II test matrix.

The first four sequences had only one tensile overload followed by 24 hours of sustained compression load. Then the specimens were constant amplitude-cycled to failure. Sequences 9 and 10 were similar but only had a single application of the compression

load and did not include the sustained compression load. Cyclic block sizes between overloads (N_{OL}) were 15,000 cycles and 30,000 cycles. The 15,000-cycle block size was the Phase I baseline condition. A maximum of five 24-hour hold periods were included in Sequences 5, 7, and 8. Two specimens were tested for Sequence 7, as shown in Figure 58; only three 24-hour hold periods were applied on the first specimen. Five hold periods were applied on the second.

As noted earlier, both creep and cycles-to-failure were recorded from these tests. The specimen life reported in Figure 58 is the cycles-to-total-specimen separation. No crack initiation times were recorded; however, experience from the Phase I program showed that crack growth under these loading conditions was only 1 - 2 percent of the cycles-to-rupture.

A comparison between these test results and some of the more pertinent and similar tests from the Phase I program is included in Table 8. In the table, Group 1 tests contain only sequences with overloads and underloads, whereas Group 2 includes the addition of the hold period in the sequence. The baseline constant amplitude cycling only is also included for comparison. The data illustrate the following basic points:

- Tension overloads produce a life lengthening effect over the basic constant amplitude loading.
- Compression underloads reduce the effect of the tension overload.
- Cyclic block size affects the induced beneficial residual stresses which produce the life-lengthening effect.
- Time dependent creep does alter the residual stress-strain state and significantly affects time to failure.

The overload/underload effects can be seen by comparing Sequence I-6 with I-8 and II-6. In all three of these sequences, the overload and underload is repeated every 15,000 cycles. The repeated overloads tend to greatly extend the specimen life. A single

initial overload/underload (Sequences II-9 and II-10) does extend the life of the baseline but the overload contribution of extending life decays with continued constant amplitude cycling. This is illustrated by comparing Sequences II-9 and II-10 with I-8 and II-6, respectively. Another indication of this decay in the overload-induced beneficial residual stress/strain state can be seen in comparing the Group 2 specimens tested with N_{OL} 15,000 and 30,000 cycles. In each case, the 30,000-cycle block size results in the shorter specimen life.

In general, the compression hold periods at 0, -7.9, and -15.8 ksi net section stress follow expected trends. The data for the -4.0 ksi compression stress do not, however. For example, Sequence II-5 should have resulted in a shorter life than Sequence II-6, but the two specimens failed at approximately the same lifetime. Sequence II-5, with the compression-hold period, actually had a longer life. It may be that the -4.0 compression stress does not sufficiently overcome the beneficial residual stresses induced by the tension overload at least within the 15,000 cycle block size between overloads. For example, in Sequence II-8 with N_{OL} = 30,000 cycles, there is a significant reduction in time-to-failure as compared to II-5 and II-6.

A similar trend has been observed in evaluating the effects of underloads on crack growth, Reference 3. In that program, various levels of compression underloads were applied immediately following tensile overloads, similar to the sequences here. Crack growth is retarded after the tensile overload due to the plastic zone formed at the crack tip. Compression load application tends to negate this effect; however, the magnitude of the compression load affects reinitiation of the crack growth. The lower the compression load, such as the -4.0 ksi here, the more constant amplitude cycles that must be applied in order to overcome the plastic zone effects. It appears that this same effect may hold true for crack initiation.

Creep strain was recorded during the compression hold periods from the transducer inside the hole and from the four strain gages immediately adjacent to the hole on the specimen surface. A summary of the measured strains is shown in Table 9 . Plots of creep strain versus time are illustrated in Figures 59 through 61 for Sequences II-5, II-7, and II-8. The data shown are from the strain transducer located inside the hole.

In general, the measured data follow expected trends; however, the magnitude of the measured strain was less than expected. The transducer measurements for Sequence 4 appear to be high, but the instrumentation was checked and no problems were found. Sequence 1 also appears not to follow the expected trends in that the change inside the hole is in the positive sense where the changes on the specimen surface were negative (decreasing strain). This phenomena was also observed during the Phase I testing, however. Variations in the material properties and homogeneity from specimen to specimen apparently have a significant impact on the stress-strain history variability.

4.4 SPECTRUM FATIGUE TESTS

A series of flight-by-flight spectrum fatigue tests was run on center circularly notched coupon specimens to evaluate the data developed from the previously described tests and to evaluate the hysteresis fatigue analysis. The test sequences developed were representative of transport wing lower surface loadings. Typical flight and ground loads data were used to develop logistics and low-level mission spectra for these test sequences. Three test sequences were developed for this study. One sequence included periodic overloads followed by sustained load-hold periods. The test specimen used was a simple center notched (open hole) coupon with a geometric stress concentration of 2.43. Three specimens were tested for each loading sequence.

Typical mean and alternating flight and ground loads for a transport wing lower surface which were used in the test sequence development are included here in Figures 62 through 66. Three typical flights were developed from the loads data and then mixed to form the three test spectra. Flight A was derived from the logistics mission data. For each flight segment, four loads equal to the five times per flight load and one load equal to the once per flight load are included. Only one taxi load was included to obtain a compression underload in the flight. Flight B was derived in the same manner, except that the low-level mission data was used. Flight C is identical to Flight B except for the inclusion of the tensile overload. The mean loads were selected to bracket the loadings used in the previous Phase I and II loading sequences, and the applied flight loads were adjusted for the appropriate means. The resulting flights are illustrated in Figure 67. The stresses shown in these figures are net section stresses.

These flights were combined into the following three spectra:

Spectrum 1

$$50\,[C + 150\,(2A + B)\,] + N\,(2A + B)$$

That is, Flight C
A
A
B
} Repeat 150 Times

Repeat 50 Times

⋮

Then,

A
A
B
} Until Failure

Spectrum 2

$$50\,[\,(C + \text{Hold}) + 150\,(2A + B)\,] + N(2A + B)$$

This spectrum included a 1-hour sustained load hold period at -9.4 ksi after each application of Flight C.

Spectrum 3

$$50\,[\,B + 150\,(2A + B)\,] + N(2A + B)$$

A sample of a strip chart recording for Spectrum 2 is illustrated in Figure 68. The specimen life, in flights-to-failure, of each specimen tested is tabulated in Table 10.

These test results tend to confound this study in that no discrimination can be made between the results of the Spectrum 1 and 2 tests. It was anticipated, based on all the preceding tests, that there would be distinguishable differences between the spectra with and without the hold periods included. The periodic overloads included in Spectra 1 and 2 do result in a life extension effect, as compared to Spectrum 3 which does not have the overload. But, at least for the transport spectra used here, the compression load and hold period do not show the life reduction that was previously demonstrated.

This is not a conclusive test since it was limited limited to one typical spectrum for a transport aircraft, but the results are discouraging. The data base developed in the preceding tests and in Reference 3 did show a pronounced effect of underload and sustained load hold periods on both cycles to crack initiation and crack growth. It is possible that these effects do show up on an individual cycle; but, for a transport spectrum, the effect is not that significant and can be accounted for by a statistical smear across the spectrum.

4.5 GENERAL TEST METHODS

Four different types of tests were performed during the Phase II experimental evaluations; namely, superscale, single-bar coupon, three-bar simplified stress concentration, and spectrum fatigue tests. All testing was performed in modern electrohydraulic servo-controlled test systems manufactured by MTS Systems Corporation. Each test system was interfaced to a digital computer which was used to command the different profiles, monitor loads and strains, and perform failsafe functions. Additionally, the computer was used to store, reduce, tabulate, and plot data in a reportable format. The data collection, reduction and display functions operated in near real time as the test progressed. The heart of each system was a PDP-11 computer and a modified BASIC programming language which was interactive. Inputs and outputs were managed through a teletype terminal and CRT supported by a hard-copy unit. A typical system containing a three-bar SSC specimen is shown in Figure 69.

A user program was written in BASIC for each different test type, and each program contained options to accommodate the different profiles required. The superscale tests were performed under load control, and outputs from the load and strain transducers were recorded at programmed time intervals throughout the tests. The time intervals were controlled by a programmable clock which resulted in precise load-strain-time history data.

The single-bar and three-bar SSC tests were also performed under load control; however, the test system computer program was written so that loading was reversed once a desired value of strain was reached during the initial tensile loading. For the SSC tests, the load reversal was based on strain in the center bar. All subsequent events in the profiles were applied under unconditional load control. Single bar strains were measured using an extensometer. Strains for the three bar tests were measured using an extensometer on the center bar and one outer bar, and strain gages on the other outer bar. (As was done for the superscale tests, load and strain data were recorded at programmed time intervals throughout the tests.) Load and strain history data for a typical three-bar test are contained in Table 7. A summary plot of these data is shown in Figures 52 and 54. Both the data tabulations and plots represent copies from the test system CRT.

The spectrum fatigue tests were performed under load control with peak-to-peak load transition. An analog representation of the three different flights contained in the baseline spectrum is shown in Figure 68. Tests for two different variations of the baseline were also performed. One variation was the inclusion of 50, one-hour hold periods at the minimum load in Flight C. The other variation was to replace Flight C with Flight B which eliminated the high tensile overload.

SECTION V
HYSTERESIS ANALYSIS PROGRAM DEVELOPMENT

The experimental data collected during both Phases I and II have been used to formulate a rather comprehensive hysteresis type of an analysis. This analysis contains the following elements:

(1) Notch Stress-Notch Strain Algorithm
   - o Locus Curves
   - o Branch Curves
   - o Neuber Analysis (Modified)

(2) Material Hardening or Softening

(3) Creep/Stress Relaxation

(4) Fatigue Damage Computation

A detailed discussion of Items 1, 2, and 4 is included in the Phase I final report, Reference 1. The creep and stress relaxation module was developed in Phase II and a discussion of this formulation is included here. Specifics of the analysis program subroutines, program input, etc. are included in Appendix A, Hysteresis Analysis Computer Program Description, and Appendix B, Hysteresis Analysis User's Guide.

5.1 NOTCH STRESS-NOTCH STRAIN ANALYSIS

The basic algorithm for the notch stress-notch strain calculations is illustrated in Figure 70. Phase I test data were used to formulate the locus curves and branch curves for the 7075-T651 material used here. For a material that has been cyclically hardened or softened it can be said that:

(1) Stress and strain will always expand along the cyclic locus curve.
(2) Excursions from the cyclic locus curve will follow branch curves.

The formulation and use of the locus curves and branch curves are discussed in detail in Reference 1. In Figure 70, a specimen can be loaded along the tension locus curve to a point A which is located at the intersection of the locus curve and the modified Neuber hyperbola. When the loading is reversed, the stress and strain will follow the branch curve, as illustrated, to the next loading condition.

Figure 71 is a typical example of the notch stress-notch strain calculations from the hysteresis analysis and its plotter option. The input loading sequence and the resultant stress-strain plot are illustrated here. These data are then used in the damage calculations within the program to predict structural life.

5.2 CYCLIC HARDENING AND SOFTENING

The rationale and data used in the development of the cyclic hardening and softening module are included in Reference 1 and in Appendix A. The hypothesis is based on the premise that an excursion along the tension locus or branch curves will harden the compression locus and branch curve. The cycles necessary to harden the material must be determined experimentally and will depend in part on the material, alloy, and strain level. For the 7075 used here, the number of cycles to fully harden the material varied from 4 cycles at a strain of 0.035 in/in to 50 cycles at 0.010 in/in. An example of the material hardening module in the analysis program is illustrated in Figure 72.

5.3 CREEP AND STRESS RELAXATION

The following two phenomenon were observed in the simple bar creep tests and the simplified stress concentration tests:

(a) When a material is loaded to a local stress σ_A and allowed to creep and then further loaded to a local stress σ_B the creep at σ_B is less than if the material were loaded directly to σ_B and allowed to creep. This is illustrated in Figure 73.

(b) When a material is loaded to a local stress σ_A and allowed to creep, and then the cycle is completely reversed and the material reloaded to σ_A and again allowed to creep, for equal hold periods the two creep levels will be the same, see Figure 74.

These observations form the basis for the creep algorithm used in the hysteresis stress-strain analysis.

The creep formulation credited to Nutting, Hoff, and Scott-Blair is used in the algorithm:

$$^{c}\varepsilon = K\sigma^{p}t^{n} \tag{1}$$

where

$^{c}\varepsilon$ is the creep strain

σ is the current stress

t is the time in hours

$K, p, \& n$ are material constants.

Based on observations of the simplified stress concentration tests, the relationship between the creep strain and the stress relaxation $^{R}\sigma$ is assumed to be proportional to the current stress:

$$\frac{^{R}\sigma}{^{c}\varepsilon} = \sigma E \tag{2}$$

where

$$\sigma = {}^{o}\sigma - {}^{R}\sigma$$

$^{o}\sigma$ is the stress at time zero

Hence, given ${}^{o}\sigma$ and t, equations (1) and (2) are used to find the creep strain ${}^{c}\varepsilon$ and the stress relaxation ${}^{R}\sigma$.

${}^{H}\varepsilon$, a creep history value, and ${}^{H}t$ the corresponding time, are used to simulate the preceding observations (a) and (b). Initially ${}^{H}\varepsilon$ and ${}^{H}t$ are zero. After a sustained load hold period ${}^{H}\varepsilon$ is set to ${}^{c}\varepsilon$ and ${}^{H}t$ to the time for the hold period. The next time a hold period is reached ${}^{H}\varepsilon$ effects the amount that the material can creep. This is done by ratioing the values obtained from equations (1) and (2) by an amount that makes ${}^{c}\varepsilon$ at time ${}^{H}t$ plus ${}^{H}\varepsilon$ equal to the creep that would have been experienced if ${}^{H}\varepsilon$ were zero. i.e.,

$$\text{Ratio} = \frac{{}^{c}\varepsilon({}^{H}t) - {}^{H}\varepsilon}{{}^{c}\varepsilon({}^{H}t)}$$

If the ratio is <0 then no creep is allowed. This satisfies (a).

After a hold period any plastic strain involved in the cycles that are reversals to the cycle immediately proceeding the hold period will subtract from ${}^{H}\varepsilon$. Hence a fully reversed cycle following a hold period will make ${}^{H}\varepsilon = 0$ which satisfies (b).

To check the algorithm three sequences shown in Figures 75,76, and 77 were analyzed using the following creep parameters.

E	58.436
K	$3.085 \times 10^{-13.44}$
P	2.11
n	.065

The first sequence, Figure 75, considers a single hold period. The second sequence, Figure 76, considers two hold periods where there is a fully reversed cycle following the first hold negating any effect on the second hold. The third sequence, Figure 77, considers two hold periods where the first hold decreases the amount of creep during the second hold. These analysis results correlate well with the coupon creep test results and the SSC specimen data discussed in 4.1 and 4.2. The analysis with the creep and stress relaxation module included was used in the data correlation studies reported in Section VI.

SECTION VI
DATA ANALYSIS AND CORRELATION

The experimental creep and stress relaxation data collected from the simple coupon, the simplified stress concentration specimen, and the super-scale specimens have been used to establish the necessary material constants, to formulate analysis algorithms for both the finite-element studies, and develop the hysteresis analysis program. Finite-element simulation studies were conducted for the SSC and the super-scale specimen tests using the creep constants determined from the simple coupon tests. The analysis results using the constants from the coupon tests do not correlate well with the observed experimental data; however, the SSC test data was used to update the constitutive data and much better correlation was obtained. These constitutive data plus the observed data from the SSC experiments were used in formulating the creep/stress relaxation module in the hysteresis analysis. The hysteresis analysis was used, in turn, to predict times to failure for the super-scale test sequences and the spectrum fatigue tests. In addition, a linear cumulative damage (Miner's) analysis method was used to predict the life of these two groups of specimens for comparison with the hysteresis analysis predictions. This data analysis and correlation is discussed in detail in the following sections.

6.1 FINITE ELEMENT ANALYSIS CORRELATION

6.1.1 Simplified Stress Concentration Specimen

A discussion of the SSC specimen finite-element analysis and an illustration of the model details are included in 3.4 and Figures 11 and 12. This model was used in the simulation of the four SSC specimen test sequences (Figure 43) discussed earlier. The tension overloads and sustained compression loadings used in the analysis were representative of the test conditions for each sequence. Element stresses for the maximum tension overload and for the -20 ksi net section sustained compression load ($\sigma_b \approx -50$ ksi) are illustrated in Figures 78 and 79.

In this model, the stresses and strains in each element are calculated at four Gaussian integration points. The data listed were calculated at the first integration point. Element No. 1 in the center bar plastic zone and Element No. 71 in the elastic outer bar are identified in these two figures. The data for these two elements were used in the correlation studies with the experimental results. The analytical stress-strain curves for these two elements are illustrated in Figure 80.

Three finite-element model runs were made, one each at a sustained net section compression stress of -12 ksi, -20 ksi, and -30 ksi. These are identified in the figure for both Element Nos. 1 and 71. A tension overload preceded each sustained underload hold period and creep data were calculated at each compression load. As can be seen in the figure, the outer bar remains elastic during the tension loading whereas the center bar does go plastic and has a maximum strain of approximately 0.016 in/in. A comparison between these analytical stress-strain curves and those from the SSC test sequences is shown in Figures 81 and 82. The agreement between the analytical results and the tests is quite good. Although these plots are labeled center bar stress and strain, the measured data for the elastic outer bars is included with this data for comparison. This elastic response of the outer bar is practically identical to the analysis. Differences in the center bar data can be attributed to the dependency of the method of calculation of the center bar stress on the measured data in all three bars (see Section 4.2.1, for example). Slight variations in material properties, dimensions, strain gage or extensometer data, etc. can account for the differences shown here.

Creep data, as measured on the center bar during SSC test Sequences 1 and 2, are illustrated in Figures 83 and 84 with the creep strains predicted from the MARC finite-element analysis. Initially, the analytical predictions were made using the material constants derived from the simple coupon data, as discussed in 4.1. The basic trends in this analysis and the tests are similar; however, as shown in the figures the correlation is rather poor. At first it was thought that the coupon creep constants would be applicable to the SSC and super-scale specimen analysis, but, as shown here, the analysis is very conservative as far as the amount of creep that is predicted. Since the SSC and super-scale specimens are more complex than the simple coupons, it was assumed that load redistribution in these two configurations (which did not occur in the coupon) could affect the magnitude of creep.

Based on this, the experimental data collected in the SSC specimen tests were used to derive a new set of material constants for the analysis. These constants are listed below along with those derived from the coupon tests for comparison.

Coupon Tests	SSC Tests
$\beta = 1.120 \times 10^{-13}$	$\beta = 1.851 \times 10^{-13}$
$p = 2.11$	$p = 2.01$
$n = 0.065$	$n = 0.067$

The correlation between the test and the analysis is, of course, greatly improved by using these SSC specimen derived constants as illustrated in Figures 83 and 84. The variation between the analysis and test is due to the calculated stresses being somewhat different from the experimental data. This again points out the extreme sensitivity of stress and strain measurements to variations in material, specimen geometry, and loadings.

6.1.2 Super-Scale Specimen

Two finite-element models were used in the analysis of the stress-strain distribution and creep around the center notch of the super-scale specimen. These two models were previously illustrated in Figures 9 and 10. One of the models used the solid, three-dimensional elements in the MARC program and the second model was constructed using the two-dimensional plate elements. The solid elements were used to attempt to determine if there is a through-the-thickness variation in the stress-strain field around the stress riser. In addition, the layered plate model discussed in 3.2 was also run to evaluate this through-thickness variation. No effect could be identified using either the 3-D elements or the layered model. The solid elements are also more expensive to run than the 2-D plate elements; therefore, only the 2-D plate elements were used throughout this analysis. A comparison of a typical element using the 2-D and 3-D elements is illustrated in Figure 85. The solid elements are much stiffer, as illustrated, and do not correlate as well as the plate element analysis with the experimental data.

Figure 86 is an enlarged view of the plate elements immediately adjacent to the stress riser. The figure also contains a listing of the elements that go plastic along with the

far-field tension stress level at which each element exceeds the proportional limit. Elements 8 and 7 are the most highly stressed elements in the model, as expected. The plastic zone adjacent to the hole, for the maximum tensile loading of 47.3 ksi net section stress, is highlighted in this figure.

Typical stress-strain curves from the finite-element analysis are illustrated in Figure 87 for Elements 8, 7, 16, and 15. The different symbols used locate the initial values, prior to creep, of stress and strain for each element at four different compression stress levels. These curves vividly illustrate the multi-linear stress-strain curve representation capabilities incorporated into the MARC analysis program as well as the different compression yield points for the elements.

Creep analyses were run at the four compression loadings listed in Figure 87 using the creep subroutine in the MARC program. Table 11 illustrates the analysis results for the -7.9 ksi loading. The analysis results for each of the four Gaussian integration points in each element are listed in the table. This analysis utilizes the creep constants from the simple coupon tests. Figures 88 through 92 are comparison plots of the analytical creep predictions and the measured data from the super-scale specimen tests.

The material constants used in these creep analyses include those developed from both the simple coupon tests and the simplified stress concentration specimen (SSC) tests. In general, the analyses using the SSC material constants agree better with the experimental data than the analyses using the coupon test constants. The experimental data for the -15.8 ksi compression loading do not agree with either analysis. This loading condition has been repeated and similar results were obtained. No explanation for this particular set of data is offered.

6.2 FATIGUE LIFE CORRELATION

Fatigue tests involving the super-scale specimens and simple, center notched coupons were conducted and the results from these tests have been compared with analysis predictions using both the hysteresis analysis and a linear damage analysis. The super-scale specimen tests included combinations of overloads, hold periods, and constant amplitude cycling, as defined in Figure 58; whereas, the notched coupons were tested under the flight-by-flight spectra described in 4.4. In addition, super-scale test data from Phase I have been included in the correlation studies discussed here.

Table 12 is a comparison of the Phase II super-scale test results with analytical predictions using both a linear damage analysis and the hysteresis analysis. The test life listed for each specimen is the number of cycles to total specimen rupture. It was demonstrated earlier that cycles to crack initiation are approximately 90-95 percent of the cycles to rupture at the stress levels used in these tests; therefore, cycles to rupture was used throughout the program as the failure criteria.

The cycles to failure from the various test sequences is variable and depends on the applied loading sequence. For example, magnitude of underload, hold period, number of overloads and number of cycles between overloads, each effect cycles to failure. The linear analysis, as shown, cannot discriminate among the different loading conditions and predicts approximately the same life (97,000 cycles) regardless of the applied loading. The hysteresis analysis on the other hand, with the capabilities for residual stress accountability and creep, does account for the differences in the loading sequences.

The results of the hysteresis analysis for these sequences are quite encouraging. At first glance, the correlation may be considered as less than anticipated; but, after a detailed study of the data, the trends are as expected but point out a need for additional parameter studies necessary for the hysteresis analysis which were not a part of the research conducted here.

The first observation from these results is the influence of the notch-root residual stress, following the overload-underload combination, on the fatigue life. That is, the magnitude of the underload is a definite factor effecting the life. Also, the effect of the

creep and stress relaxation during the hold periods is accounted for with the analysis. For example, the trends in Sequences 1 through 4 and 9 and 10 illustrate the effect of underload magnitude on the residual or mean stress during constant amplitude cycling. Sequences 5 and 6 illustrate the creep and stress relaxation accountability. Although not exact, the hysteresis analysis-to-test correlation for Sequences 5, 6, 7, and 8 is considered quite good. More on this will be discussed later.

The correlation for the sequences with only an initial overload-underload combination (Sequences 1 through 4 and 9 and 10) is not as good as that for Sequences 5 through 8 although the trends are as expected. The reason for this can be (and quite probably is) associated with micro crack growth through the induced plastic zone around the notch as well as a cyclic change in the notch stress and notch strain. The cyclic change in the notch stress and notch strain was observed during the simplified stress concentration specimen tests and is illustrated in Figures 53 and 56. The hysteresis analysis as currently formulated does not consider either of these phenomena.

When the initial overload-underload combination is applied, a plastic zone is established immediately adjacent to the notch. If no other overloads were applied, such as in Sequence 1, and the specimen is only constant amplitude cycled; micro crack coalescing and growth progresses slowly through this zone and can then accelerate once it passes through the plastic zone. The hysteresis analysis assumes a constant micro crack growth, for example, or a continuous plastic zone and does not consider any possible acceleration. This is one reason the analysis predicts a longer life than demonstrated in these test sequences with the initial overload-underload only. When there are periodic overloads in the sequence this would tend to retard micro crack growth by enlarging or reinforcing the initial plastic zone and resulting in a more constant rate of micro crack growth. The number of cycles between overloads would also be an influence on specimen life. Both of these can be seen by comparing Sequences 5, 7, and 10, for example. This is one reason why better correlation between analysis and test was shown for those test sequences which included multiple overload-underload combinations (either with or without hold periods).

The cyclic creep, as discussed earlier, from an initial favorable compression mean stress to a more positive mean stress value,can also reduce the specimen life.

The experiments conducted here were limited and were not designed to evaluate these possible effects of the plastic zone and subsequent micro crack coalescing and growth through this zone, or the effect of the cyclic changes in residual stress. Therefore, the current hysteresis analysis does not include either of these phenomena in its present form. If sufficient data were collected, however, additional modules can be added to the current analysis program to perhaps include the accuracy for these specific loading conditions.

Table 13 illustrates the test-to-analysis correlation for additional sequences, some of which are from the Phase I program. Again, the correlation is considered quite good. One surprise was the excellent correlation for Sequence 1. Here, only an initial tension overload was applied, no underload, and the correlation is quite good. This is contrary to the trends just discussed for those sequences which have the initial overload-underload combination. The initial notch mean stress was more compressive than any of the sequences with an initial overload-underload combination and this may have effected the micro crack growth through the plastic zone or the cyclic stress changes.

A final comparison of the test results and the analytical predictions is included in Table 14. Here, the results of the spectrum fatigue tests are compared with analytical predictions for both a linear damage analysis and the hysteresis analysis. Once again the linear analysis predicts approximately the same life for each of the three test spectra. The three test spectra were described in 4.4 and are typical of a transport wing lower surface loading conditions. The hysteresis analysis does distinguish between the three different spectra and follows the test trends quite well.

It was pointed out earlier that the hold periods included in these spectra did not demonstrate the significant reduction in life shown in the other sequence tests; however, the analytical predictions show the same results. These spectra may not have been a good combination of loading conditions to demonstrate this phenomena. Certainly, other

load combinations, type of aircraft, and spectra should be evaluated before definite conclusions can be drawn.

SECTION VII
OBSERVATIONS AND CONCLUSIONS

The following observations and conclusions are based on the results of both the Phase I and Phase II program:

1. Overloads and underloads induce a plastic zone around a stress concentration. The plasticity induced by overloads results in a life lengthening effect in structures. Underloads can reduce life lengthening effects produced by overloads.

2. Creep and stress relaxation occur in this plastic zone at the stress concentration during sustained load hold periods. This creep and relaxation is a complex function of both notch stress and notch strain.

3. Finite element methods of analysis can be used to successfully model the elastic-plastic stress-strain state around stress concentrations.

4. The cyclic period between overload-underload combinations has a significant impact on specimen life. Multiple overload-underload combinations result in a longer life than a single application of an overload-underload.

5. There is evidence of a cyclic dependent change in mean stress which may affect specimen life.

6. A hysteresis type of stress-strain analysis more closely represents complex loadings and specimen fatigue life than does a linear analysis method.

7. Spectrum fatigue tests conducted here are inconclusive as to effect of sustained load hold periods on time to crack initiation.

8. The loading events included in the test sequences do occur in service and may effect component and full scale tests, test spectra development, and interpretation of data.

TABLE 1- SUMMARY OF PHASE I EXPERIMENTAL RESULTS

TEST SEQUENCE DEFINITION

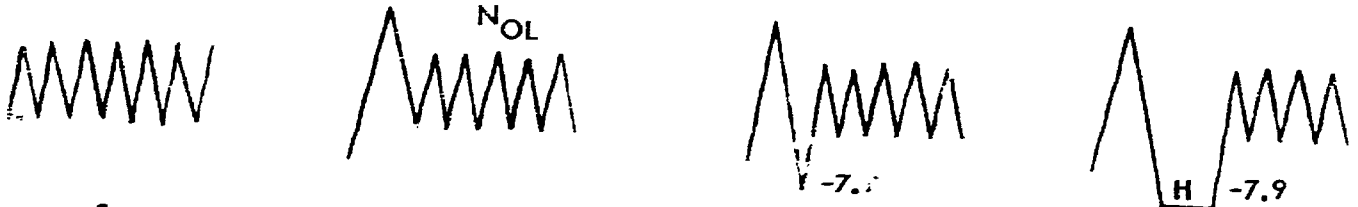

A B C D

SEQUENCE	HOLD PERIOD (H - HOURS)	CYCLES BETWEEN OVERLOADS (N_{OL} CYCLES x 10^{-3})	CRACK INITIATION (CYCLES x 10^{-3})
A	-	-	48
B	-	15	2,000 NF
B	-	1	1,000
C	-	15	715
C	-	1	309
D	24	15	141
D	1	15	337
D	24	1	101
D	1	1	154

NF = No Failure

TABLE 2 - TEMPERATURE AND UNDERLOAD EFFECTS FROM PHASE I TEST SEQUENCES

	SEQUENCE	TEST CONDITIONS	CRACK INITIATION (CYCLES x 10^{-3})
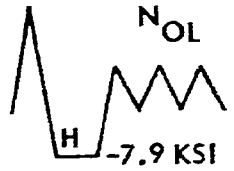	13	H = 24 HR. - N_{OL} = 15,000 CYCLES	141
	14	H = 1 HR. - N_{OL} = 15,000	337
	16	H = 24 HR. - N_{OL} = 1,000	101
	17	H = 1 HR. - N_{OL} = 1,000	154
Temperature = +160°F	20	H = 24 HR. - N_{OL} = 15,000	114
	21	H = 1 HR. - N_{OL} = 15,000	149
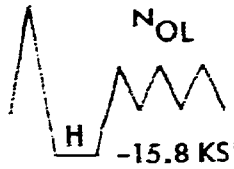	15	H = 24 HR. - N_{OL} = 15,000	114
	18	H = 24 HR. - N_{OL} = 1,000	130
	19	H = 1 HR. - N_{OL} = 1,000	60

H = Sustained Load Hold Period, Hours

N_{OL} = Cycles Between Overloads

TABLE 3 - SUMMARY OF CREEP FORMULATIONS

Equation	Investigator	Comments
$\dot{\epsilon} = k\sigma^p$ k, p are material constants	Bailey, Norton	1. Good for low stresses 2. Represents only secondary creep 3. Uniaxial stress 4. Tension 5. Small $\dot{\epsilon}$
$\dot{\epsilon} = k\rho^{\frac{\sigma}{\sigma_c}}$ k, σ_c are material constants	Ludwitt	1. Represents only secondary creep 2. Uniaxial stress 3. Is not zero for zero stress 4. Tension 5. Small $\dot{\epsilon}$
$\dot{\epsilon} = c(\rho^{\frac{\sigma}{\sigma_c}} - 1)$ c, σ_c are material constants	Soderberg	1. Represents only secondary creep 2. Uniaxial stress 3. Gives $\dot{\epsilon} = 0$ for $\sigma = 0$ 4. Tension 5. Small $\dot{\epsilon}$
$\dot{\epsilon} = D \sinh \frac{\sigma}{\sigma^+}$ D, σ^+ are material constants	Nadai, Eyring	1. Represents only secondary creep 2. Nearly linear for low stresses and nonlinear for higher stresses 3. Tension 4. Small $\dot{\epsilon}$ 5. Uniaxial stress
$\epsilon^c = k\sigma^p t^n$ k, p, n are material constants	Nutting, Hoff, Scott-Blair	1. Primary and most of secondary creep 2. n is almost always less than 0.5 3. Uniaxial stress

$\dot{\epsilon}$ - Creep Strain Rate
ϵ^c - Creep Strain
σ - Stress
t - Time

TABLE 3 - SUMMARY OF CREEP FORMULATIONS (Cont'd)

Equation	Investigator	Comments
$\dot{\epsilon}_{ij} = \frac{3}{2} c \sigma_e^{p-1} S_{ij}$ c, p material constants σ_e - equivalent stress S_{ij} - deviatoric stress	Odqvist	1. Multi-axial case 2. Secondary creep only
$\dot{\epsilon}_{ij} = \frac{3}{2} cn\sigma_e^{p-1} S_{ij} t^{n-1}$ c,p,n are material constants σ_e - equivalent stress S_{ij} - deviatoric stress	Lai, Findley, Onaran	1. Multi-axial case 2. Primary and most of secondary creep

TABLE 4 - LAYERED PLATE MODEL ANALYSIS RESULTS

INCREMENT 0 1st YIELD	ELEMENT NO. 1		ELEMENT NO. 2	
Gaussian Integration Point	$\sigma(10^4$ psi)	$\epsilon(10^{-3}$ in./in.)	$\sigma(10^4$ psi)	$\epsilon(10^{-3}$ in./in.)
1	7.674	7.452	7.675	7.452
2	7.458	7.452	7.458	7.452
3	5.663	5.814	5.663	5.814
4	5.699	5.814	5.701	5.814
5	7.674	7.452	7.675	7.451
6	7.459	7.452	7.461	7.451
7	5.663	5.814	5.662	5.813
8	5.700	5.814	5.704	5.813
Avg.	6.623	6.633	6.625	6.633

INCREMENT 6 CREEP 30 HR.	ELEMENT NO. 1		ELEMENT NO. 2	
Gaussian Integration Point	$\sigma(10^4$ psi)	$\epsilon(10^{-3}$ in./in.)	$\sigma(10^4$ psi)	$\epsilon(10^{-3}$ in./in.)
1	7.261	7.915	7.261	7.915
2	6.688	7.915	6.690	7.915
3	5.870	6.140	5.870	6.140
4	5.877	6.140	5.879	6.140
5	7.261	7.915	7.264	6.914
6	6.690	7.915	6.697	7.914
7	5.870	6.140	5.871	6.139
8	5.878	6.140	5.884	6.139
Avg.	6.424	7.028	6.427	7.027

TABLE 4 - LAYERED PLATE MODEL ANALYSIS RESULTS (Cont'd)

INCREMENT 0 1st YIELD	ELEMENT NO. 3		ELEMENT NO. 4	
Gaussian Integration Point	$\sigma(10^4$ psi)	$\epsilon(10^{-3}$ in./in.)	$\sigma(10^4$ psi)	$\epsilon(10^{-3}$ in./in.)
1	4.965	4.741	4.965	4.741
2	5.102	4.741	5.102	4.741
3	3.349	3.448	3.349	3.448
4	3.409	3.448	3.409	3.448
5	4.965	4.741	4.965	4.741
6	5.102	4.741	5.102	4.741
7	3.349	3.448	3.349	3.448
8	3.409	3.448	3.410	3.448
Avg.	4.206	4.095	4.206	4.095

INCREMENT 6 CREEP 30 HR.	ELEMENT NO. 3		ELEMENT NO. 4	
Gaussian Integration Point	$\sigma(10^4$ psi)	$\epsilon(10^{-3}$ in./in.)	$\sigma(10^4$ psi)	$\epsilon(10^{-3}$ in./in.)
1	5.233	4.977	5.233	4.976
2	5.400	4.977	5.401	4.976
3	3.454	3.573	3.454	3.573
4	3.521	3.573	3.522	3.573
5	5.233	4.977	5.233	4.976
6	5.401	4.977	5.402	4.976
7	3.454	3.573	3.455	3.572
8	3.522	3.573	3.523	3.572
Avg.	4.402	4.275	4.403	4.274

TABLE 5 - SIMPLE BAR CREEP TESTS

TEST	INITIAL STRAIN	APPROX. FIRST LEVEL CREEP STRESS	APPROX. FIRST LEVEL CREEP STRAIN	APPROX. SECOND LEVEL STRESS/STRAIN	COMMENTS
1	0.016	-50	-	-66	From MARC Analysis, Element No. 8 at -7.9 ksi
2	0.016	-66	-	-50	Typical for notch stress analysis from Phase I at -15.8 ksi
3	0.016	-40	-	-66	Additional stress levels to solve for creep constants
4	0.016	-35	-	-50	
5	0.016	-	+0.0025	- 0.003	Repeat No. 1 with strain control
6	0.016	-	-0.0040	- 0.001	Repeat No. 2 with strain control

NOTES:
1. Tests 1 - 4 were run under load control and creep strain was measured during hold periods.
2. Tests 5 and 6 were run under strain control and load relaxation was measured during hold period.
3. First and Second Level creep defined in sketch below.

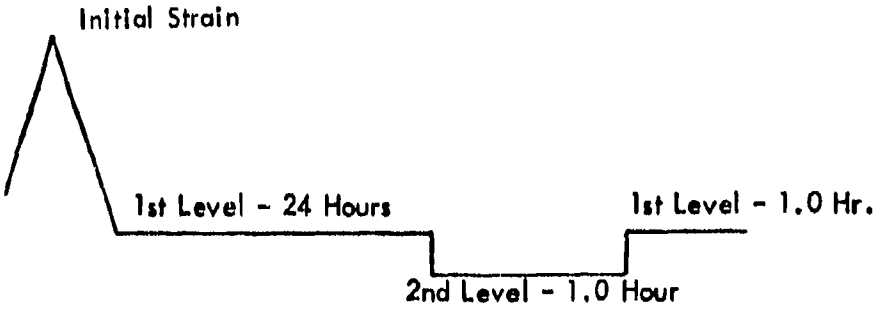

TABLE 6 - SIMPLE BAR CREEP/STRESS RELAXATION DATA

SPECIMEN NUMBER	HOLD PERIOD DEFINITION		MEASURED CREEP STRAIN OR STRESS RELAXATION
	Applied Stress or Strain	Time	
1A	-50 ksi -66 -50	24 hrs 1.0 1.0	1100 μin/in 540 0
1B	-50 ksi -66 -50	24 hrs 1.0 1.0	1035 μin/in 850 0
2A	-66 ksi -50 -66	24 hrs 1.0 1.0	2300 μin/in 0 0
2B	-66 ksi -50 -66	24 hrs 1.0 1.0	2015 μin/in 0 0
3A	-40 ksi -66 -40	24 hrs 1.0 1.0	600 μin/in 1550 0
3B	-40 ksi -66 -40	24 hrs 1.0 1.0	650 μin/in 1350 80
4A	-35 ksi -50 -35	24 hrs 1.0 1.0	300 μin/in 100 0
4B	-35 ksi -50 -35	24 hrs 1.0 1.0	380 μin/in 85 0
5A	0.0025 in/in -0.0030 0.0025	24 hrs 1.0 1.0	6.10 ksi 7.60 1.10
5B	0.0025 in/in -0.0030 0.0025	24 hrs 1.0 1.0	5.20 ksi 6.28 0.68
6A	-0.0040 in/in -0.0010 -0.0040	24 hrs 1.0 1.0	10.70 ksi 0.50 0.50
6B	-0.0040 in/in -0.0010 -0.0040	24 hrs 1.0 1.0	10.50 ksi 0.64 0

TABLE 7 - SAMPLE OF TABULATED STRAIN DATA FOR SIMPLIFIED STRESS CONCENTRATION SPECIMEN TESTS

THREE BAR TEST
PASS NO. 1
SEQUENCE NO. 1--REPEAT

RAMP THRU PEAK STRESS TO START OF 24 HR. HOLD

	MTS EXTENSOMETERS		STRAIN GAGES OUTER BAR	
STRESS, KSI	OUTER BAR STRAIN, MICRO. IN/IN	CENTER BAR STRAIN, MICRO. IN/IN	FRONT STRAIN, MICRO. IN/IN	BACK STRAIN, MICRO. IN/IN
2.58	167	353	147	161
4.75	349	733	308	328
6.93	506	1086	469	495
9.15	688	1484	627	668
11.38	841	1863	786	830
13.50	998	2262	947	1000
15.73	1166	2650	1111	1170
17.95	1299	3039	1275	1337
20.13	1471	3437	1436	1504
22.30	1619	3817	1597	1671
24.53	1782	4234	1759	1838
26.70	1935	4641	1917	2002
28.98	2097	5066	2081	2172
31.10	2240	5473	2251	2333
33.38	2403	5907	2406	2503
35.55	2551	6332	2571	2673
37.78	2699	6766	2738	2840
39.90	2861	7237	2908	3013
42.13	3014	7861	3092	3198
44.30	3234	9082	3321	3435
46.48	3468	10828	3576	3696
48.65	3707	12809	3840	3960
50.72	3941	15224	4098	4221
50.87	3955	15342	4109	4235
51.03	3960	15451	4127	4250
51.08	3965	15550	4136	4259
51.23	3974	15668	4150	4274
51.28	3994	15785	4165	4288
51.43	4013	15903	4177	4303
0.00	0	0	0	0
46.58	3659	15170	3810	3928
32.16	2637	12411	2708	2808
17.70	1648	9643	1630	1706
3.29	611	6875	577	616
-11.13	-468	3953	-466	-498
-20.08	-1170	1701	-1126	-1246

TABLE 7 (Continued)

24 HOUR HOLD

	EXTENSOMETERS		STRAIN GAGES			
STRESS, KSI	OUTER STRAIN, MICRO. IN/IN	CENTER STRAIN, MICRO. IN/IN	FRONT STRAIN, MICRO. IN/IN	REAR STRAIN, MICRO. IN/IN	TIME INTERVAL	ELAPSED TIME
-20.18	-1175	1601	-1146	-1257	0.2 SEC.	0.2 SEC.
-20.18	-1185	1565	-1149	-1260	0.2 SEC.	0.4 SEC.
-20.18	-1194	1538	-1152	-1263	0.2 SEC.	0.6 SEC.
-20.18	-1199	1520	-1155	-1266	0.2 SEC.	0.8 SEC.
-20.18	-1194	1511	-1152	-1266	0.2 SEC.	1.0 SEC.
-20.18	-1194	1511	-1152	-1263	0.2 SEC.	1.2 SEC.
-20.18	-1218	1330	-1172	-1284	5.0 SEC.	55.0 SEC.
-20.18	-1223	1312	-1172	-1284	5.0 SEC.	60.0 SEC.
-20.18	-1218	1321	-1170	-1284	5.0 SEC.	65.0 SEC.
-20.18	-1223	1312	-1172	-1284	5.0 SEC.	70.0 SEC.
-20.18	-1218	1312	-1170	-1284	5.0 SEC.	75.0 SEC.
-20.18	-1223	1303	-1172	-1287	5.0 SEC.	80.0 SEC.
-20.18	-1218	1312	-1172	-1284	5.0 SEC.	85.0 SEC.
-20.18	-1232	1212	-1181	-1298	5.0 MIN.	25.0 MIN.
-20.18	-1232	1203	-1181	-1298	5.0 MIN.	30.0 MIN.
-20.23	-1237	1194	-1181	-1301	5.0 MIN.	35.0 MIN.
-20.23	-1232	1203	-1181	-1301	5.0 MIN.	40.0 MIN.
-20.18	-1237	1194	-1181	-1301	5.0 MIN.	45.0 MIN.
-20.33	-1223	1122	-1196	-1316	60.0 MIN.	19.0 HRS
-20.33	-1223	1122	-1199	-1316	60.0 MIN.	20.0 HRS
-20.33	-1242	1158	-1199	-1319	60.0 MIN.	21.0 HRS
-20.28	-1223	1158	-1199	-1316	60.0 MIN.	22.0 HRS
-20.28	-1242	1086	-1199	-1319	60.0 MIN.	23.0 HRS

TABLE 8 - PHASE I AND PHASE II SUPER-SCALE TEST SPECIMEN COMPARISON

Sequence Number	Test Conditions	Cycles To Failure
I-1	Constant Amplitude Baseline $F_m = 15$, $F_v = \pm 10$	47,647
Group 1		
I-6	+47.3, N_{OL} = 15,000, CA	1,977,450 (NF)
I-8	+47.3, -7.9, N_{OL} = 15,000, CA	712,000
II-6	+47.3, -4.0, N_{OL} = 15,000, CA	1,269,770
II-9	+47.3, -7.9, CA	286,838
II-10	+47.3, -4.0, CA	131,956
Group 2		
I-13	+47.3, 24 Hr. @ -7.9, N_{OL} = 15,000, CA	141,329
II-7	+47.3, 24 Hr. @ -7.9, N_{OL} = 30,000, CA	88,000
II-5	+47.3, 24 Hr. @ -4.0, N_{OL} = 15,000, CA	1,375,000
II-8	+47.3, 24 Hr. @ -4.0, N_{OL} = 30,000, CA	581,557

NOTE: Roman numerals refer to Phase I or II in the sequence identification.

TABLE 9 - CREEP STRAINS FROM SUPER-SCALE SEQUENCE TESTS

Sequence Number	Maximum Measured Strain Change (μ in/in)				
	Transducer	S.G. No. 1	S.G. No. 2	S.G. No. 3	S.G. No. 4
1	+131	-209	-258	-149	-177
2	-248	-352	-305	-229	-213
3	-203	-200	-190	-120	-150
4	-509	-122	-125	- 86	- 86
5	-187	-140	-160	- 80	- 80
7	-300	-200	-200	-130	-100
8	-350	-190	-270	-130	-110

TABLE 10- SPECTRUM FATIGUE TEST RESULTS

SPECTRUM 1	SPECTRUM 2	SPECTRUM 3
30,710 Flights	29,861 Flights	8,458 Flights
29,858	31,932	8,245
30,218	30,020	8,233
Average: 30,262 Flights	30,604 Flights	8,312 Flights

TABLE 11 - FINITE-ELEMENT CREEP ANALYSIS
SUPER-SCALE SPECIMEN, -7.9 KSI COMPRESSION

Time (Hours)	Gaussian Integration Point	Element 8	
		σ_r (ksi)	ϵ^c (10^{-4} in/in)
Time = 0	1	-47.48	0
	2	-41.34	0
	3	-47.85	0
	4	-41.78	0
	Avg.	-44.61	
Time = 0.5	1	-46.47	- 9.104
	2	-40.59	- 7.029
	3	-46.82	- 9.147
	4	-41.01	- 7.064
	Avg.	-43.72	- 8.086
Time = 3.0	1	-45.88	- 9.989
	2	-40.14	- 7.742
	3	-46.22	-10.04
	4	-40.56	- 7.781
	Avg.	-43.20	- 8.888
Time = 13.7	1	-45.34	-10.80
	2	-39.73	- 8.398
	3	-45.68	-10.85
	4	-40.14	- 8.442
	Avg.	-42.72	- 9.622
Time = 24.5	1	-45.12	-11.13
	2	-39.57	- 8.664
	3	-45.46	-11.18
	4	-39.97	- 8.708
	Avg.	-42.53	- 9.921

TABLE 12 - COMPARISON OF EXPERIMENTAL DATA WITH ANALYTICAL LIFE PREDICTIONS FOR SUPER-SCALE TEST SPECIMENS

TEST SEQUENCE DEFINITION (1)	TEST LIFE (CYCLES)	ANALYTICAL LIFE $\Sigma \frac{n}{N}$	ANALYTICAL LIFE HYSTERESIS
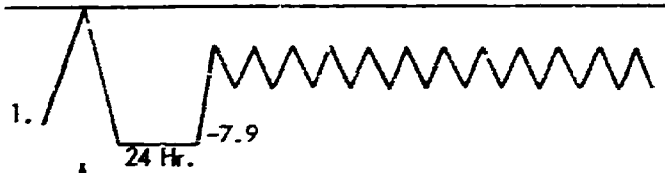	80,018	97,955	562,000
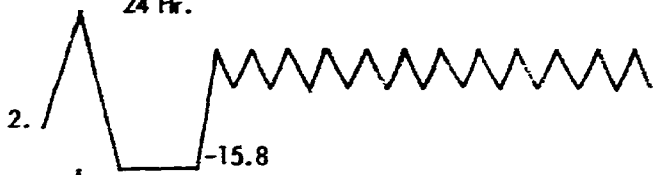	49,567	97,920	334,400
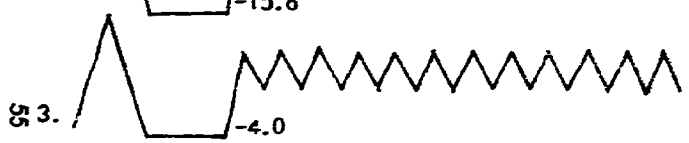	44,277	97,972	695,000
	135,801	97,987	841,300
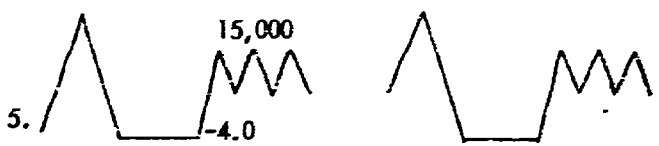	1,375,000	97,604	653,200
	1,269,770	97,604	712,000

(1) See Also Figure 58

TABLE 12 - COMPARISON OF EXPERIMENTAL DATA WITH ANALYTICAL LIFE PREDICTIONS FOR SUPER-SCALE TEST SPECIMENS (Continued)

TEST SEQUENCE DEFINITION [1]	TEST LIFE (CYCLES)	ANALYTICAL LIFE $\Sigma \frac{n}{N}$	ANALYTICAL LIFE HYSTERESIS
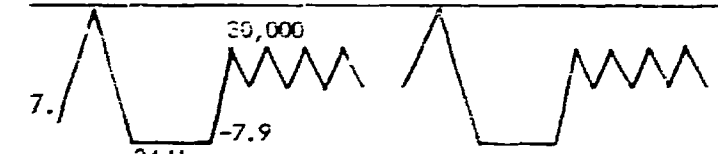	214,546 88,000	97,765	532,000
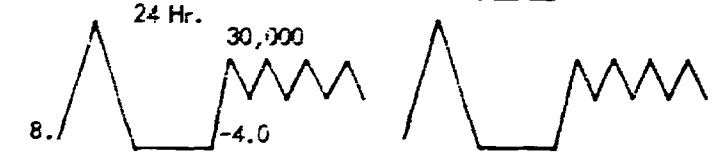	581,557	97,821	666,700
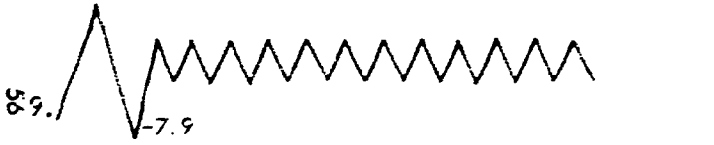	286,838	97,955	950,500
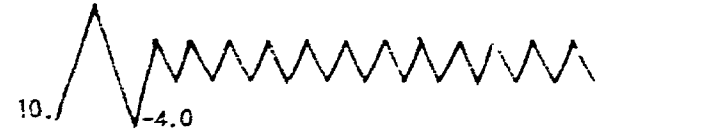	131,956	97,927	771,000

(1) See Also Figure 58

TABLE 13 - ANALYSIS AND EXPERIMENTAL RESULTS FOR TEST SEQUENCES INCLUDING OVERLOADS AND UNDERLOADS

TEST SEQUENCE DEFINITION	TEST LIFE (CYCLES)	ANALYTICAL LIFE $\Sigma \frac{n}{N}$	ANALYTICAL LIFE HYSTERESIS
1. 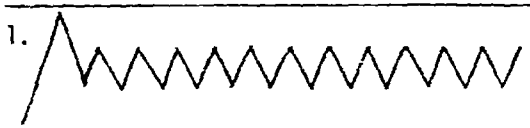	910,000 (1)	~ 97,000	978,000
2. 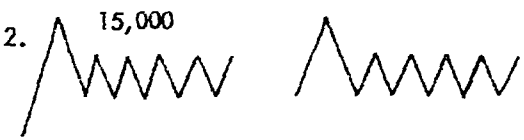	1.98×10^6 N.F.		950,500
3. 	286,800		646,300
4. 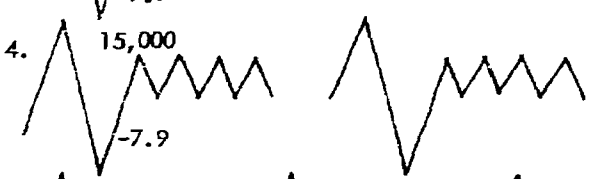	715,000		615,800
5. 	308,000		364,400

(1) Test data from Reference 4.

TABLE 13 - ANALYSIS AND EXPERIMENTAL RESULTS FOR TEST SEQUENCES INCLUDING OVERLOADS AND UNDERLOADS (Continued)

TEST SEQUENCE DEFINITION	TEST LIFE (CYCLES)	ANALYTICAL LIFE $\Sigma \frac{n}{N}$	ANALYTICAL LIFE HYSTERESIS
6. 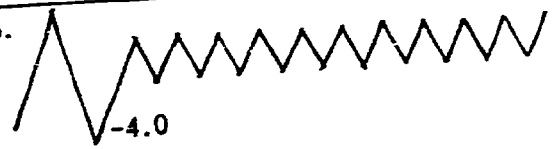	132,000	~97,000	771,000
7. 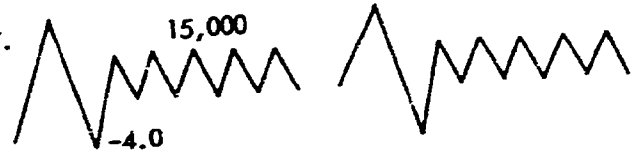	1,269,770		712,200

TABLE 14 - EXPERIMENTAL AND ANALYTICAL LIFE COMPARISON FOR SPECTRUM FATIGUE TESTS

TEST (1) SPECTRUM	TEST LIFE (2) (FLIGHTS)	ANALYTICAL LIFE LINEAR DAMAGE $\Sigma\frac{n}{N}$	ANALYTICAL LIFE HYSTERESIS ANALYSIS
1	30,262	15,460	43,282
2	30,604	15,460	46,106
3	8,312	15,920	8,681

(1) Spectrum 1: 50 [Flt. C + 150 (2 Flt. A + Flt. B)] + N (2 Flt. A + Flt. B)

Spectrum 2: 50 [(Flt. C + Hold Period) + 150 (2 Flt. A + Flt. B)] + N (2 Flt. A + Flt. B)

Spectrum 3: 50 [Flt. B + 150 (2 Flt. A + Flt. B)] + N (2 Flt. A + Flt. B)

(2) Average of Three Tests

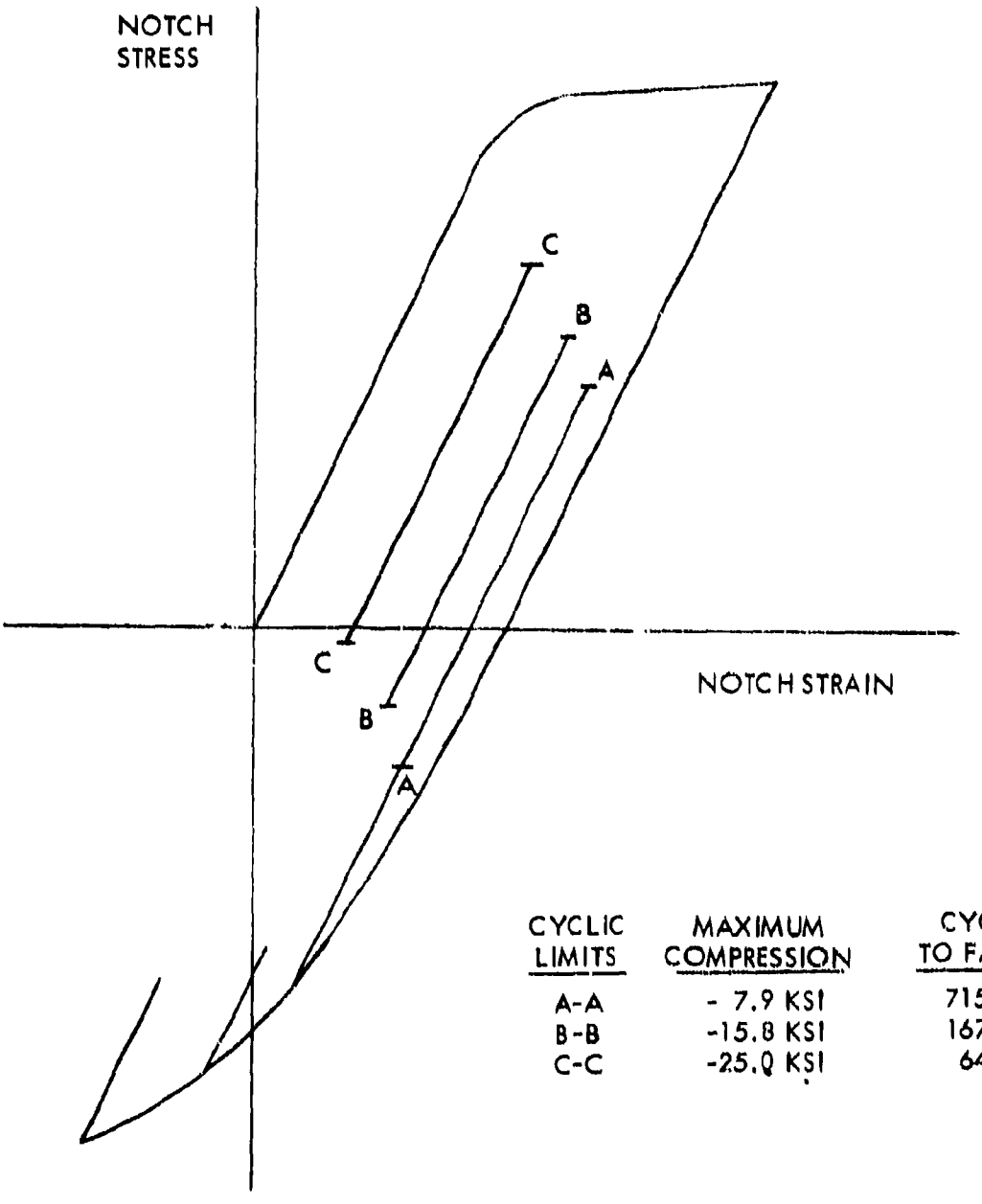

CYCLIC LIMITS	MAXIMUM COMPRESSION	CYCLES TO FAILURE
A-A	- 7.9 KSI	715,000
B-B	-15.8 KSI	167,000
C-C	-25.0 KSI	64,000

Figure 1. Underload Effects on Cycles to Crack Initiation

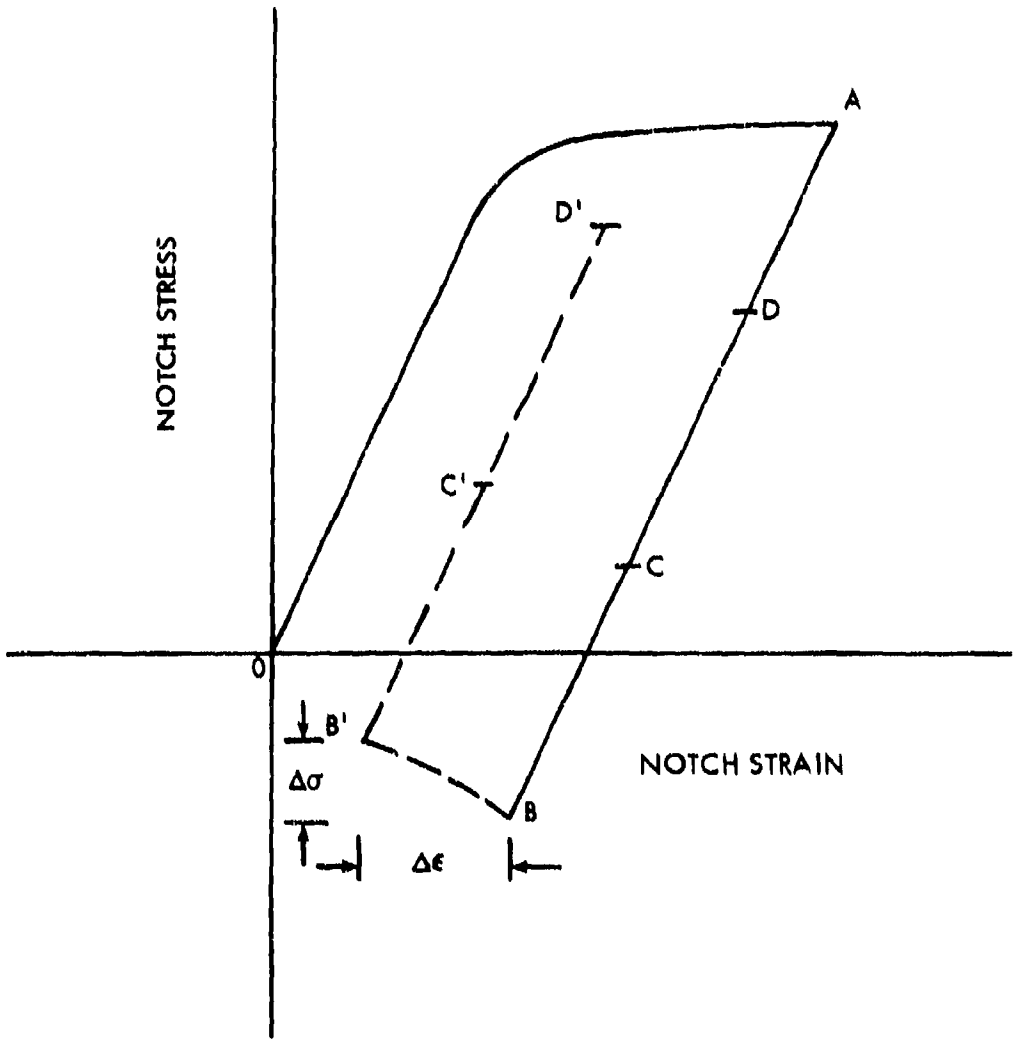

Figure 2. Hypothesis of Complexity of Time Dependent Stress-Strain Change

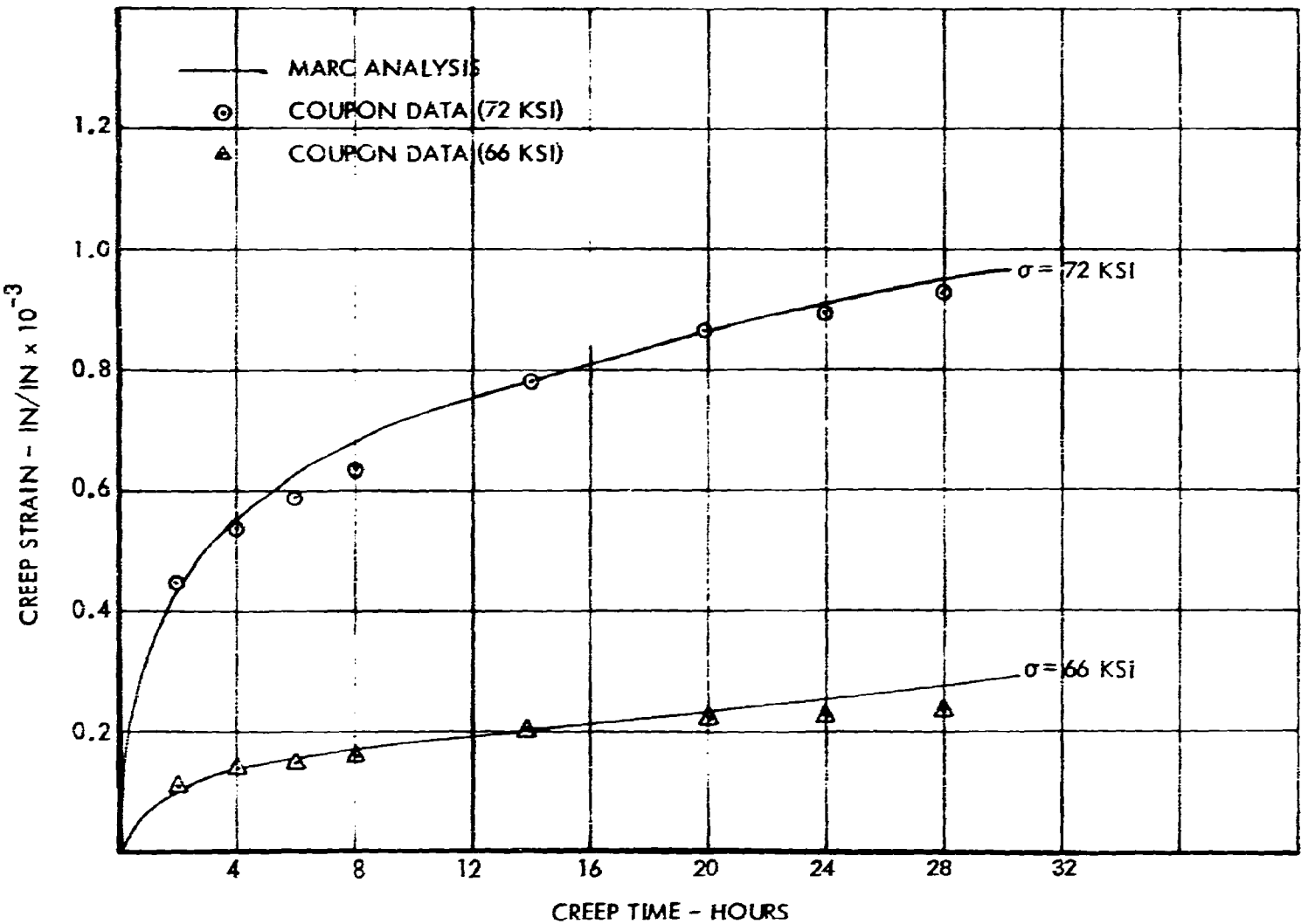

Figure 3. Comparative Creep Data - Finite Element Simulation Versus Coupon Test Data

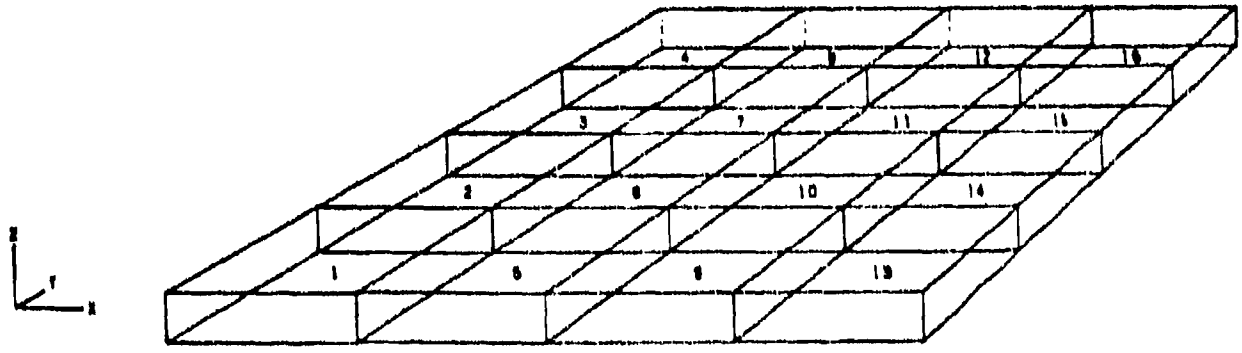

Figure 4. Simple Plate Finite Element Model

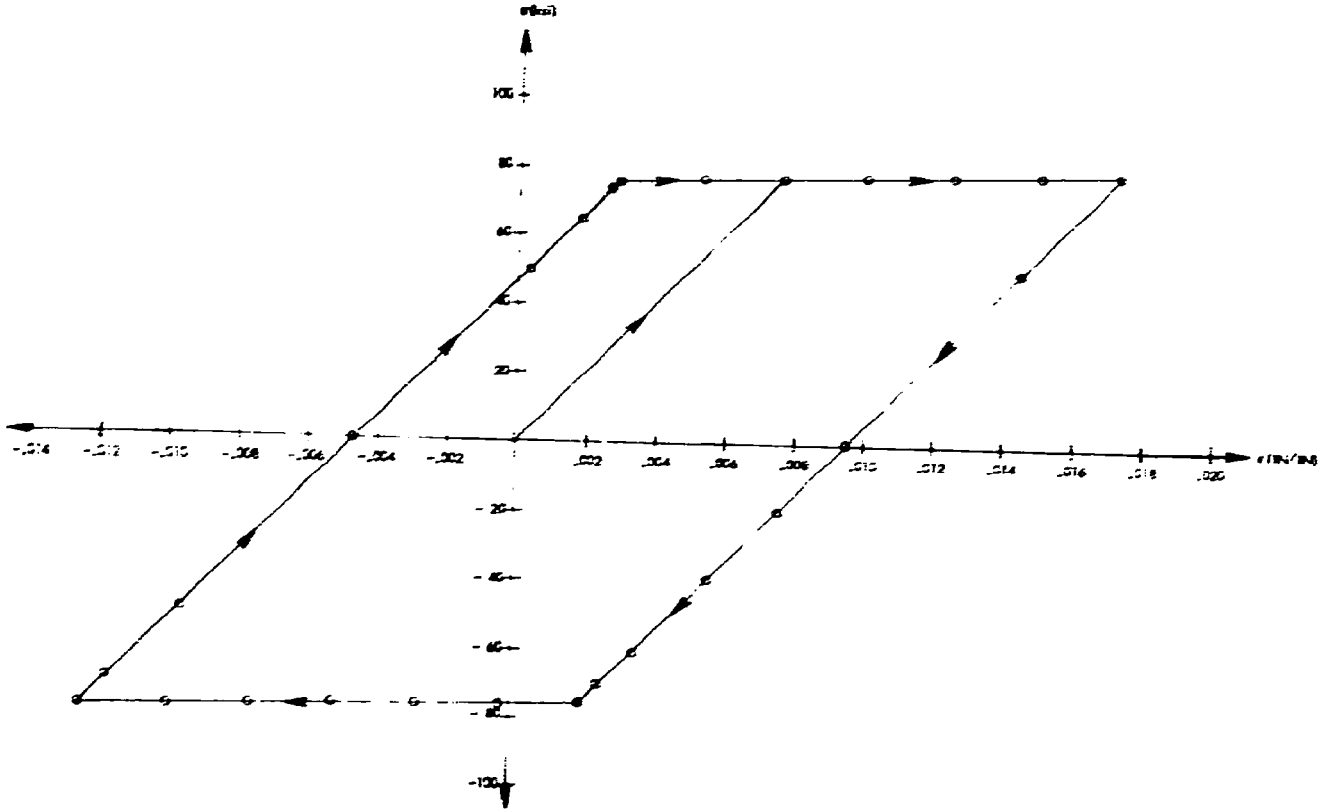

Figure 5. MARC Bilinear Stress-Strain Representation

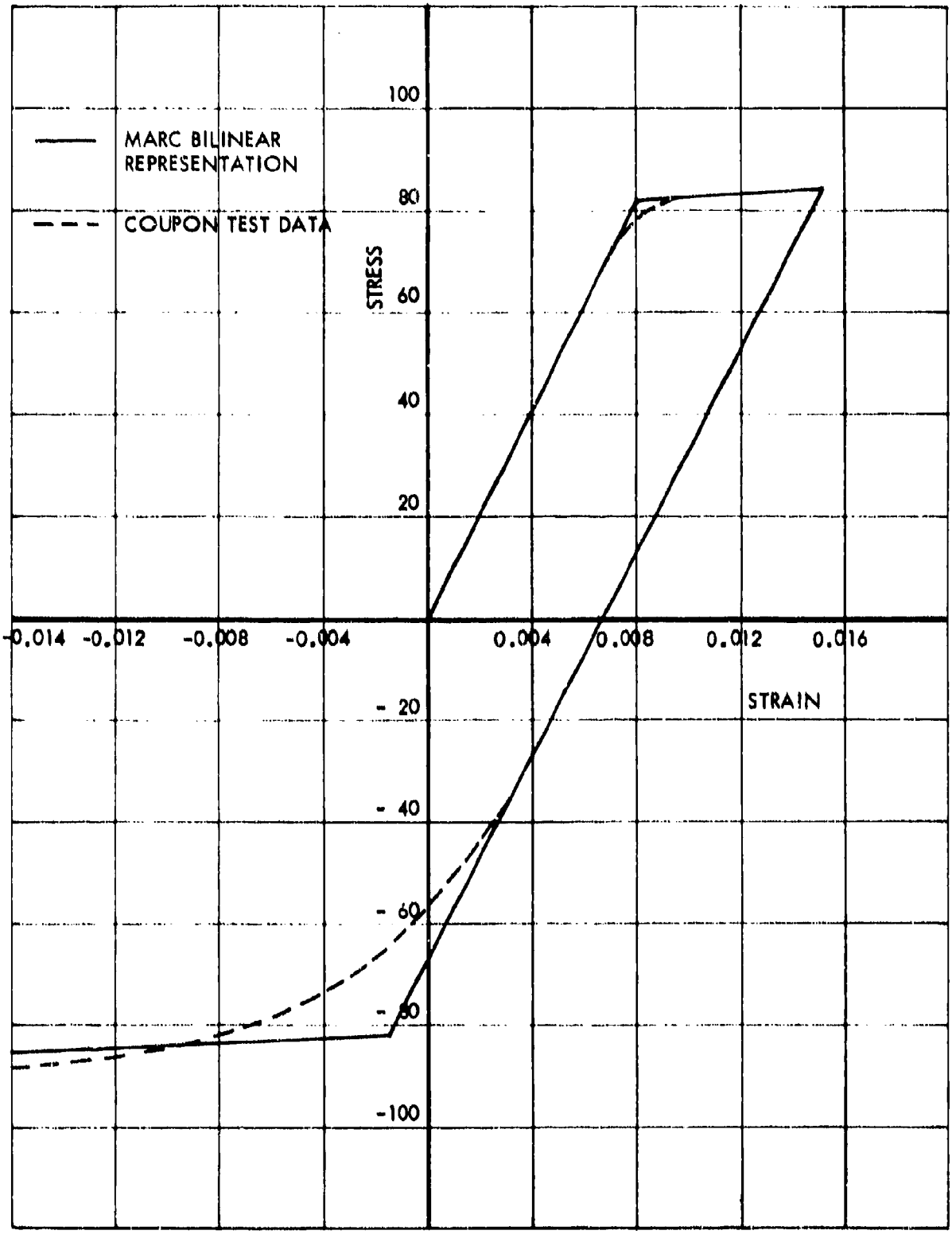

Figure 6. Comparison of Coupon Test and MARC Representation of Stress-Strain Data

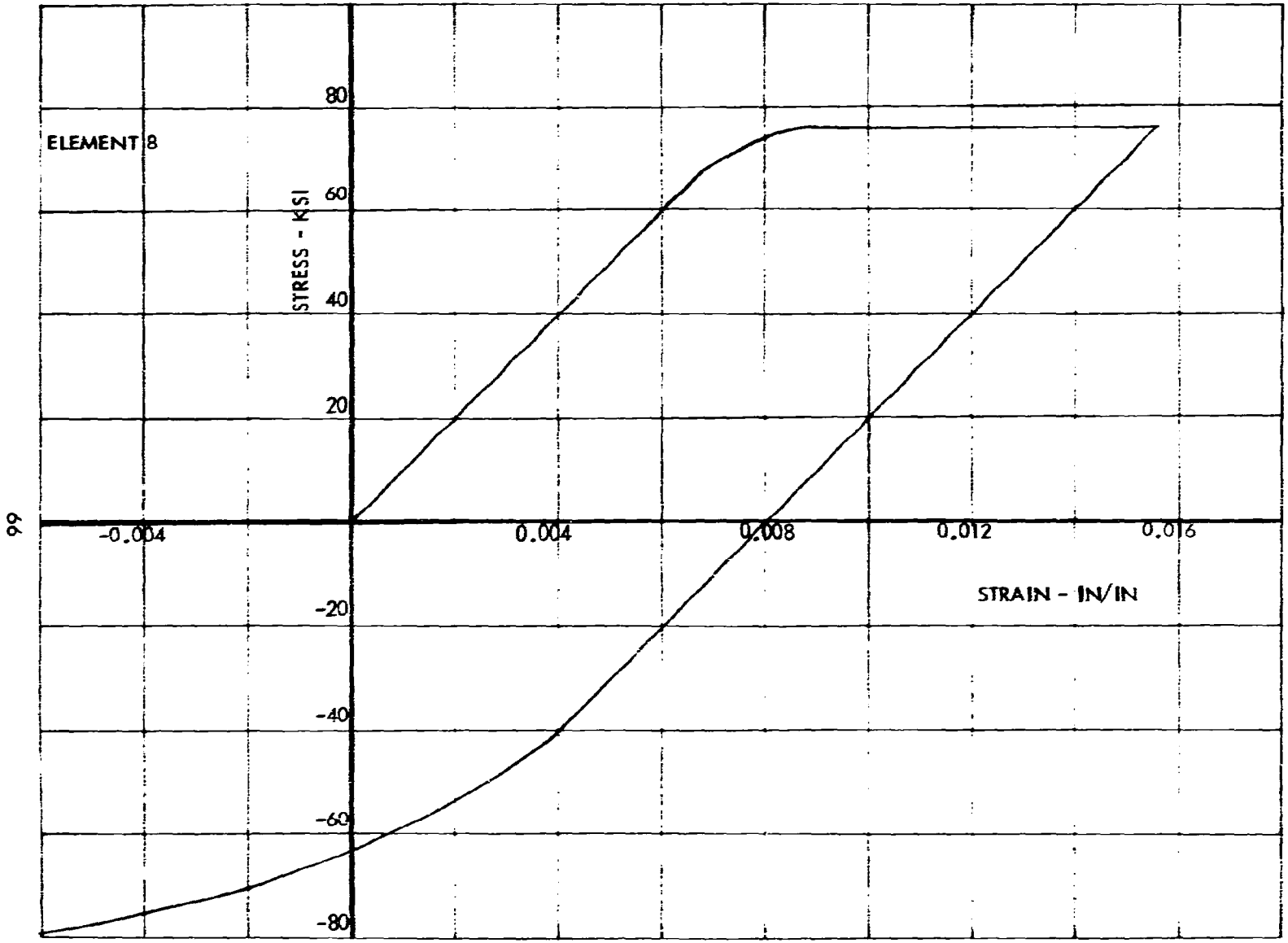

Figure 7. Tension Compression Stress-Strain Curve
Element No. 8

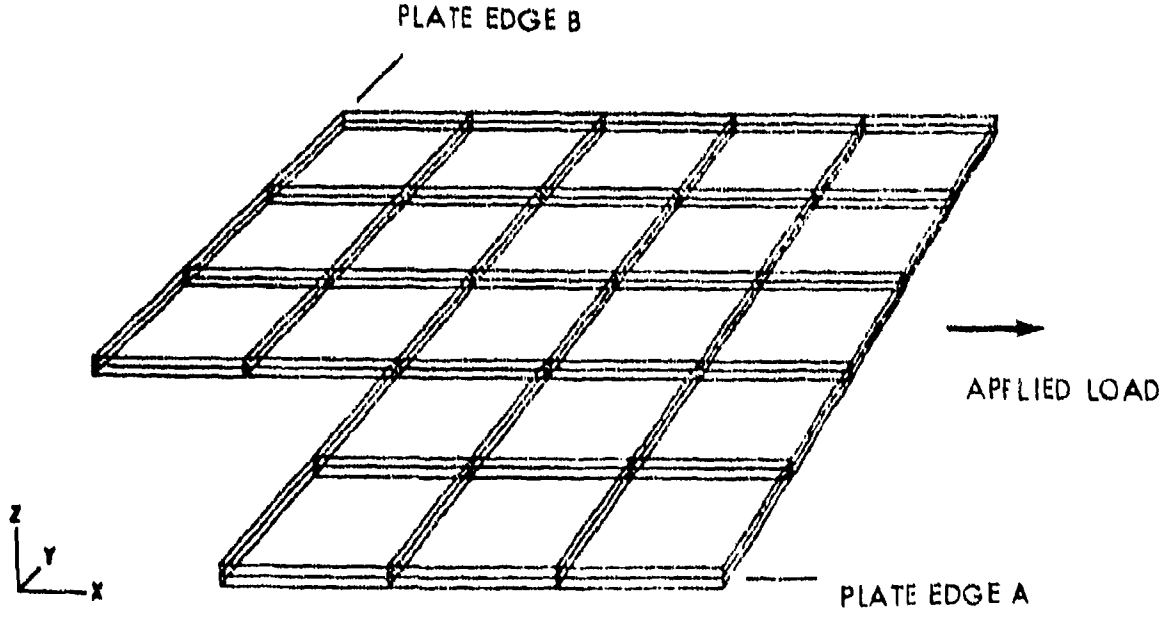

Figure 8. Layered Finite Element Model

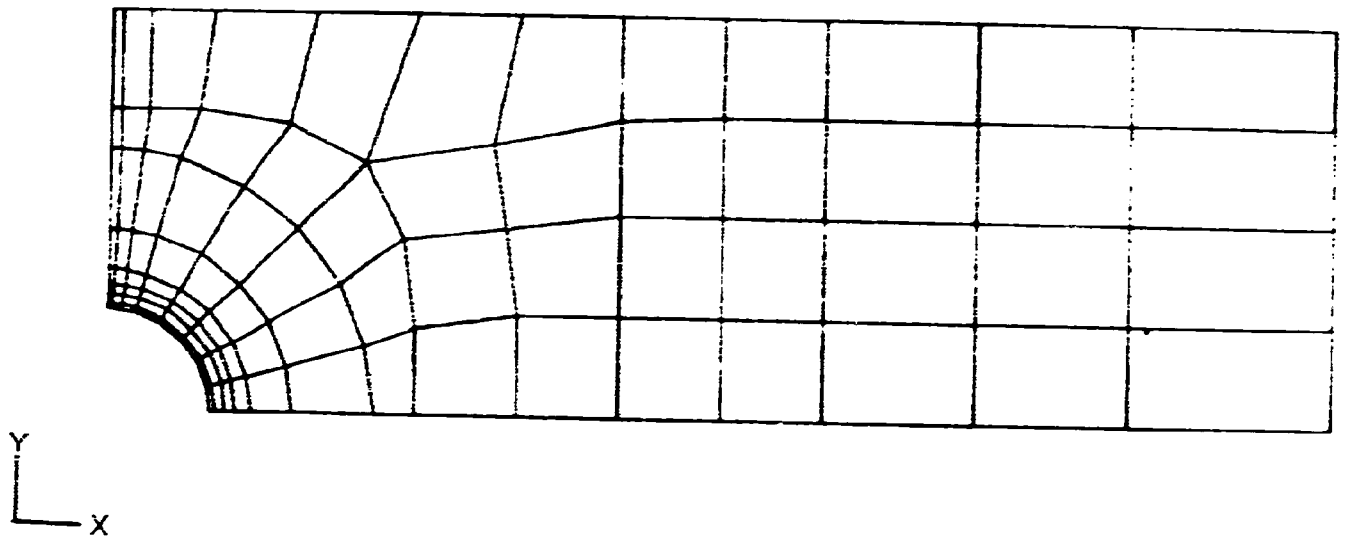

Figure 9. Super-Scale Finite Element Model

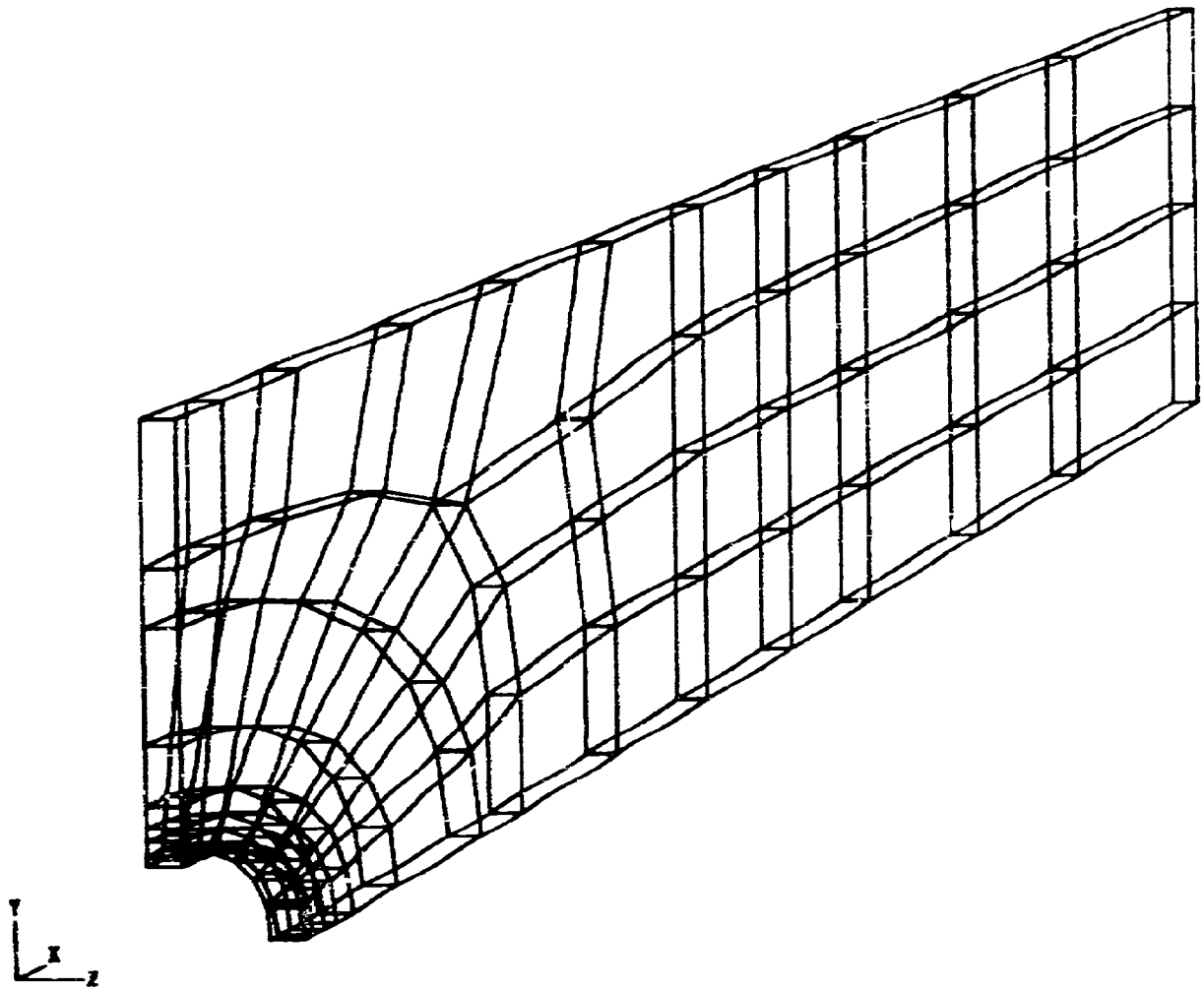

Figure 10. Three-Dimensional Super-Scale Model

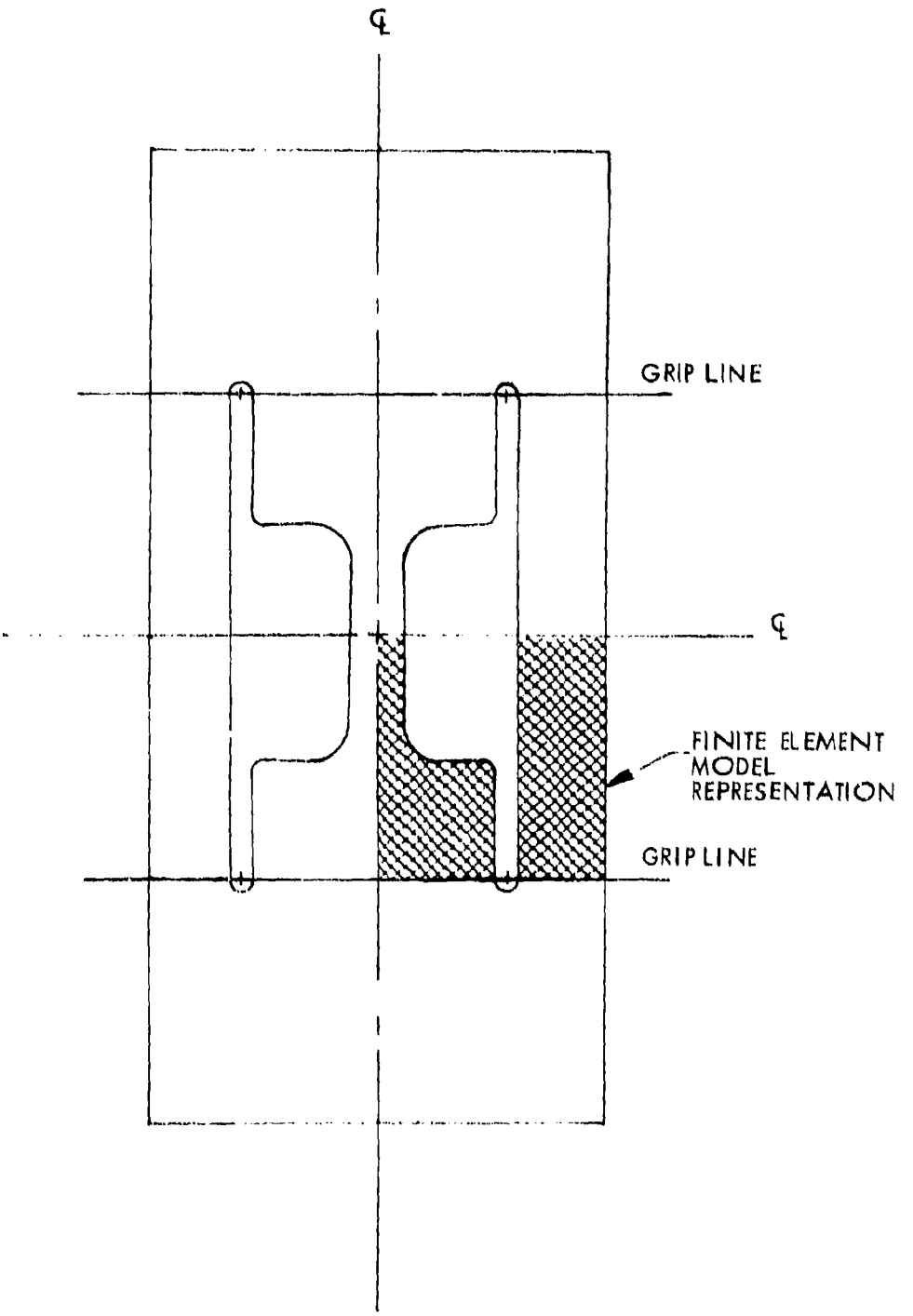

Figure 11. Area of Simplified Stress Concentration Specimen To Be Represented by Finite Element Simulation

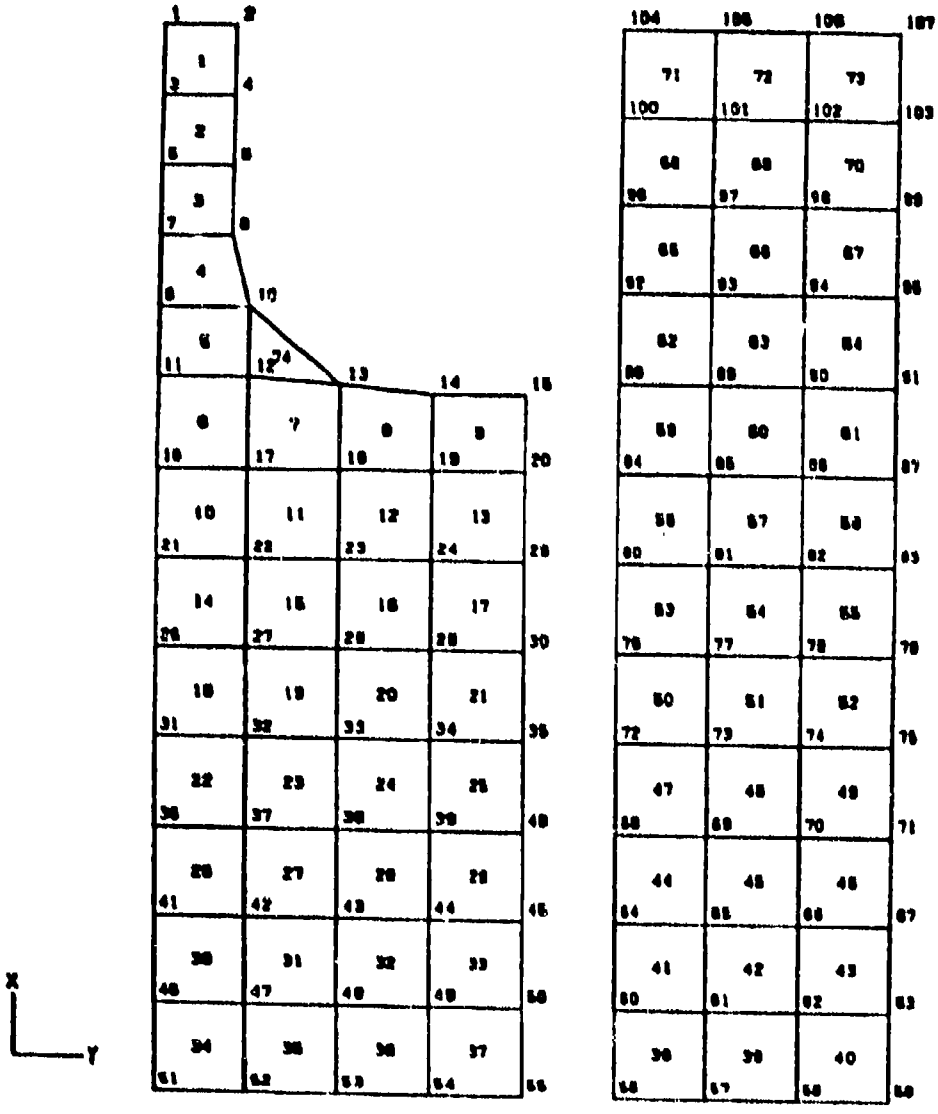

Figure 12. Finite-Element Model for Simplified Stress Concentration Specimen

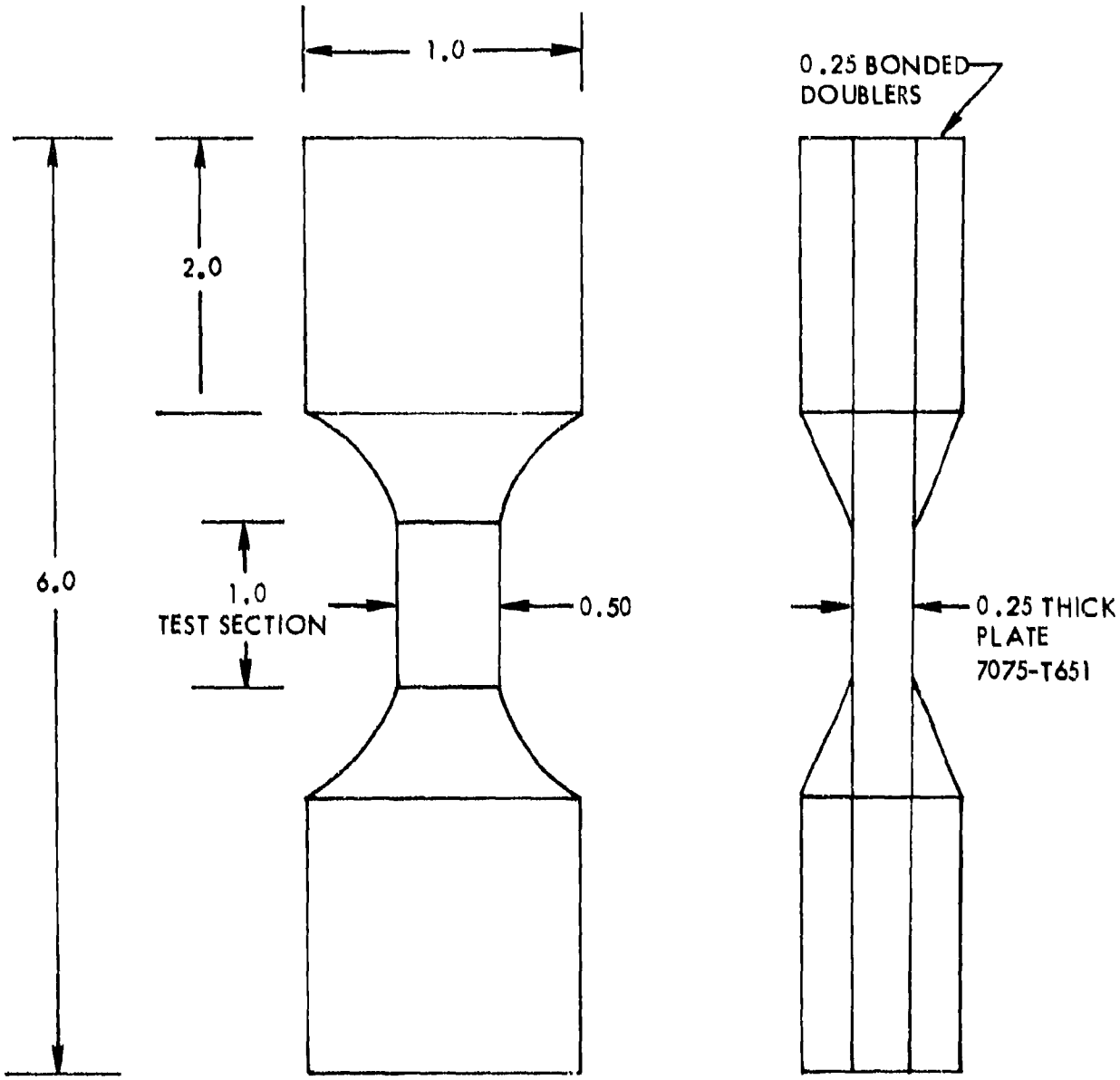

Figure 13. Coupon Specimen for Creep and Stress Relaxation Tests

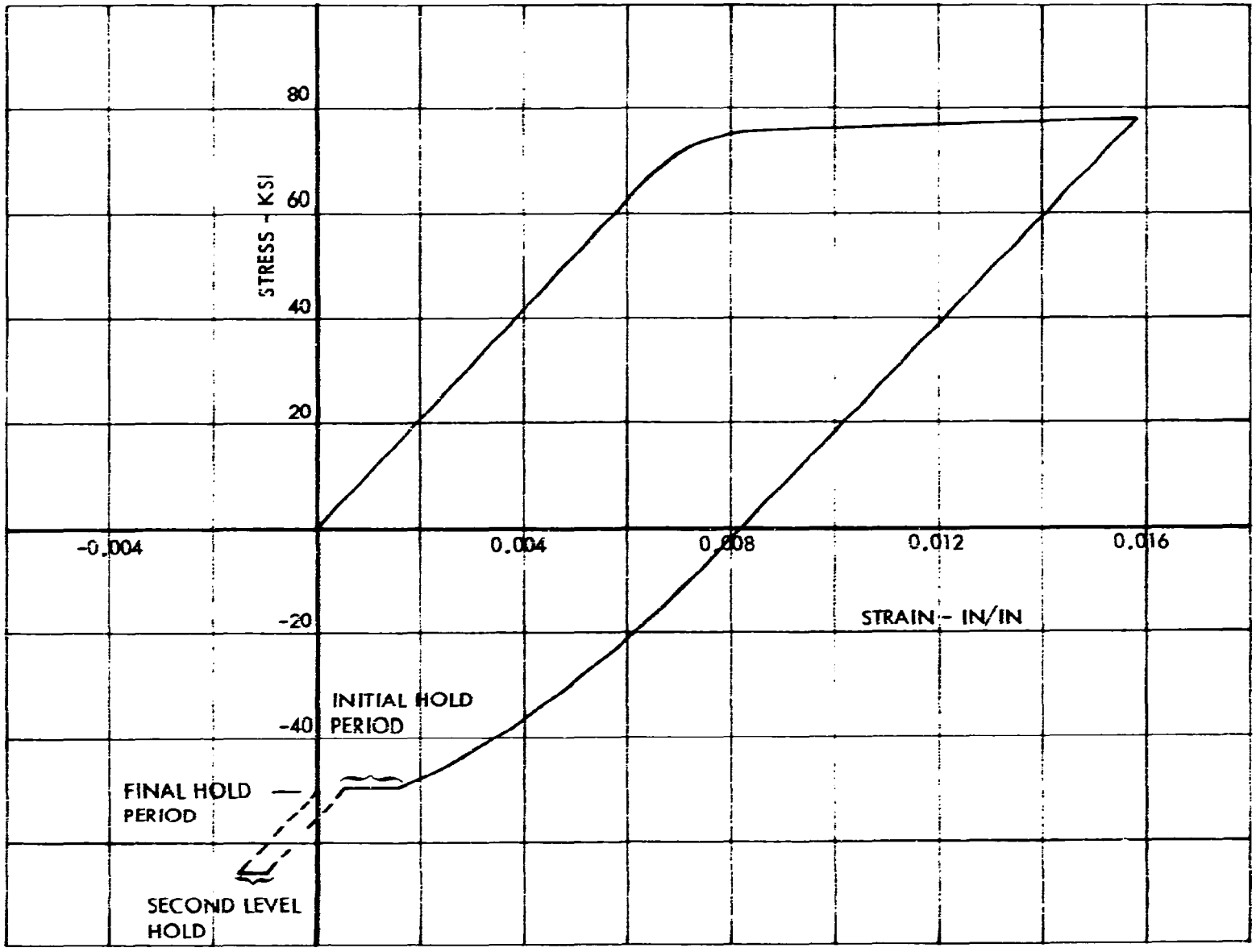

Figure 14. Stress-Strain Curve, Coupon Specimen 1A Load Control Test

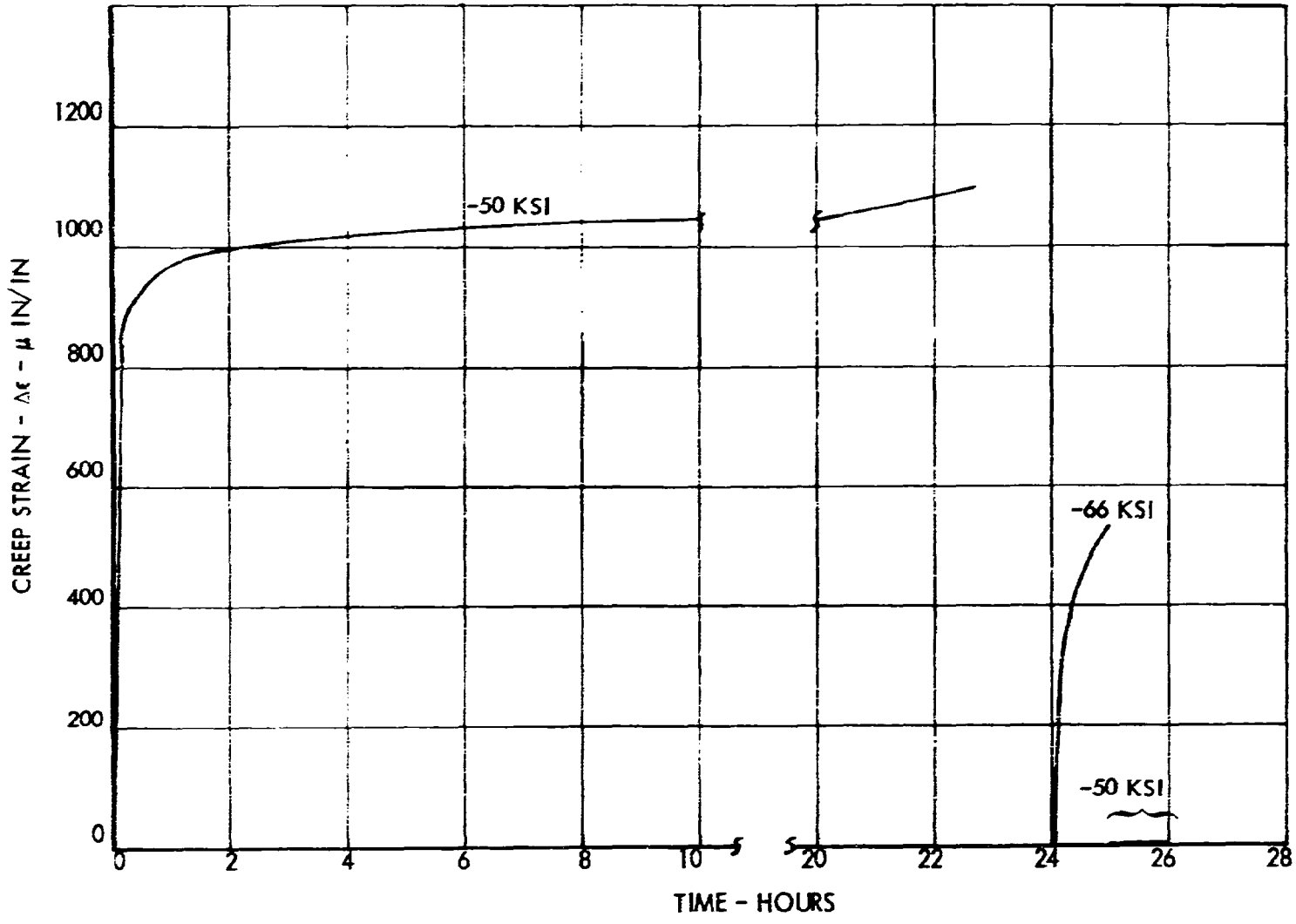

Figure 15. Coupon 1A Creep Strain

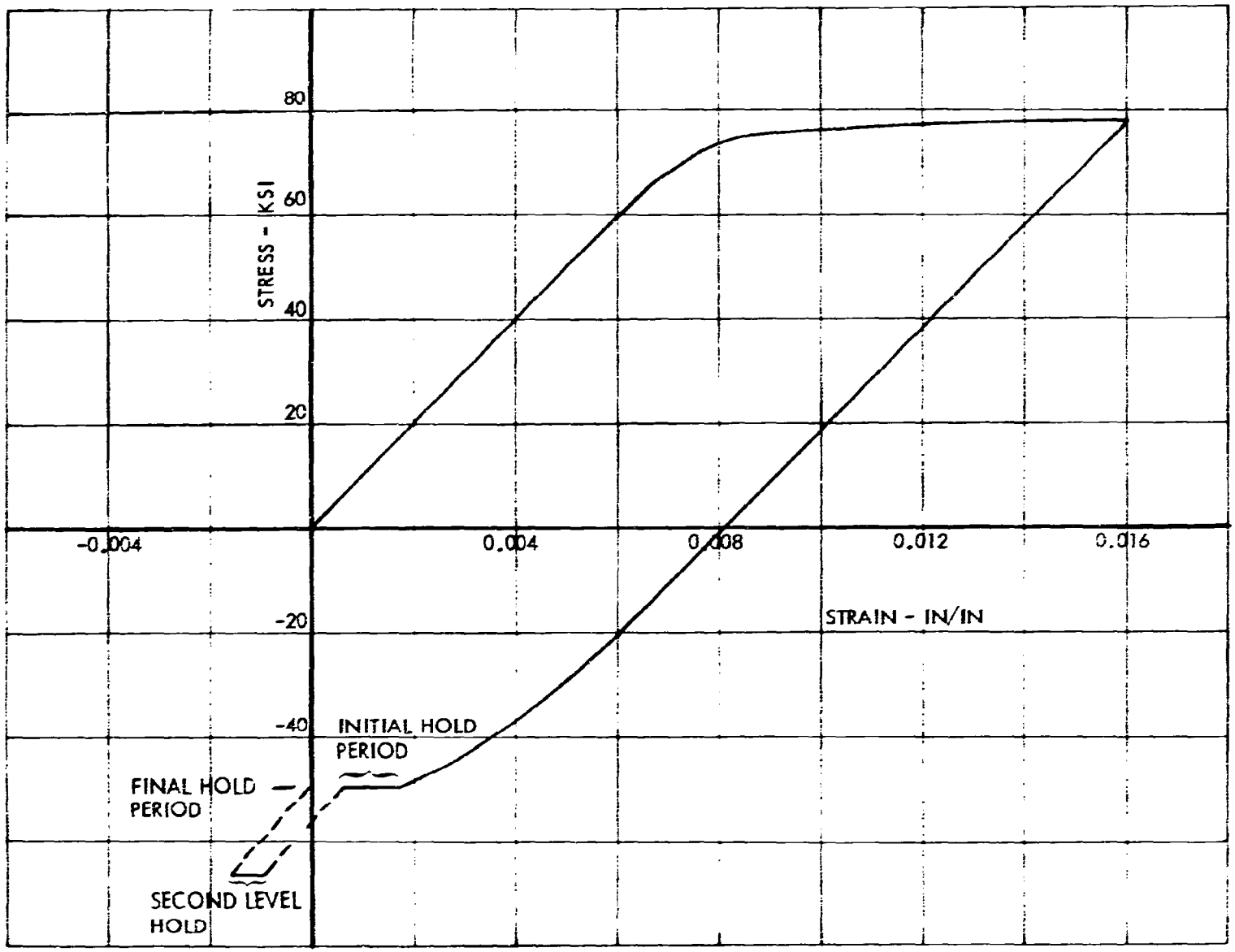

Figure 16. Stress-Strain Curve, Coupon Specimen 1B
Load Control Test

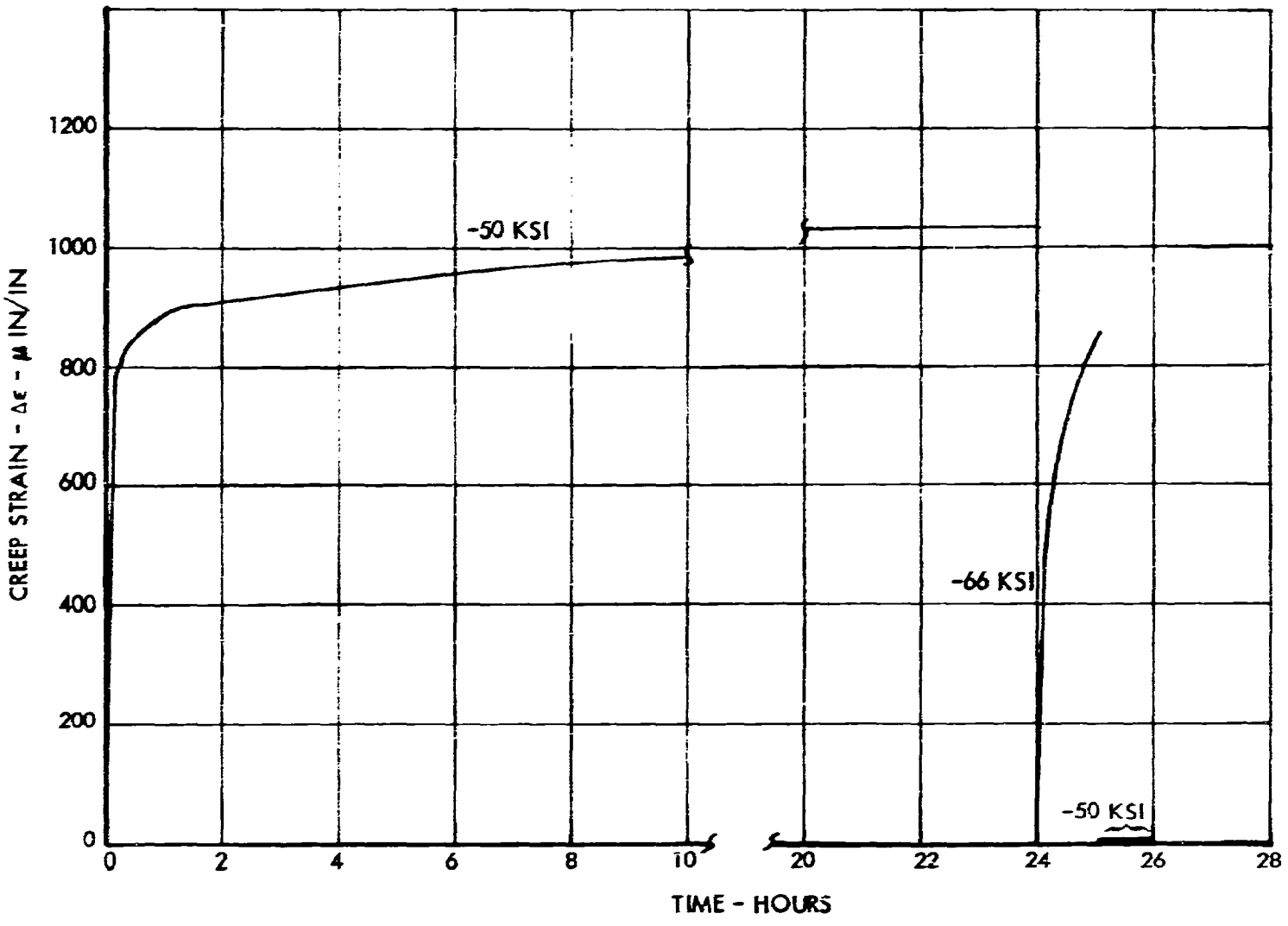

Figure 17. Coupon 18 Creep Strain

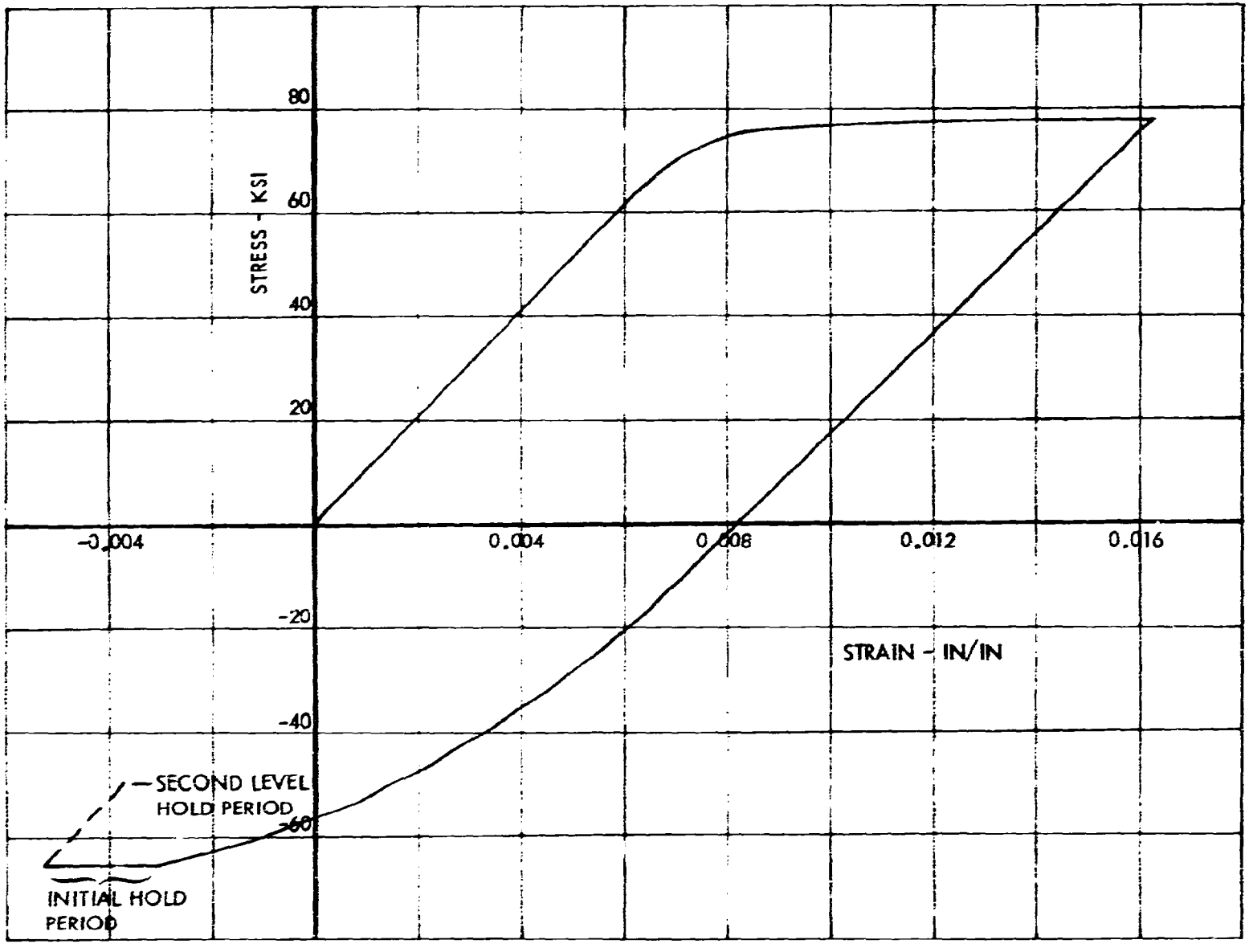

Figure 18. Stress-Strain Curve, Coupon Specimen 2A Load Control Test

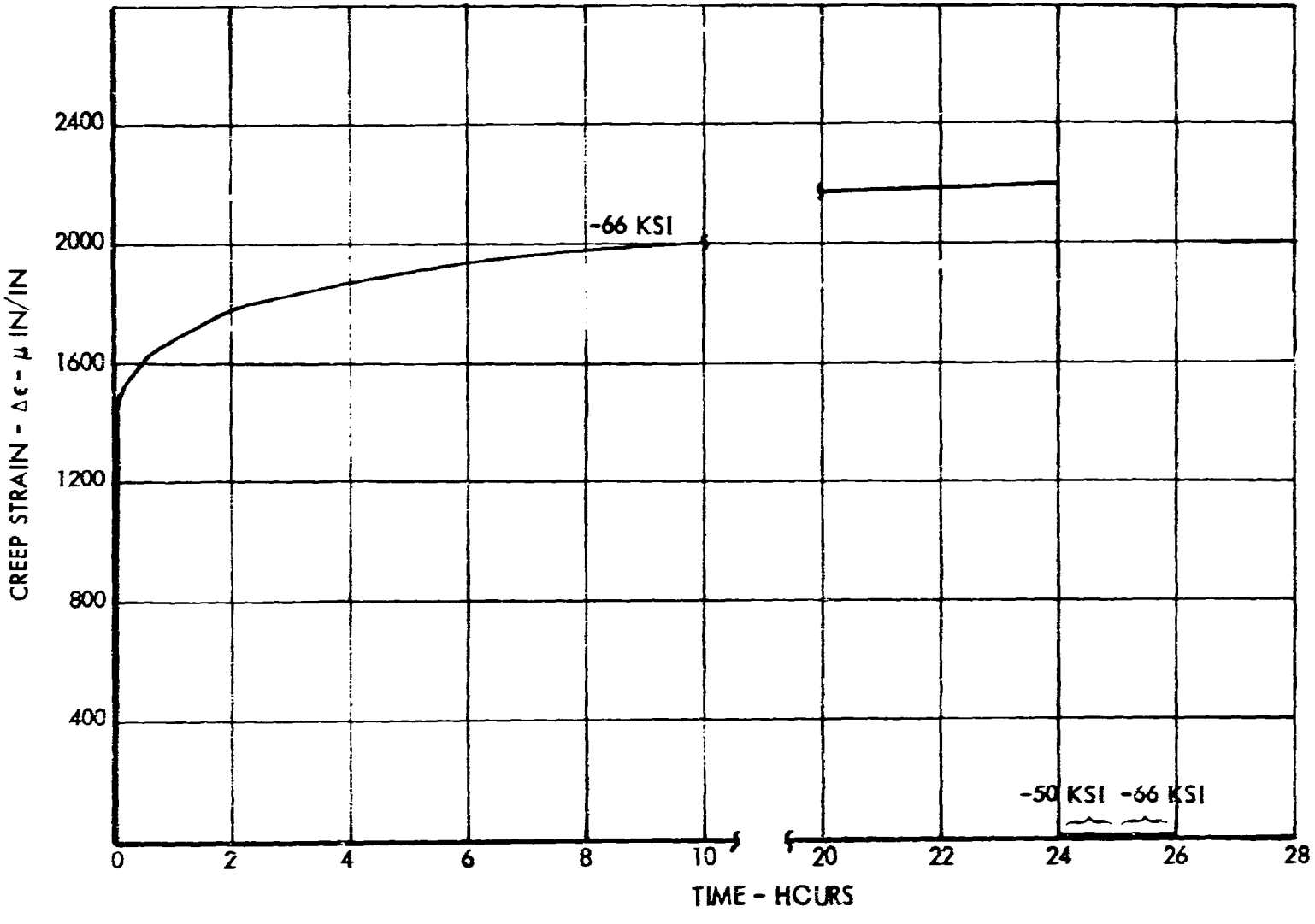

Figure 19. Coupon 2A Creep Strain

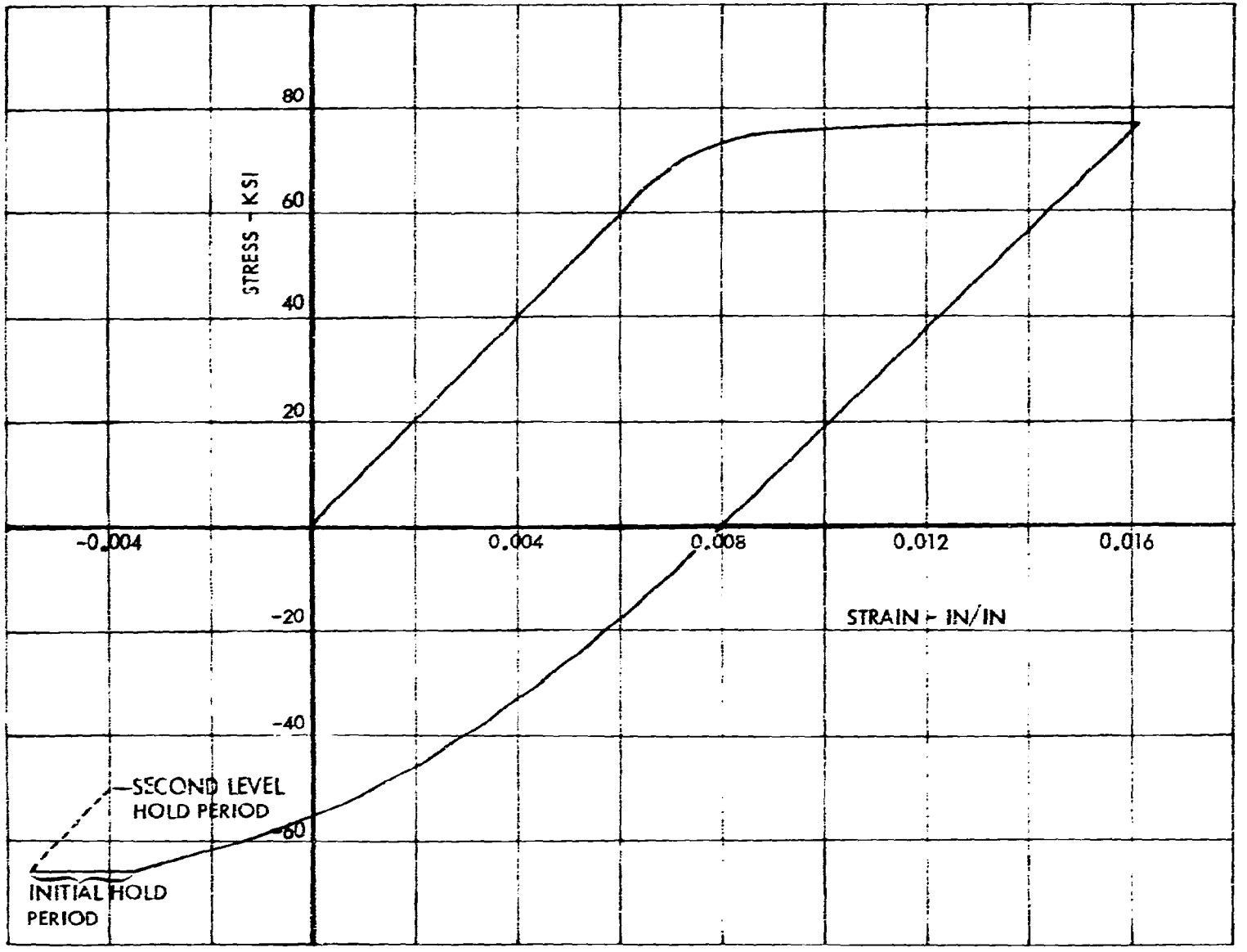

Figure 20. Stress-Strain Curve, Coupon Specimen 2B
Load Control Test

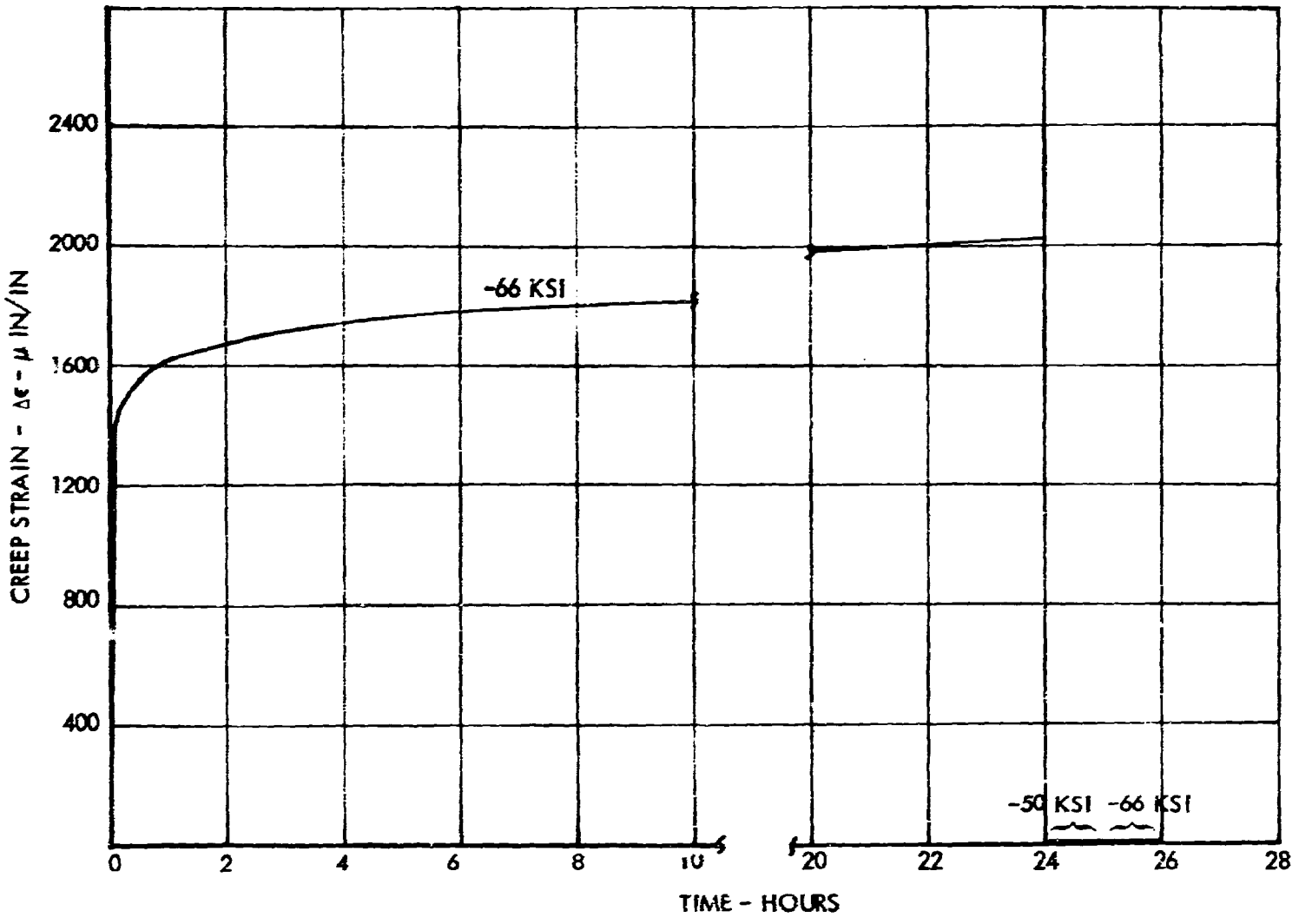

Figure 21. Coupon 2B Creep Strain

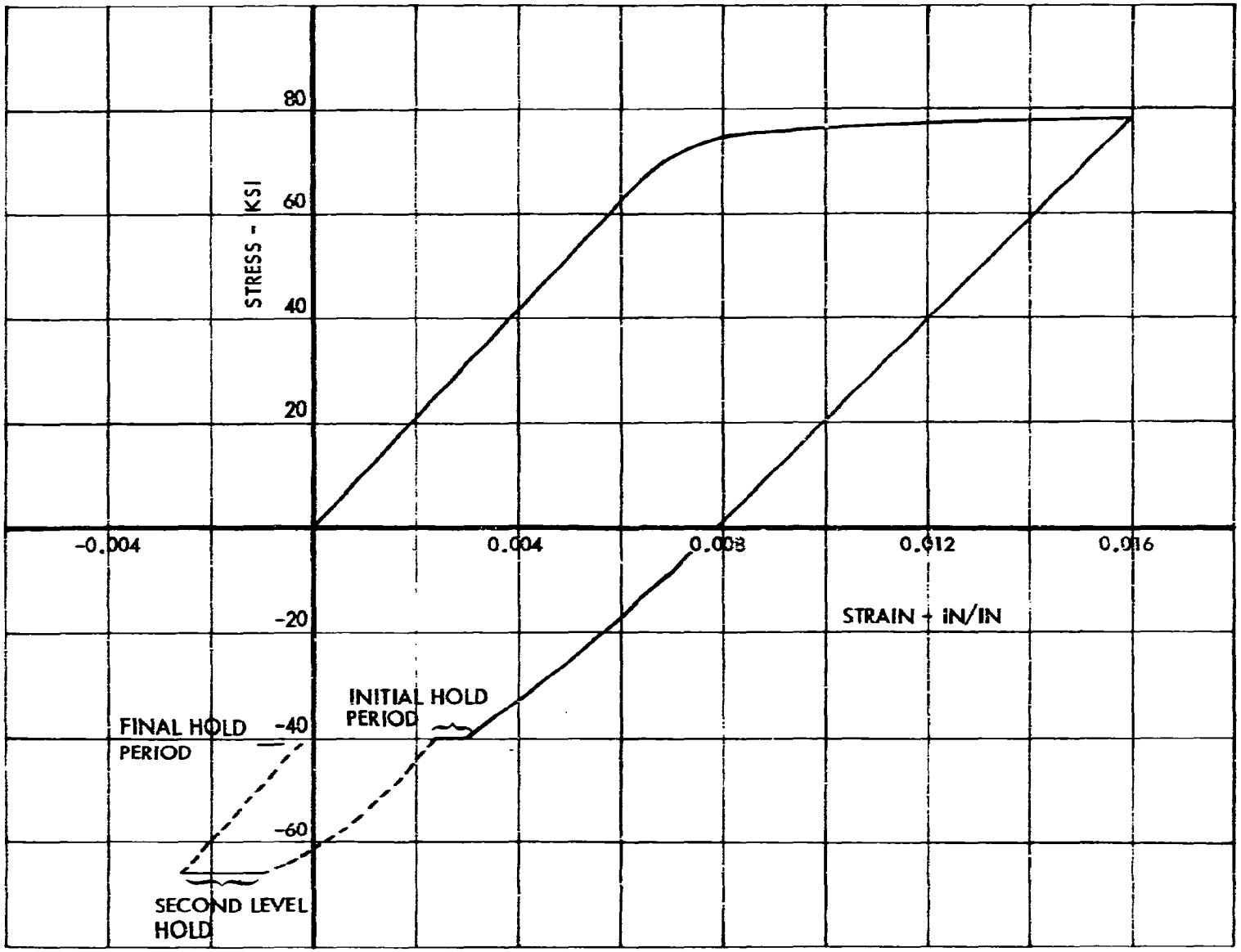

Figure 22 . Stress-Strain Curve, Coupon Specimen 3A
Load Control Test

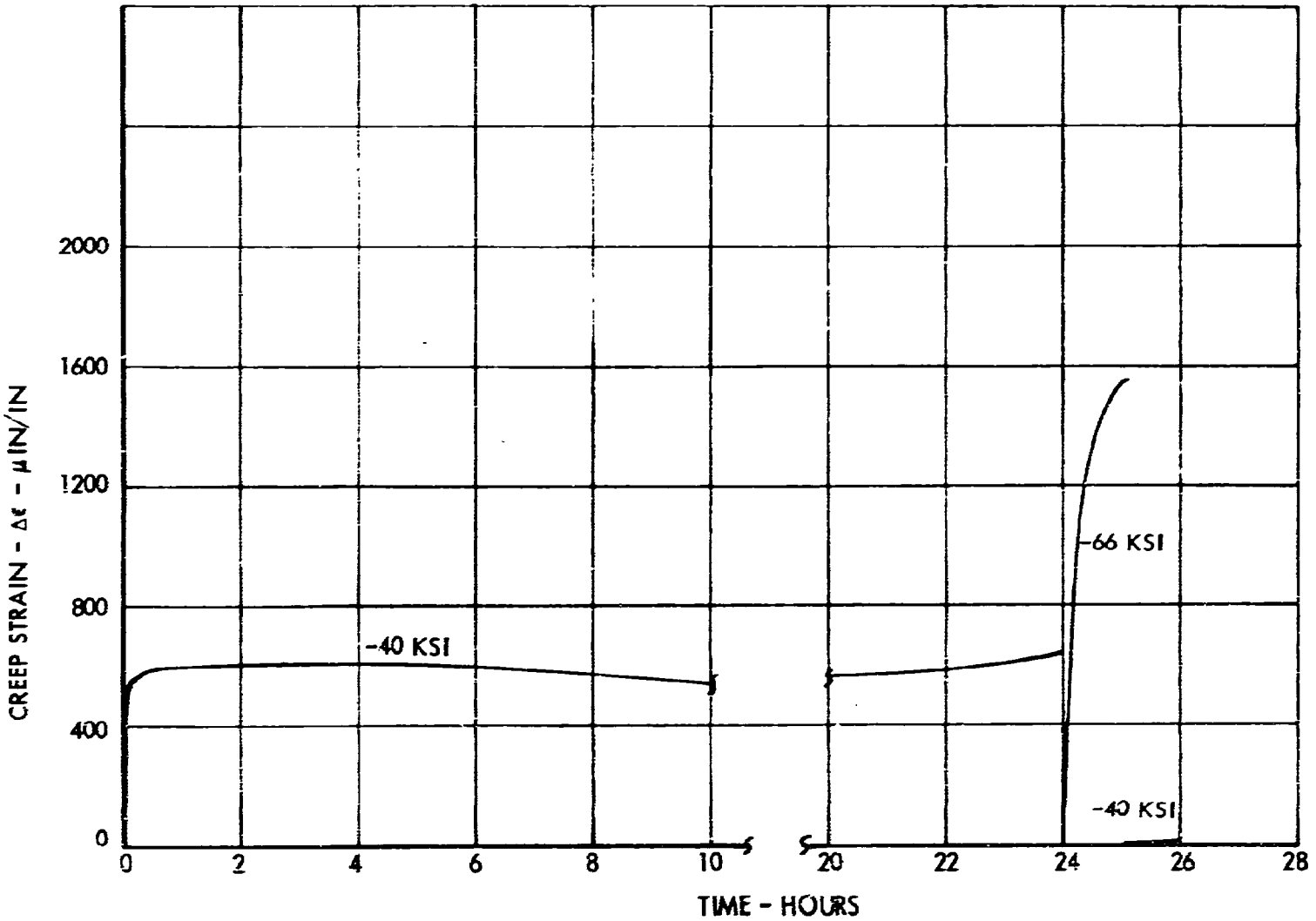

Figure 23. Coupon 3A Creep Strain

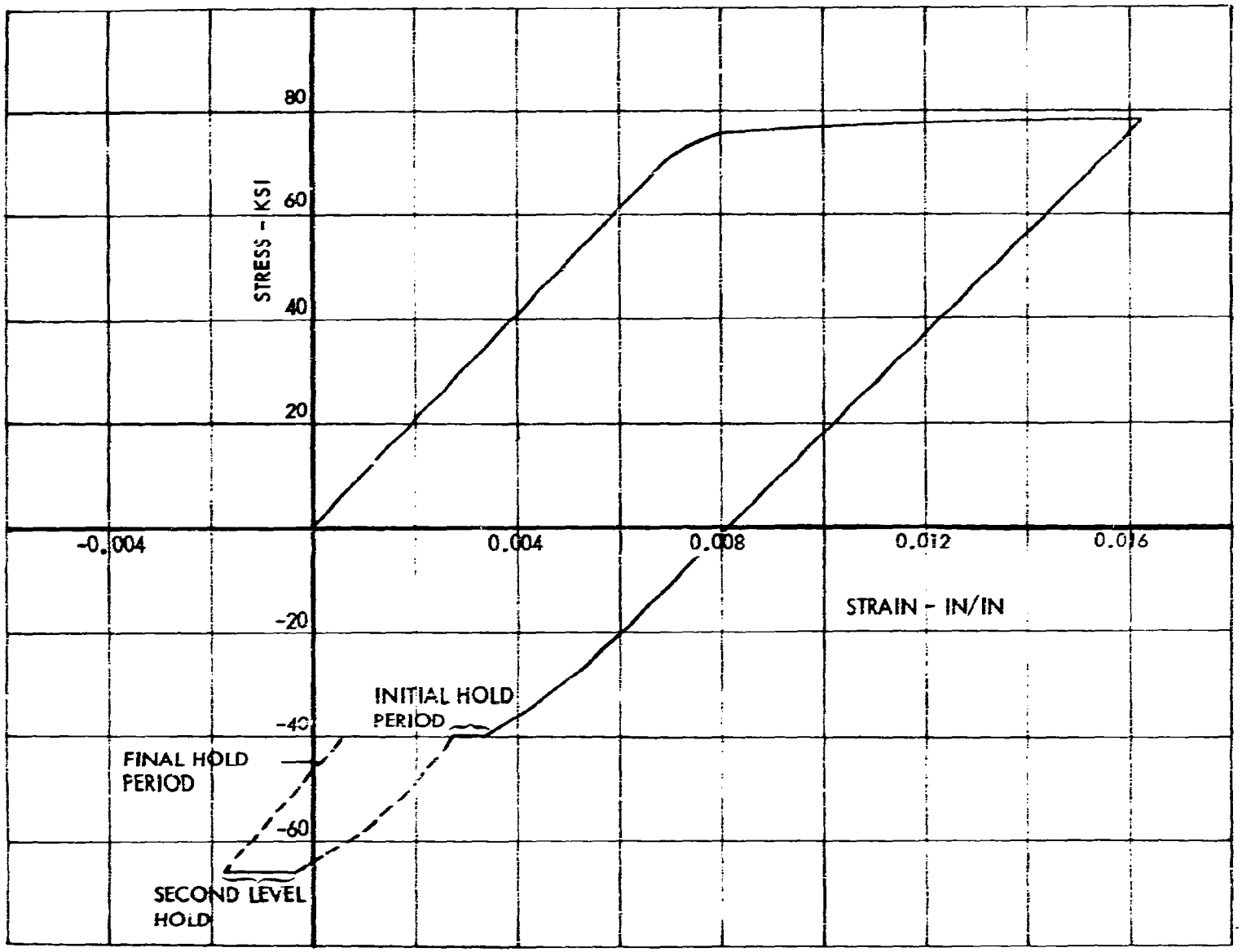

Figure 24. Stress-Strain Curve, Coupon Specimen 3B
Load Control Test

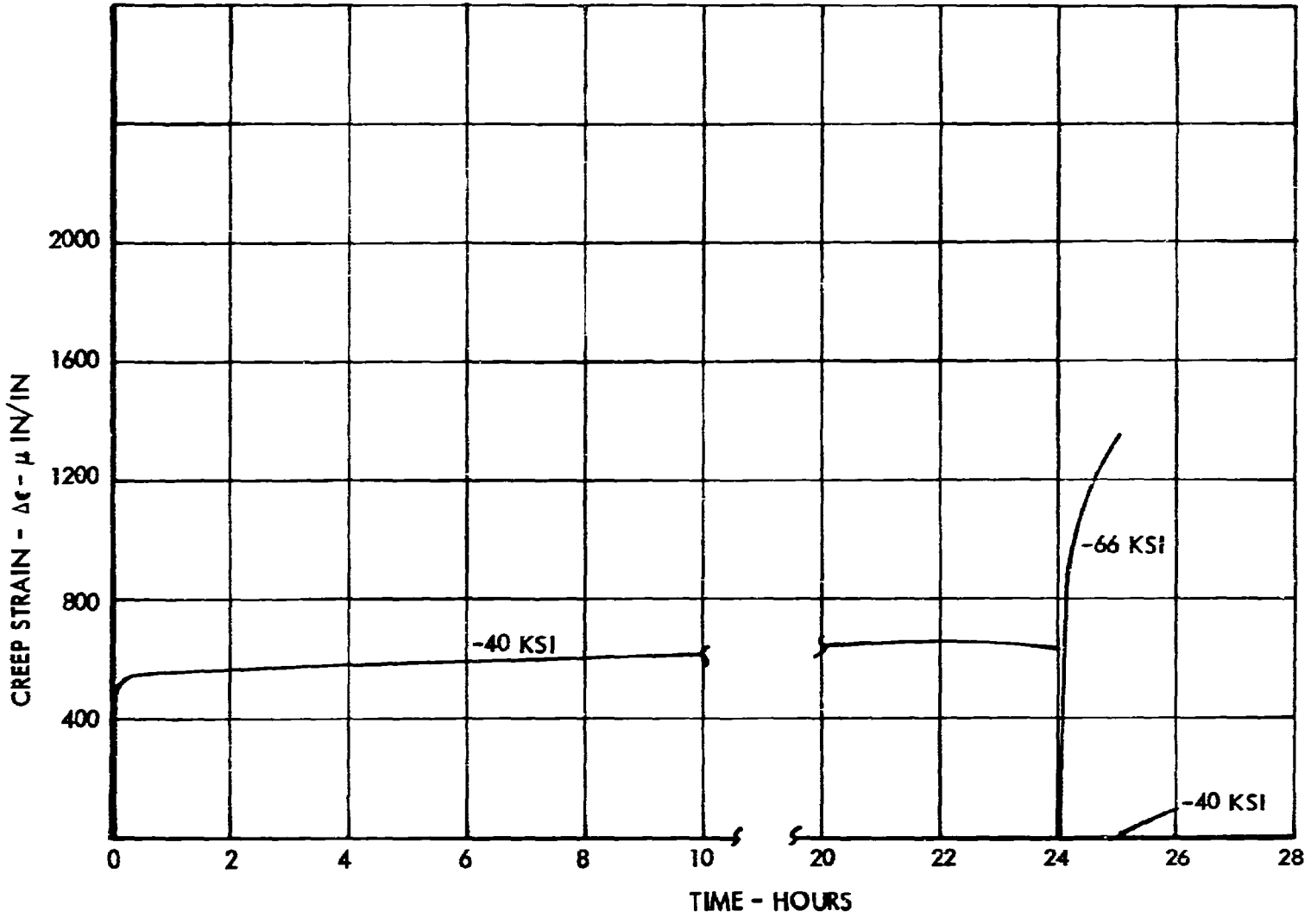

Figure 25. Coupon 3B Creep Strain

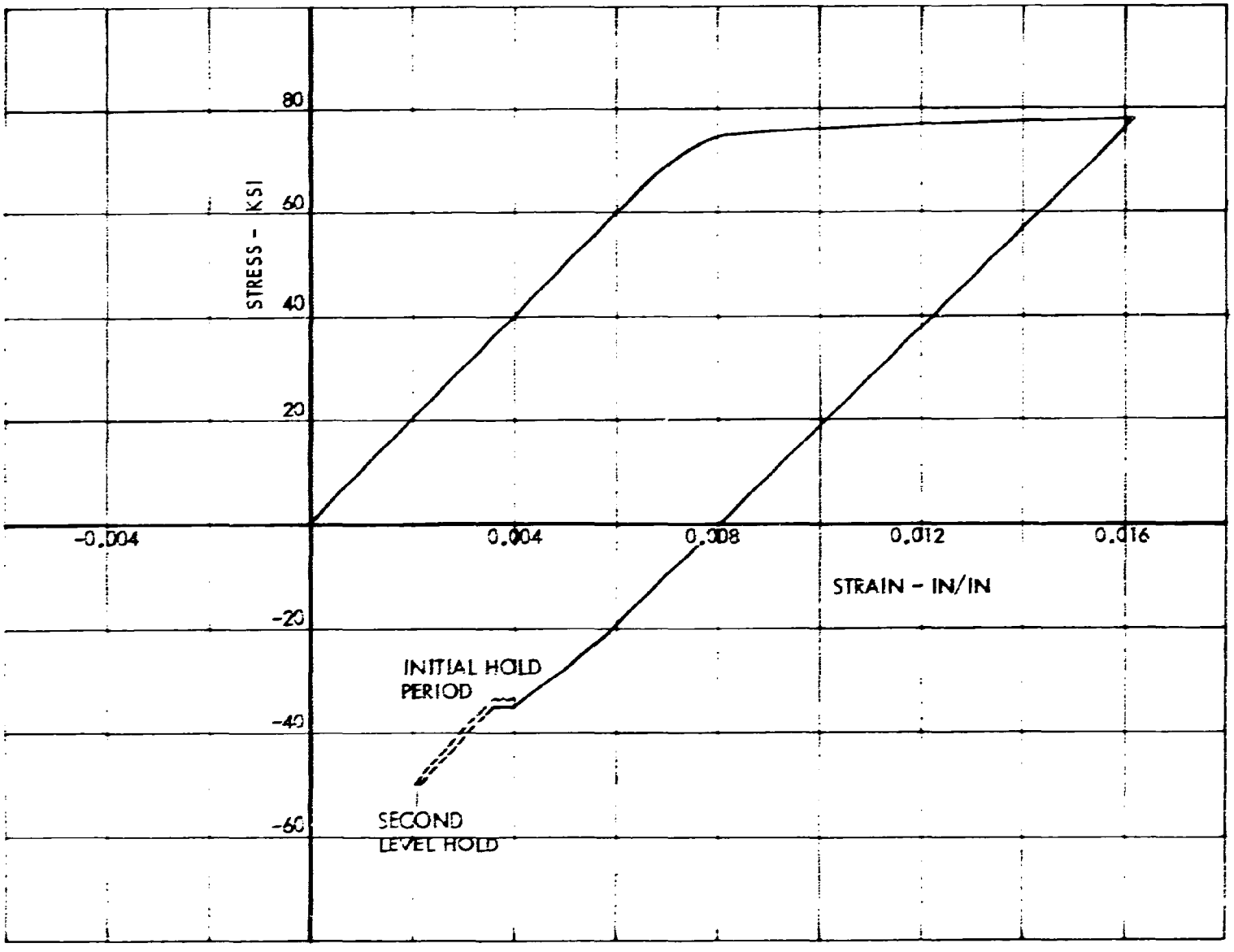

Figure 26. Stress-Strain Curve, Coupon Specimen 4A
Load Control Test

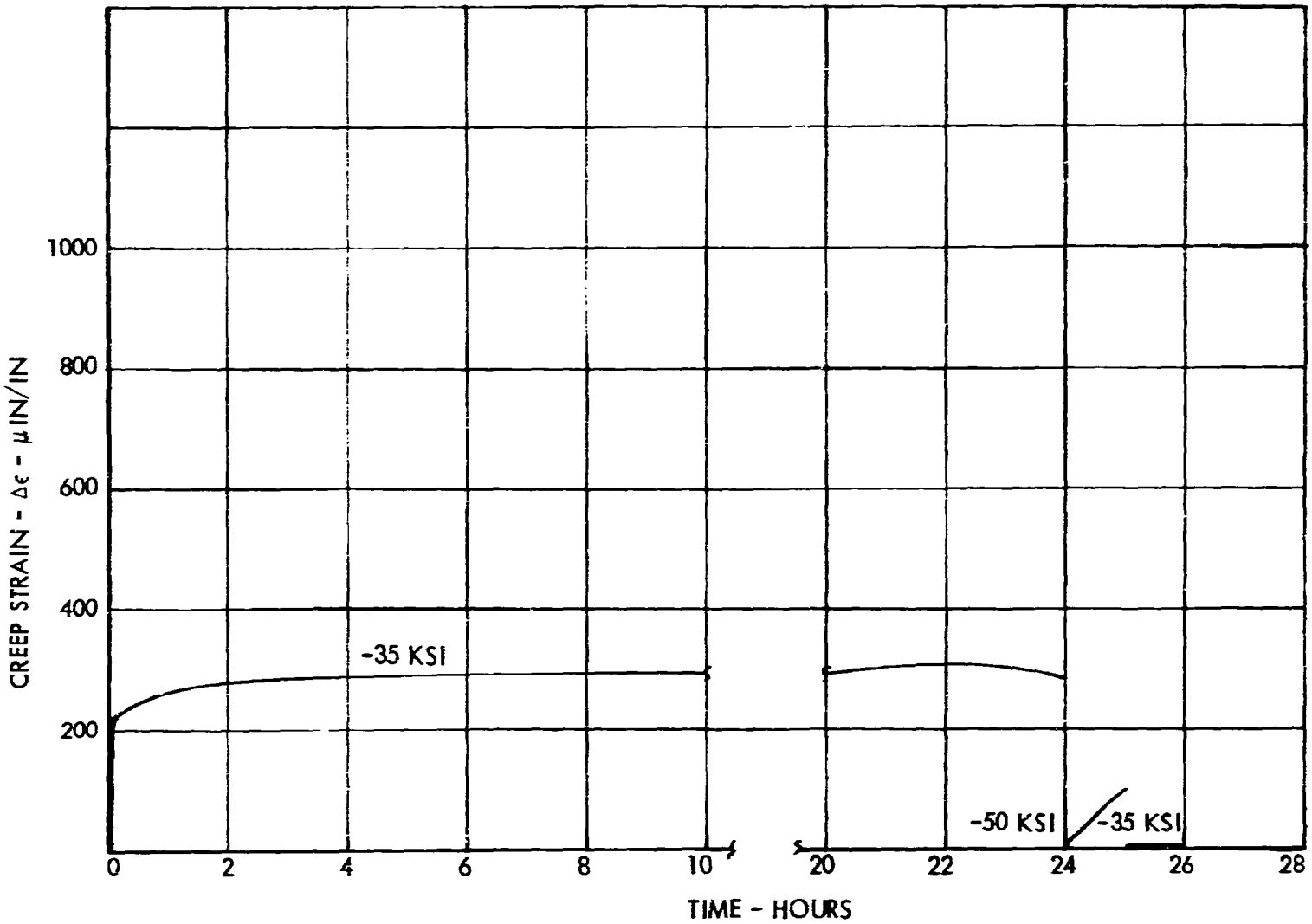

Figure 27. Coupon 4A Creep Strain

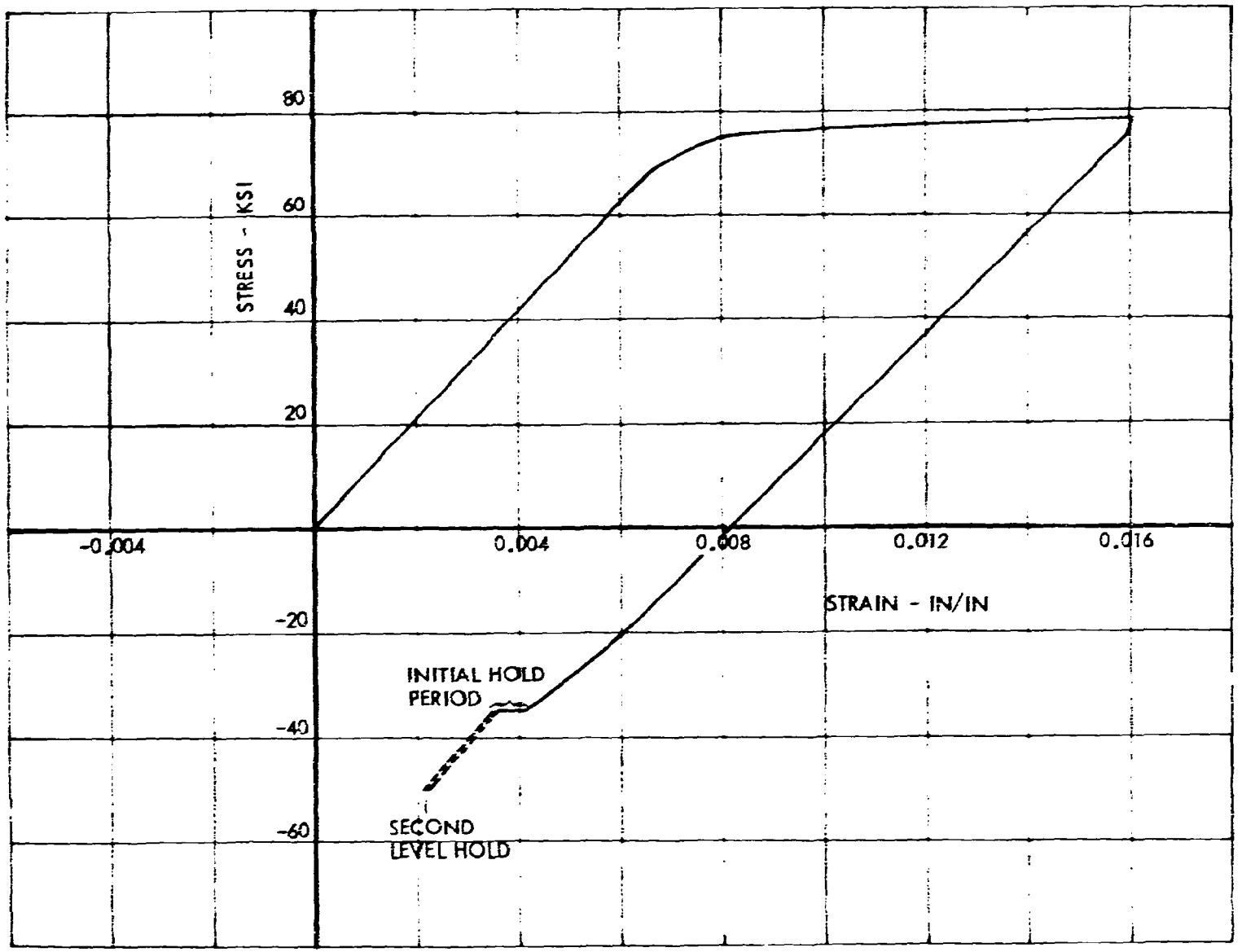

Figure 28. Stress-Strain Curve, Coupon Specimen 48
Load Control Test

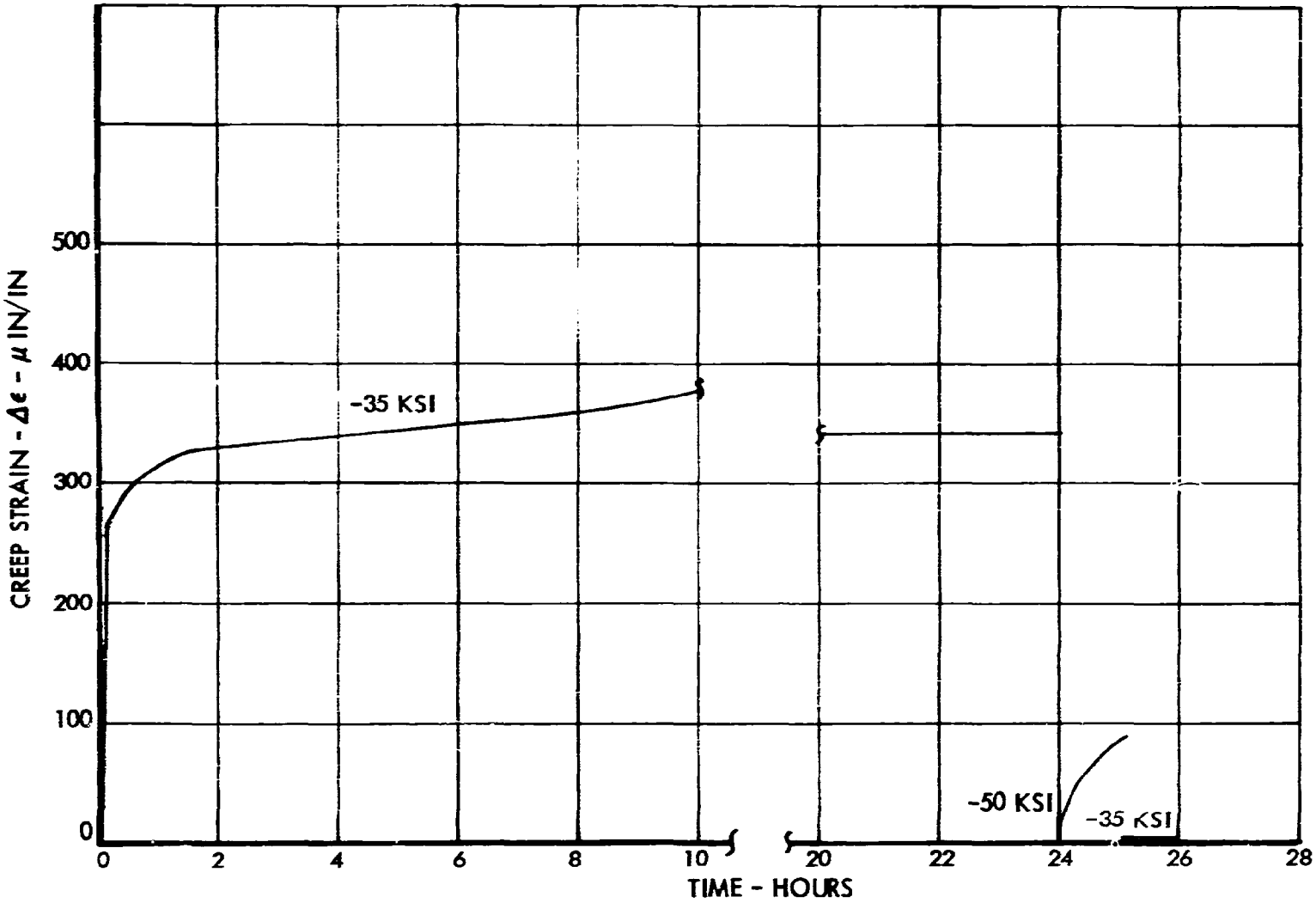

Figure 29. Coupon 4B Creep Strain

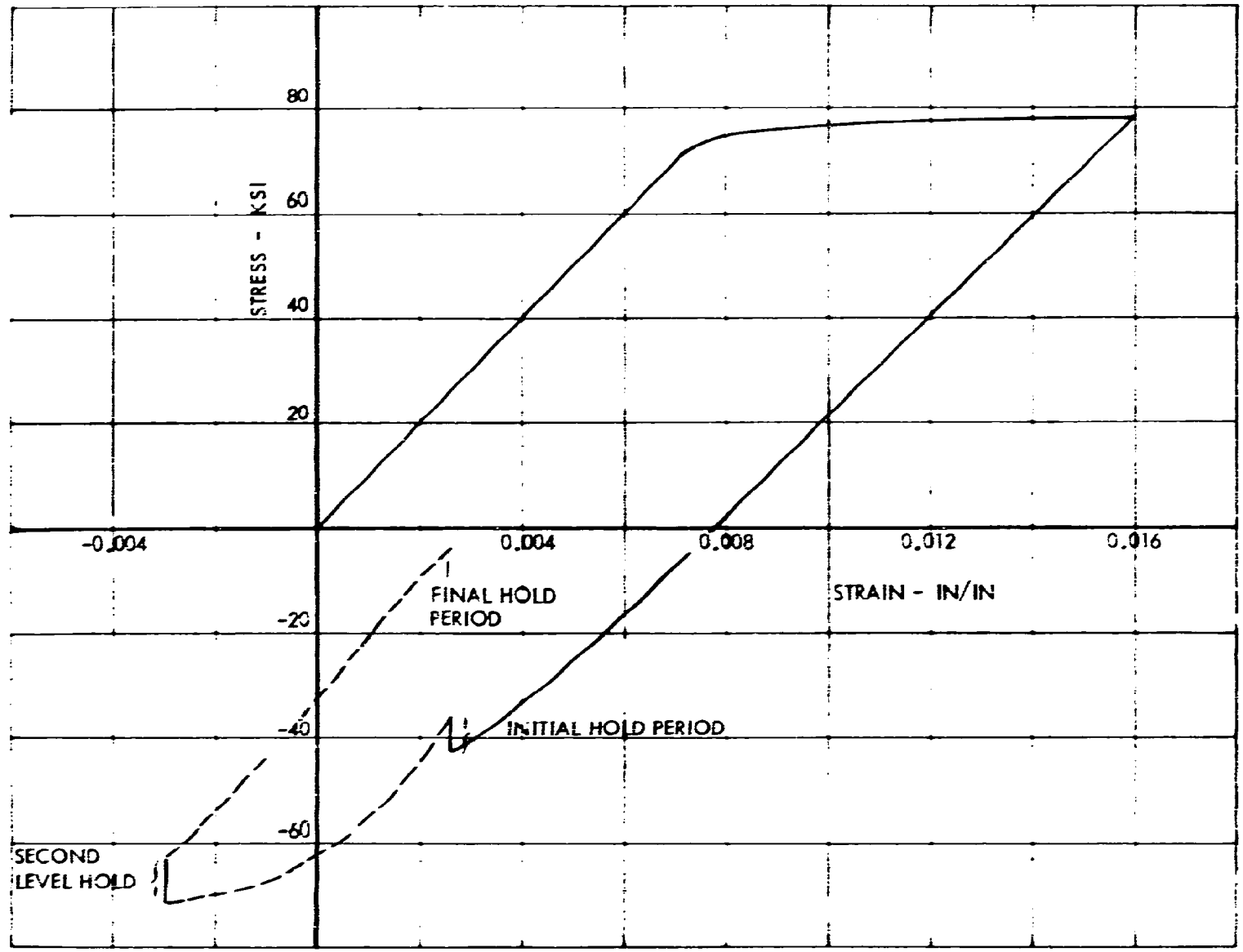

Figure 30. Stress-Strain Curve, Coupon Specimen 5A
Strain Control Test

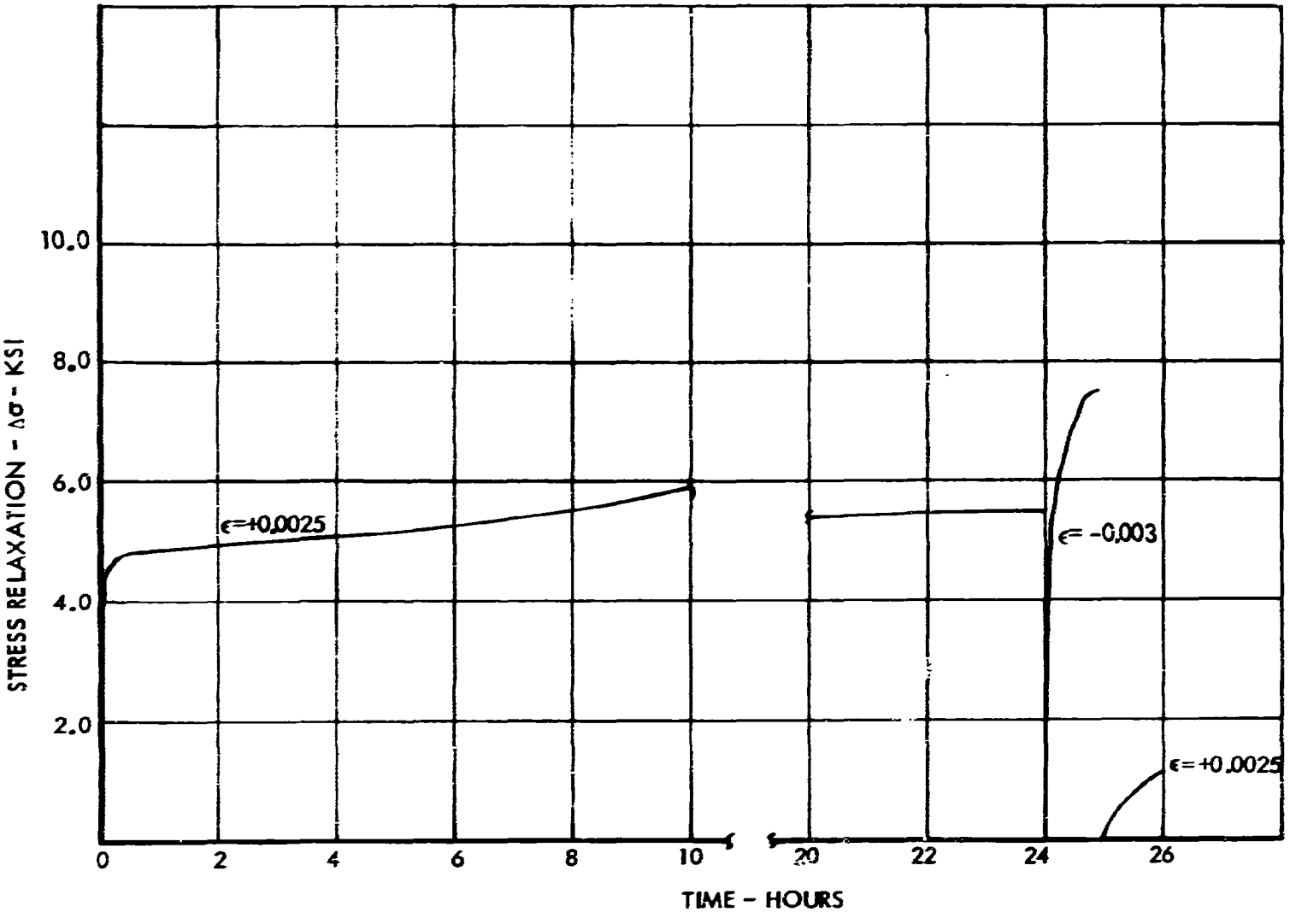

Figure 31. Coupon 5A Stress Relaxation

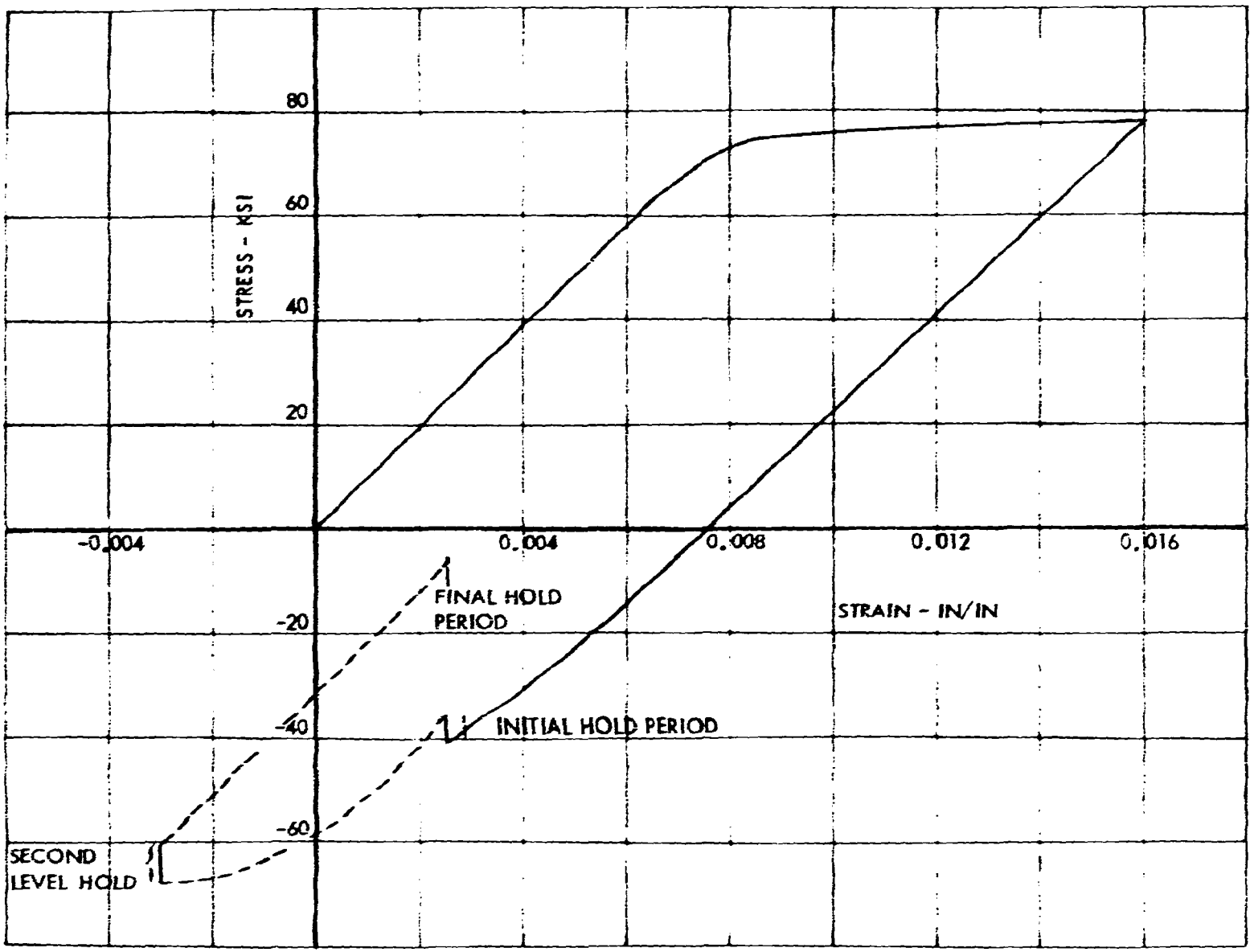

Figure 32. Stress-Strain Curve, Coupon Specimen 5B
Strain Control Test

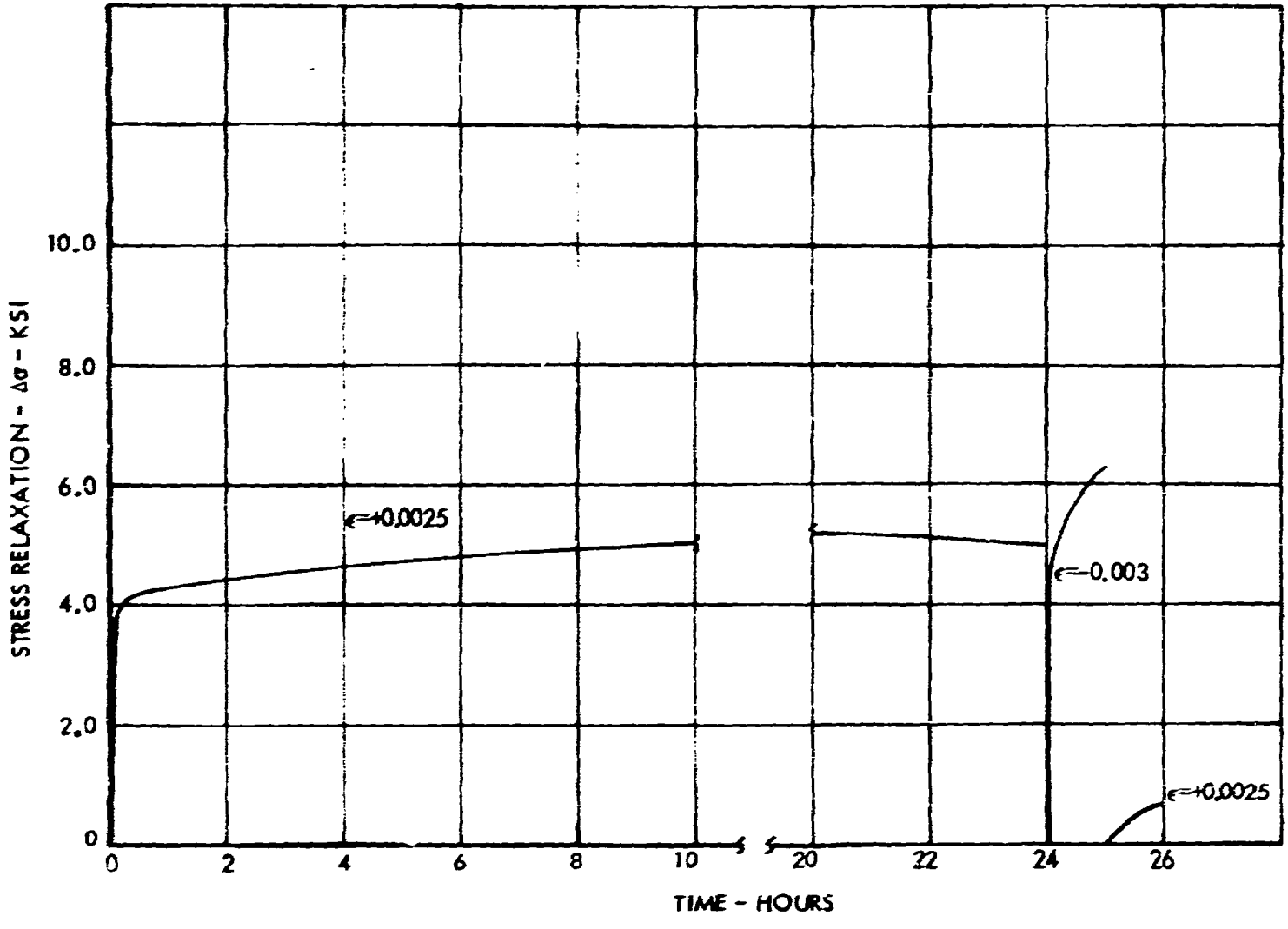

Figure 33. Coupon 5B Stress Relaxation

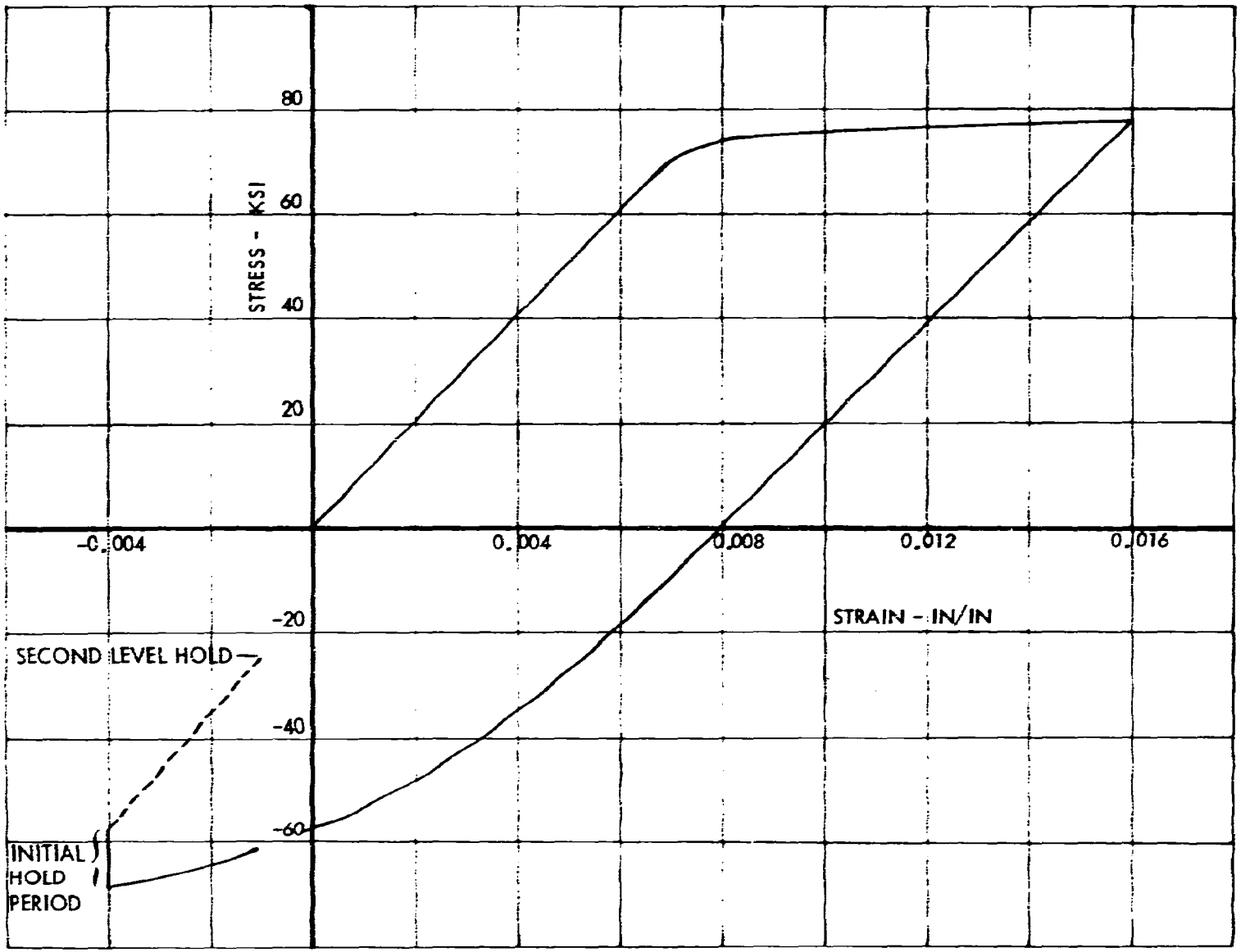

Figure 34. Stress-Strain Curve Coupon Specimen 6A
Strain Control Test

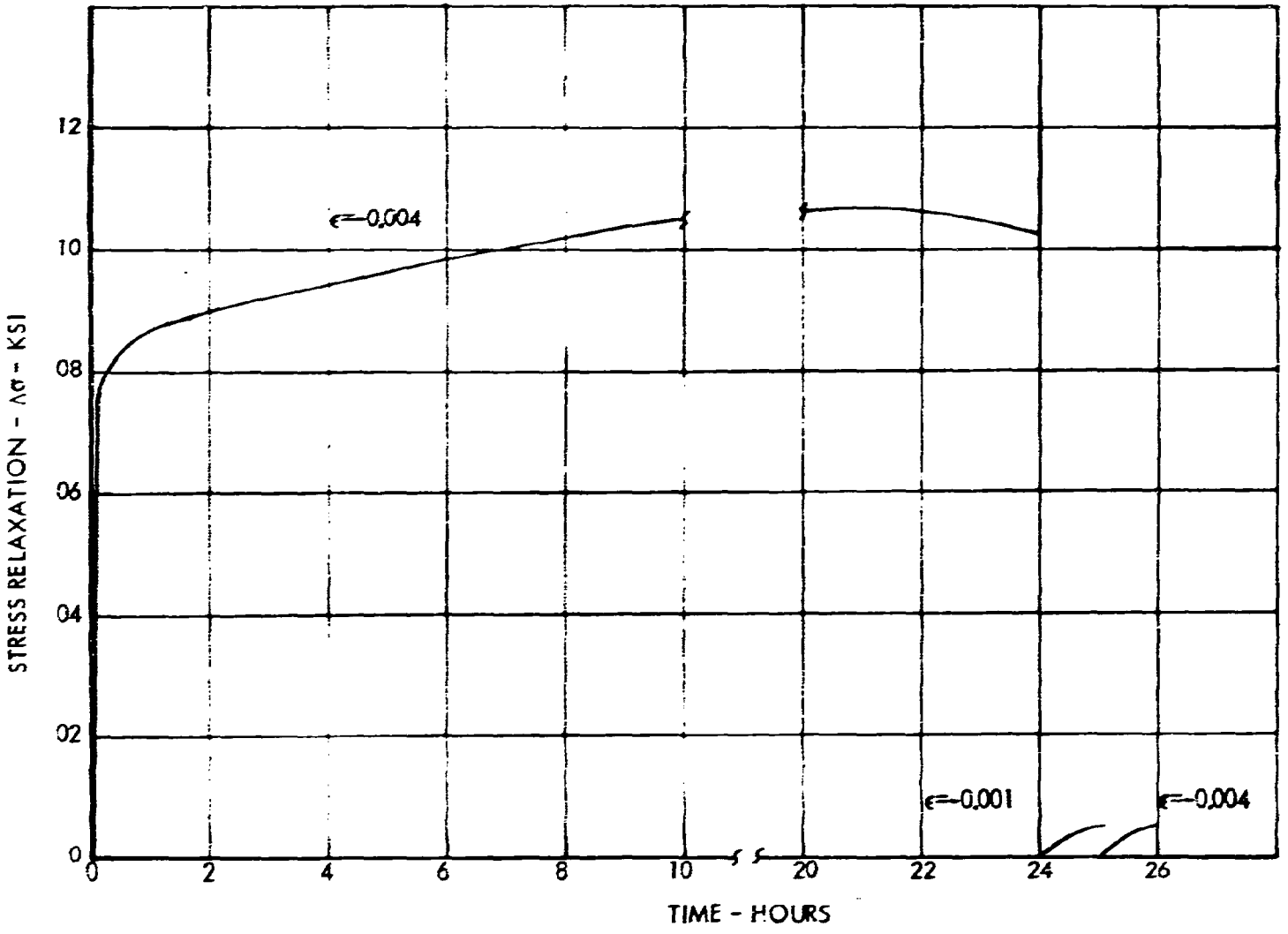

Figure 35. Coupon 6A Stress Relaxation

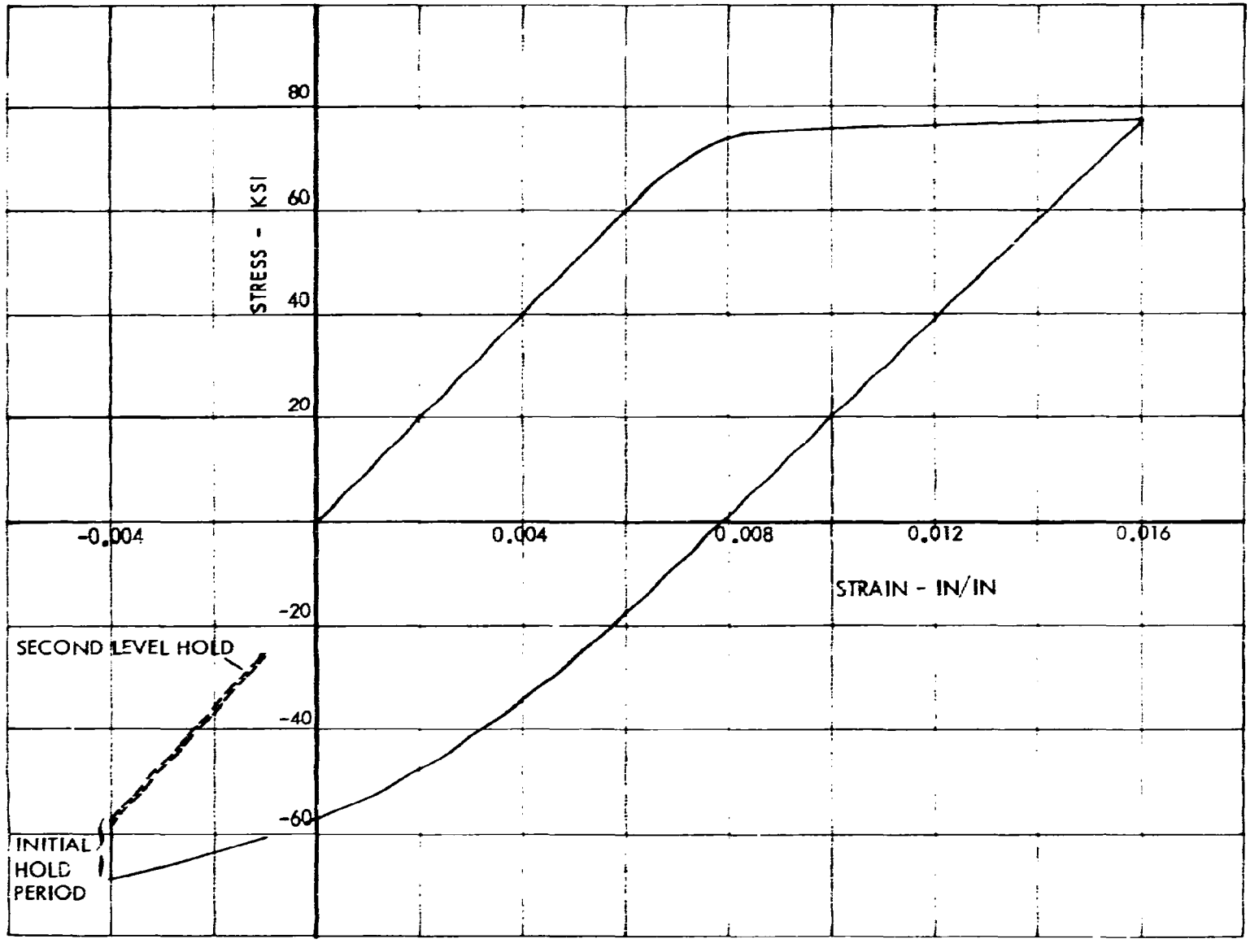

Figure 36. Stress-Strain Curve Coupon Specimen 6B
Strain Control Test

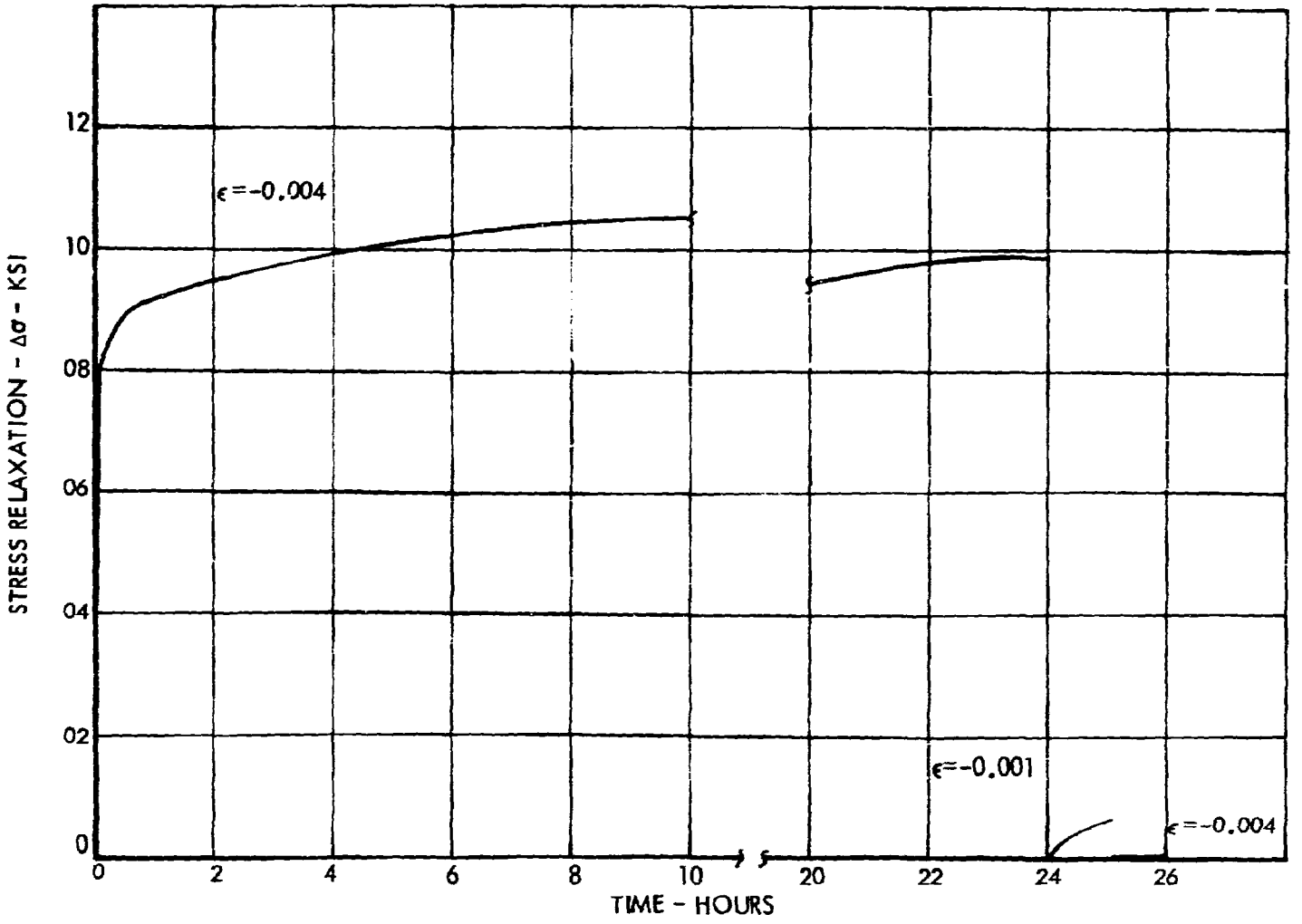

Figure 37. Coupon 6B Stress Relaxation

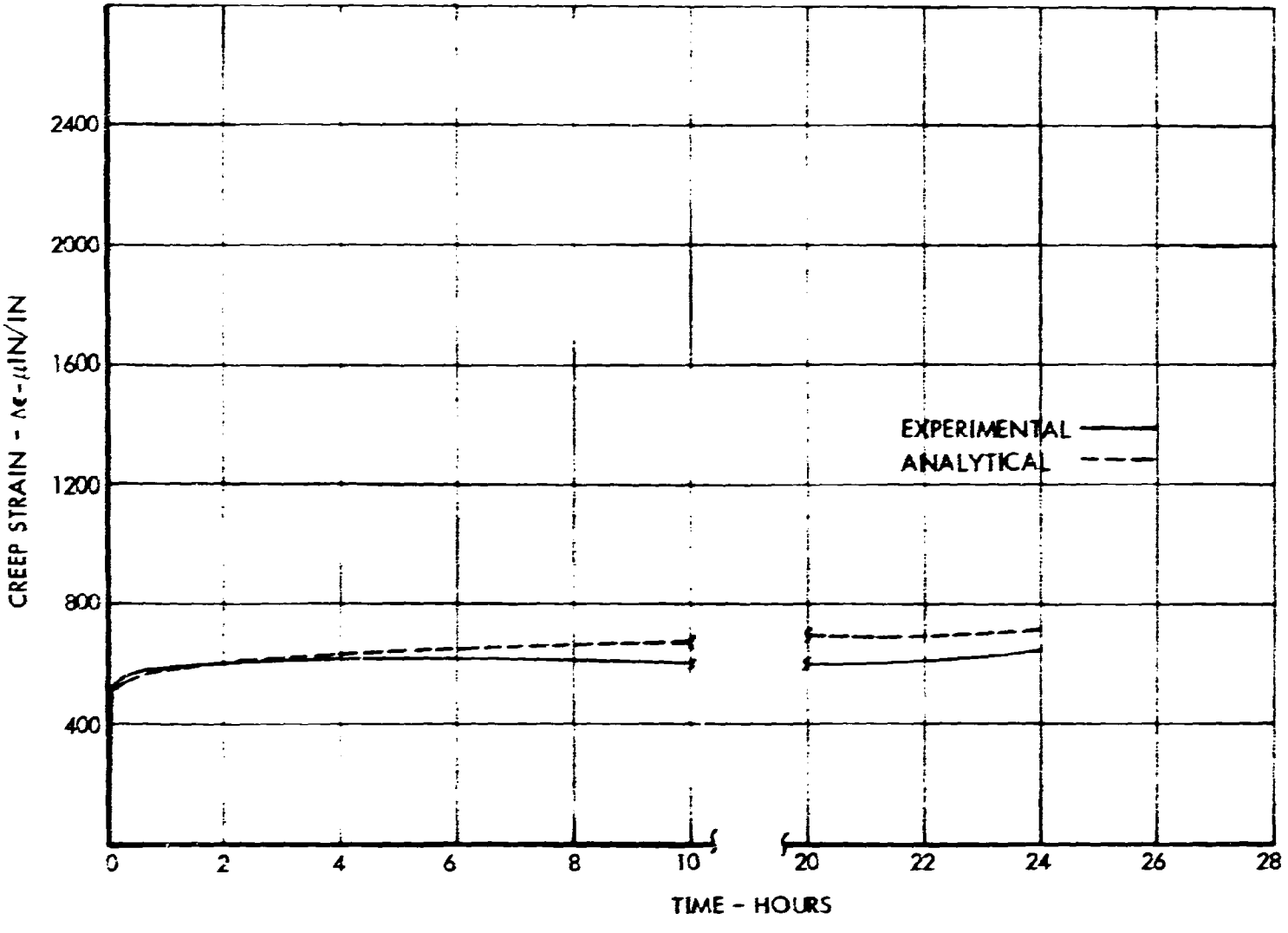

Figure 38. Comparison of Predicted and Measured Creep at -40 Ksi

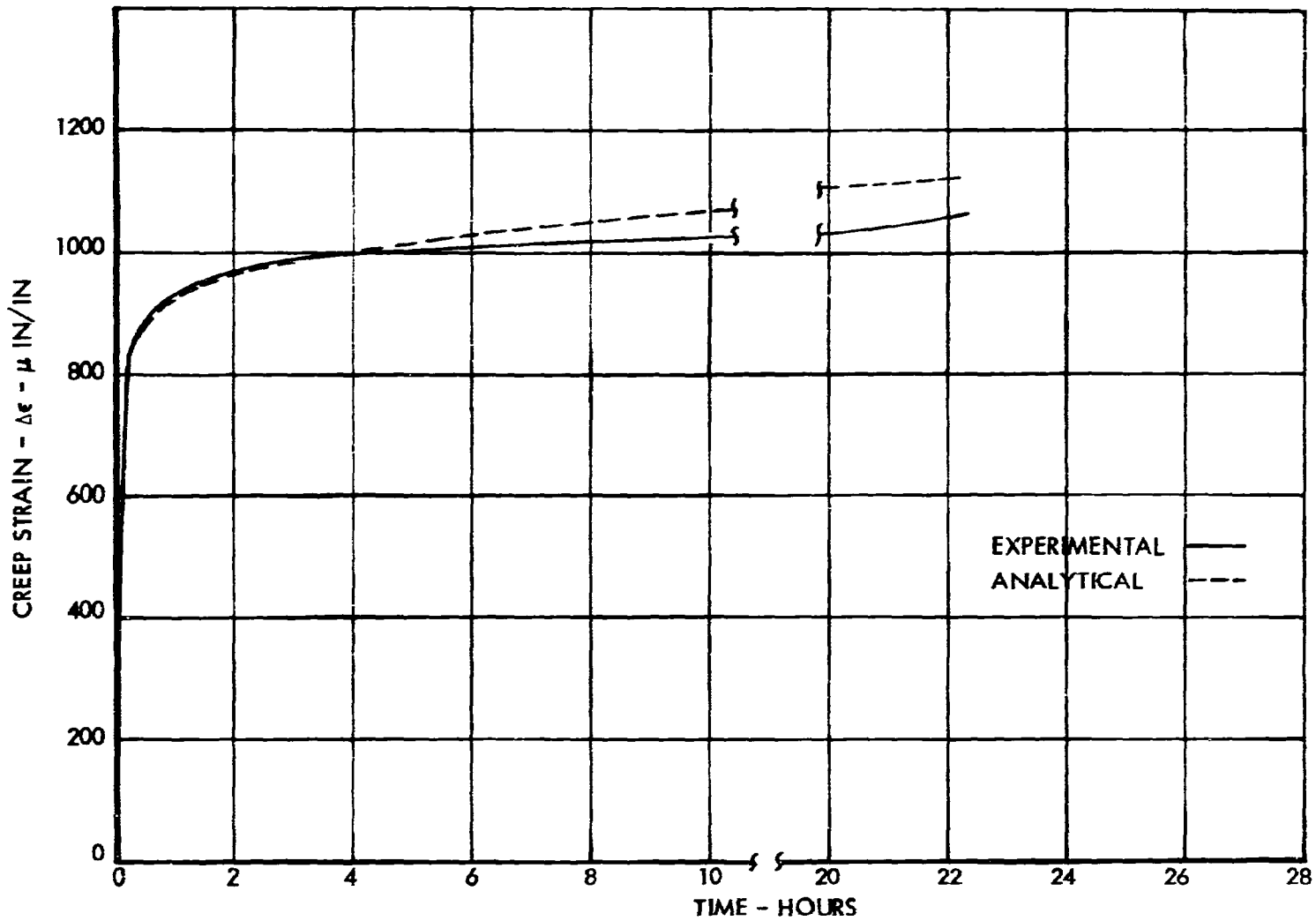

Figure 39. Comparison of Predicted and Measured Creep at -50 Ksi

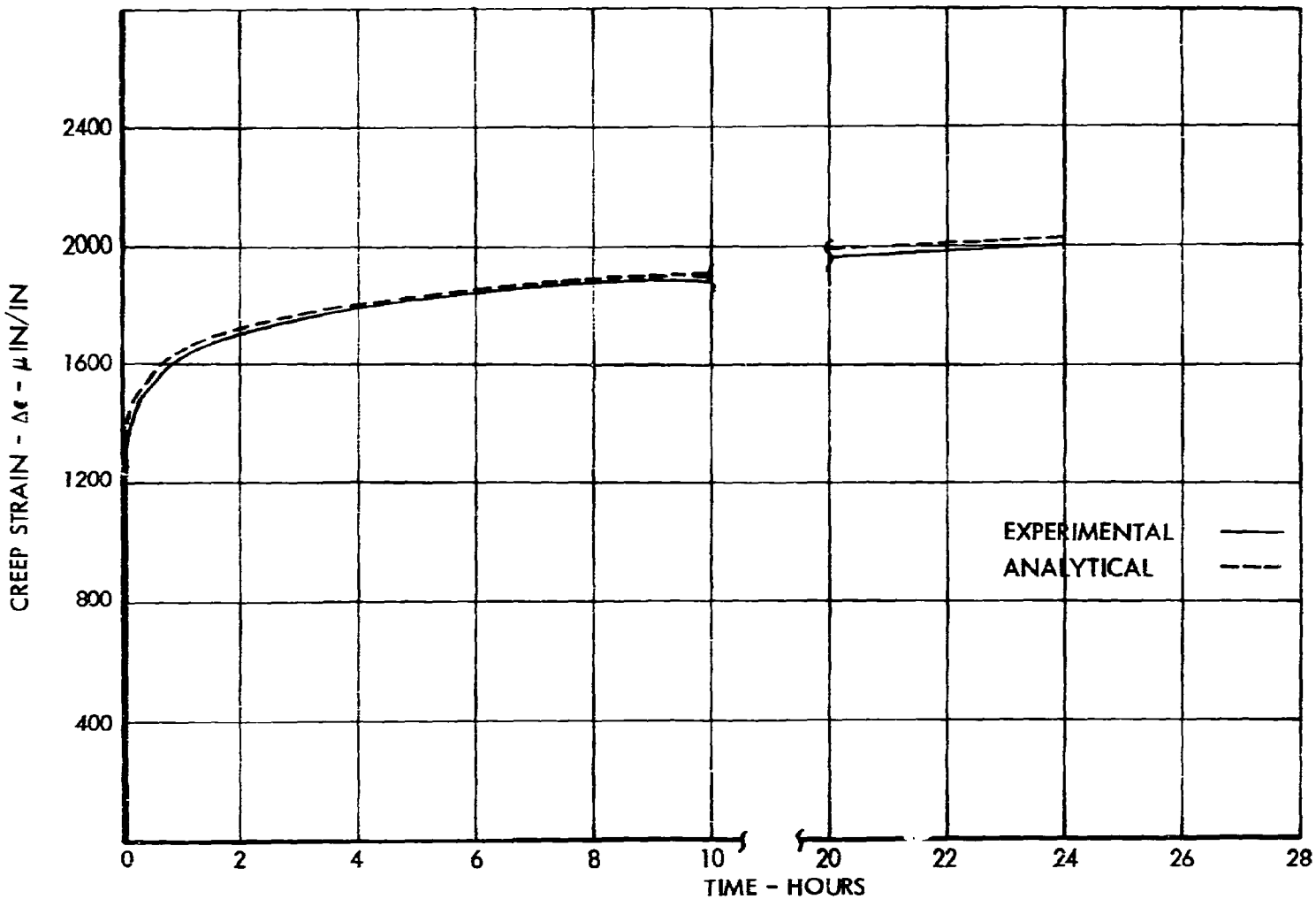

Figure 40. Comparison of Predicted and Measured Creep at -66 Ksi

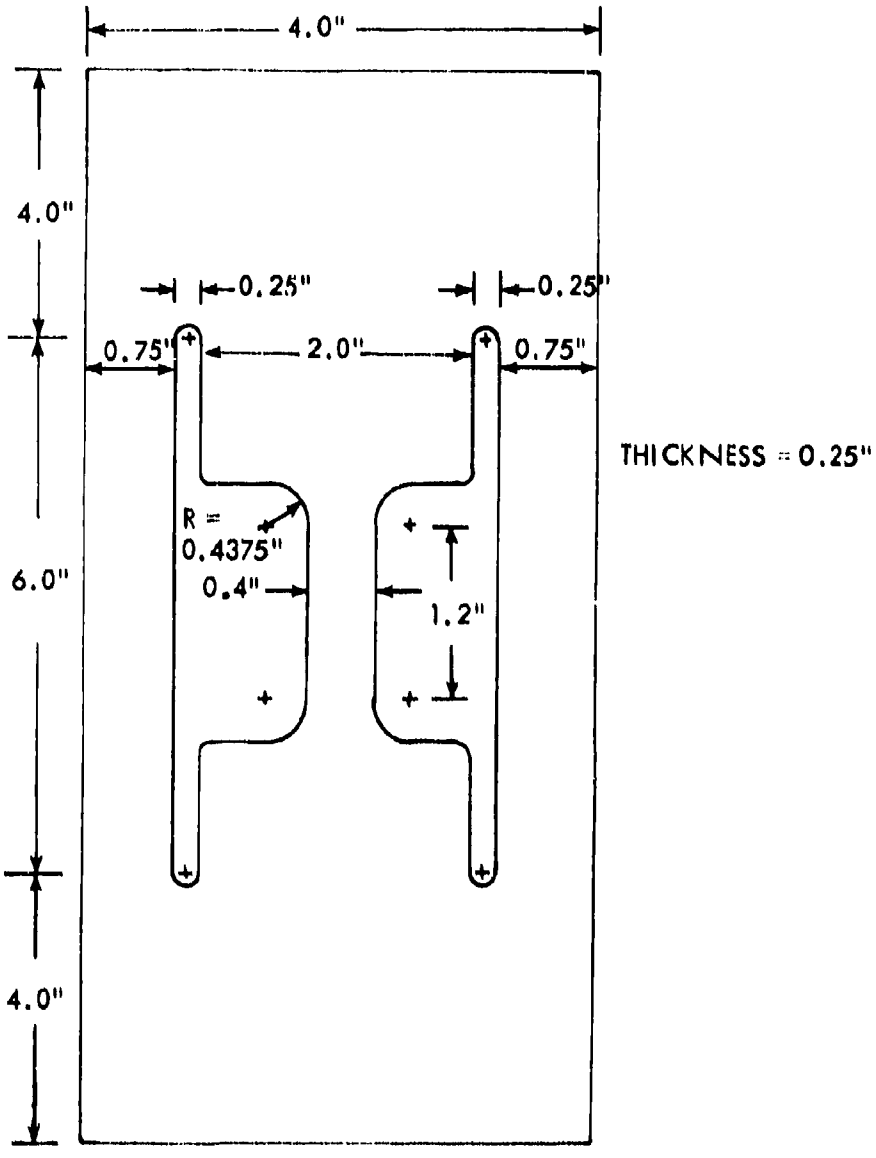

Figure 41. Simplified Stress Concentration Specimen

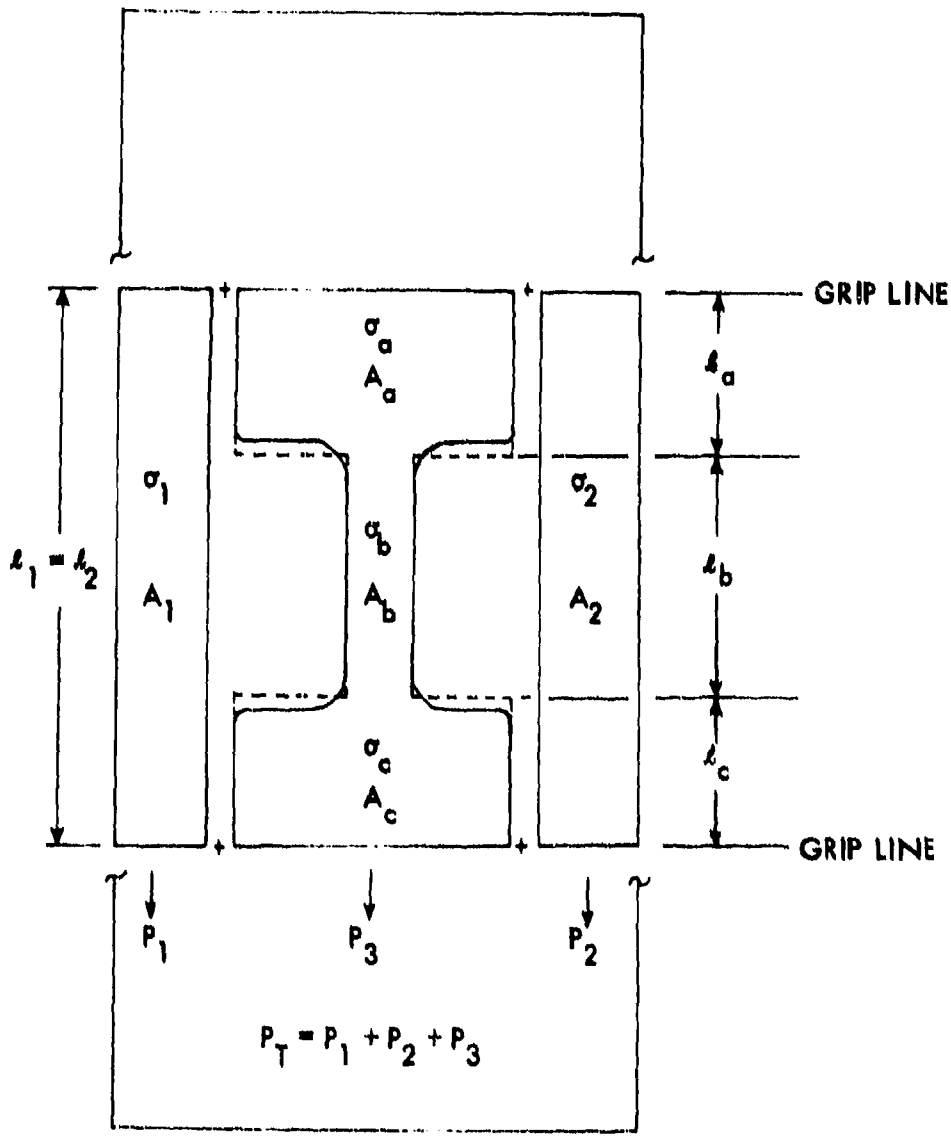

Figure 42. Schematic Representation of Simplified Stress Concentration Specimen

TEST SEQUENCE	LOADING CONDITIONS	COMMENTS
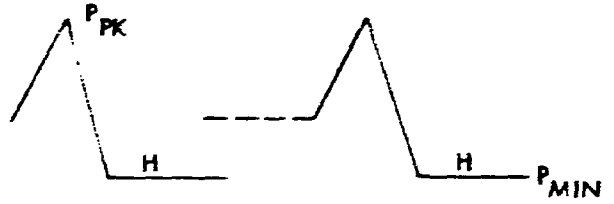	P_{PK} = 25 KIPS P_{MIN} = -9.5 KIPS H = 24 HRS. ϵ_{PK} ≅ 0.016 IN/IN ϵ_{MIN} ≅ 0.0015 IN/IN	Two Specimens Tested. See Data in Figures 45 through 48. Test for Creep/Stress Relaxation Only.
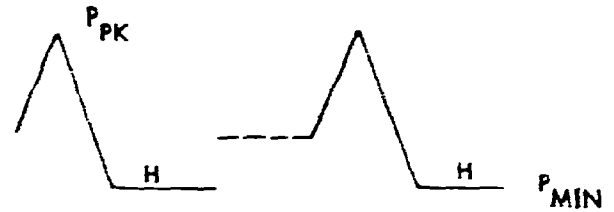	P_{PK} = 25 KIPS P_{MIN} = -5.8 KIPS H = 24 Hrs. ϵ_{PK} ≅ 0.016 IN/IN ϵ_{MIN} ≅ 0.0035 IN/IN	One Specimen Tested. See Figures 49 and 50. Creep/Stress Relaxation Only.
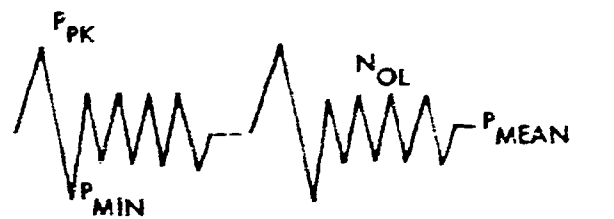	P_{PK} = 25 KIPS, P_{MIN} = -9.8 KIPS P_{MEAN} = 8.8 KIPS N_{OL} = 1000 CYCLES $-0.0001 \leq \epsilon_{MIN} \leq +0.0036$ $+0.008 \leq \epsilon_{MEAN} \leq +0.0098$	Fatigue Tests. Two Specimens Tested. See Figures 51 through 53.
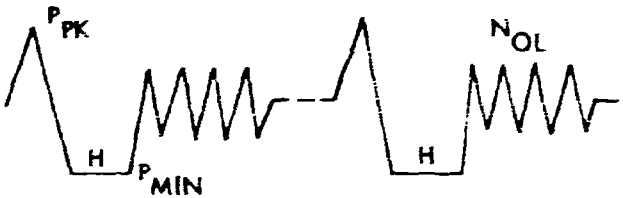	P_{PK} = 25 KIPS, P_{MIN} = -9.8 KIPS P_{MEAN} = 8.8 KIPS N_{OL} = 1000 CYCLES $0.0013 \leq \epsilon_{MIN} \leq 0.0026$ $0.0078 \leq \epsilon_{MEAN} \leq 0.0092$ H = 1.0 HR.	Fatigue Test. One Specimen Only. See Figures 54 and 55.

NOTE: 1) P is defined as total load (P_T)

2) ϵ is center bar strain

3) H is sustained load hold time.

4) N_{OL} is number of cycles between overloads.

Figure 43. Test Sequence Definition For Simplified Stress Concentration Specimens

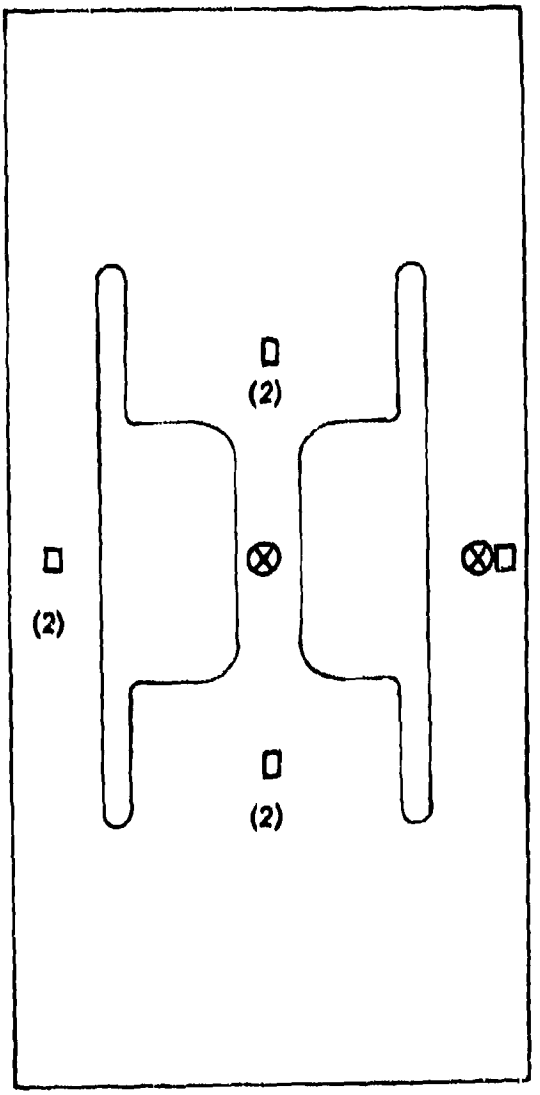

⊗ EXTENSOMETER

□ STRAIN GAGE

(2) GAGES BOTH SIDES

Figure 44. Instrumentation Locations For Simplified Stress Concentration Specimens

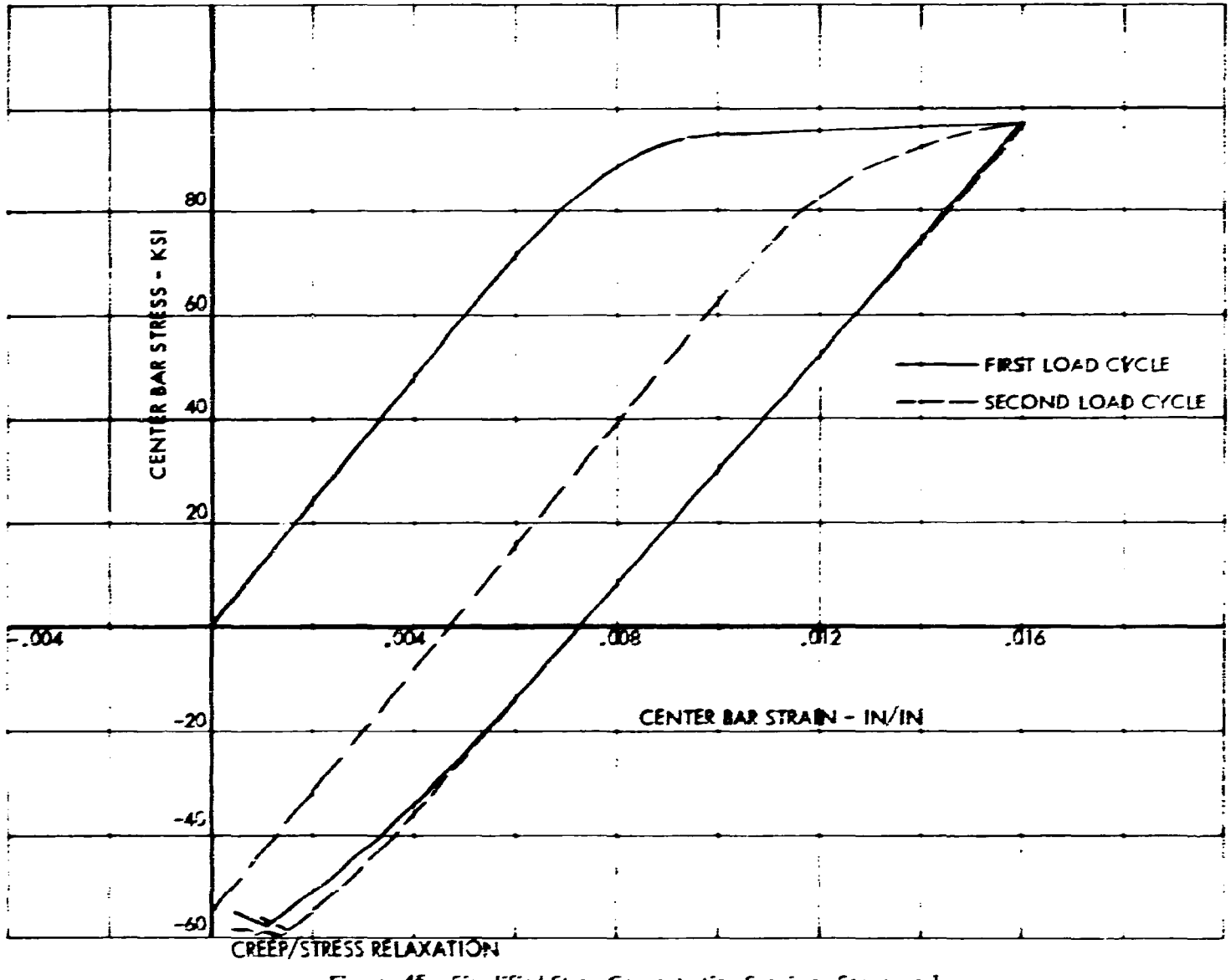

Figure 45. Simplified Stress Concentration Specimen Sequence 1
Center Bar Stress-Strain Data

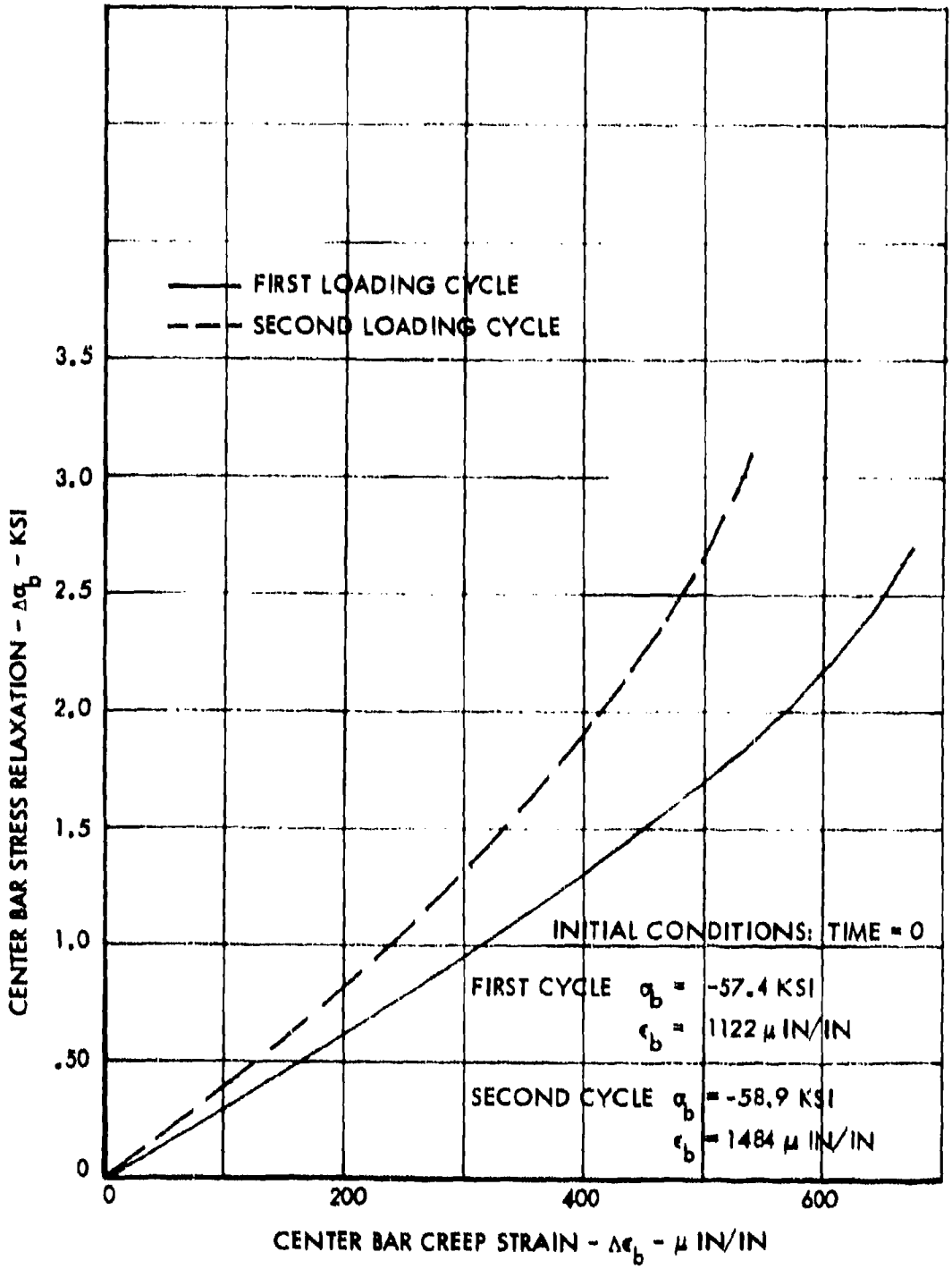

Figure 46. Creep/Stress Relaxation Measurements From Simplified Stress Concentration Specimen - Sequence 1

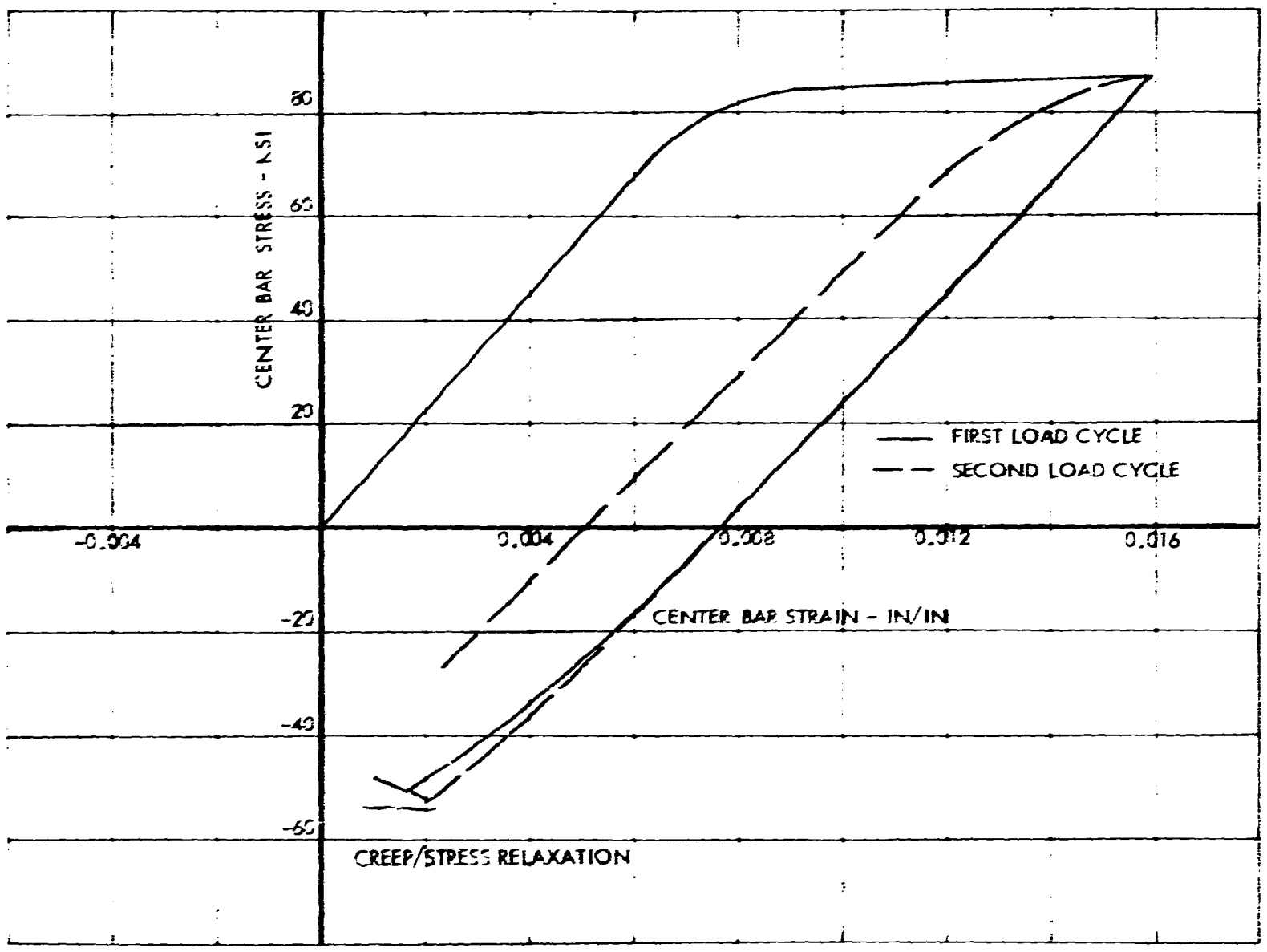

Figure 47. Simplified Stress Concentration Specimen - Center Bar Stress-Strain Data Sequence No. 1 Repeat

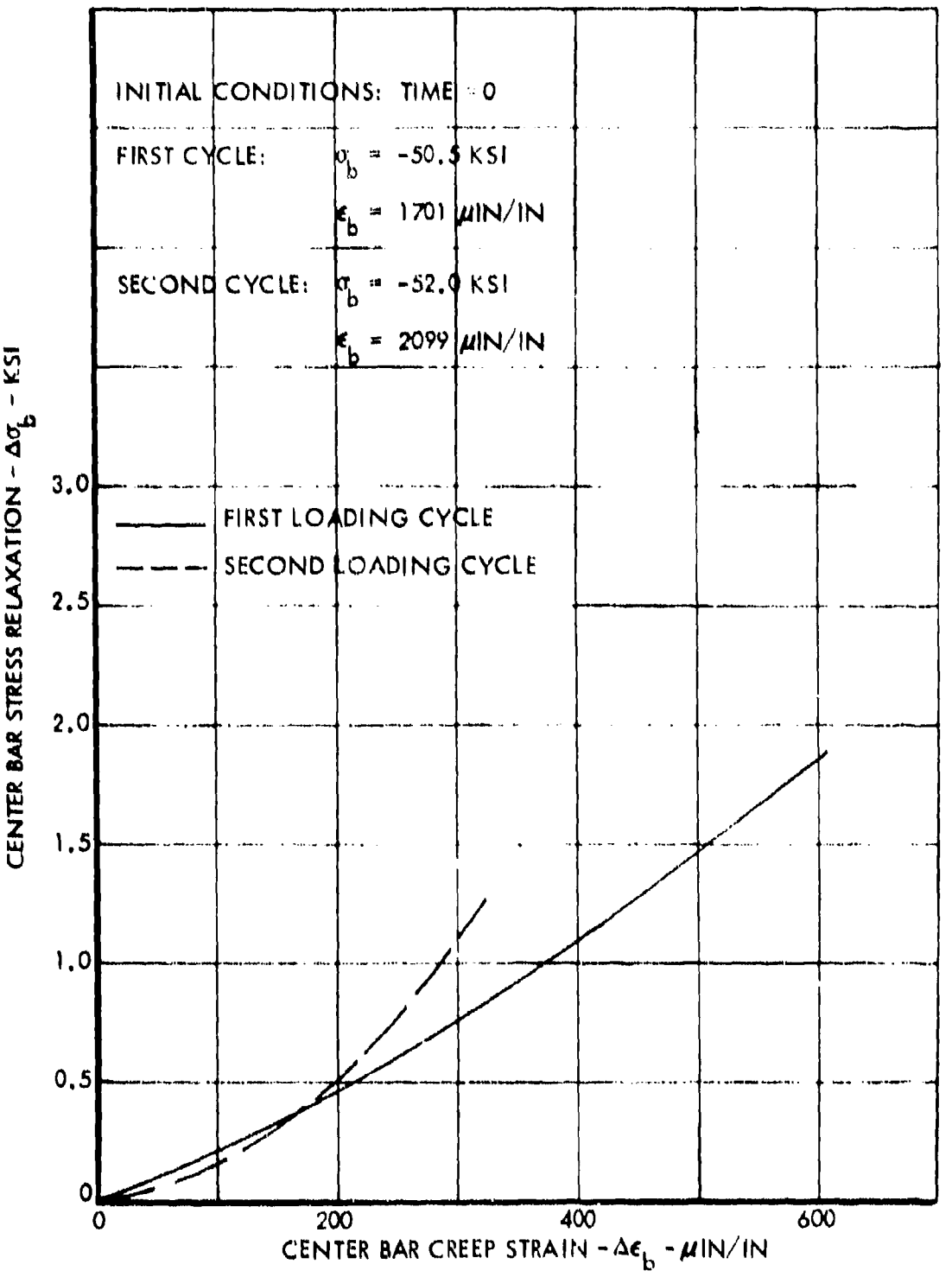

Figure 48. Creep/Stress Relaxation Measurements From Simplified Stress Concentration Specimen - Repeat Sequence 1.

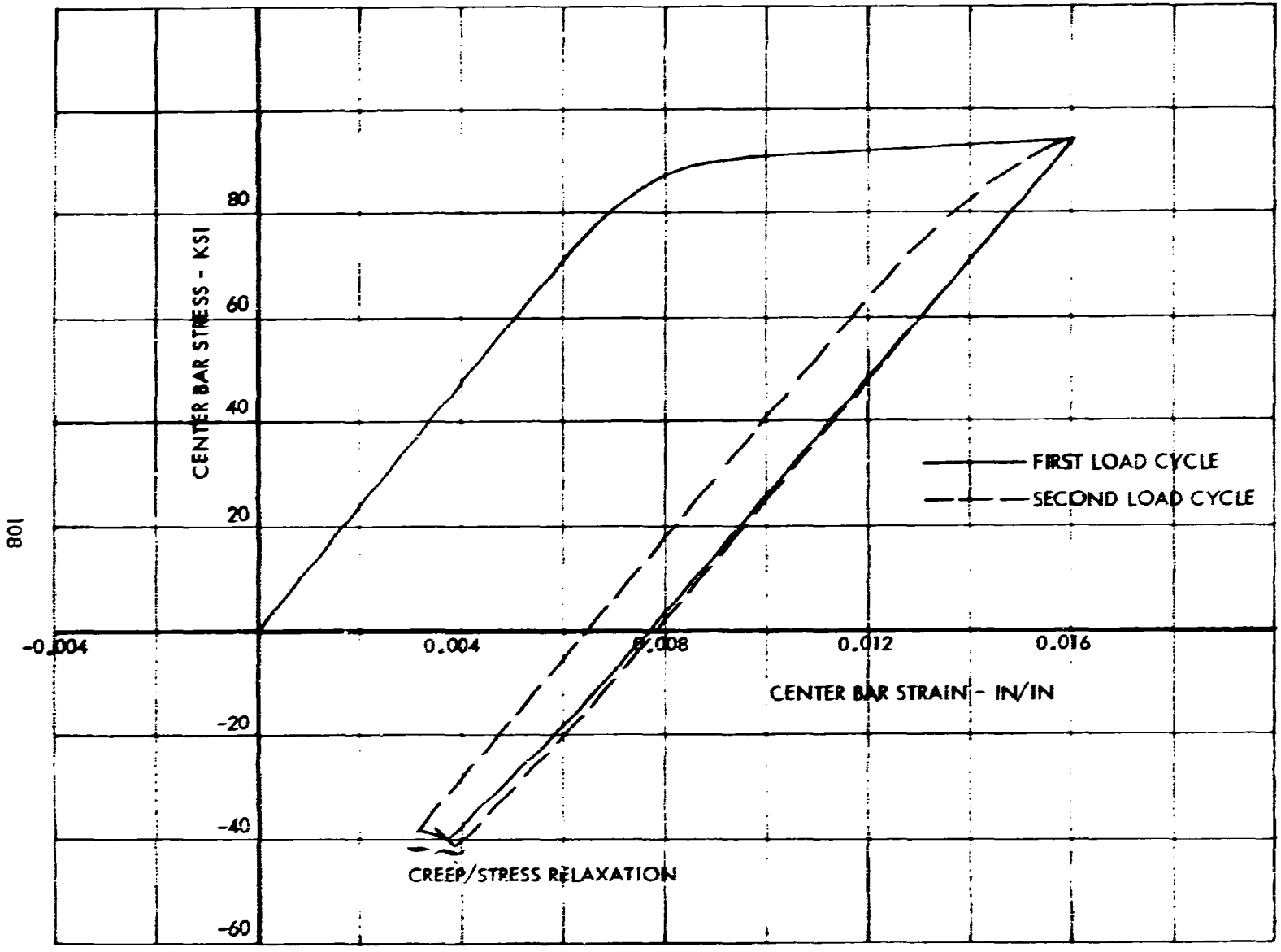

Figure 49. Simplified Stress Concentration Specimen Sequence 2
Center Bar Stress-Strain Data

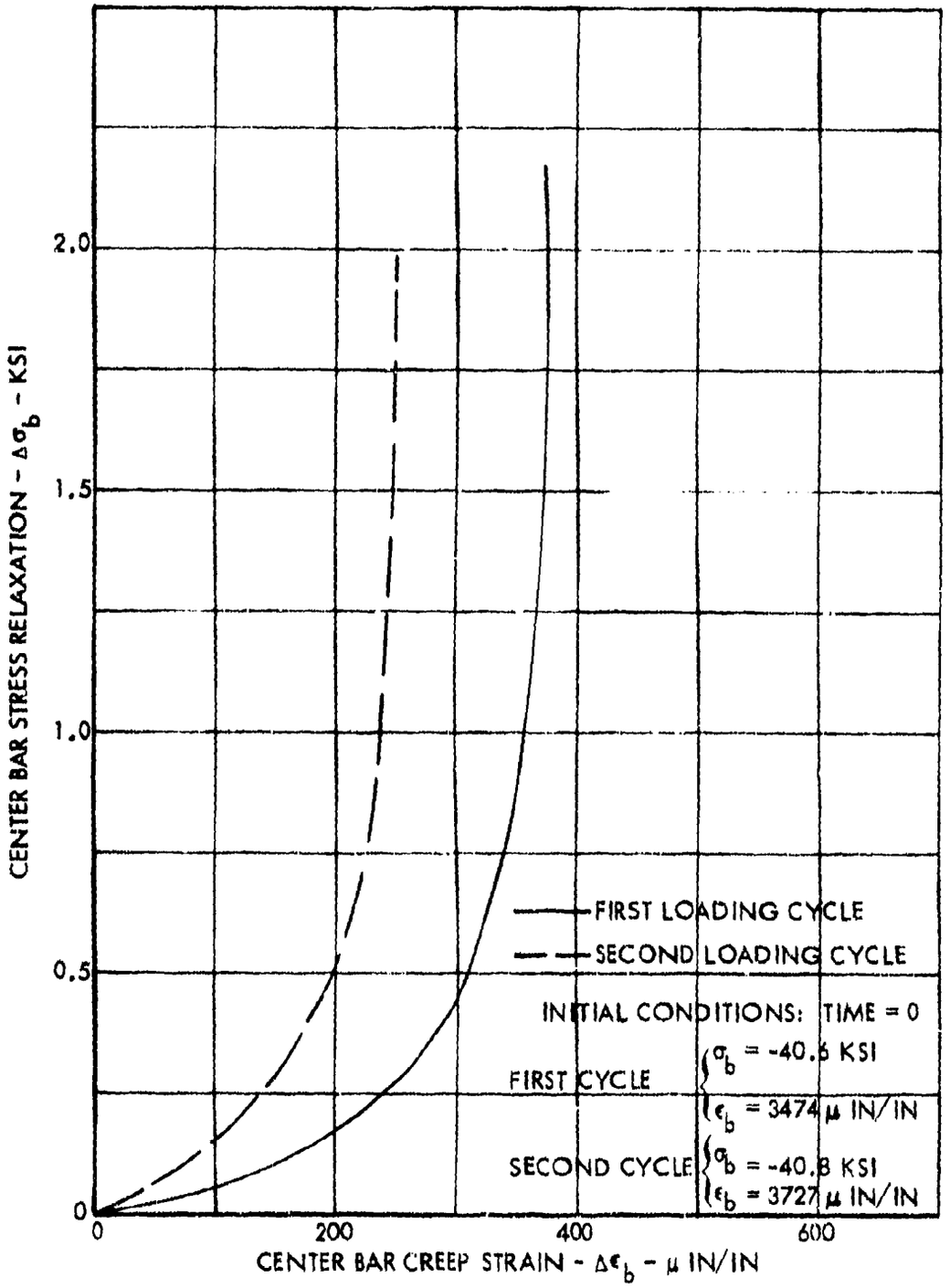

Figure 50. Creep/Stress Relaxation Measurements From Simplified Stress Concentration Specimen - Sequence 2

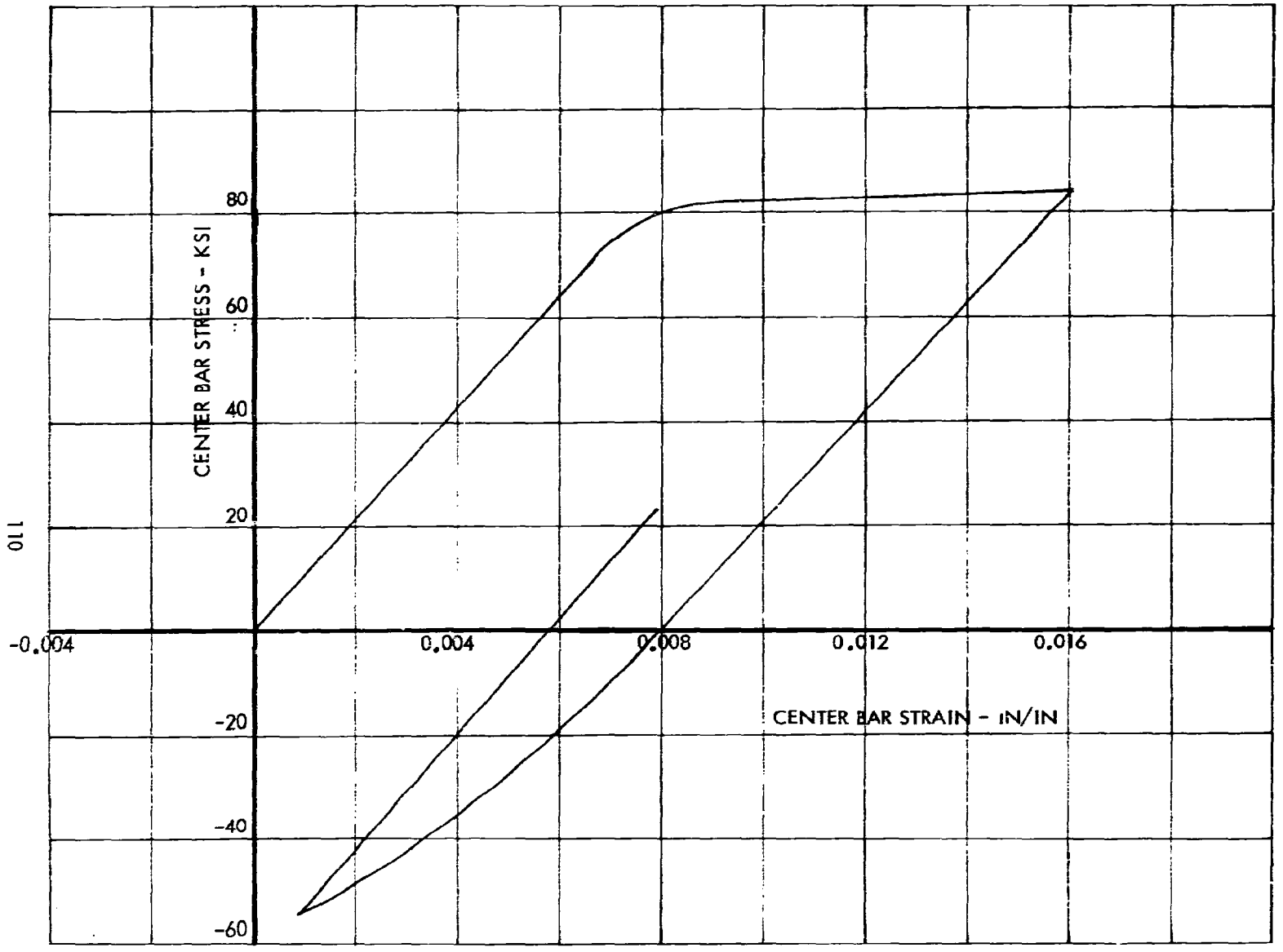

Figure 51. Simplified Stress Concentration Specimen, Sequence 3-1
Center Bar Stress-Strain Data

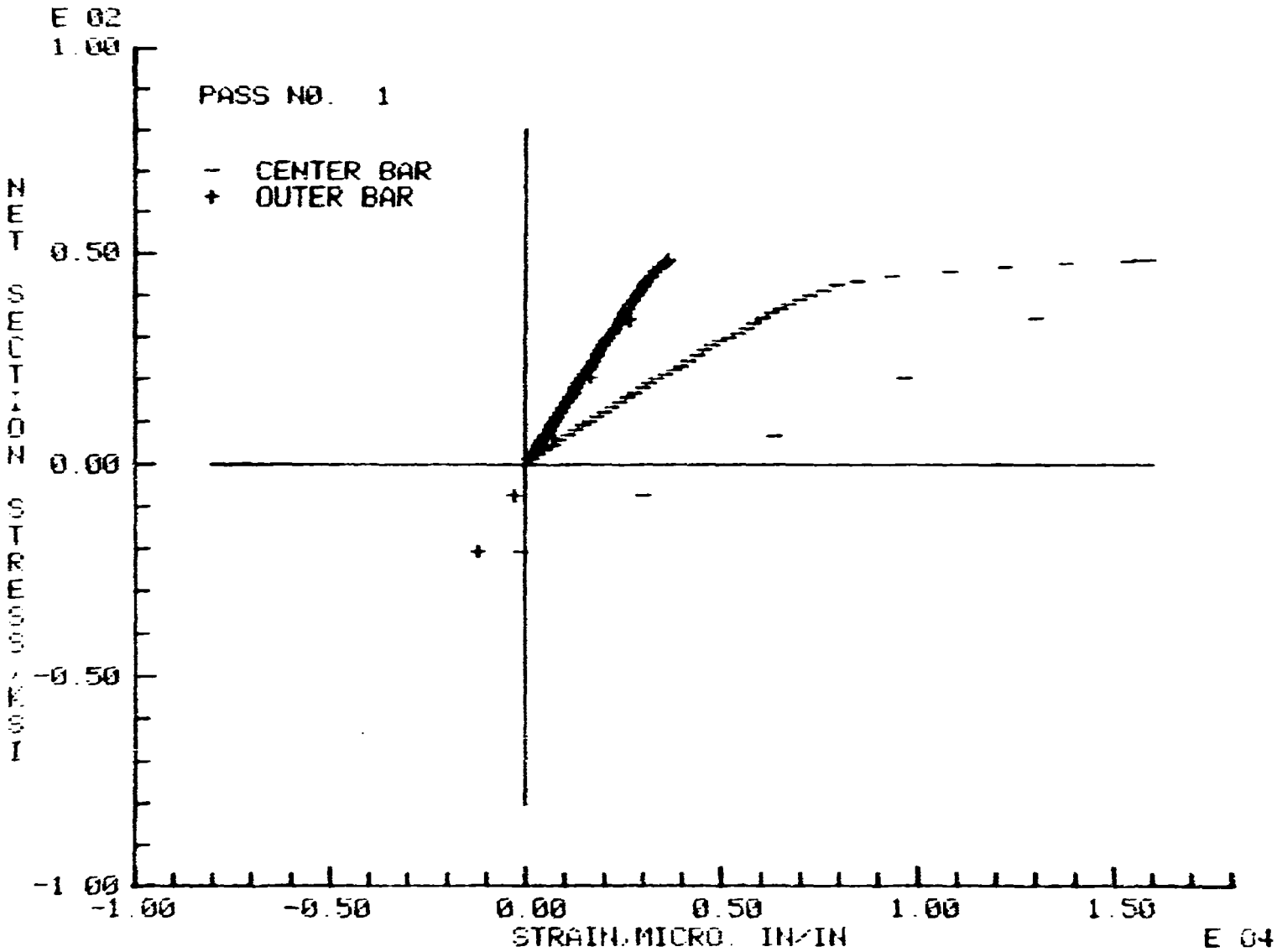

Figure 52. Typical Stress-Strain Data for Simplified Stress Concentration Specimen - Sequence 3, Specimen 2

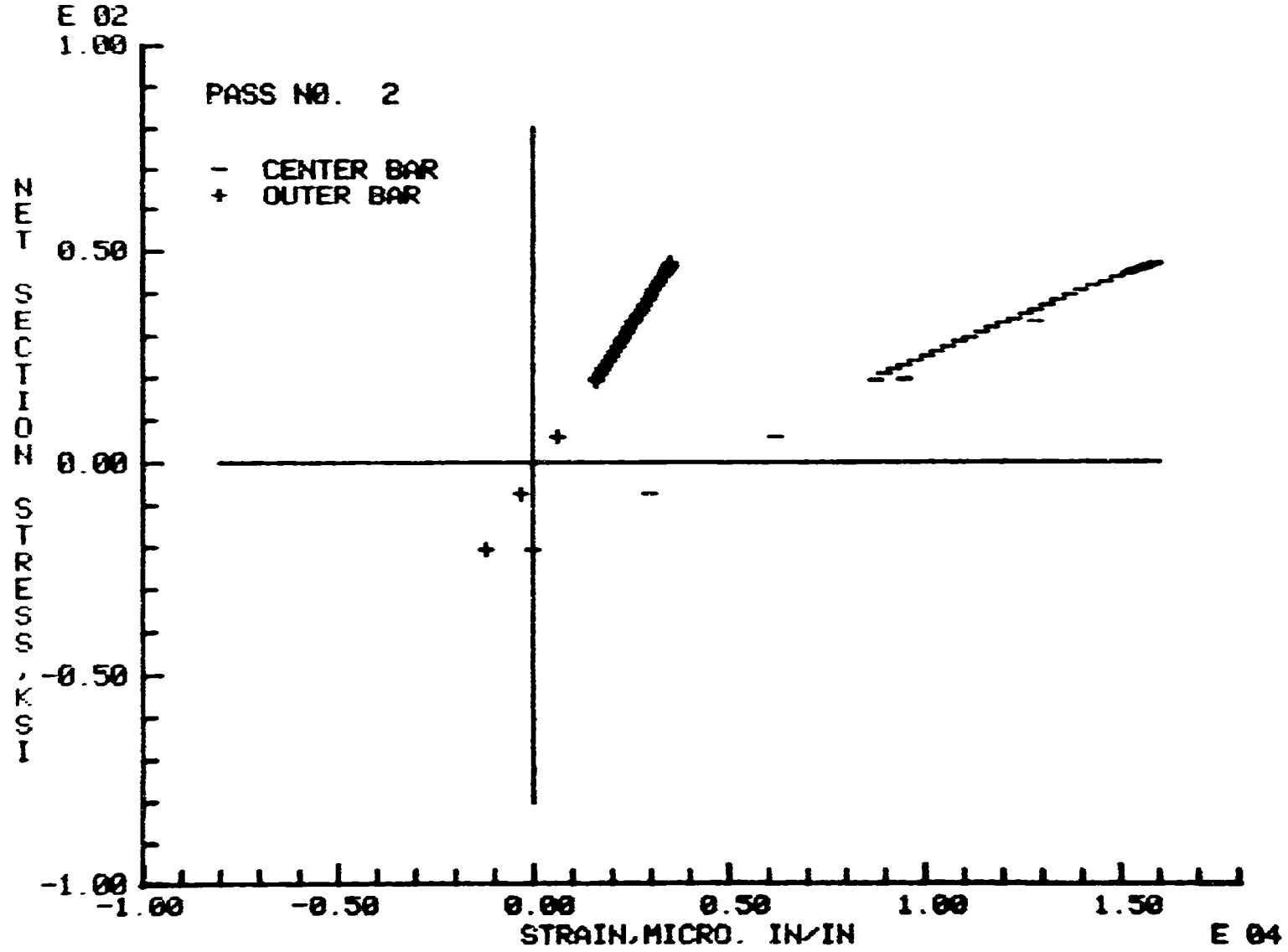

Figure 52. (Continued)

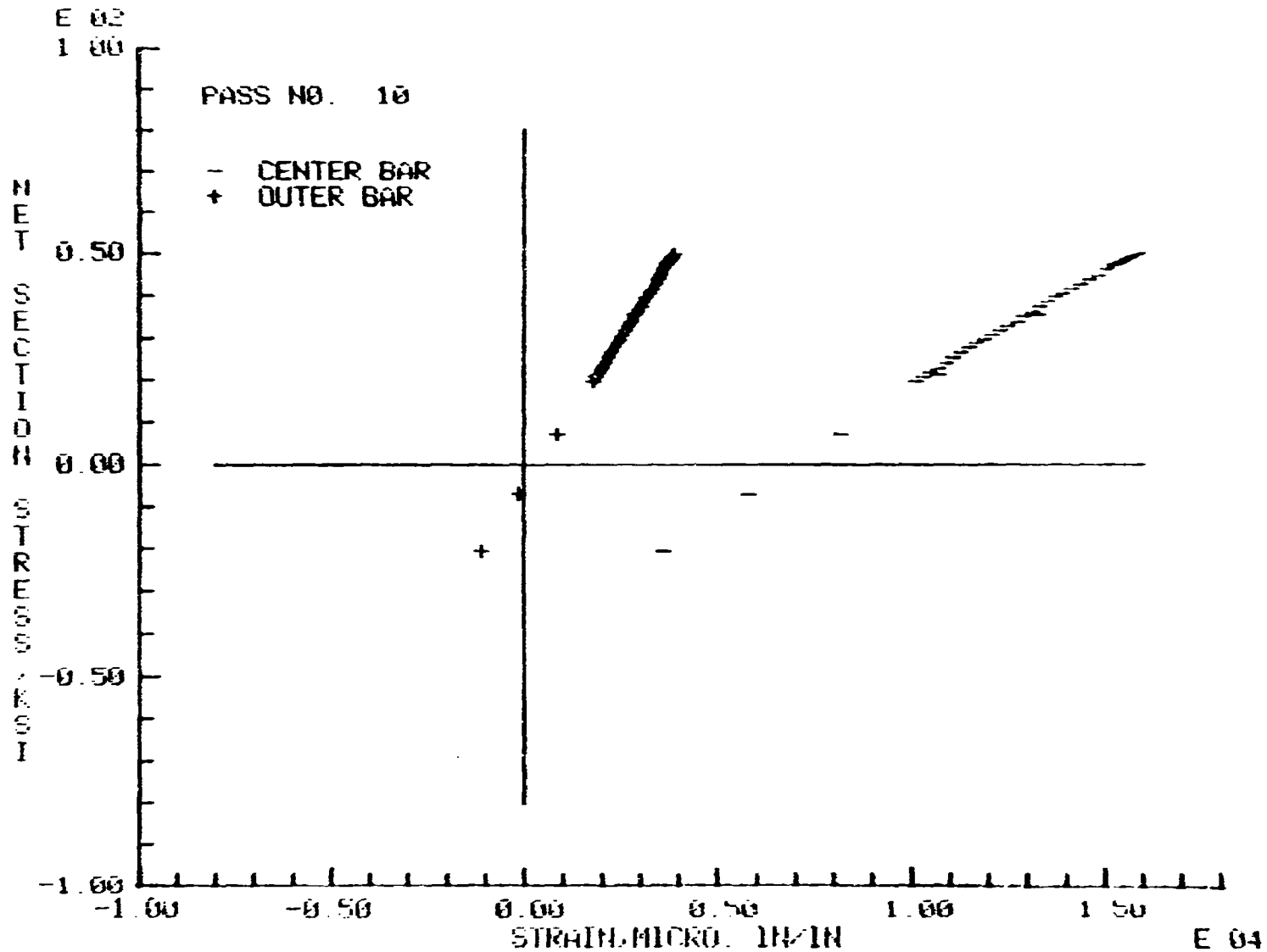

Figure 52. (Concluded)

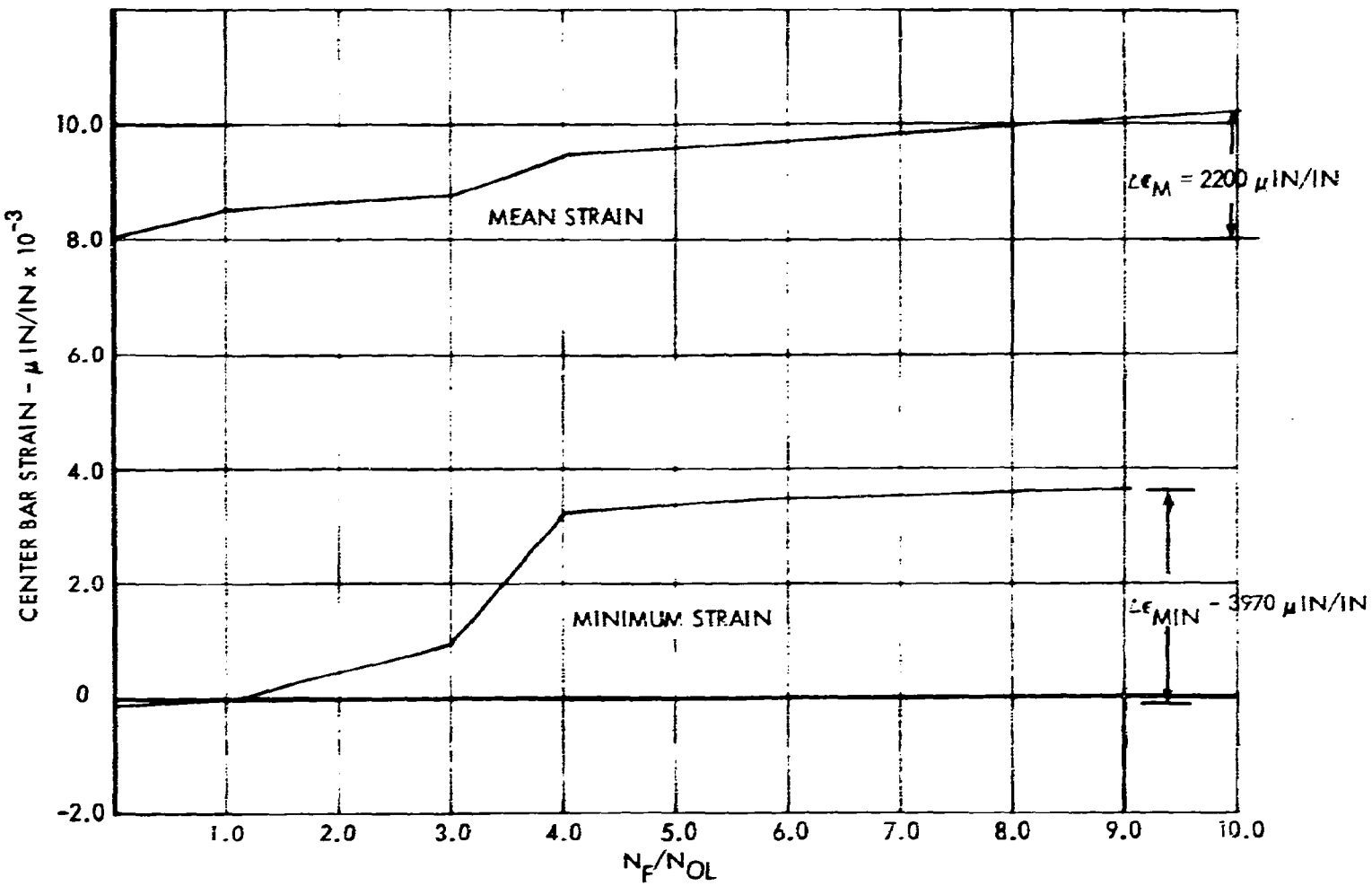

Figure 53. Strain Time History - Simplified Stress Concentration Specimen, Sequence No. 3 Test

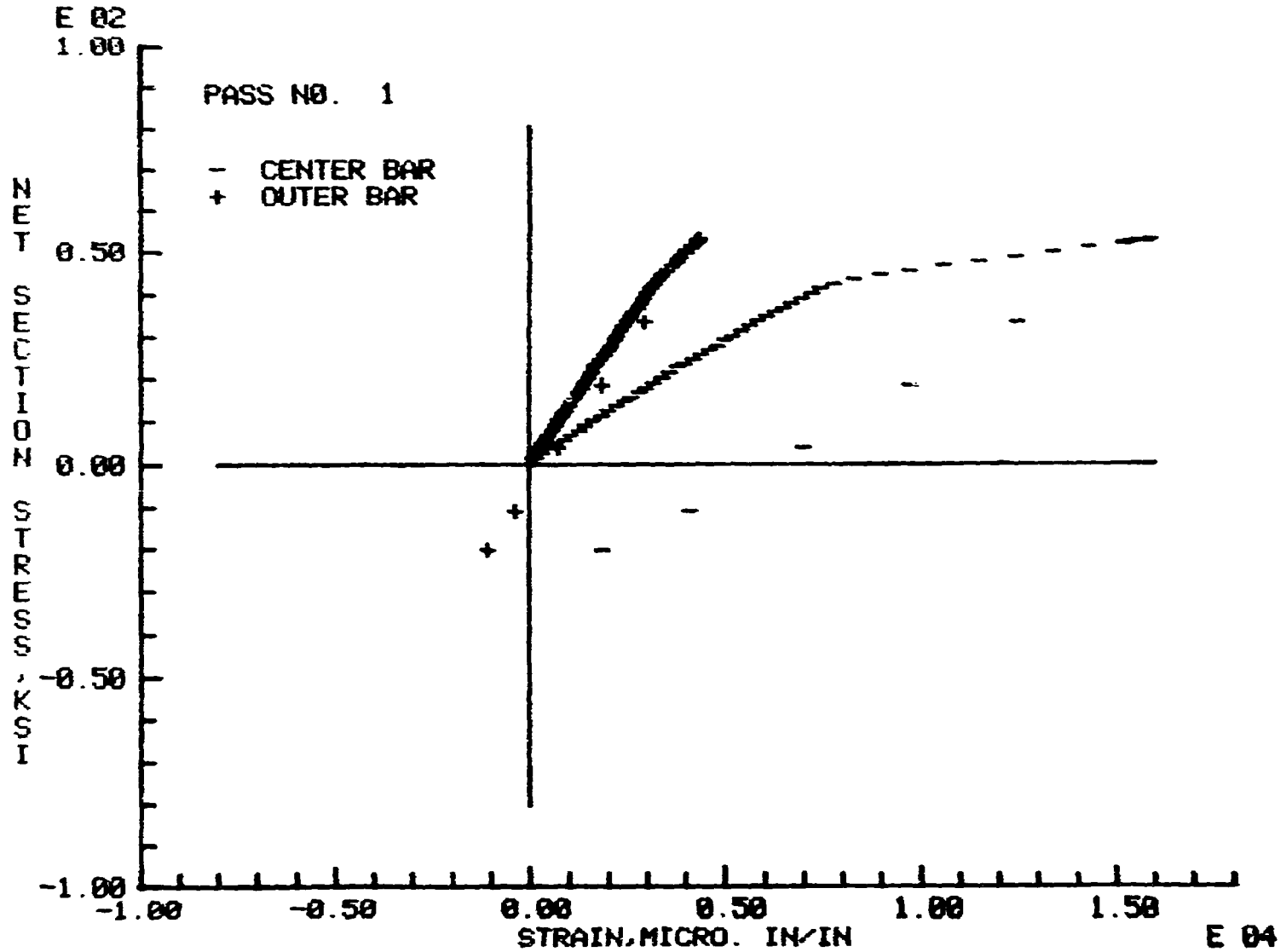

Figure 54. Stress-Strain Curve for Simplified Stress Concentration Specimen - Sequence 4

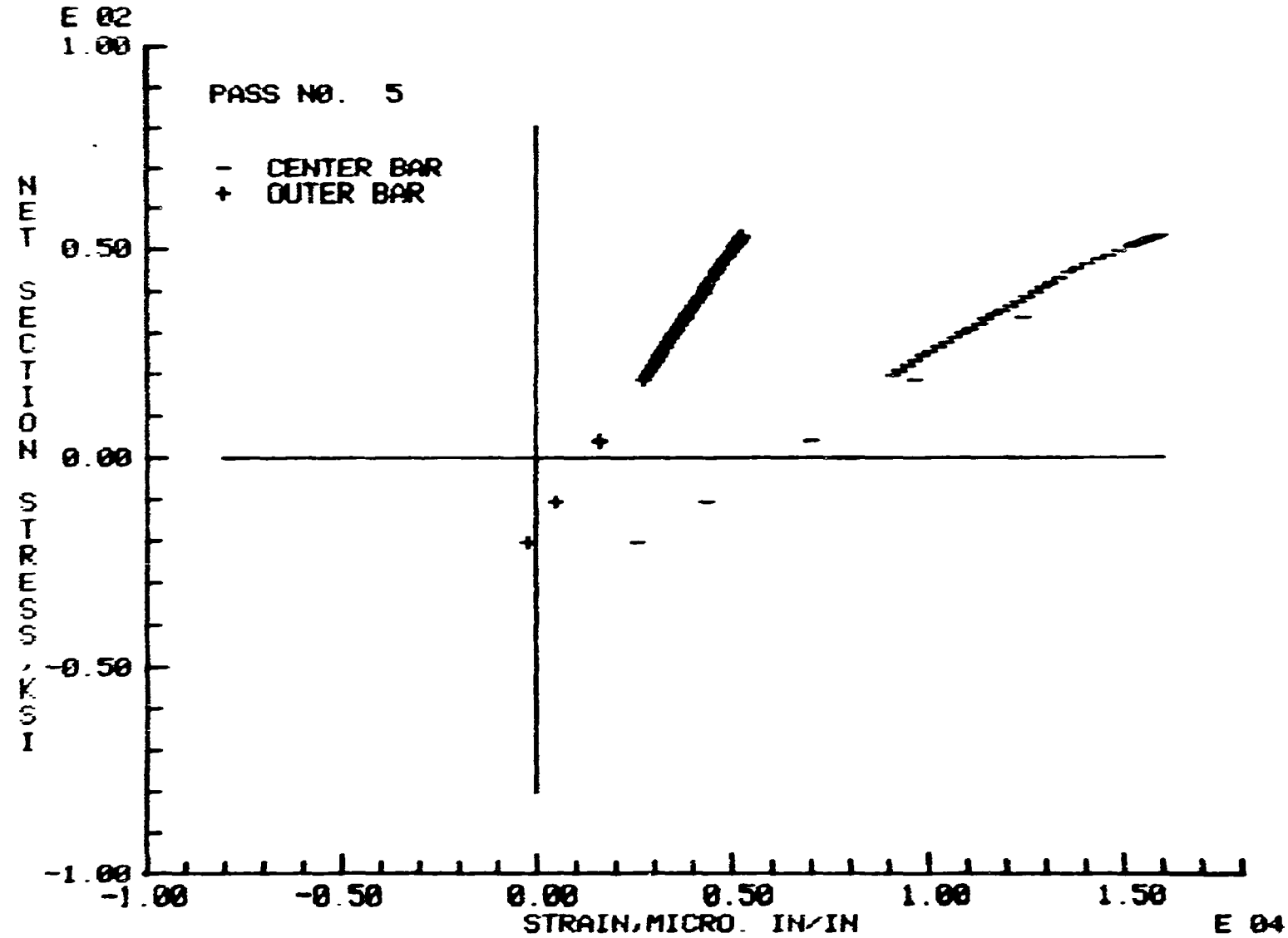

Figure 54. (Continued)

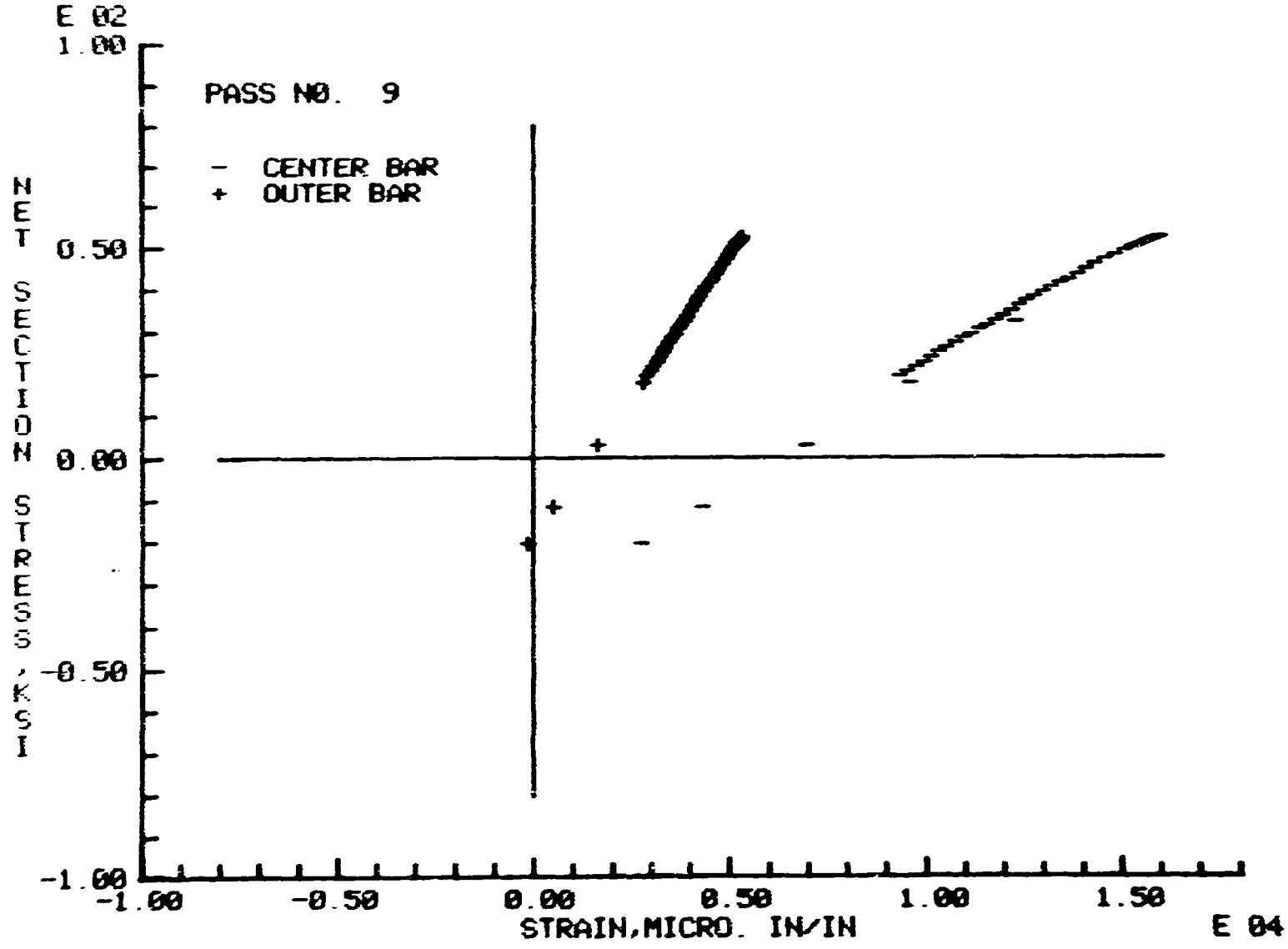

Figure 54. (Concluded)

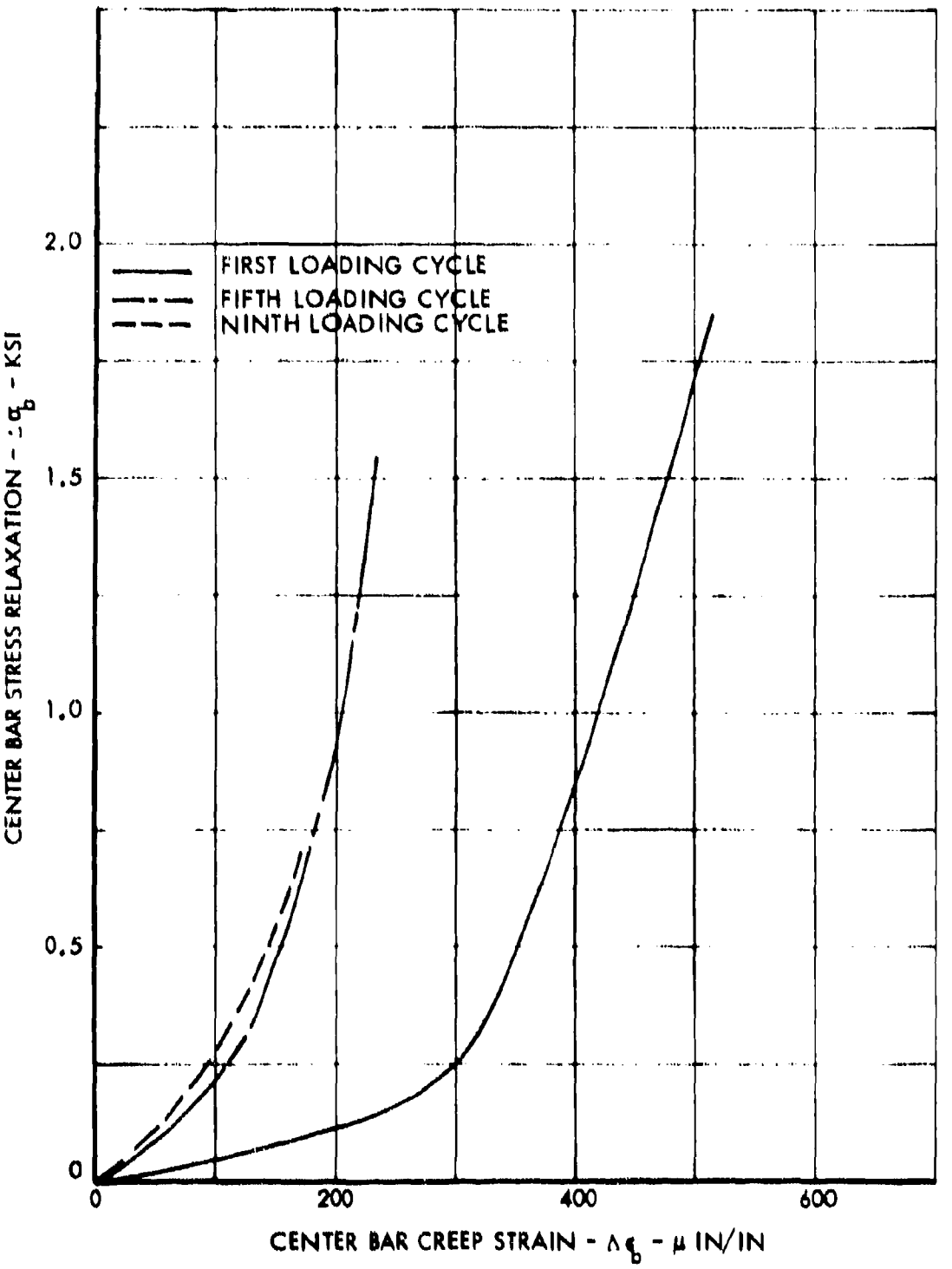

Figure 55. Creep/Stress Relaxation Measurements From Simplified Stress Concentration Specimen - Sequence No. 4

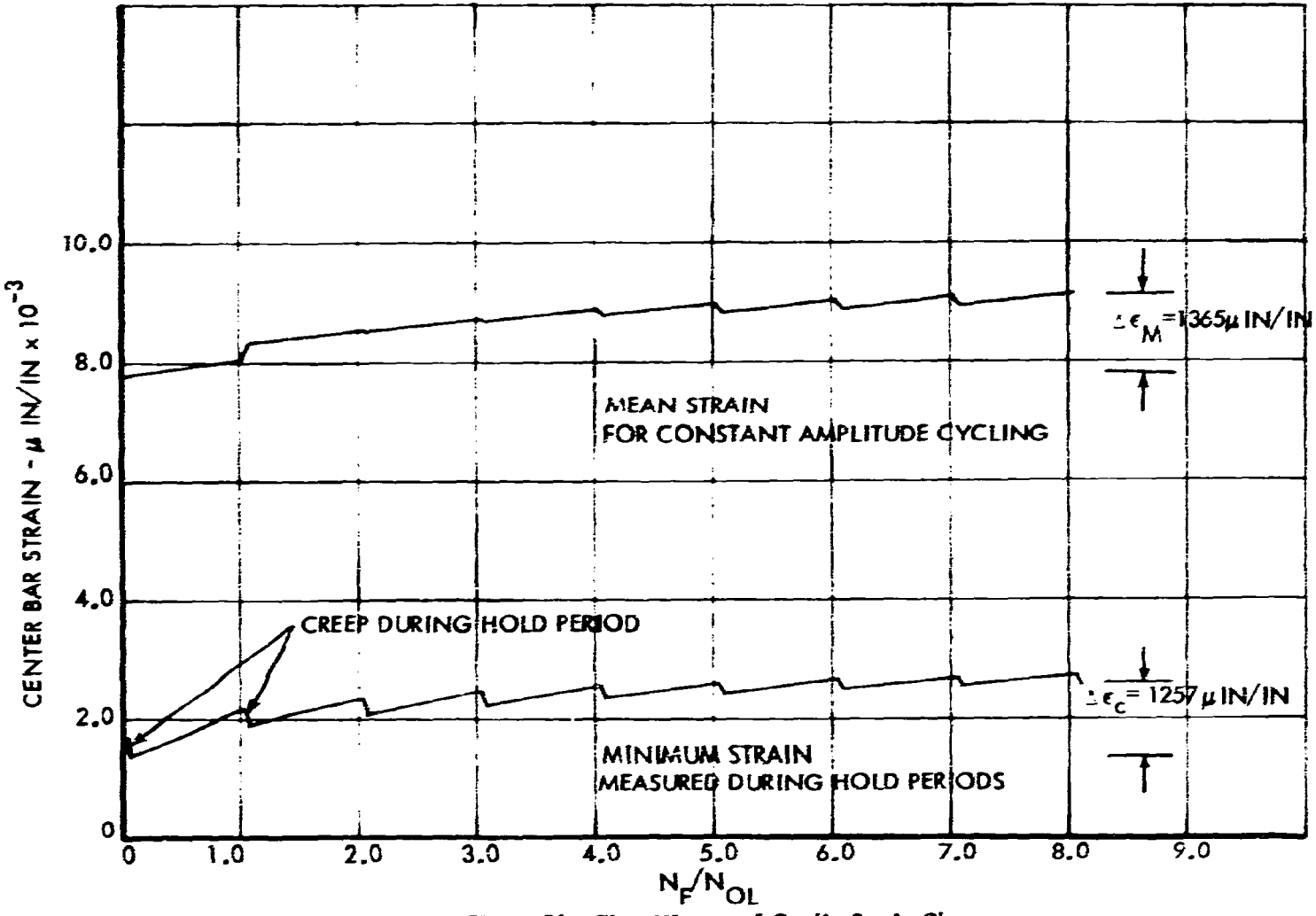

Figure 56. Time History of Cyclic Strain Change
Sequence No. 4

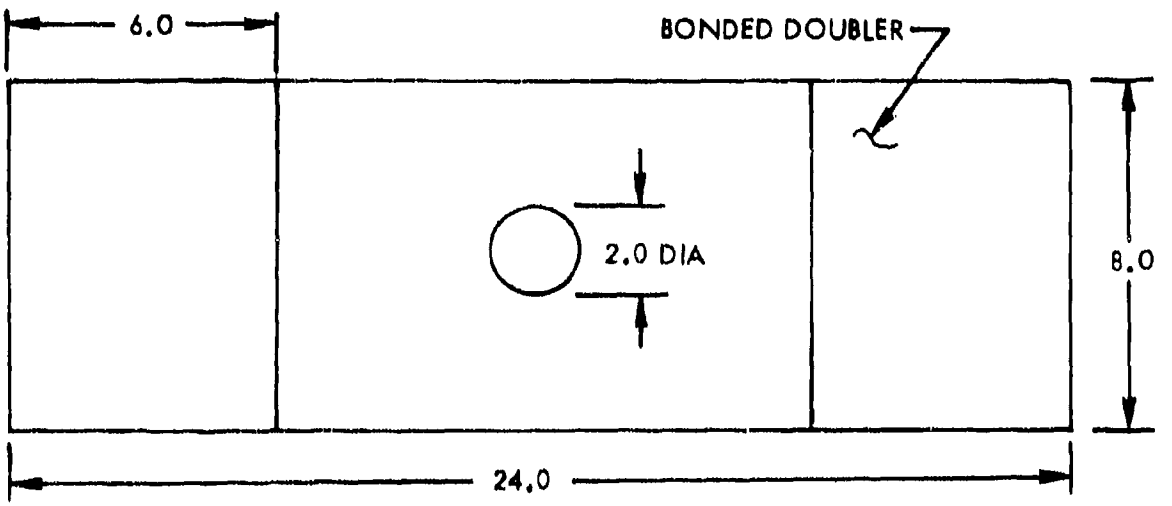

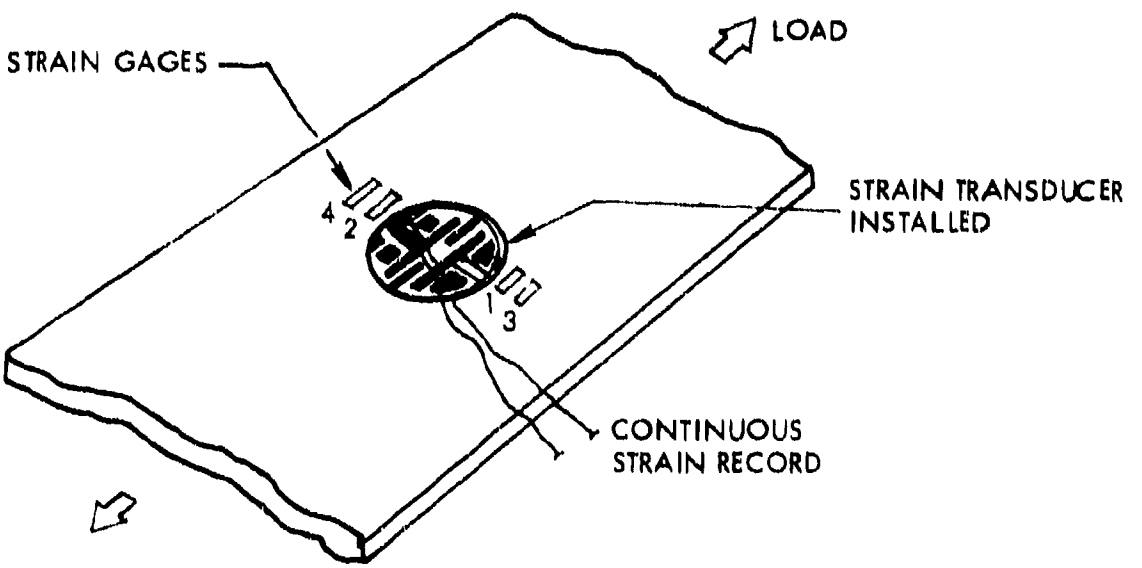

Figure 57. Super-Scale Test Specimen

SEQUENCE DEFINITION	TEST CONDITIONS	TEST LIFE
1. 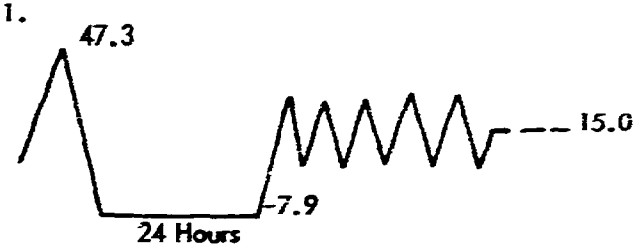	TY - 24 Hours @ -7.9 - CA, F_M = 15	80,018 Cycles
2. 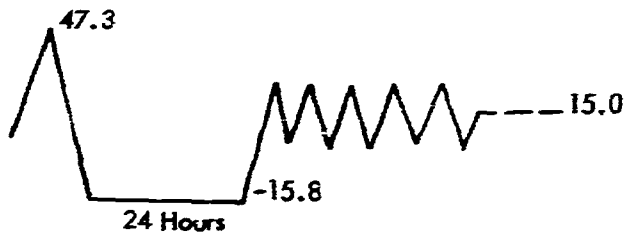	TY - 24 Hours @ -15.8 - CA, F_M = 15	49,867 Cycles
3. 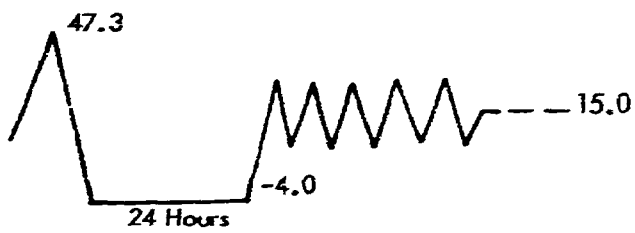	TY - 24 Hours @ -4.0 - CA, F_M = 15	44,277 Cycles
4. 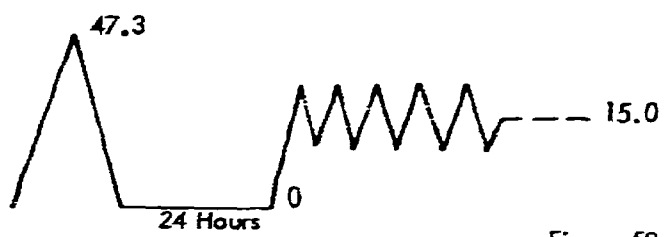	TY - 24 Hours @ Zero - CA, F_M = 15	135,801 Cycles

Figure 58. Super-Scale Specimen Test Summary

SEQUENCE DEFINITION	TEST DEFINITIONS	TEST LIFE
5. 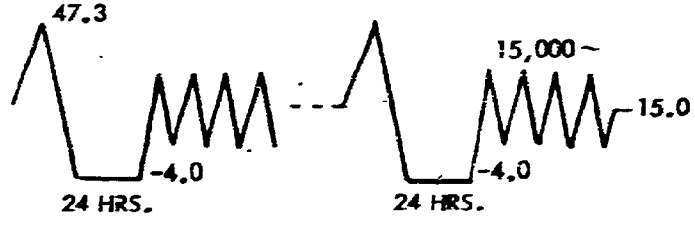	TY, 24 Hours @ -4.0 KSI CA, F_M = 15, F_V = ±10 N_{OL} = 15,000	1,375,000 Cycles
6. 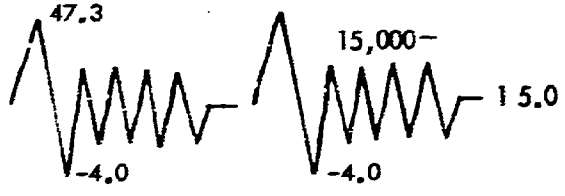	TY, -4.0 KSI, CA. F_M = 15, F_V = ±10 N_{OL} = 15,000	1,269,770 Cycles
7. 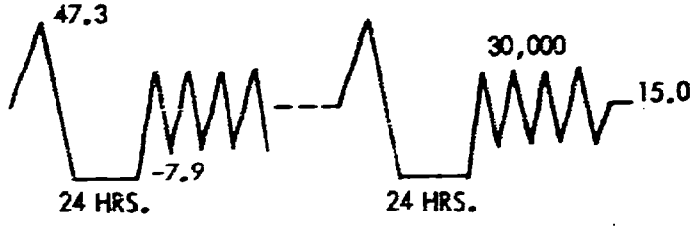	TY, 24 Hours @ -7.9 KSI, CA, F_M = 15, F_V = ±10 N_{OL} = 30,000	214,546 Cycles ① 88,000 Cycles ②

① Three 24-hour hold periods then cycled to failure.

② Five 24-hour hold periods then cycled to failure.

Figure 58. (Continued)

SEQUENCE DEFINITION	TEST DEFINITION	TEST LIFE
8. 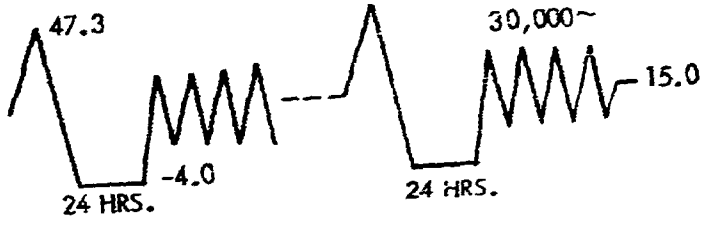	TY, 24 Hours @ -4.0 KSI CA, F_M = 15, F_V = ± 10, N_{OL} = 30,000 Cycles	581,557 Cycles
9. 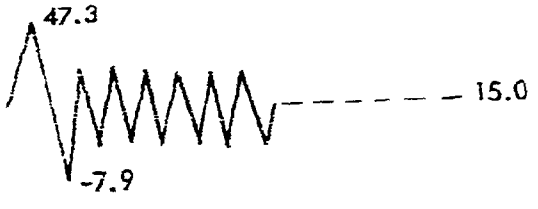	TY, -7.9 KSI CA, F_M = 15, F_V = ± 10 KSI	286,838 Cycles
10. 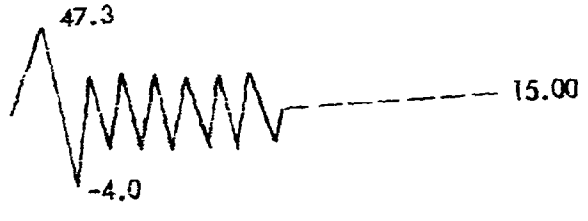	TY, -4.0 KSI CA, FM = 15, F_V = ± 10 KSI	131,956 Cycles

TY = +47.3 KSI Overload
CA = Constant Amplitude, F_M = 15 KSI, F_V = ±10 KSI
N_{CL} = Cycles Between Overloads

Figure 58. (Concluded)

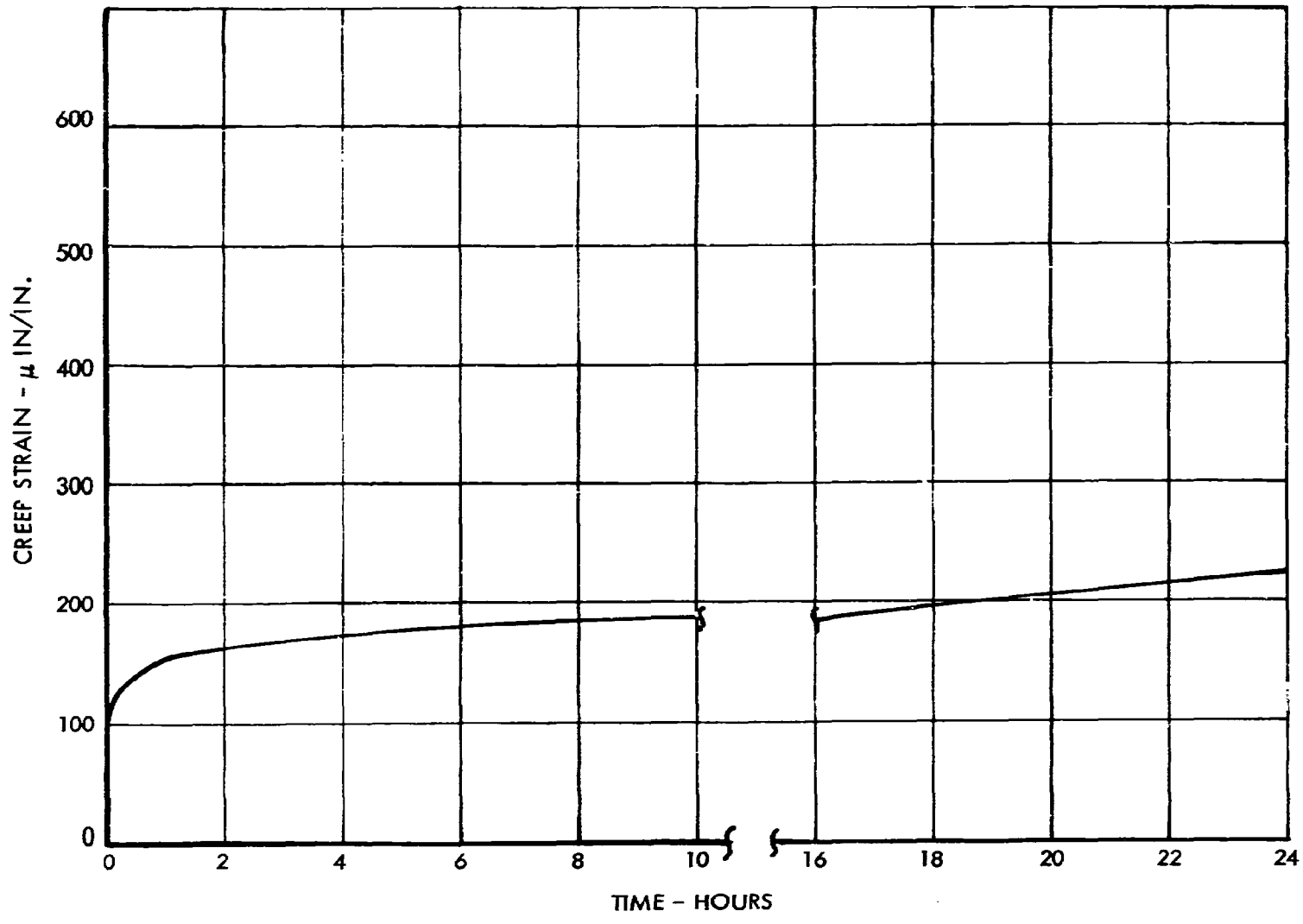

Figure 59. Creep Strain - Super-Scale Test Sequence 5

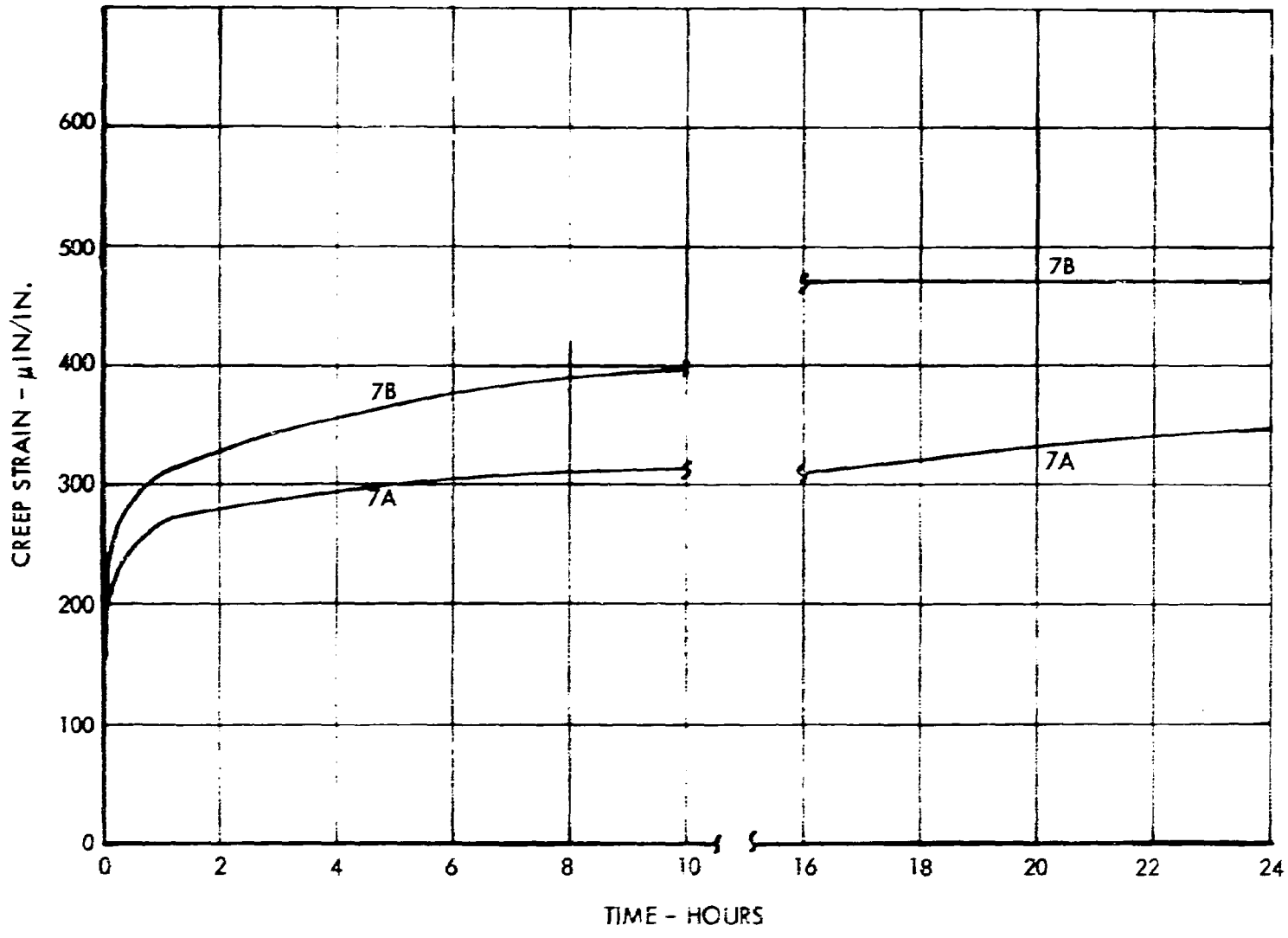

Figure 60. Creep Strain – Super-Scale Test Sequences 7A and 7B

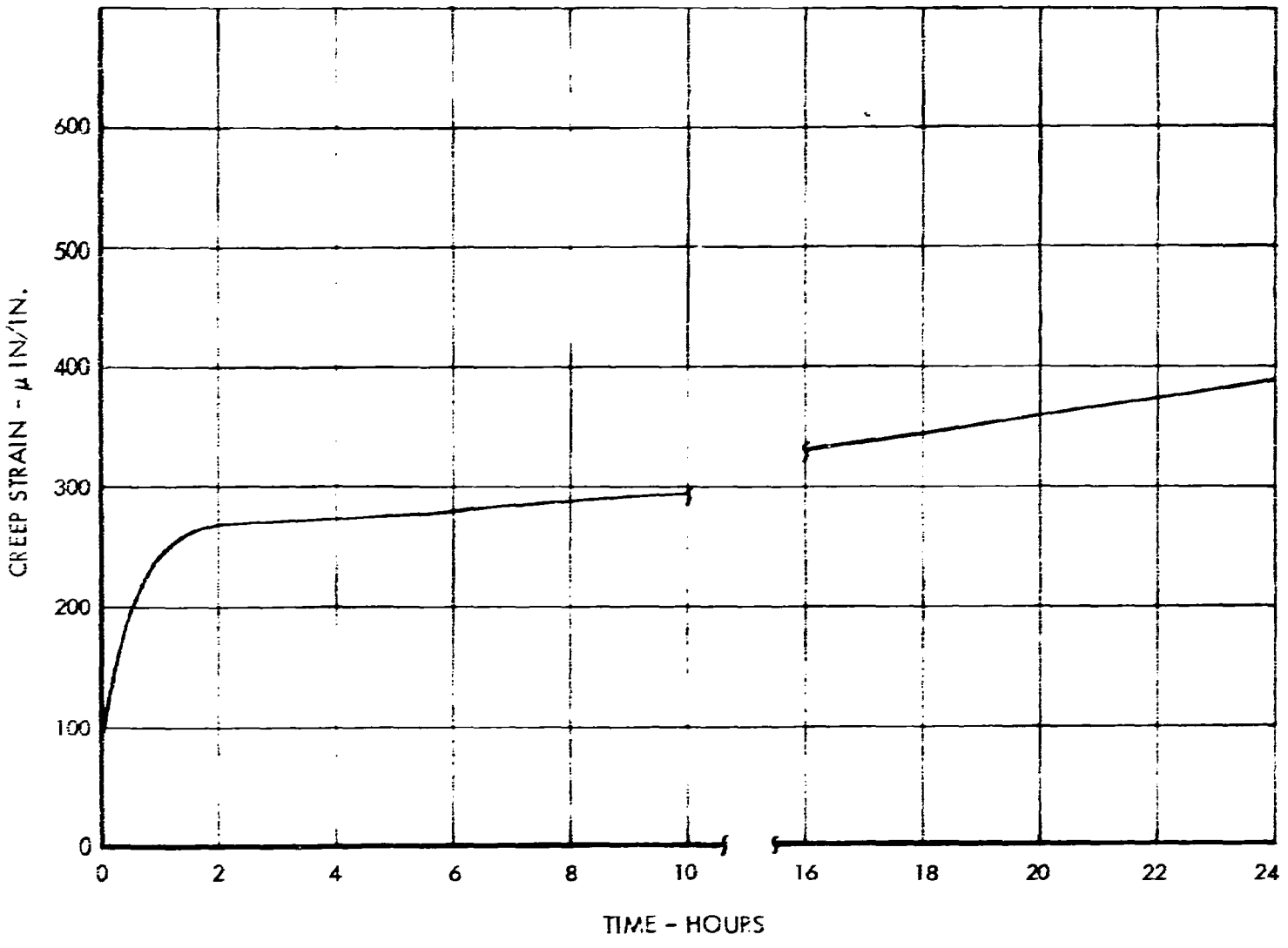

Figure 61. Creep Strain - Super-Scale Test Sequence 8

Figure 62. Typical Wing Lower Surface Mean Stresses - Transport Logistics Mission

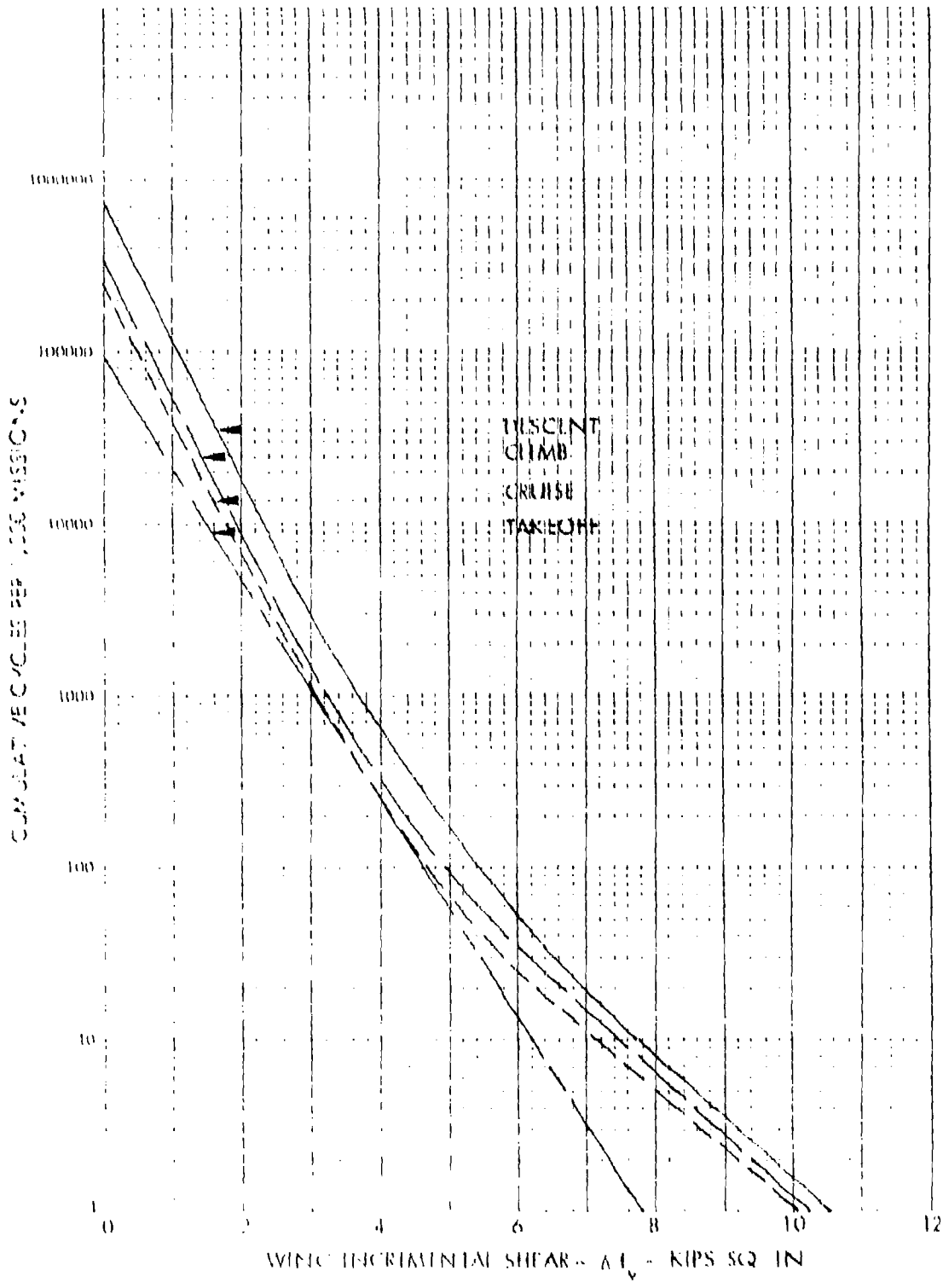

Figure 63. Wing Lower Surface Flight Spectra - Transport Logistics Mission

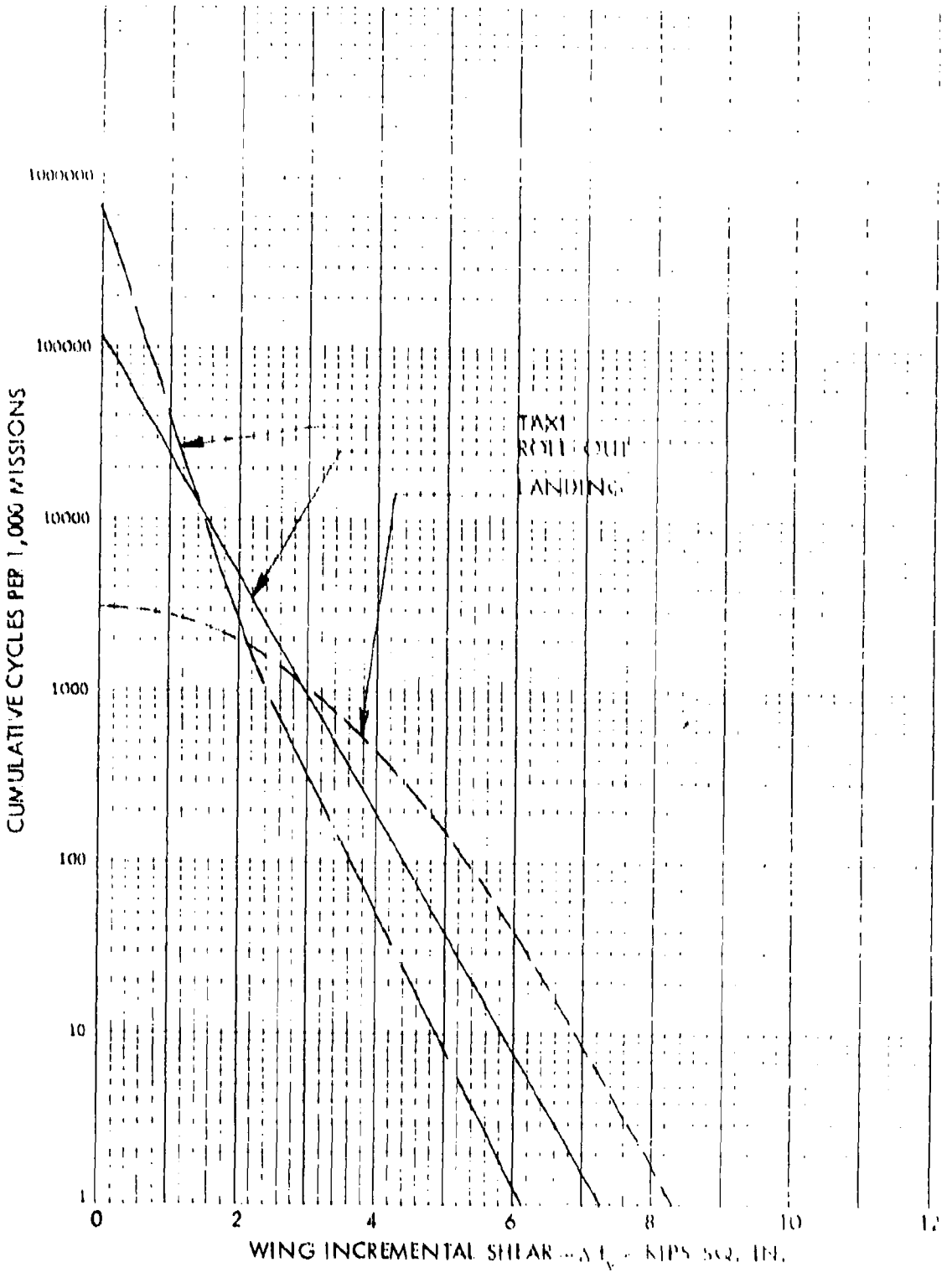

Figure 64. Wing Lower Surface Taxi Spectra – Transport Logistics Mission

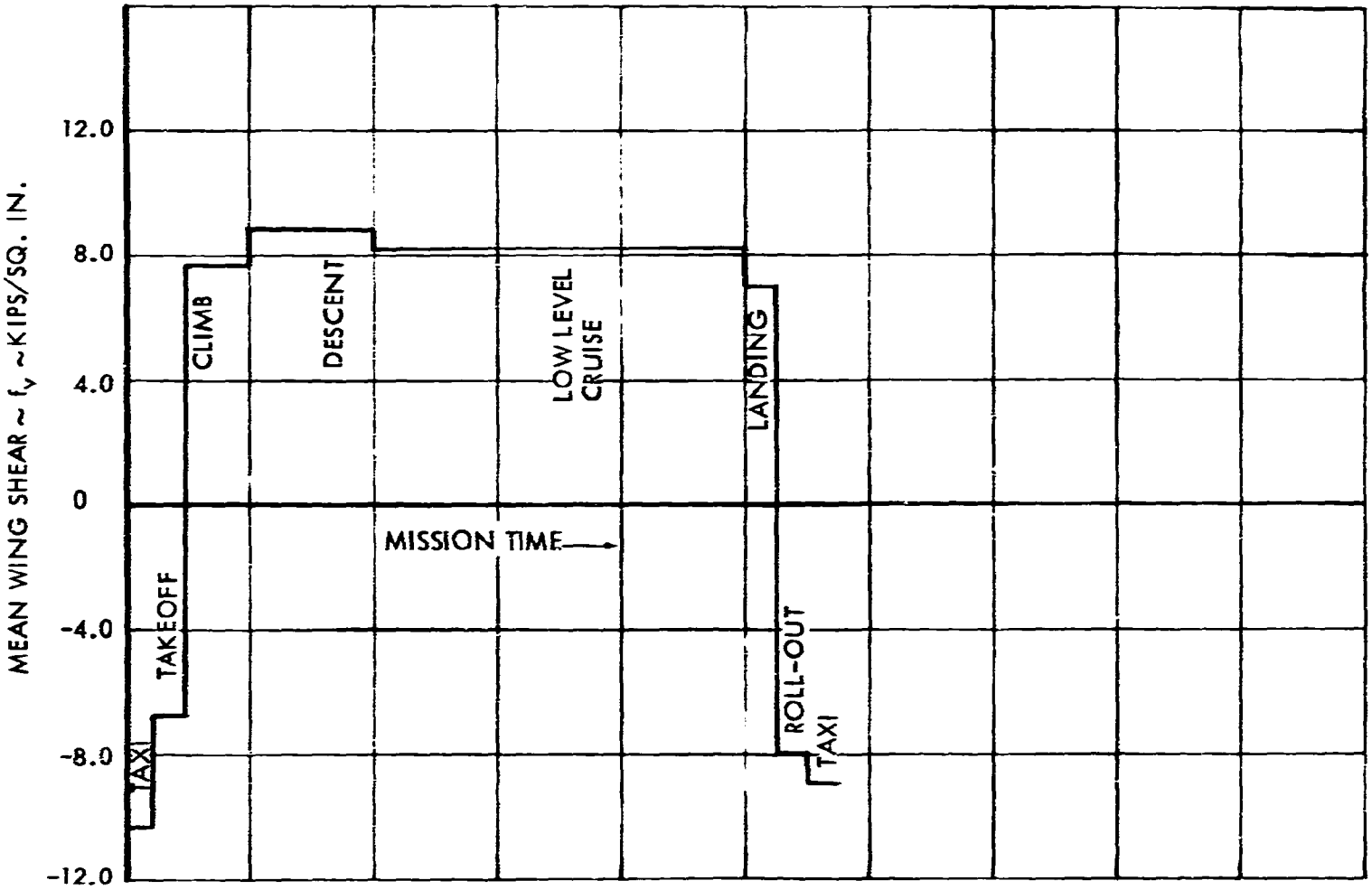

Figure 65. Typical Wing Lower Surface Mean Stresses - Transport Low Level Mission

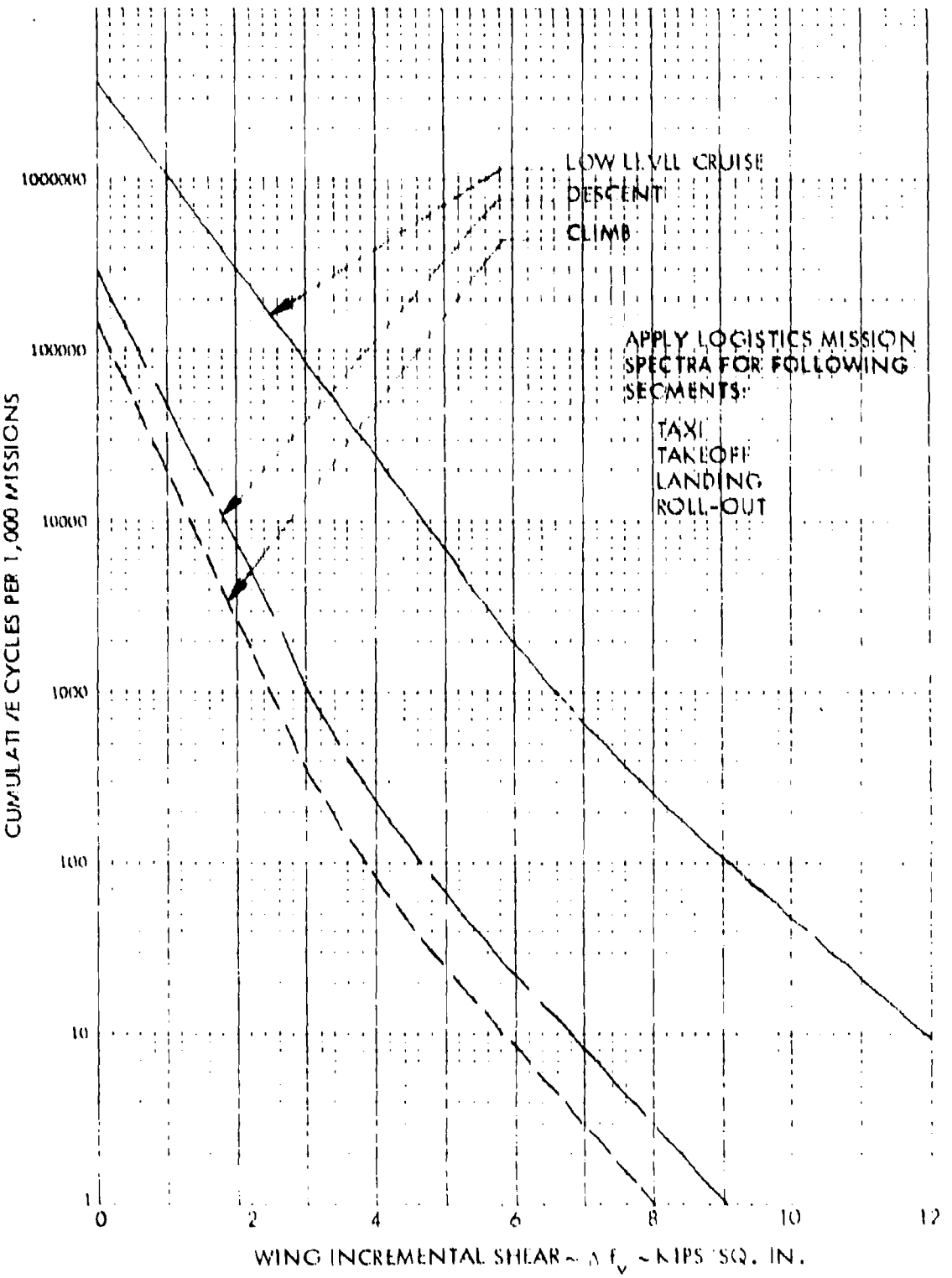

Figure 66. Wing Lower Surface Flight Spectra - Transport Low Level Mission

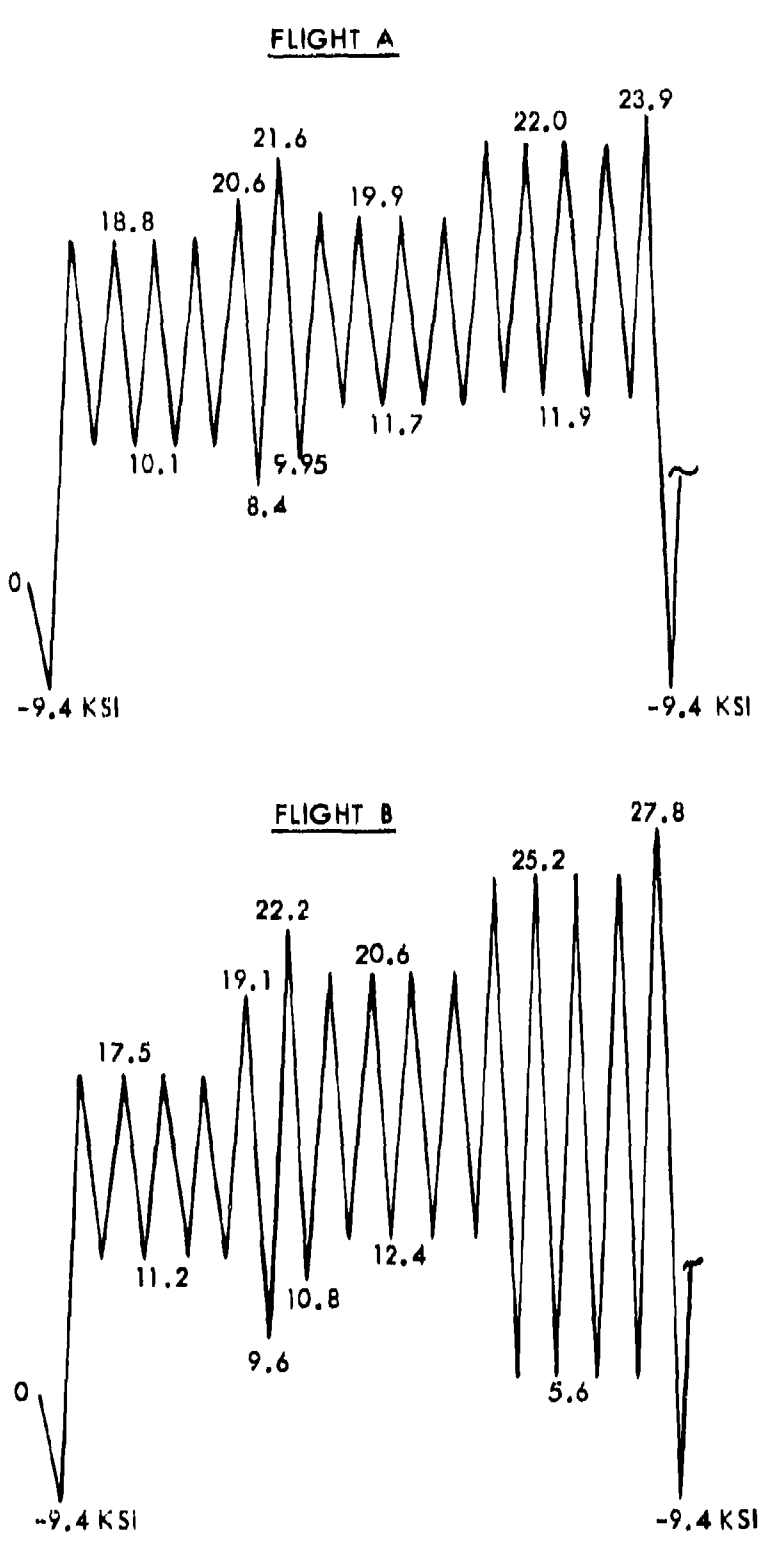

Figure 67. Flight Definition For Spectrum Fatigue Tests

FLIGHT C

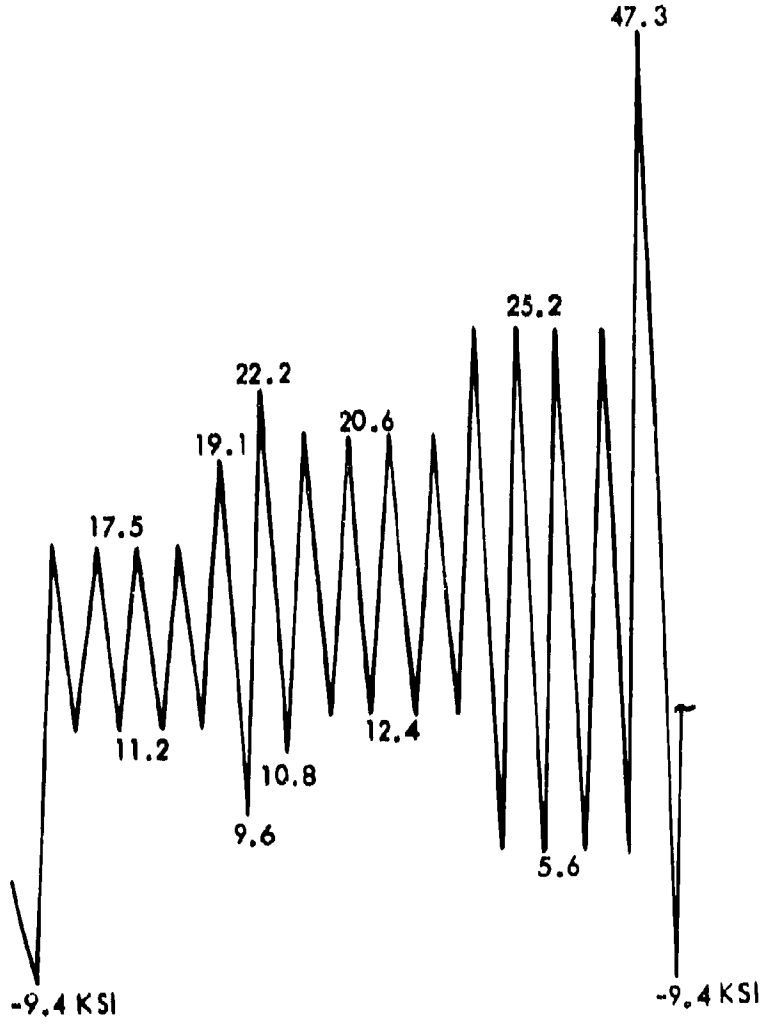

Figure 67. (Continued) Flight Definition For Spectrum Fatigue Tests

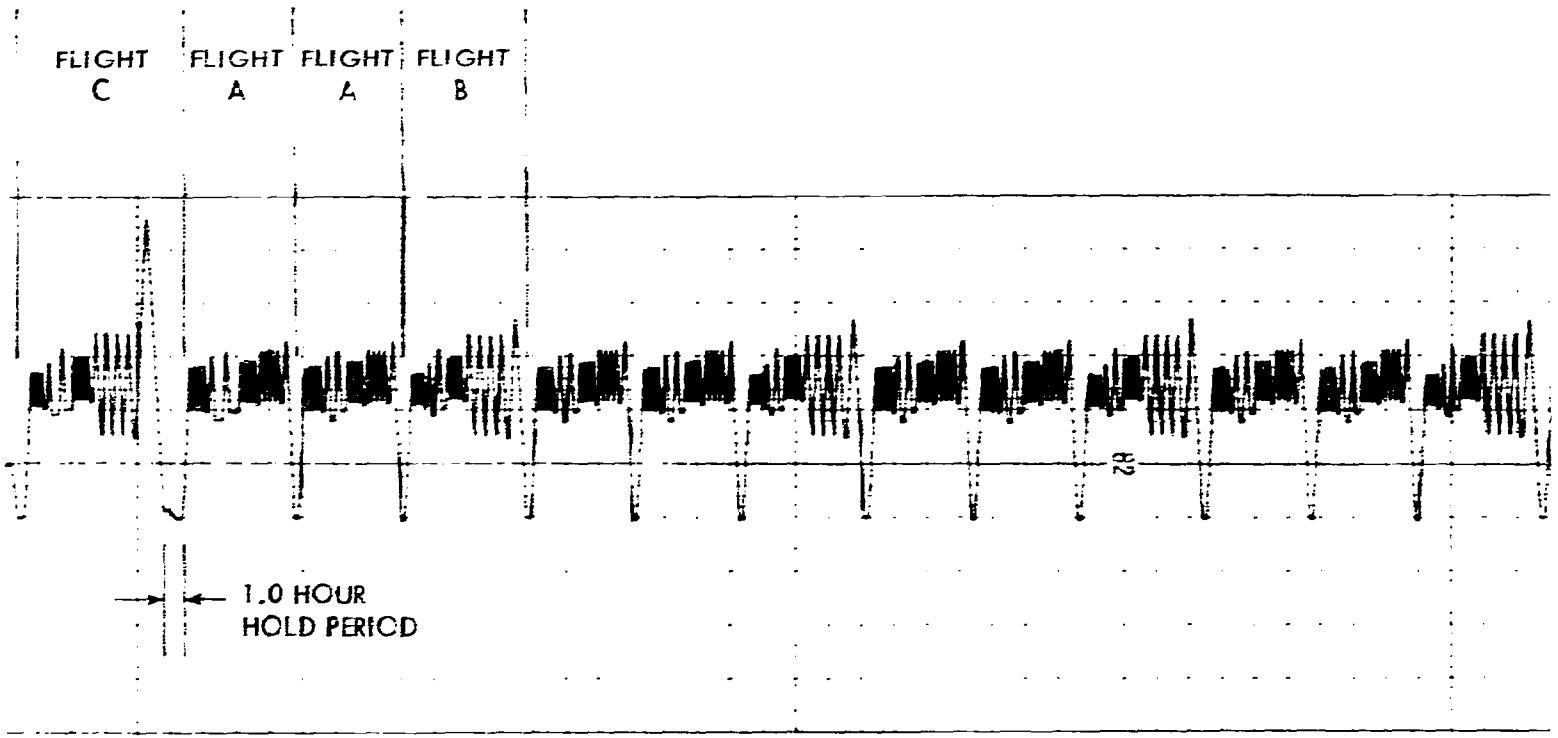

Figure 68. Sample of Strip Chart Record of Spectrum 2 Fatigue Loading

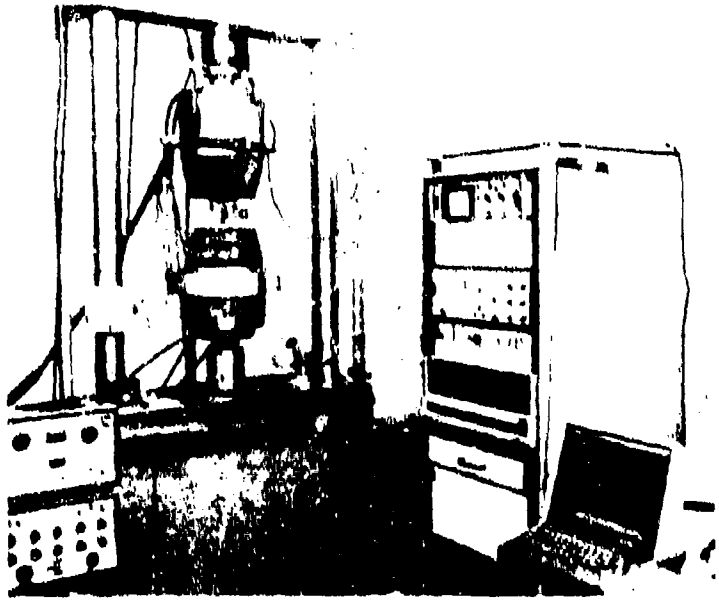

a. Computer Controlled Test Equipment

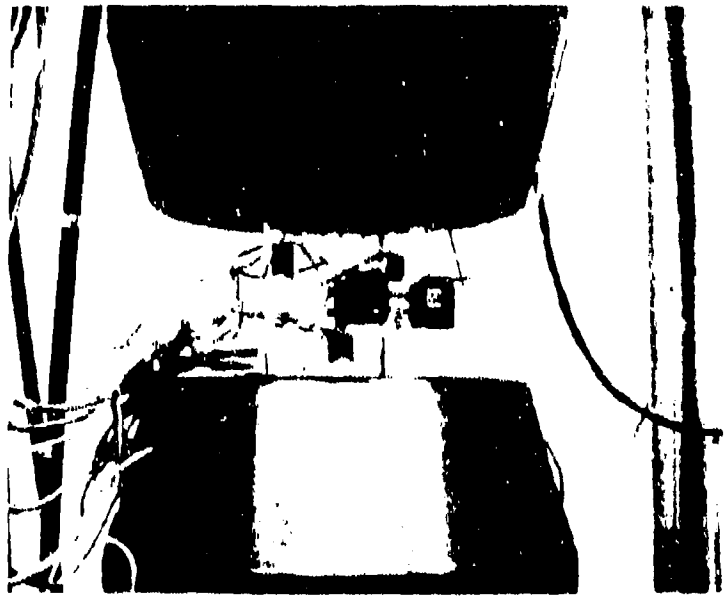

b. Extensometer and Strain Gages Located on Simplified Stress Concentration Specimen

Figure 69. Test Equipment and Test Arrangement for Simplified Stress Concentration Specimen

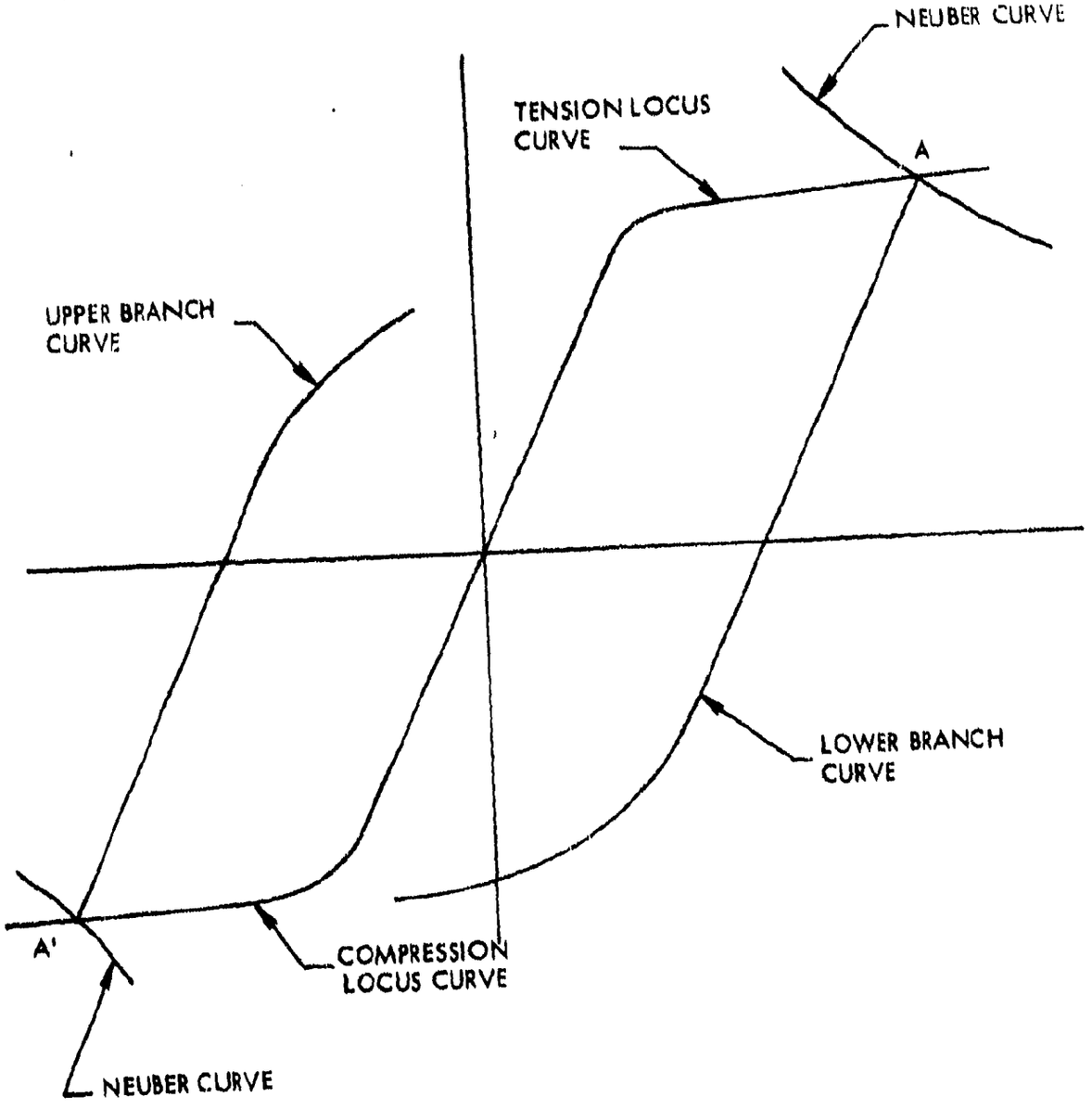

Figure 70. Material Response Algorithm for Hysteresis Analysis Formulation

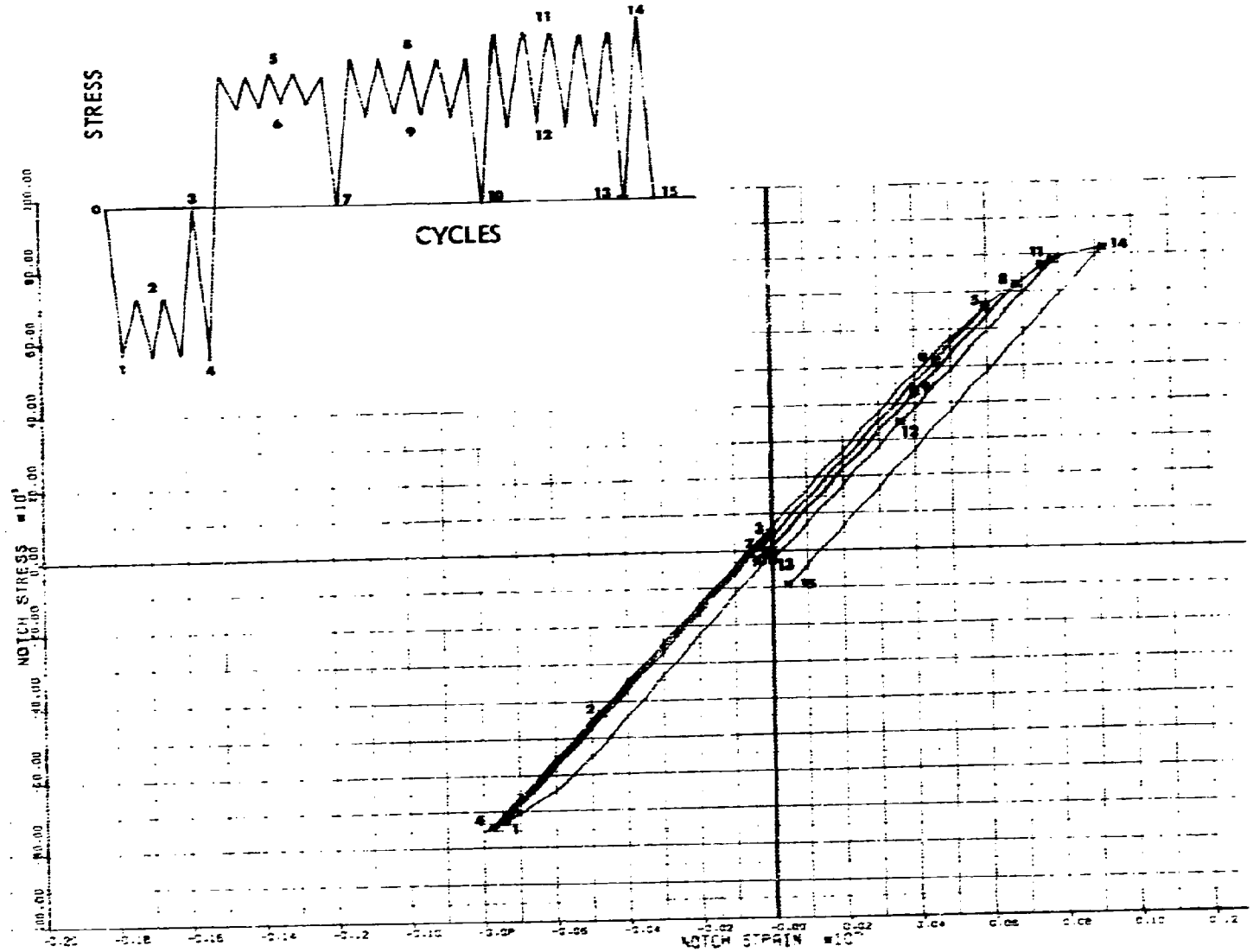

Figure 71. Notch Stress-Notch Strain from Hysteresis Analysis

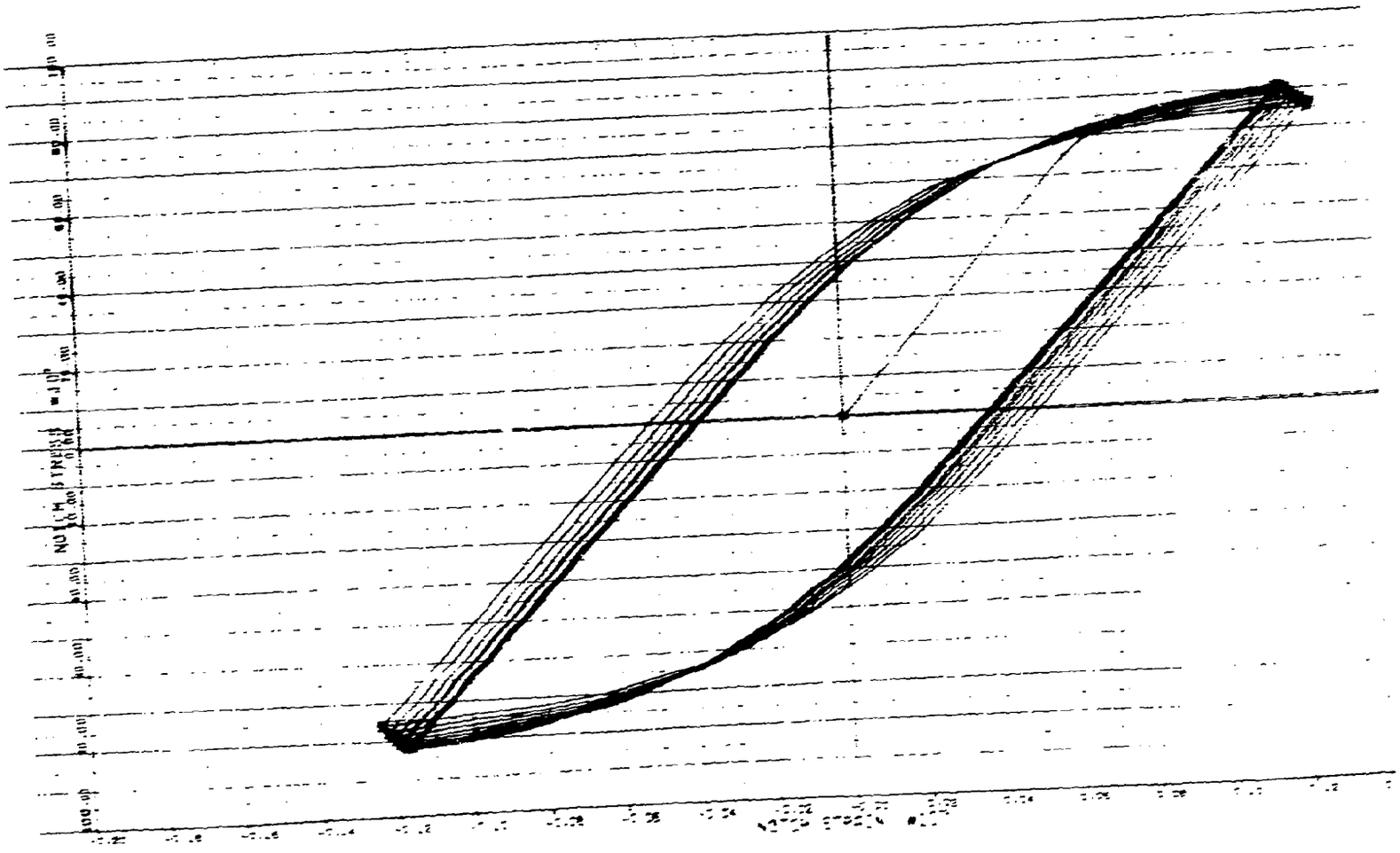

Figure 72. Example of Cyclic Hardening from Hysteresis Analysis

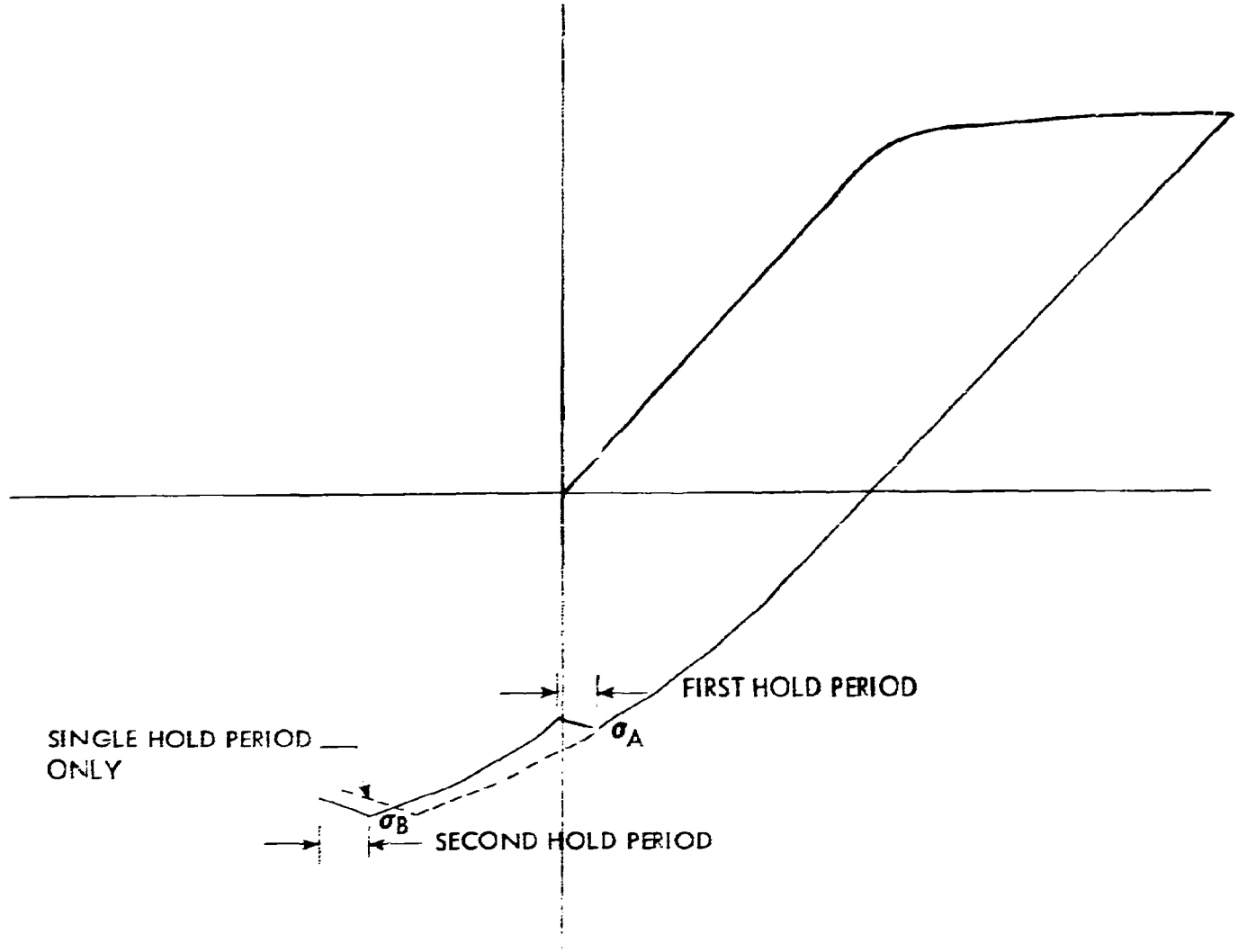

Figure 73. Illustration of Single and Multiple Level Creep During Sustained Load Hold Periods

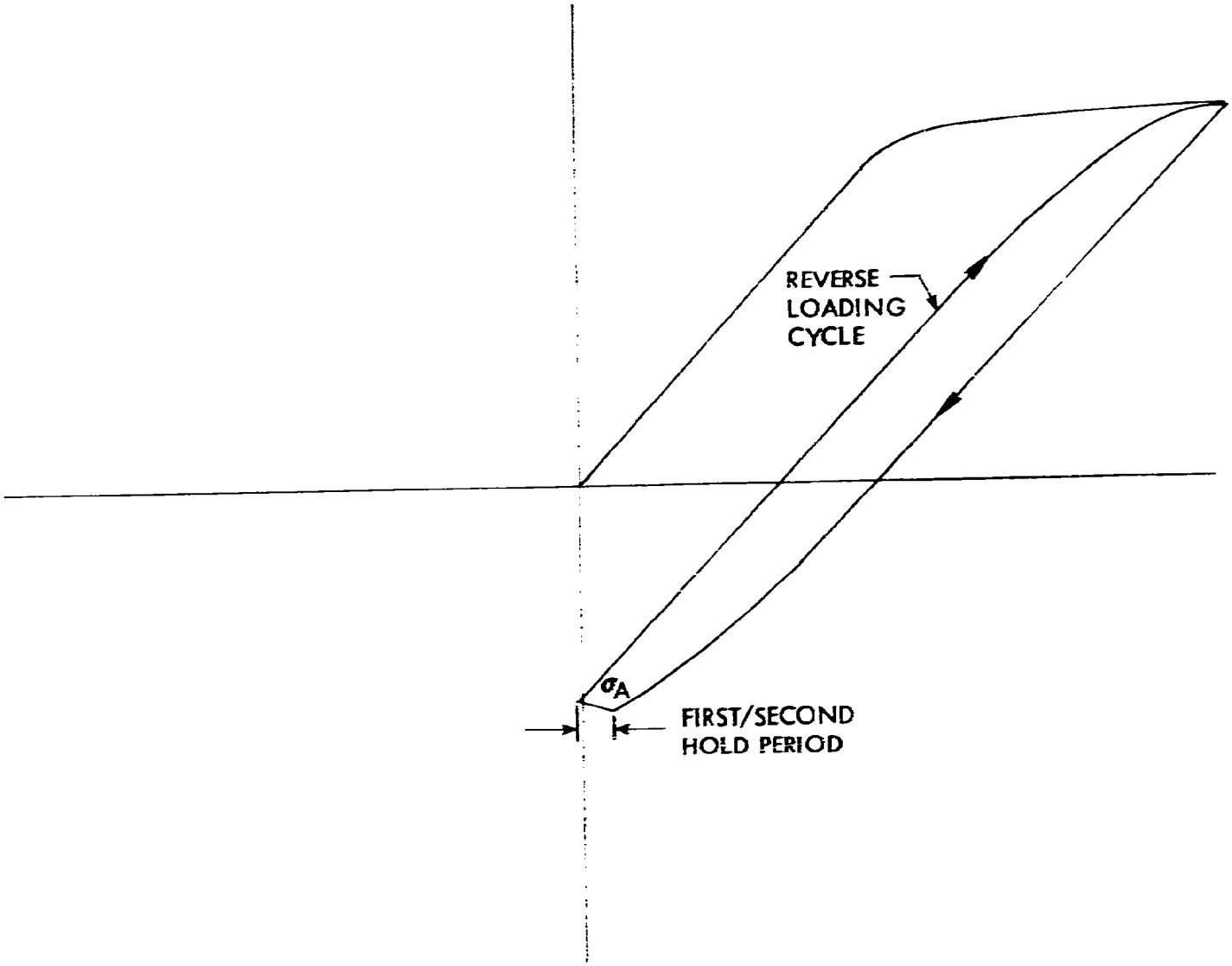

Figure 74. Illustration of Creep During Sustained Load Hold Periods with Completely Reversed Loading

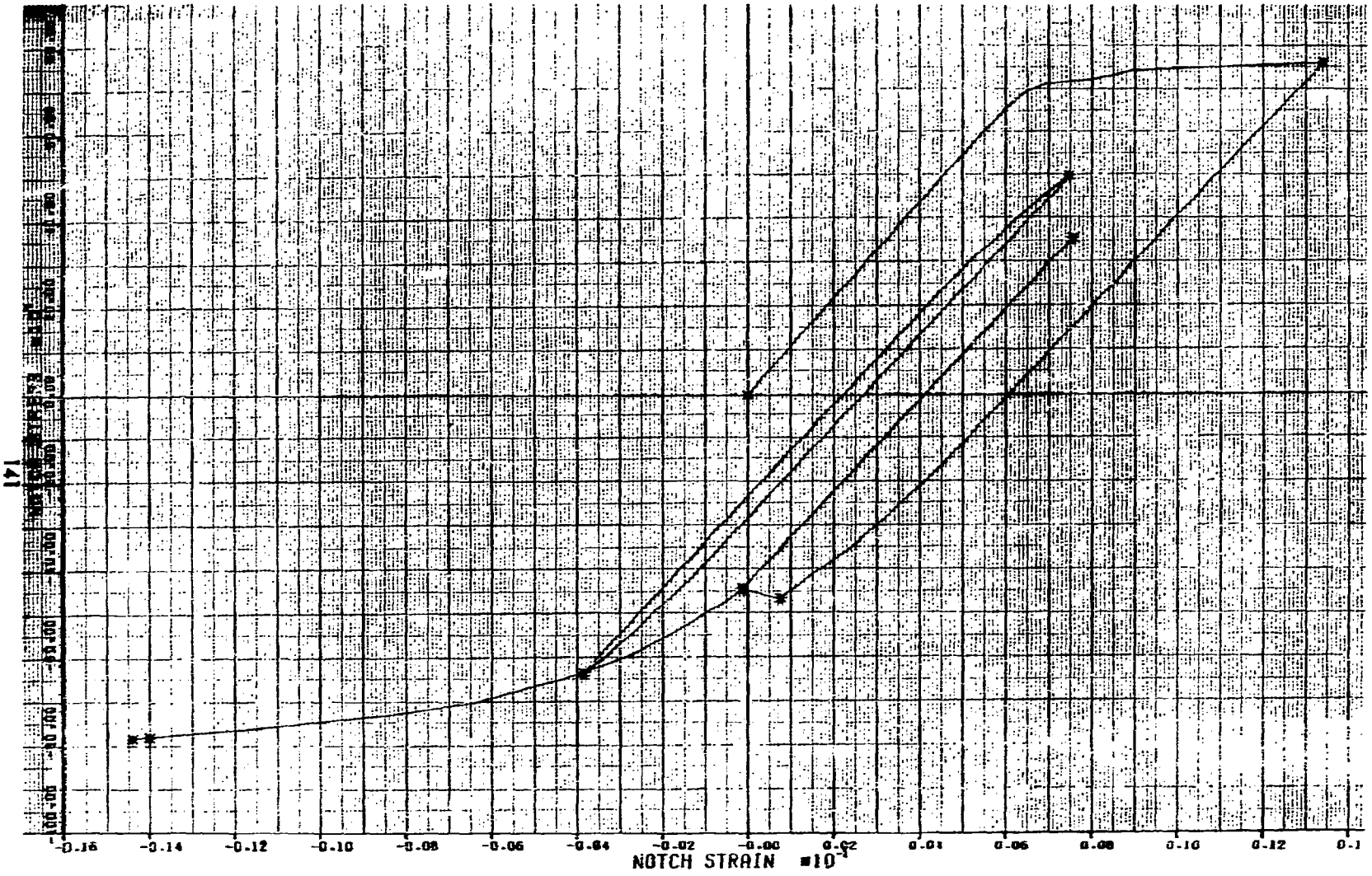

Figure 75. Hysteresis Analysis for Loading Sequence with a Single Sustained Load Hold Period

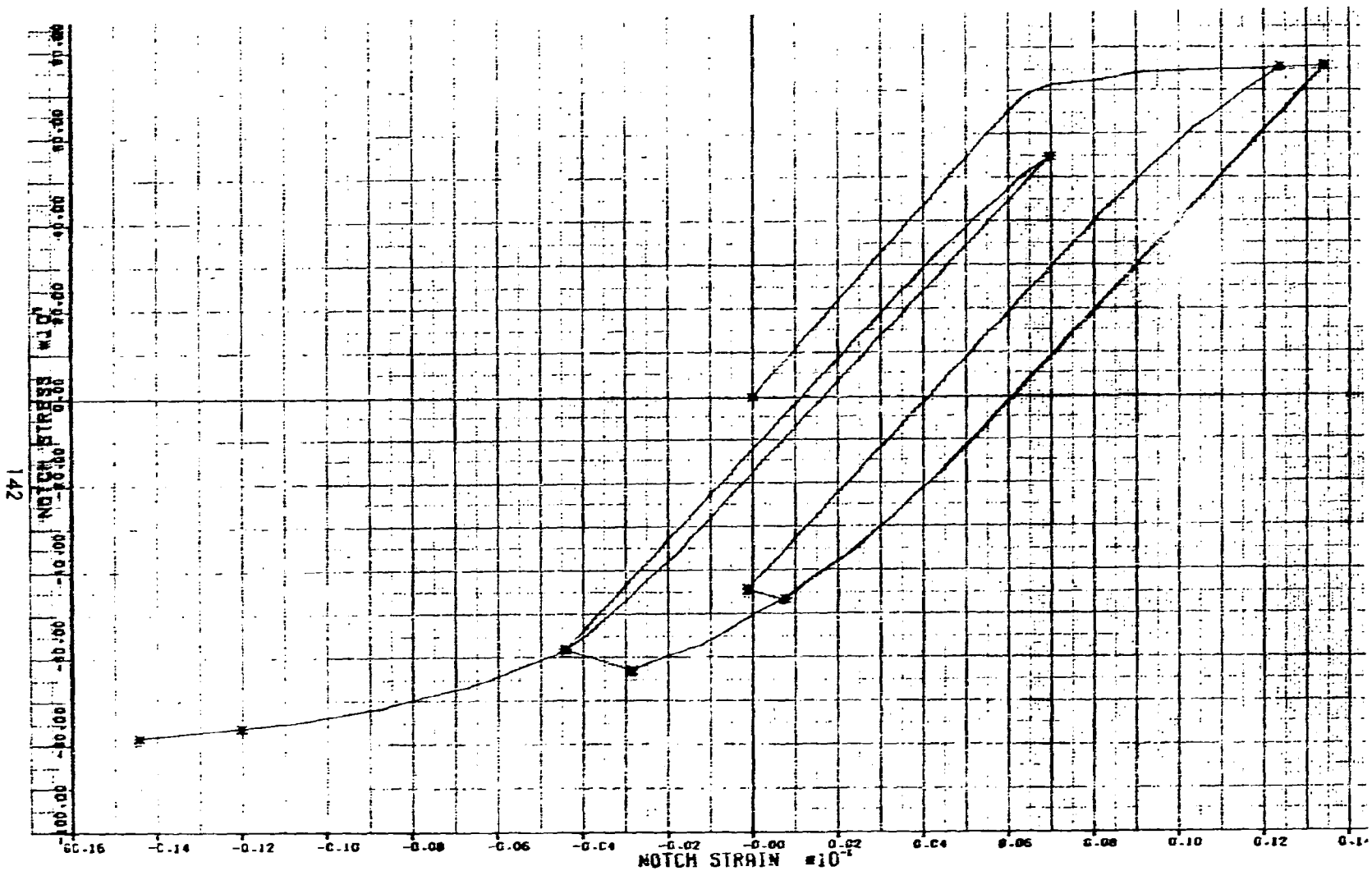

Figure 76. Hysteresis Analysis for Loading Sequence with Two Sustained Load Hold Periods and Completely Reversed Loading

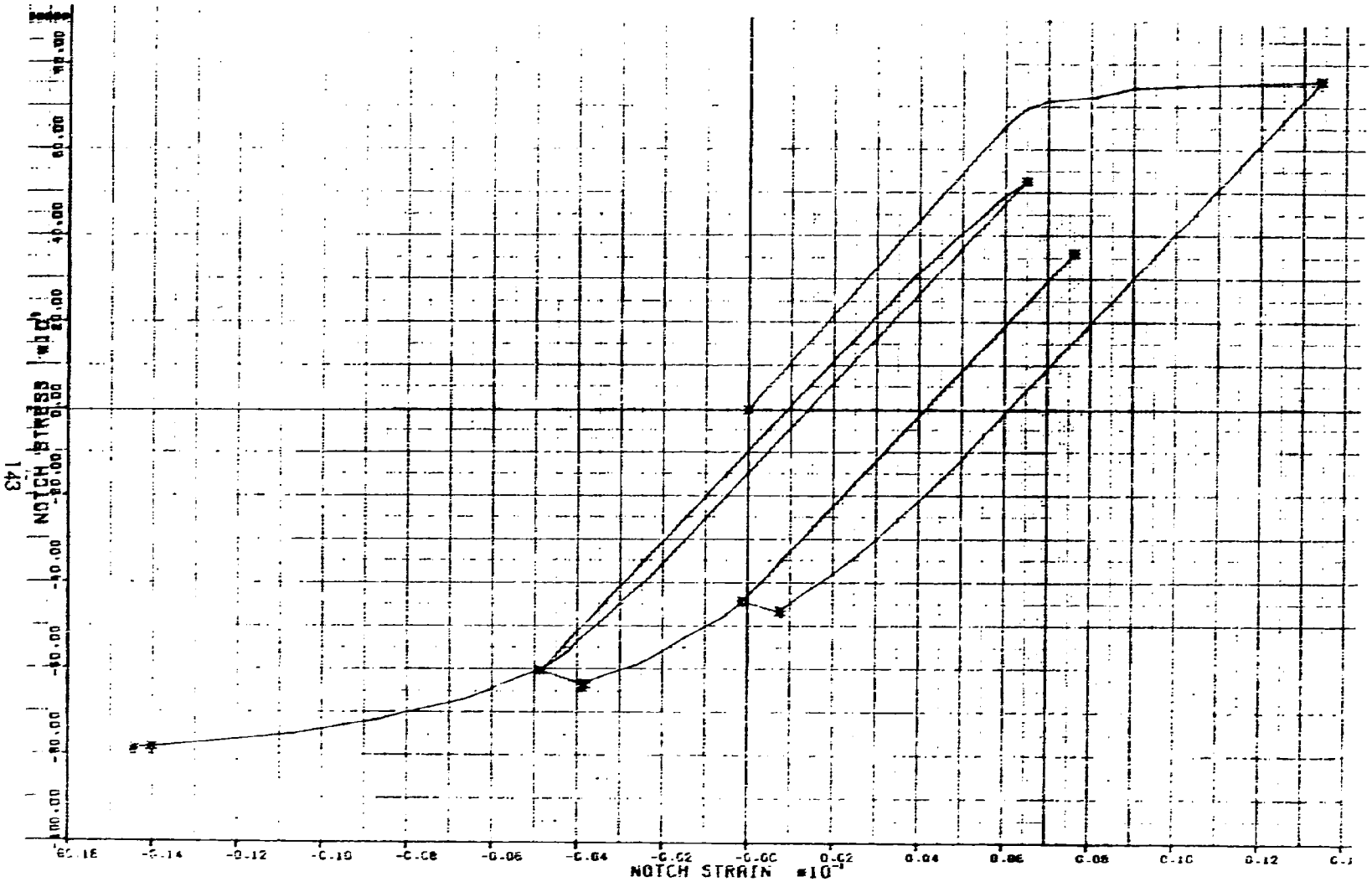

Figure 77. Hysteresis Analysis for Loading Sequence with Two Sustained Load Hold Periods

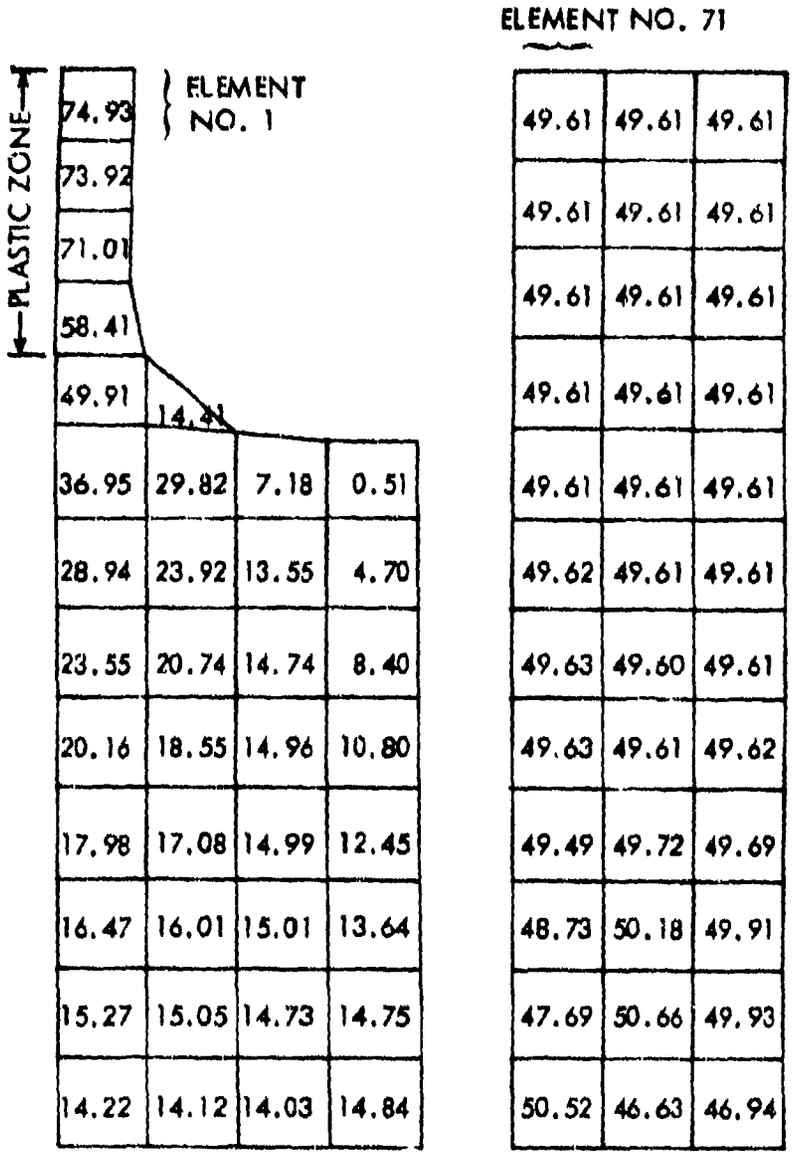

(1) All Stresses in ksi

(2) Applied Load = 13,060 lbs.

Figure 78. Finite Element Analysis Stress Distribution For Maximum Applied Tensile Load For Simplified Stress Concentration Specimen

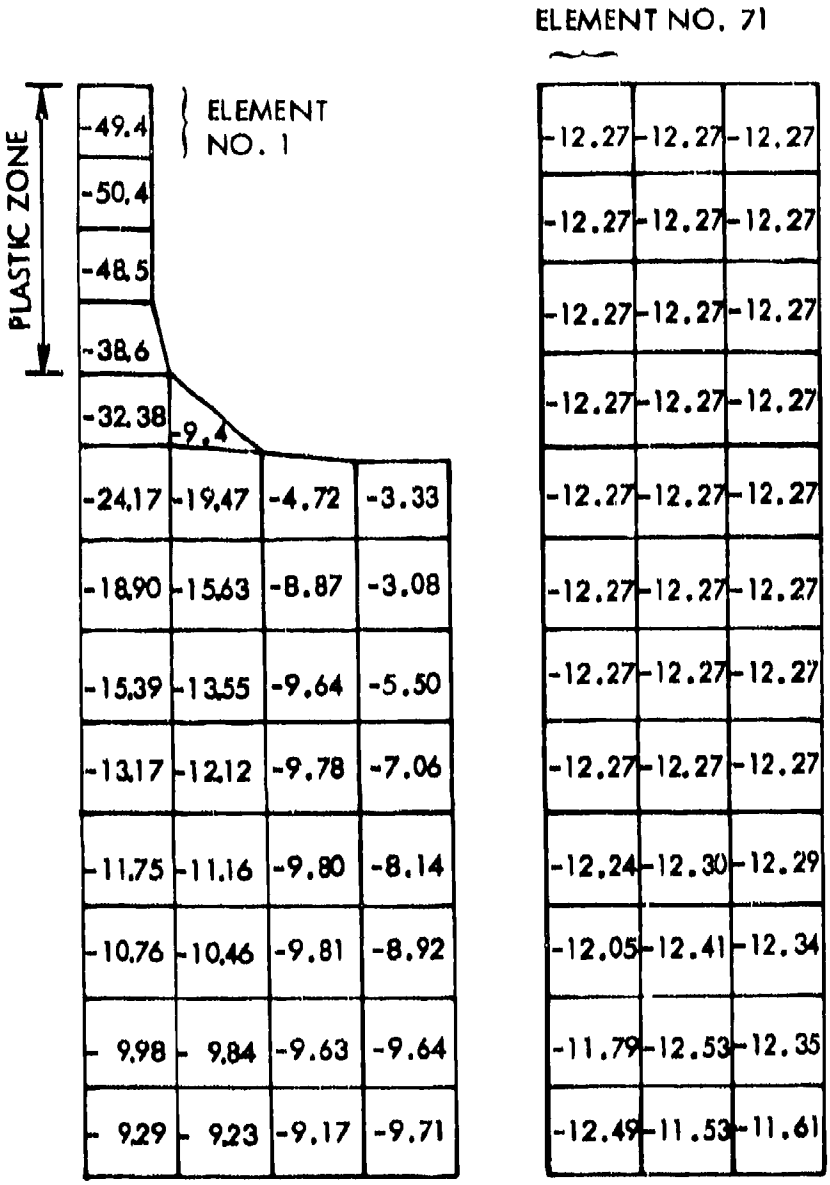

(1) All Stresses in ksi

(2) Net Section Compression Stress = -20 ksi

Figure 79. Finite Element Analysis Stress Distribution For Sustained Compression Loading On Simplified Stress Concentration Specimen

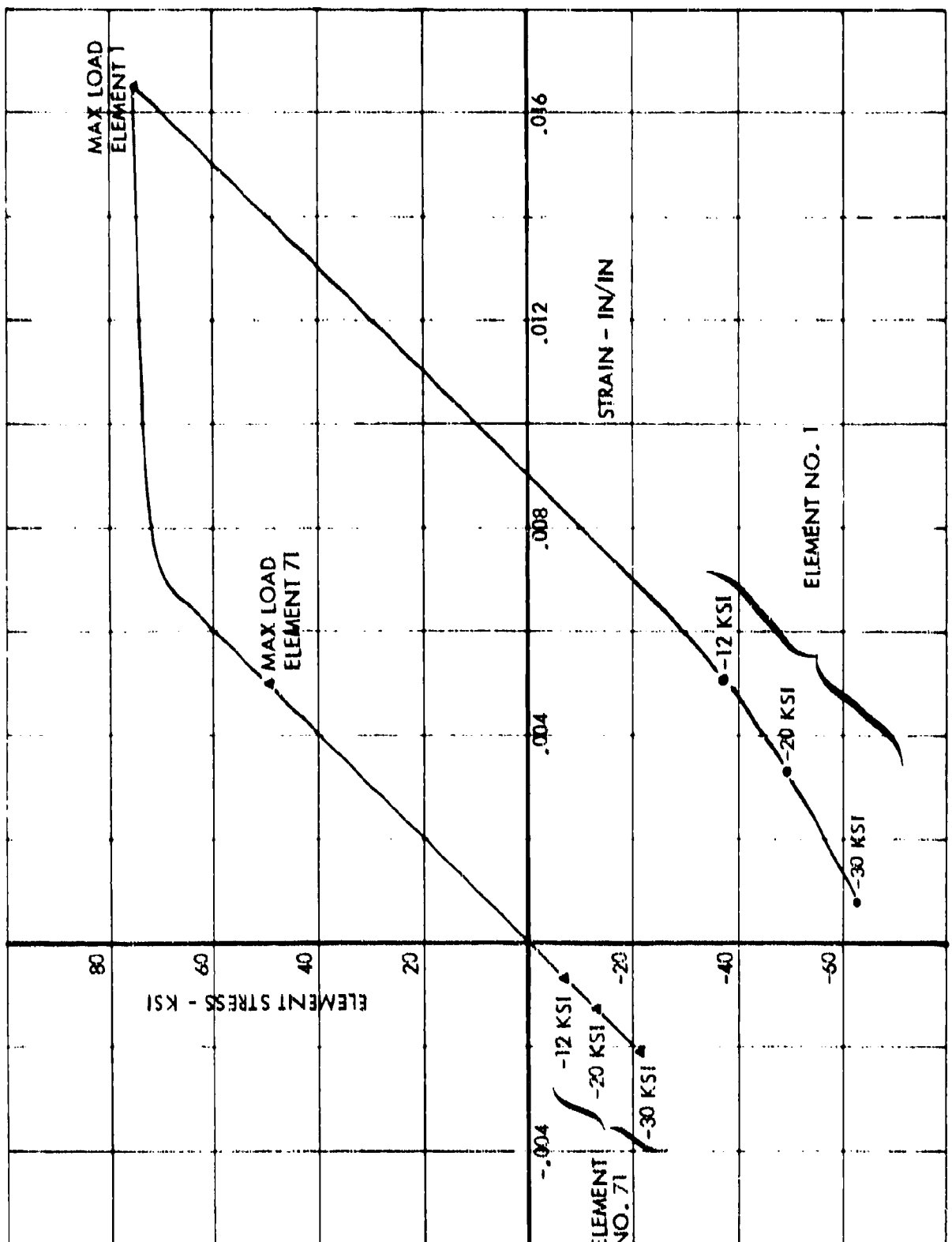

Figure 80. Analytical Stress-Strain Curve for Simplified Stress Concentration Specimen

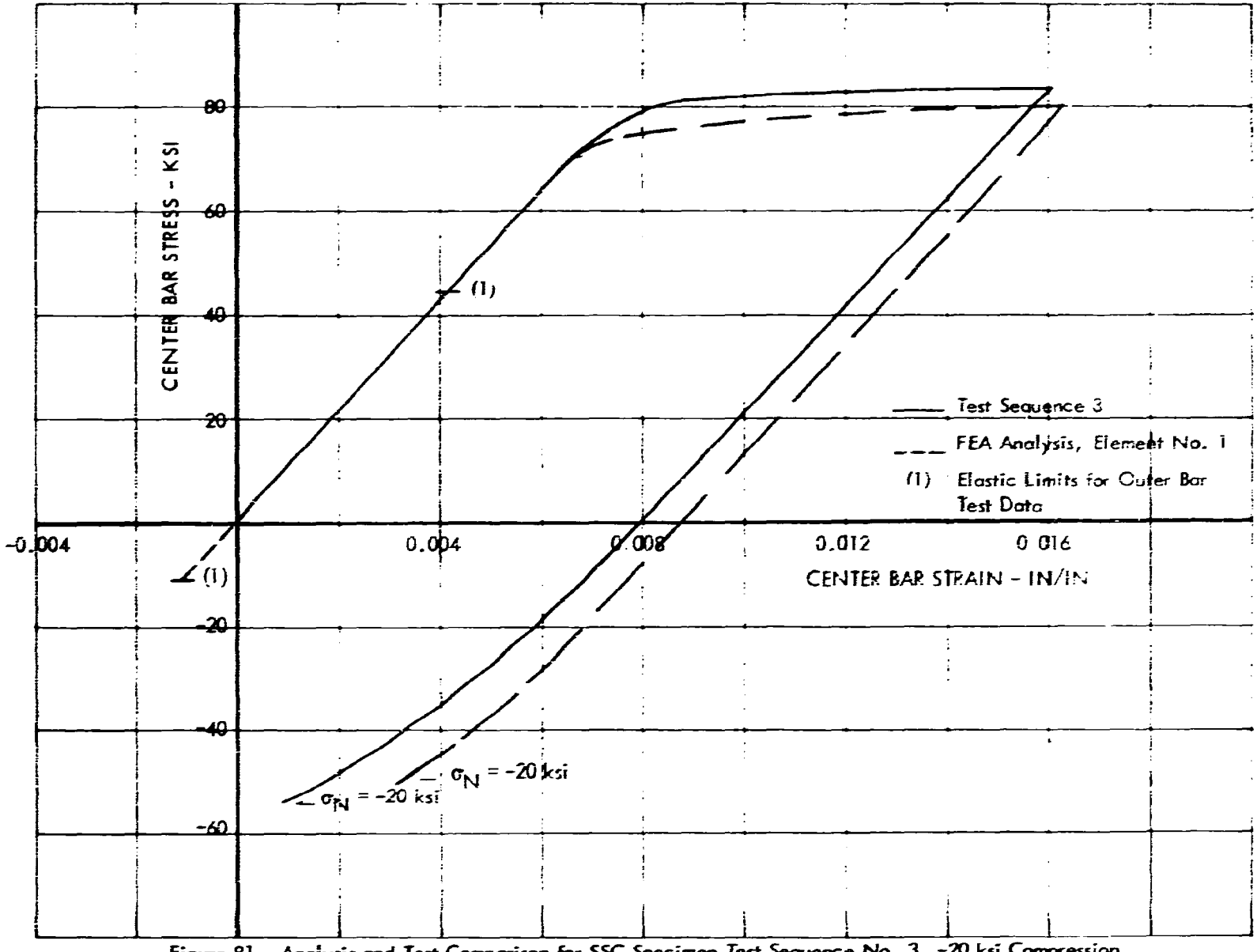

Figure 81. Analysis and Test Comparison for SSC Specimen Test Sequence No. 3, -20 ksi Compression

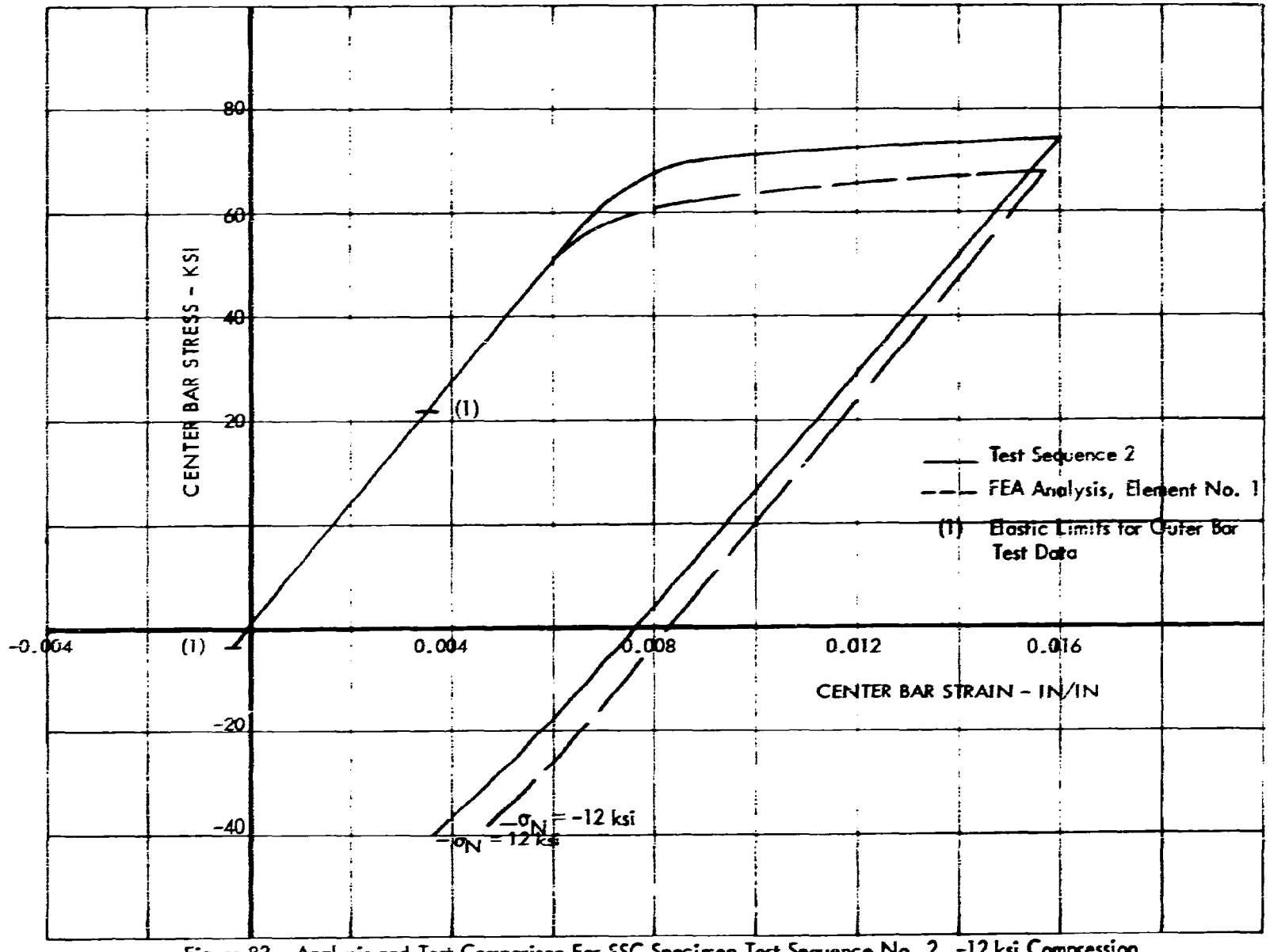

Figure 82. Analysis and Test Comparison For SSC Specimen Test Sequence No. 2, -12 ksi Compression

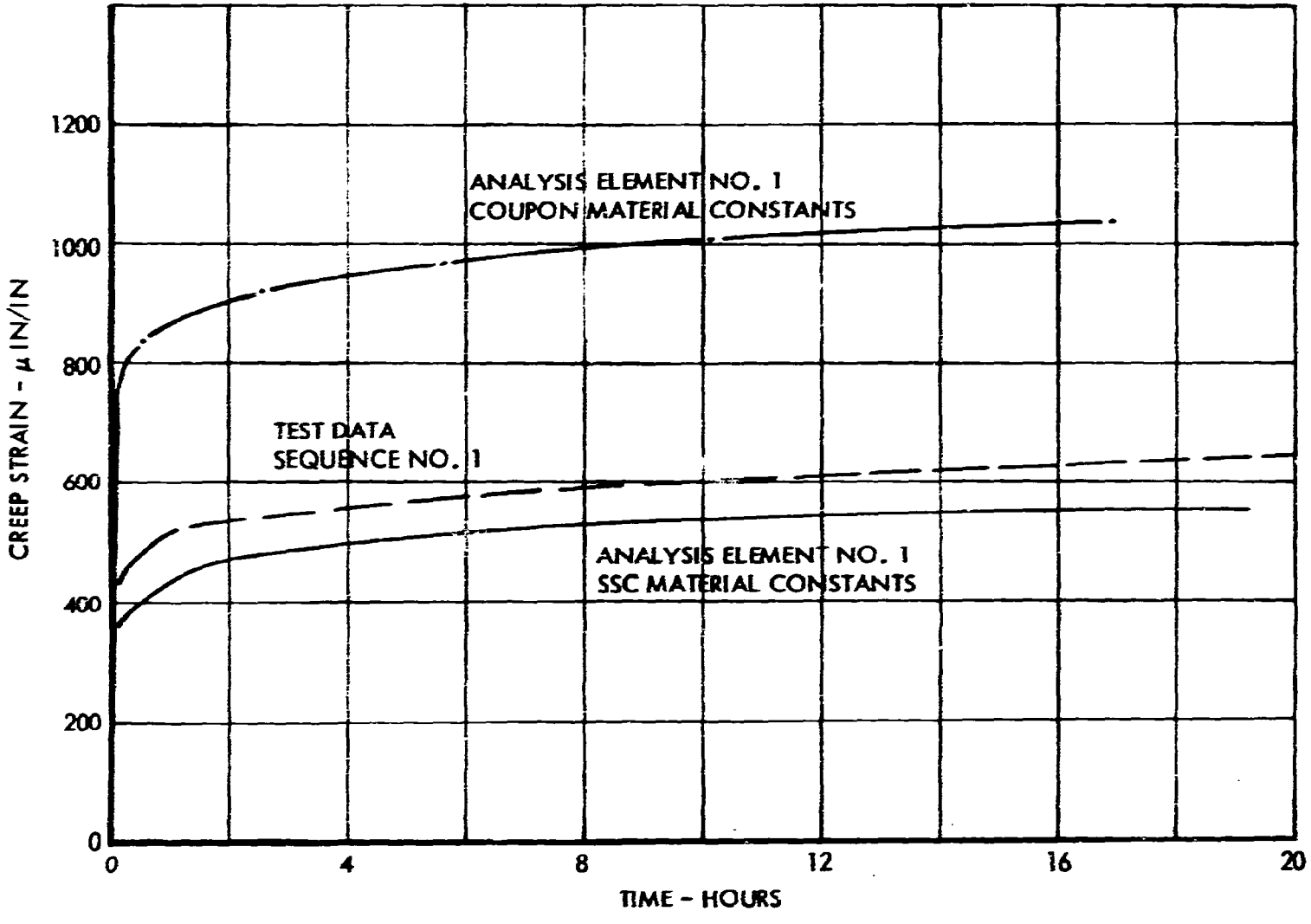

Figure 83. Analytical Creep Predictions Versus Center Bar Test Results - Simplified Stress Concentration Specimen, Applied Net Section Stress -20 ksi

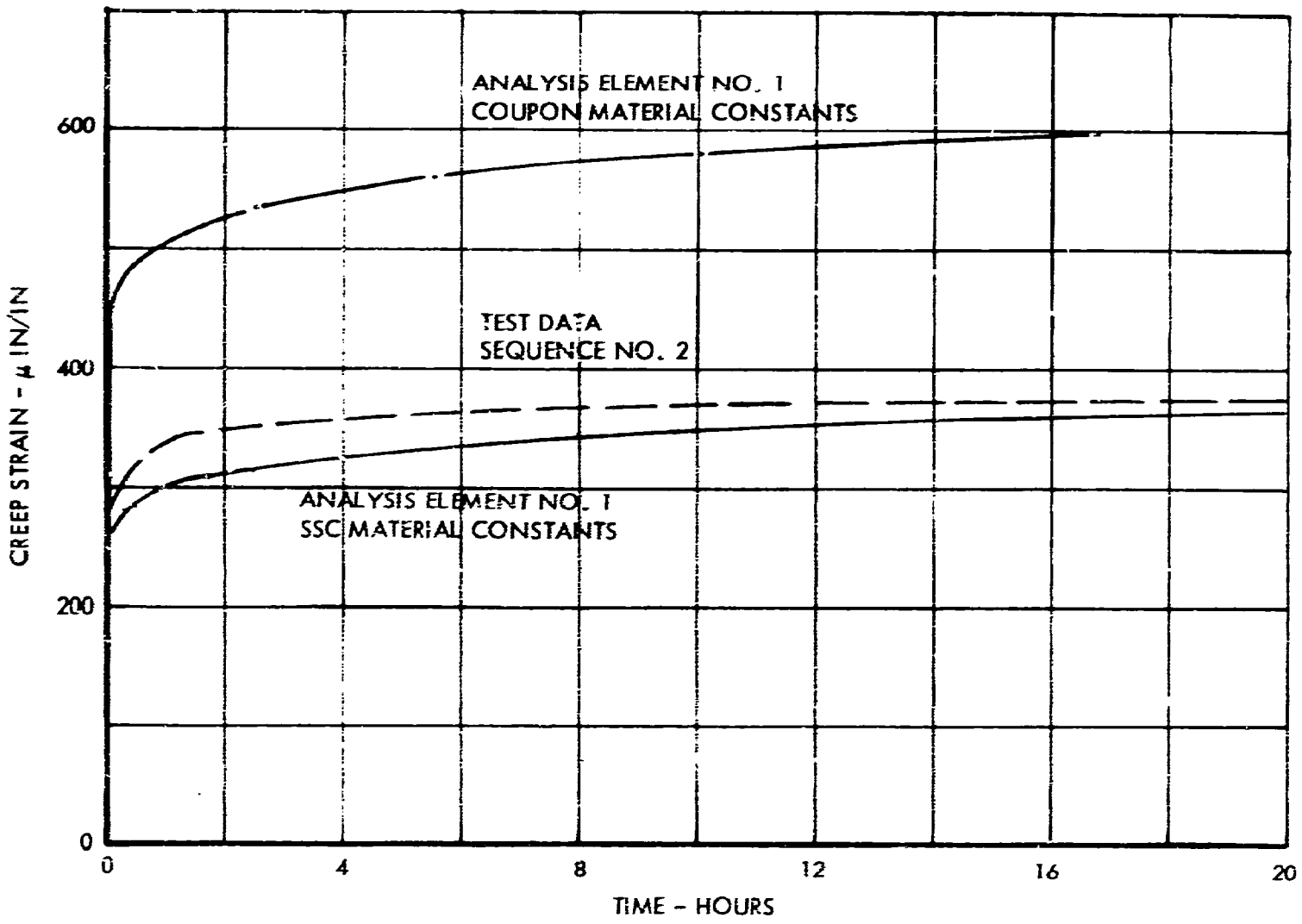

Figure 84. Analytical Creep Predictions Versus Center Bar Test Results - Simplified Stress Concentration Specimen - Applied Net Section Stress -12.0 ksi

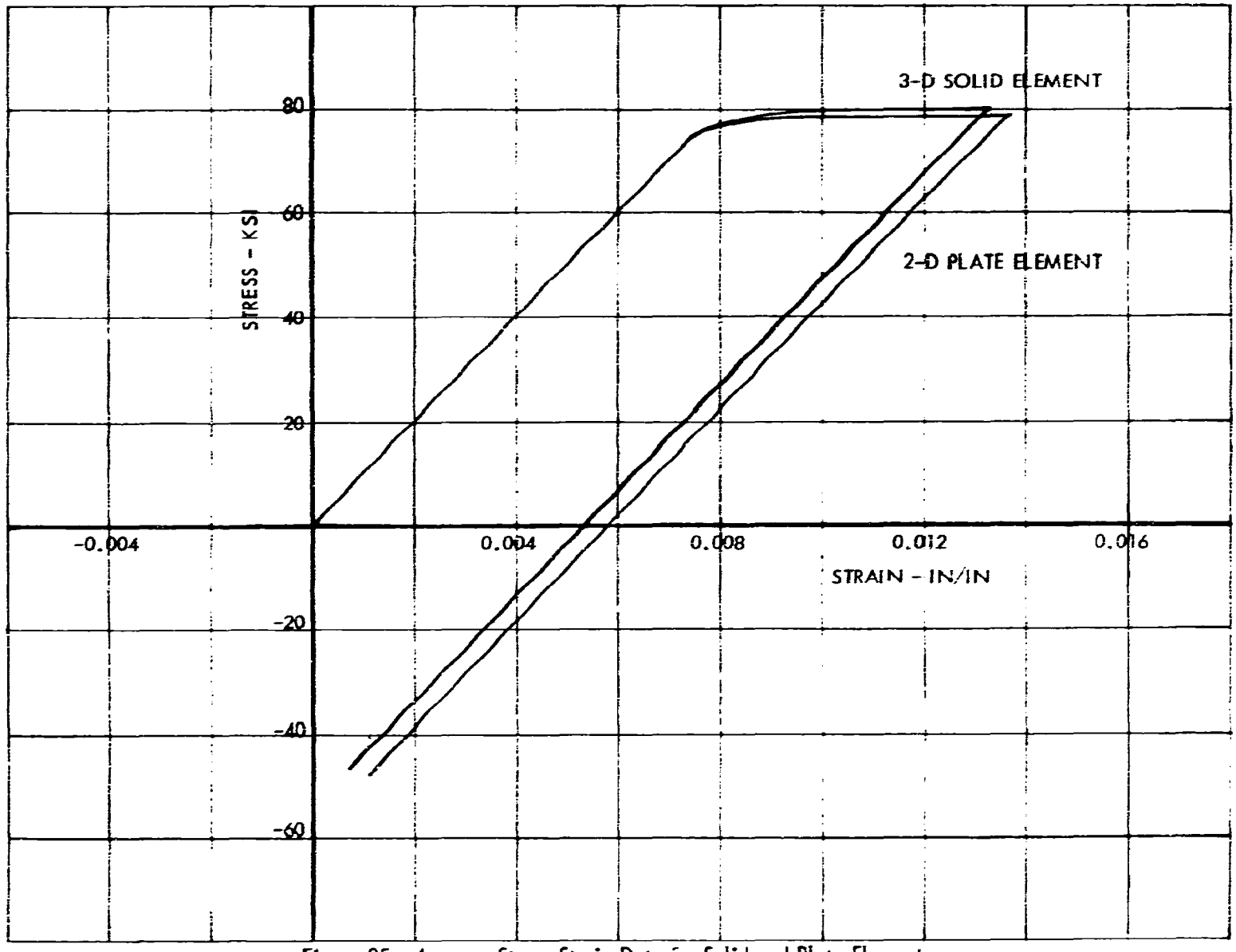

Figure 85. Average Stress-Strain Data for Solid and Plate Elements

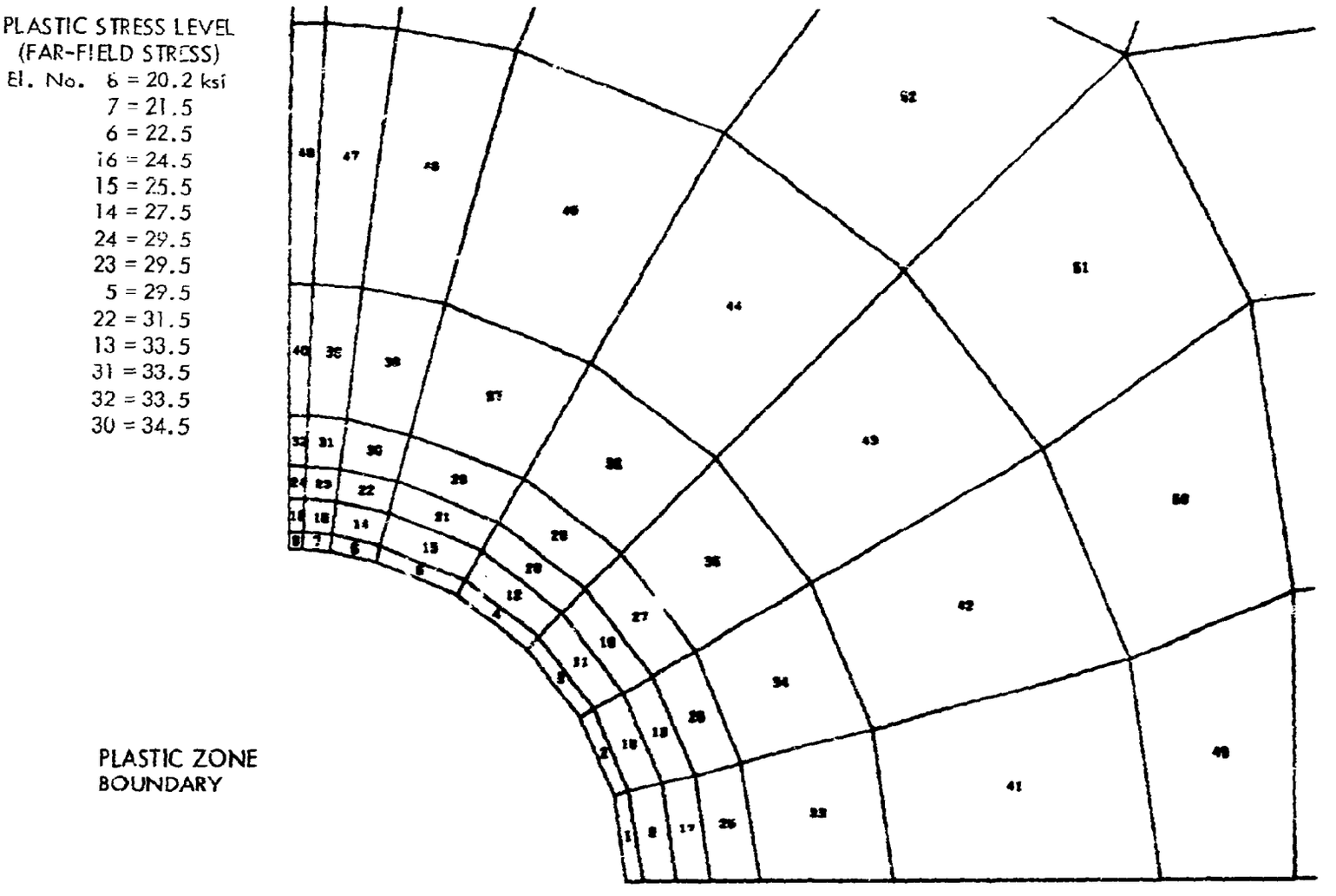

Figure 86. Plastic Zone Definition Around Stress Riser In Super-Scale Specimen

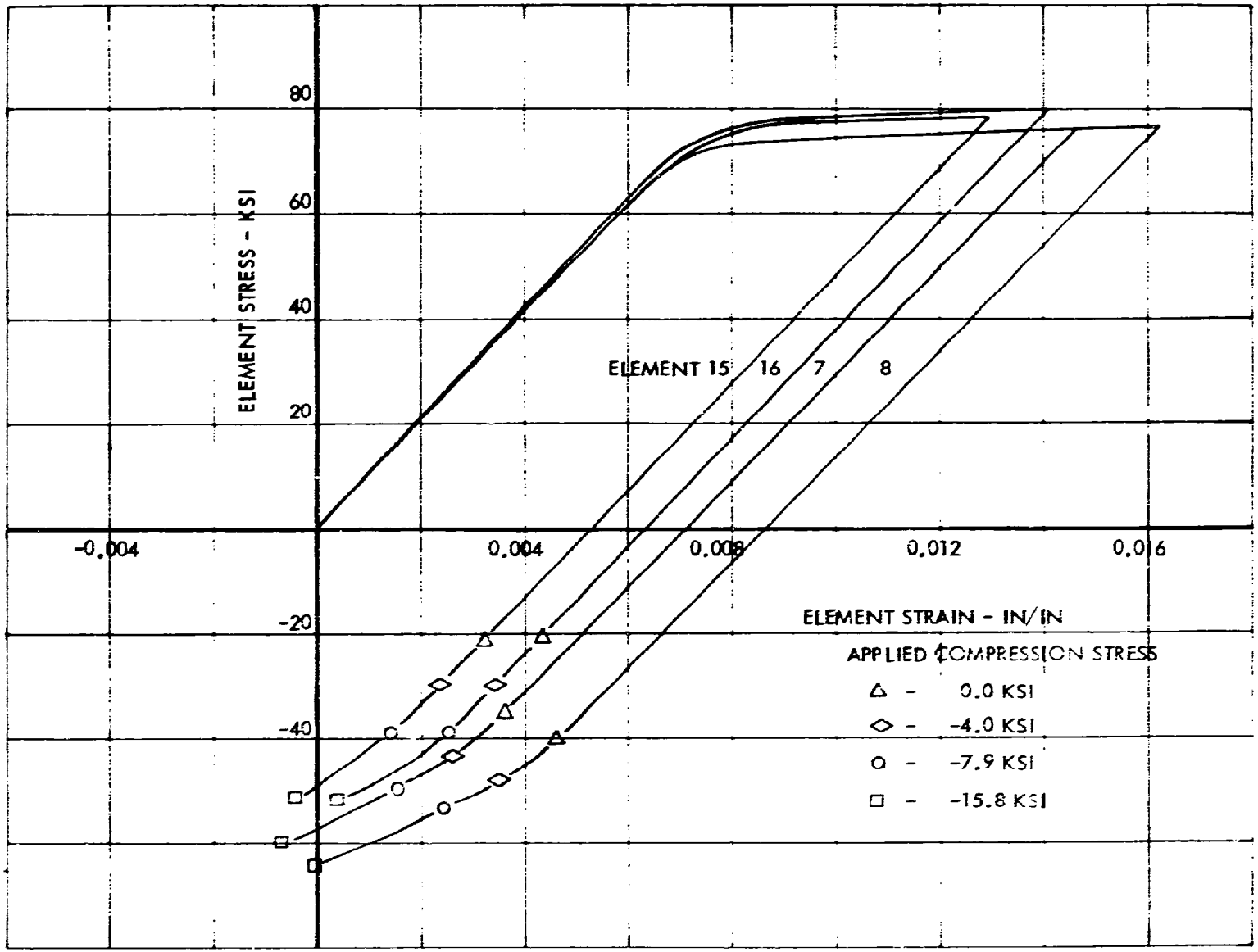

Figure 87. Stress-Strain Curve Super-Scale Specimen 2-D Finite Element Analysis Results

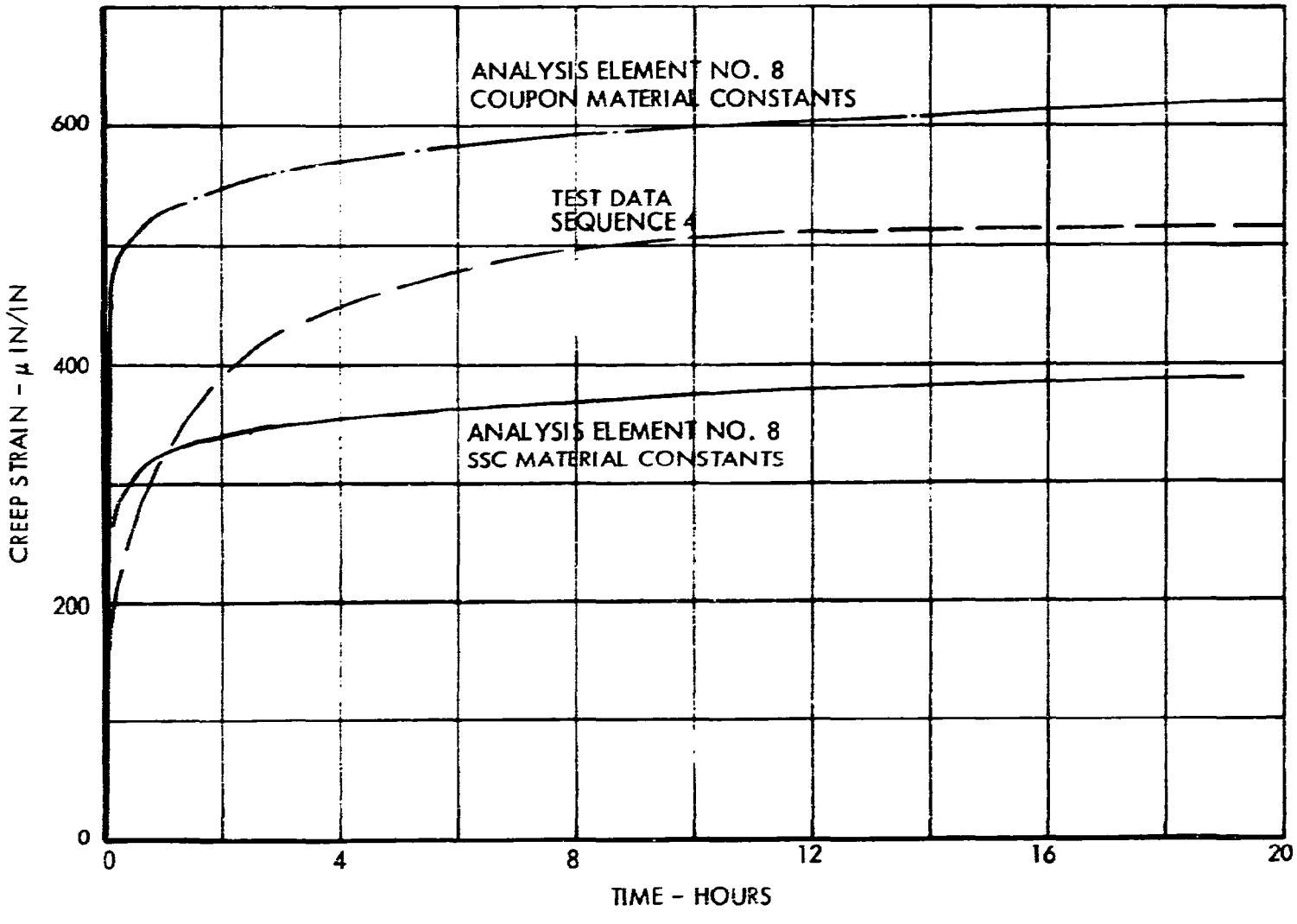

Figure 88. Analytical Creep Predictions Versus Transducer Measurements Super-Scale Specimen, Zero Net Section Stress

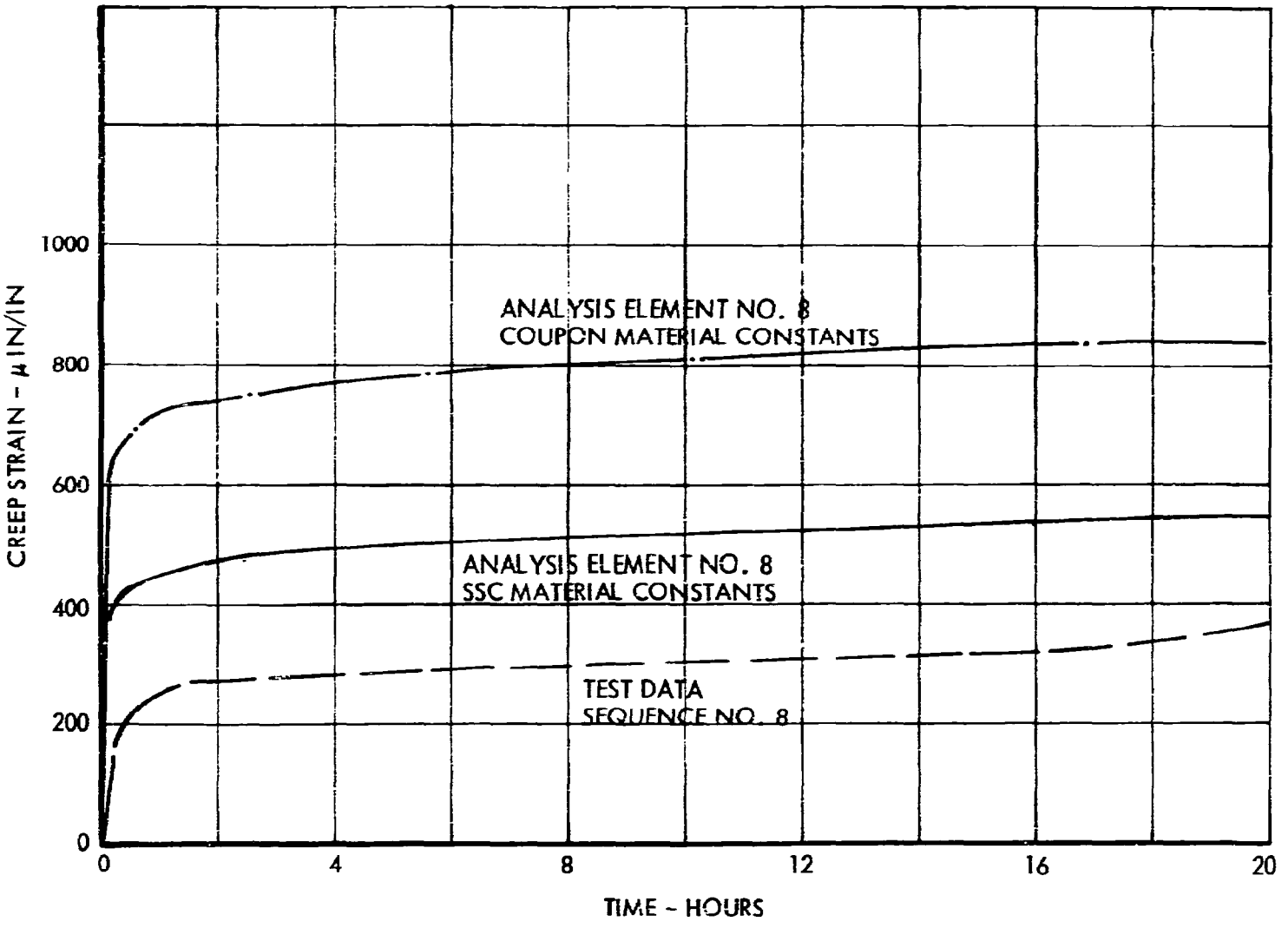

Figure 89. Analytical Creep Predictions Versus Transducer Measurements Super-Scale Specimen, -4.0 ksi Net Section Stress

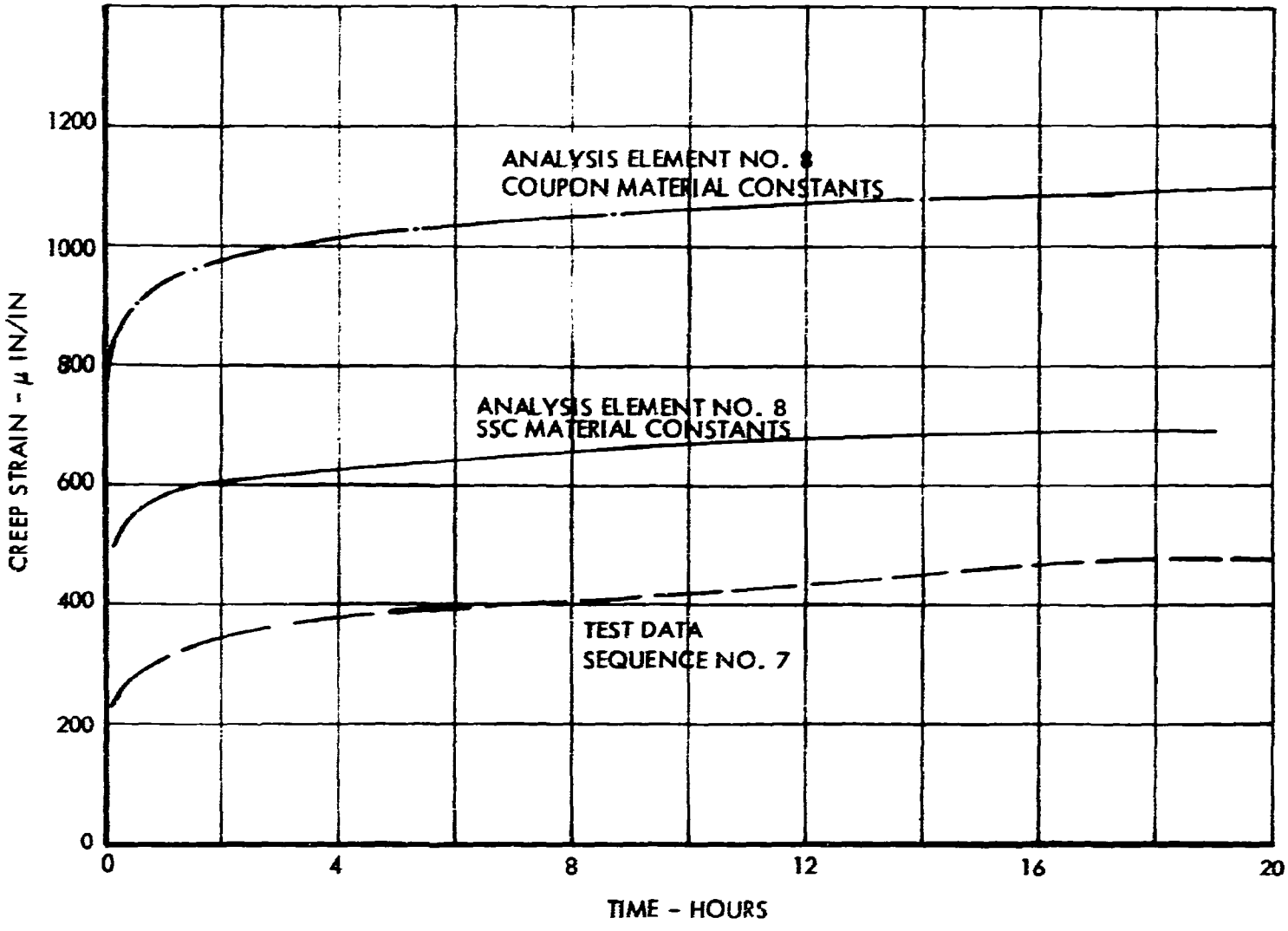

Figure 90. Analytical Creep Predictions Versus Transducer Measurements Super-Scale Specimen, -7.9 ksi Net Section Stress

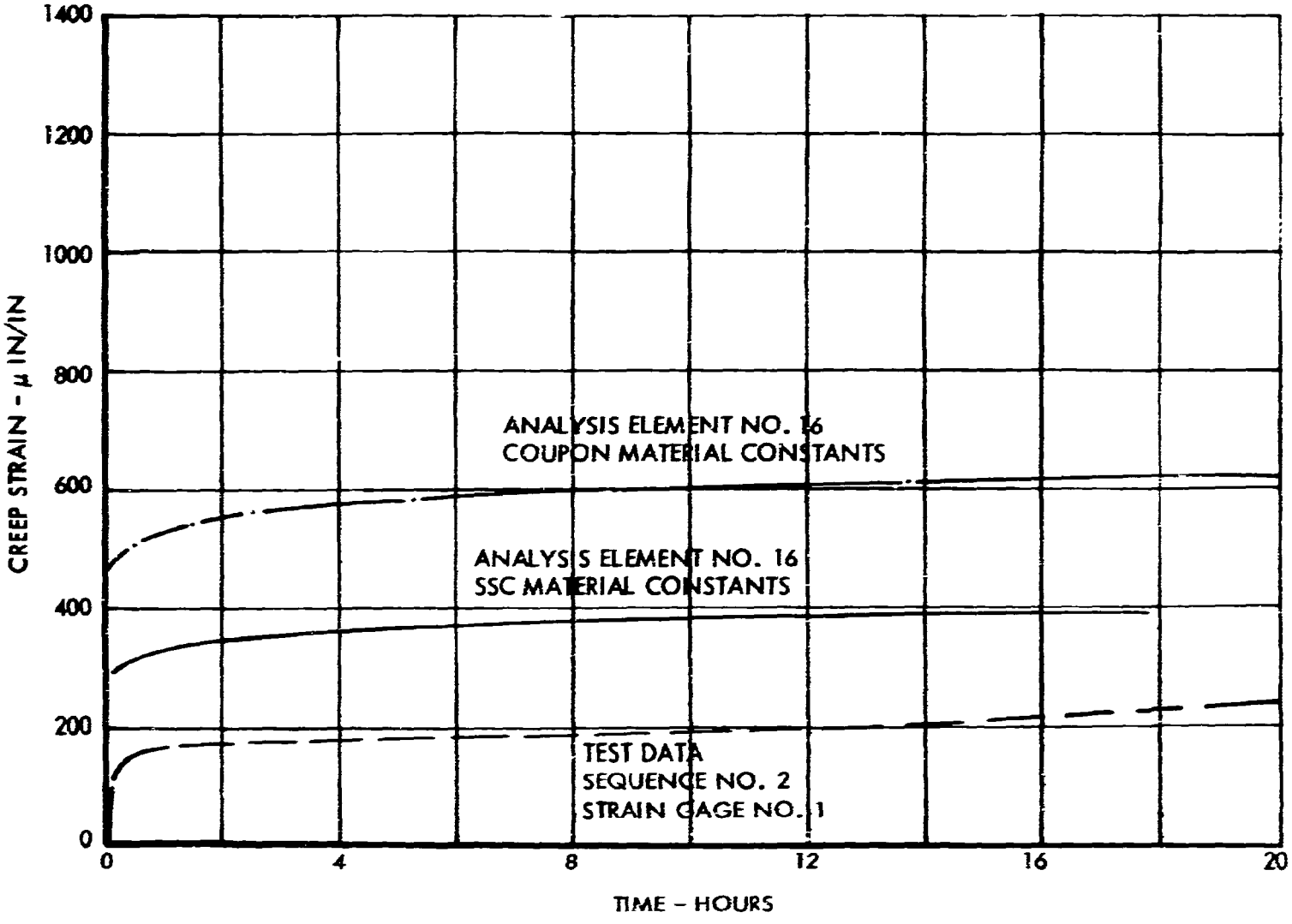

Figure 91. Analytical Creep Predictions Versus Strain Gage Measurements
Super-Scale Specimen, -7.9 ksi Net Section Stress

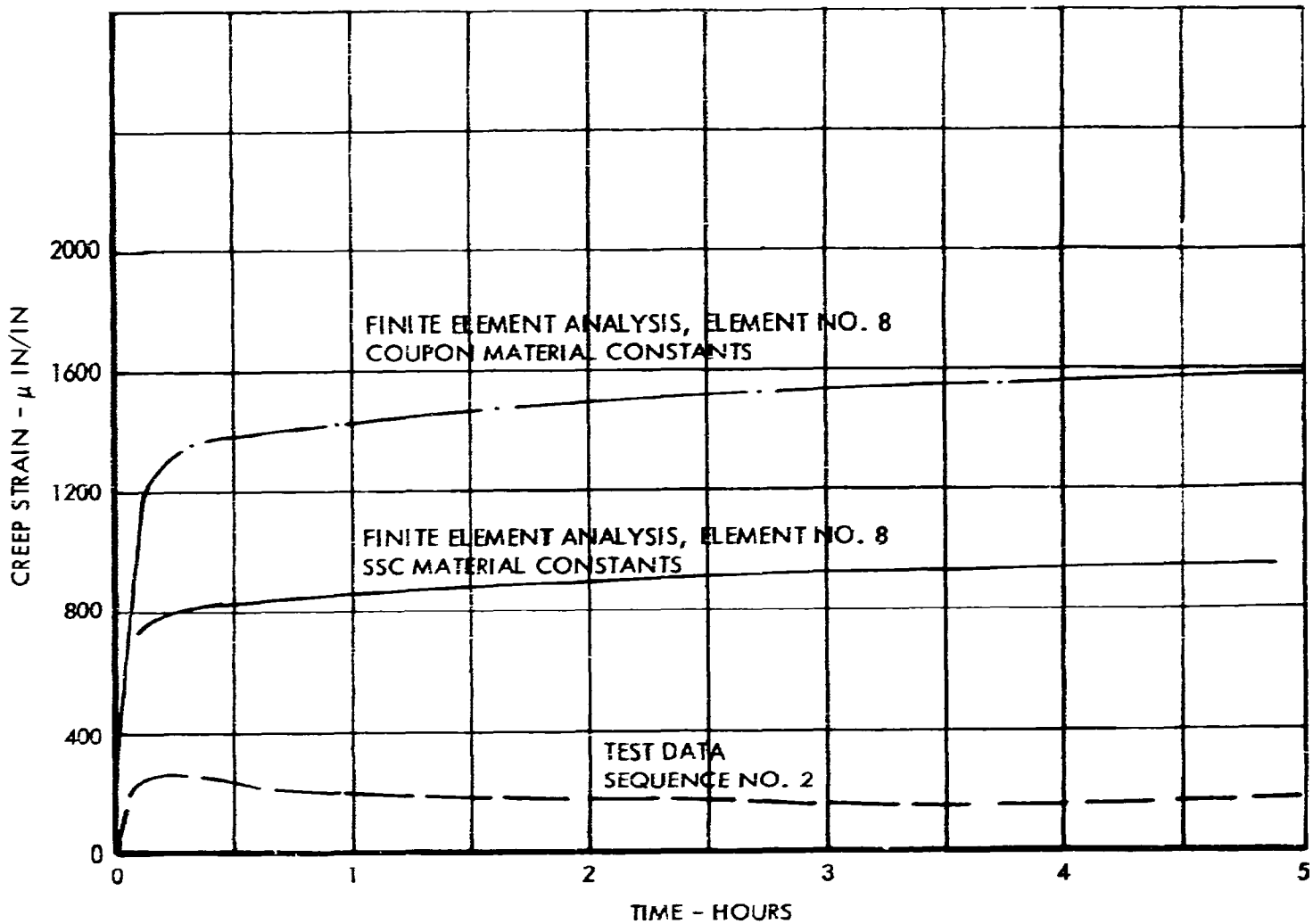

Figure 92. Analytical Creep Predictions Versus Transducer Measurements
Super-Scale Specimen, -15.8 ksi Net Section Stress

APPENDIX A

HYSTERESIS ANALYSIS COMPUTER PROGRAM DESCRIPTION

INDEX

A1.1 INTRODUCTION

Appendix A describes the computer program used to calculate fatigue damage. The program takes the true peak stresses for a notch and converts them into mean and alternating stresses through a rain flow counting technique. It then uses these stresses with unnotched S/N data and Miner's rule to calculate the damage. The derivation of the peak stresses for the notch is based on Neuber's equation. The effects of crack, stress relaxation, and material hardening or softening on these stresses are included in the program.

The following sections describe the main program and 21 subroutines comprising the program. The calling sequence for the subroutines is shown in Figure A1.

		MAIN	DRIVER	CREEPER	ADJUST	ORIGIN	MAKPLT	INCBC	ILABC	INCLC	LPTLC	LPTBC	RAIN
1.	MAIN												
2.	DRIVER	x											
3.	CREEPER	x											
4.	ADJUST	x											
5.	ORIGIN			x			x	x	x				
6.	MAKPLT	x	x										
7.	INCBC		x	x									
8.	INLABC			x	x								
9.	INCLC		x										
10.	LPTLC			x	x								
11.	LPTBC					x							
12.	RAIN	x											
13.	SPECT	x											
14.	CRVTRP	x											
15.	CREEP			x									
16.	LINBR								x				
17.	BCRPLT			x			x						
18.	FDSKT			x									
19.	DAMAGE												x
20.	DETERM									x			
21.	LINSEC										x	x	
22.	BINTS							x					

Figure A1. Calling Sequence for the Subroutines

A1.2 LIST OF SYMBOLS

$\varepsilon BC_B, \sigma BC_B$	arrays of strain, εBC, and stress, σBC, defining the branch curve in the branch curve system.
$\varepsilon MCT, \sigma MCT$	arrays of strain, εMCT, and stress, σMCT, defining the tension part of the monotonic locus curve.
$\varepsilon MCC, \sigma MCC$	arrays defining the compression part of the monotonic locus curve.
$\varepsilon CCT, \sigma CCT$	arrays defining the tension part of the cyclic locus curve.
$\varepsilon CCC, \sigma CCC$	arrays defining the compression part of the cyclic locus curve.
$\varepsilon LCT, \sigma LCT$	arrays defining the tension part of the hardened locus curve.
$\varepsilon LCC, \sigma LCC$	arrays defining the compression part of the hardened locus curve.
$D\varepsilon$, NCH	arrays defining the number of cycles to fully harden, $D\varepsilon$, versus half the plastic strain, $D\varepsilon$.
SI, PC	arrays defining the % hardening, PC, versus Σ 1/NCH, SI.
ε, σ	general stress strain coordinates in the basic system.
B	subscript defining the branch curve coordinate system.
N, F	subscript N defines a coordinate system that has its origin at $(\varepsilon H(N), \sigma H(N))$ with an orientation defined by F. If F = +1 the orientation is parallel to the basic system. F = -1 the orientation is rotated 180° to the basic system.
$\varepsilon H, \sigma H$	arrays defining the history of peak notch strains and stresses.
$\varepsilon P, \sigma P$	arrays defining all the peak notch strains and stresses.
DLOAD or DSKTS	loading term used in Neuber's equation: $\dfrac{E \times \varepsilon \times \sigma}{\left(1 - \left(\dfrac{\lvert\varepsilon\rvert}{A}\right)^{\ell}\right)^2} = DLOAD^2$
E	Young's modulus

ℓ, A	material constants.
$\bar{E}, K, p, n$	creep constants.

A2.1 MAIN PROGRAM

Purpose

The main program reads the input data and controls the output and calls the various subroutines that execute the analysis.

Procedure

The flow for the main program shown in Figure A2 proceeds through the following stages:

(1) The arrays defining the material stress/strain curves and the material constants are read. These are in general passed to the subroutines through common blocks.

(2) The subroutine SPECT is called which reads and organizes the load spectrum into peak farfield stresses.

(3) The main program computes the loading increments DLOAD(J) from the peak farfield stresses.

(4) Subroutine DRIVER calculates the peak notch strains and stresses ($\varepsilon H, \sigma H$) and ($\varepsilon P, \sigma P$) for a loading increment.

(5) Subroutine CPVTRP hardens or softens the locus curves due to the current loading increment.

(6) Subroutine ADJUST adjusts the history of peak notch strains and stresses ($\varepsilon H, \sigma H$) to reflect the hardening of the locus curve.

(7) Subroutine CREEPER allows the notch stresses to creep if a hold period is called.

Stages (4) through (7) are repeated for all the loading increments.

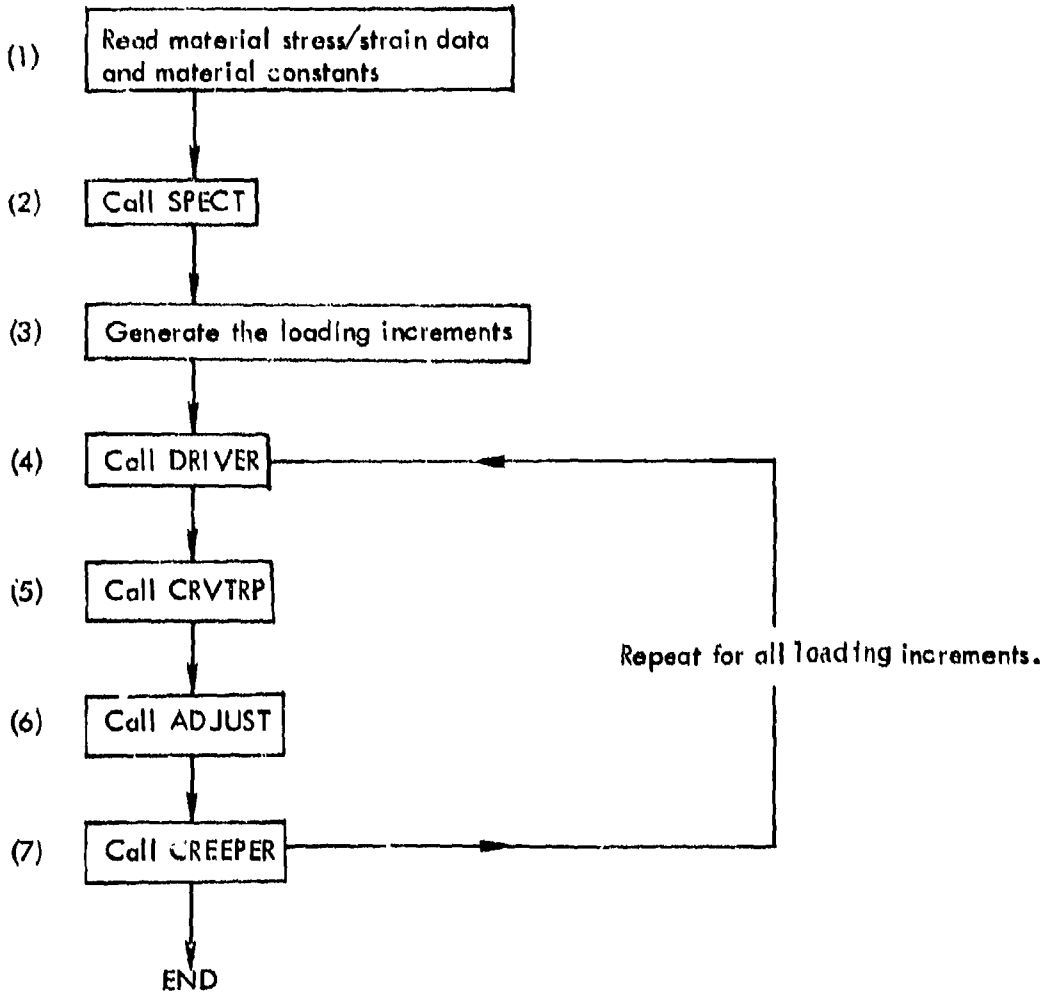

Figure A2. MAIN Program Flow

A2.2 SUBROUTINE DRIVER (DLOAD(J))

Purpose

This subroutine uses the J^{th} loading increment, DLOAD(J), to calculate the peak strains and stresses $\varepsilon P(J)$, $\sigma P(J)$, and updates the history arrays of stresses and strains εH, σH, and the history array of the loading increments DSKTS.

Procedure

If NP is the current number of active history points, in entering subroutine DRIVER the analysis follows the following flow, see Figure A3.

(1) If $NP \geq 3$ the last point calculated will be on a branch curve and the trace for the current loading increment will proceed from the point $(\varepsilon H(NP), \sigma H(NP))$ along the branch curve that passes through the points $(\varepsilon H(NP-1), \sigma H(NP-1))$ and $(\varepsilon H(NP), \sigma H(NP))$.

(2) If $|DLOAD(J)| < |DSKTS(NP-1)|$ the new point $(\varepsilon H(NP+1), \sigma H(NP+1)$ will be found on this branch curve between the points $(\varepsilon H(NP-1), \sigma H(NP-1))$ and $(\varepsilon H(NP), \sigma H(NP))$, Figure A4.a.

(3) If, however, $|DLOAD(J)| \geq |DSKTS(NP-1)|$ the current loading increment is numerically greater than the previous loading increment and the trace will pass beyond the point $(\varepsilon H(NP-1), \sigma H(NP-1))$. In this instance the loading increment is adjusted so that it is relative to the point $(\varepsilon H(NP-2), \sigma H(NP-2))$ and loading is considered from this point along a branch curve that passes through the points $(\varepsilon H(NP-2), \sigma H(NP-2))$ and $(\varepsilon H(NP-3), \sigma H(NP-3))$, Figure A4.b.

(4) If $NP < 2$ loading is along the locus curve to point $(\varepsilon H(2), \sigma H(2))$. A pseudo point $(\varepsilon H(1), \sigma H(1))$ is found on the opposite end of the locus curve, Figure A5. This is necessary to position the branch curve for the next loading increment.

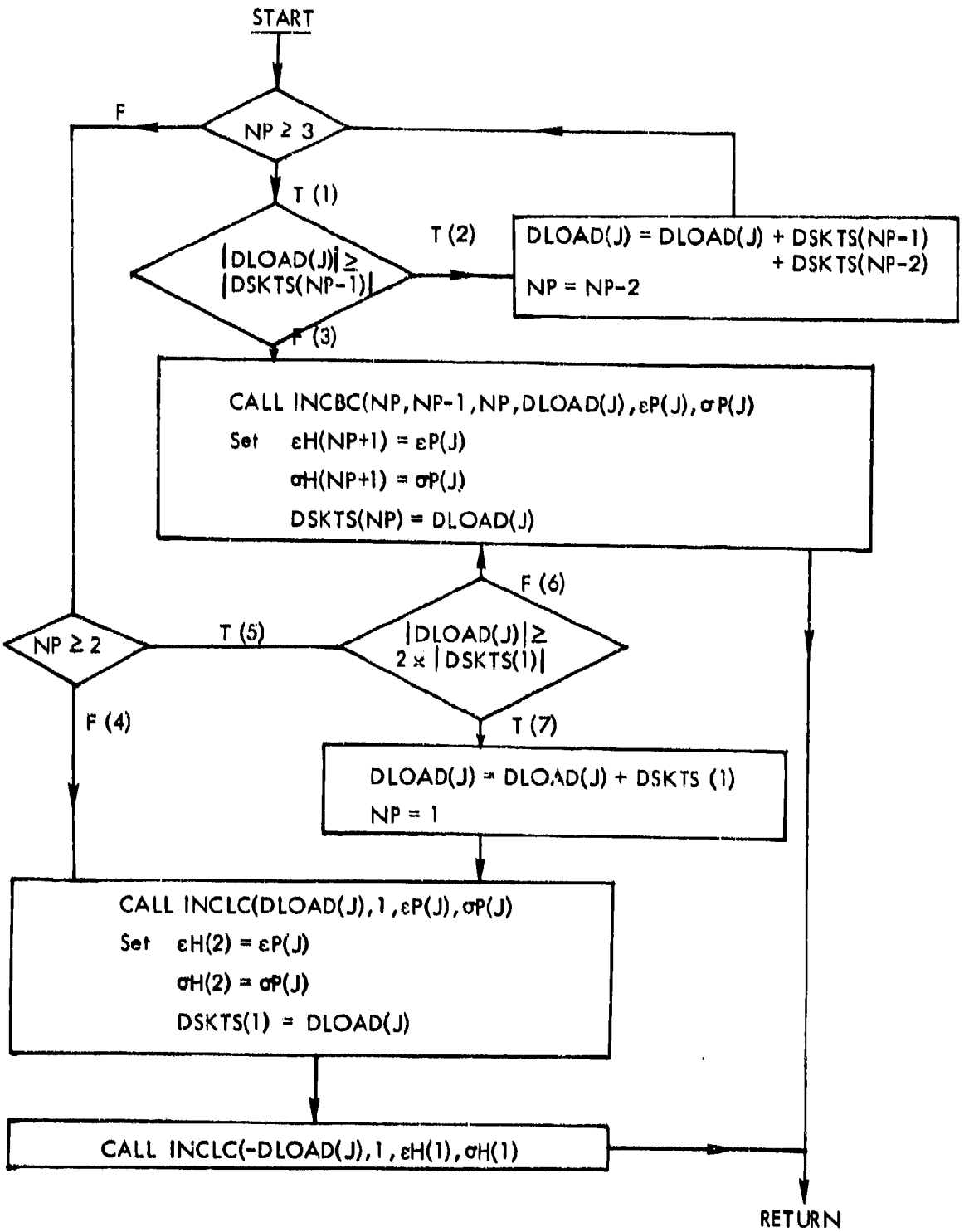

Figure A3. Analysis Flow for Subroutine DRIVER

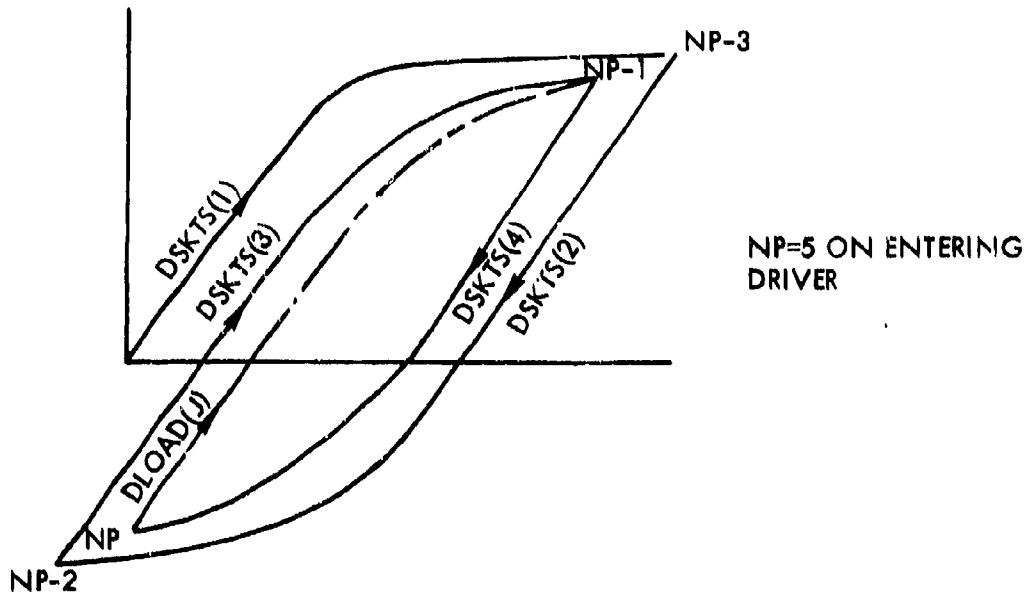

Figure A4.a. Current Loading Increment if NP ≥ 3 and | DLOAD(J) | < | DSKTS(NP-1) |

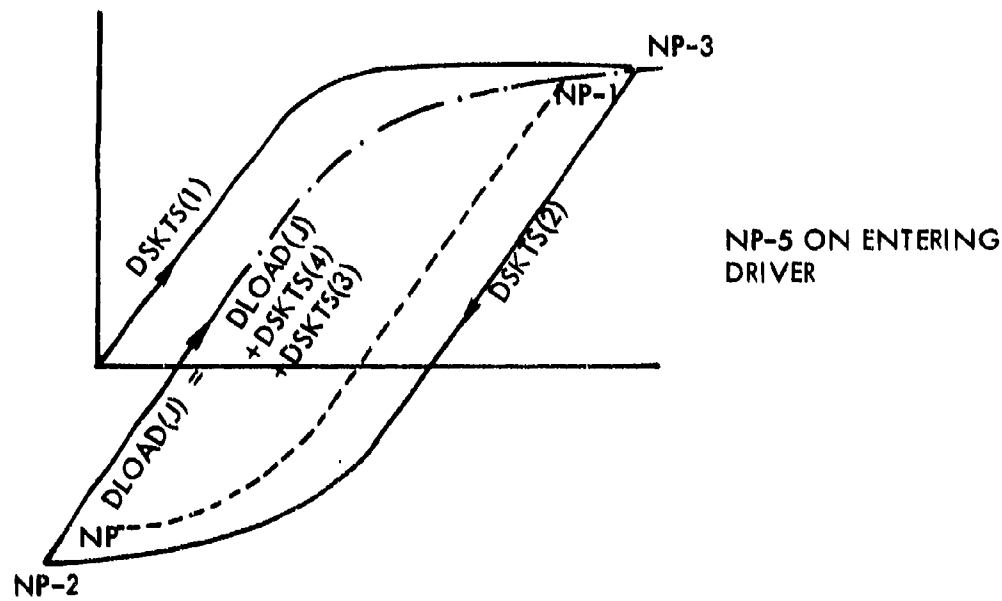

Figure A4.b. Current Loading Increment if NP ≥ 3 and | DLOAD(J) | ≥ | DSKTS(NP-1) |

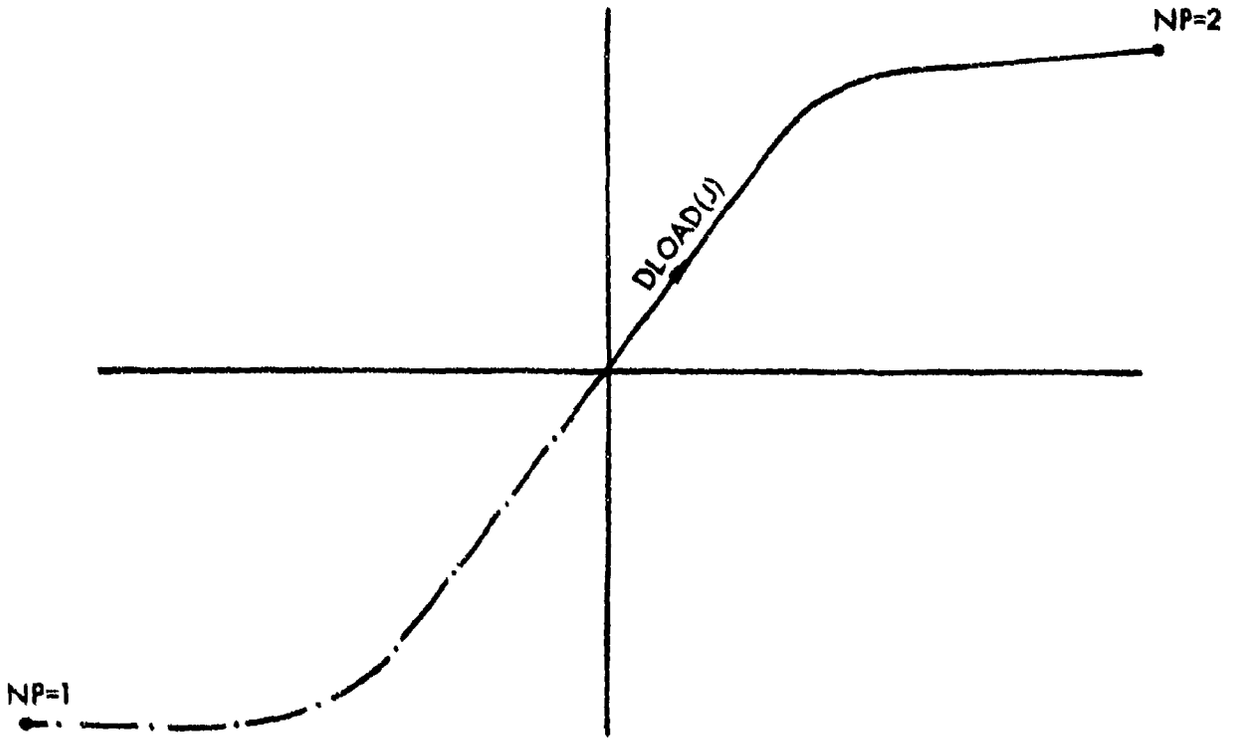

Figure A5. Loading Along the Locus Curve for NP=2

(5) If NP = 2 the trace for the current loading increment proceeds from point ($\varepsilon H(2)$, $\sigma H(2)$) on the locus curve along the branch curve that passes through the points ($\varepsilon H(2)$, $\sigma H(2)$) and ($\varepsilon H(1)$, $\sigma H(1)$).

(6) If $|DLOAD(J)| < 2 \times |DSKTS(1)|$ the new point ($\varepsilon H(3)$, $\sigma H(3)$) will be found on this branch curve between the points ($\varepsilon H(1)$, $\sigma H(1)$) and ($\varepsilon H(2)$, $\sigma H(2)$), Figure A6.a.

(7) If, however, $|DLOAD(J)| \geq 2 \times |DSKTS(1)|$ the trace will pass through the point ($\varepsilon H(1)$, $\sigma H(1)$) and then follow the locus curve. In this instance the loading increment is adjusted so that it is relative to the origin of the plot and loading is considered to follow the locus curve, Figure A6.b.

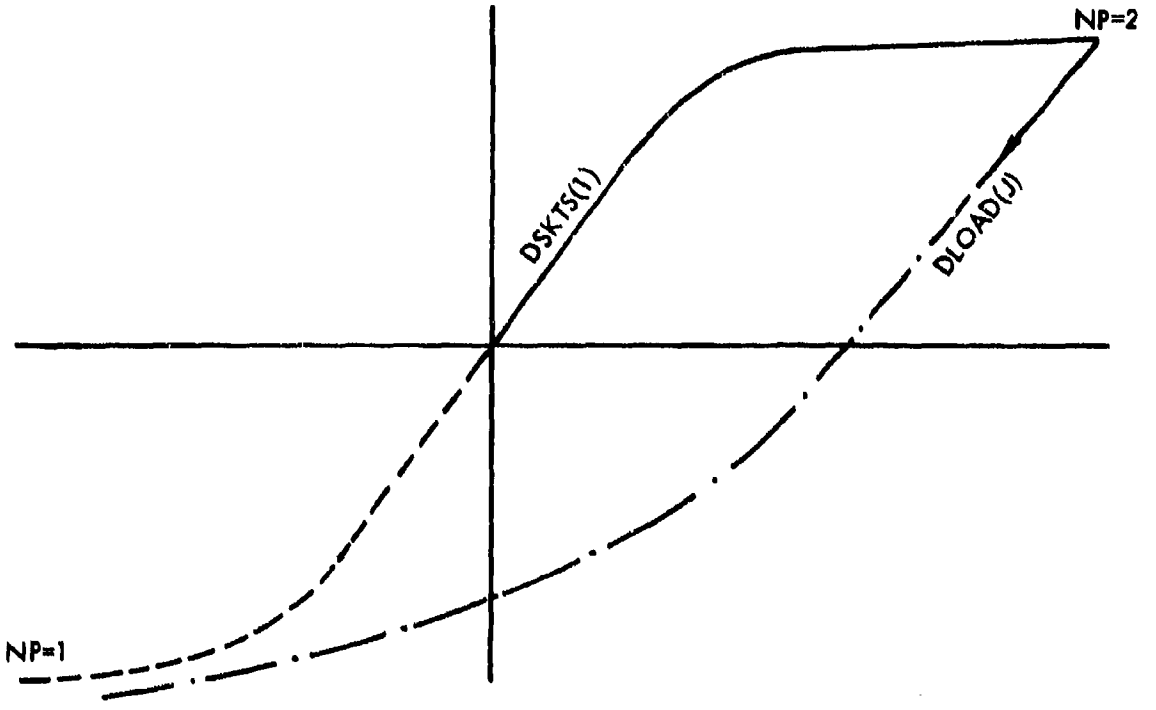

Figure A6.a. Loading for NP=2 and | DLOAD(J) | < 2 x | DSKTS(1) |

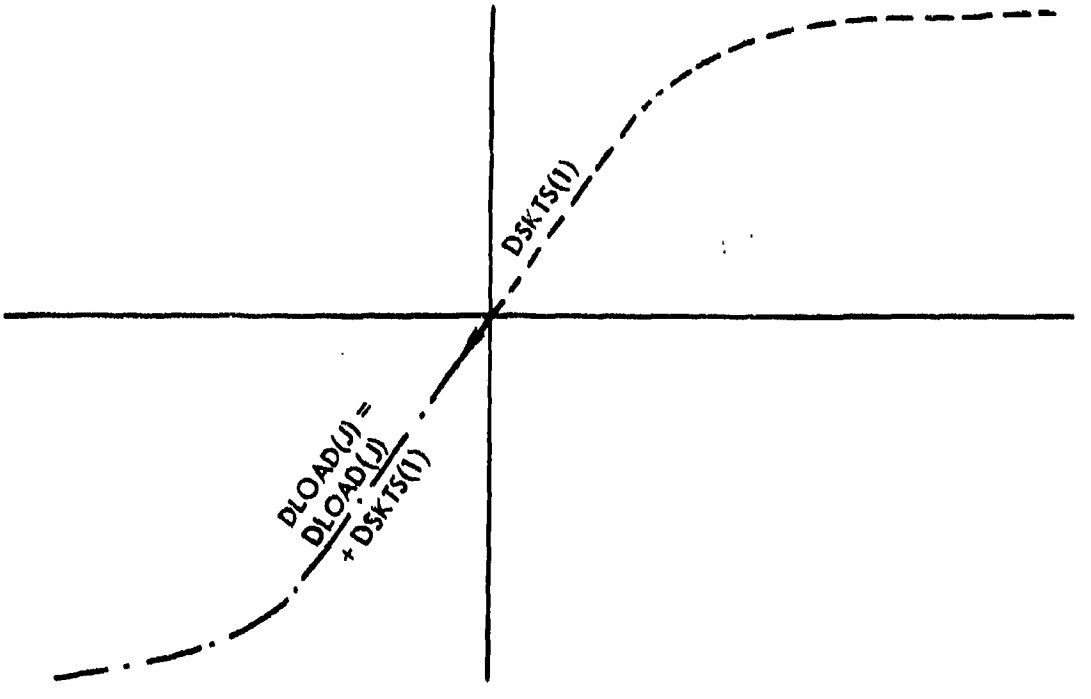

Figure A6.b. Loading for NP=2 and | DLOAD(J) | ≥ 2 x | DSKTS(1) |

A2.3 SUBROUTINE CREEPER(T)

Purpose

This subroutine calls the subroutine CREEP which calculates the creep strain and stress relaxation for the hold period T. The amount of creep for a hold period is affected by any previous creep, and this subroutine keeps up with the history of previous creeps and modifies the current effect appropriately. It also modifies the history arrays εH and σH of strains and stresses to reflect the creep.

Procedure

Consider a hold period, T, after the NP^{th} history point $(\varepsilon H(NP), \sigma H(NP))$ has been calculated. Also consider that the effect of previous creeping is defined by the values CREP and TCREP then the effect on the current hold period is

$$PCT = \frac{\left|\sigma H(NP)^p \times TCREP^n - CPEP\right|}{\left|\sigma(NP)^p \times TCREP^n\right|} \qquad (1)$$

If $PCT < 0$ no creep is allowed. The material is then allowed to creep has the point $(\varepsilon H(NP), \sigma H(NP))$ to the new point $(\varepsilon NP, \sigma NP)$ by calling CREEP

$$\text{CALL CREEP } (\varepsilon H, \sigma H, PCT, NP, T, \varepsilon NP, \sigma NP) \qquad (2)$$

This history of previous creeping is then modified

$$CREP = CREP + \left|(\varepsilon NP - \sigma NP/E) - (\varepsilon H(NP) - \sigma H(NP)/E)\right|$$
$$TCREP = T$$

The history arrays $(\varepsilon H, \sigma H)$ are then modified to reflect this new point by calling subroutines ORIGIN, LPTLC, and ILABC.

A2.4 SUBROUTINE ADJUST (NI)

Purpose

This subroutine adjusts the NP history points ($\varepsilon H, \sigma H$) to be consistant with the hardened locus curve.

Procedure

The adjustment always starts with the point NI in the locus curve (NI = 1 or 2). This is done by projecting the initial point ($\varepsilon H(NI)$, $\sigma H(NI)$) into the new locus curve along a line whose slope is E, Figure A7. This is done by calling subroutine LPTLC

CALL LPTLC ($\varepsilon H(NI), \sigma H(NI), E, \varepsilon HA, \sigma HA$)

Then ($\varepsilon HA, \sigma HA$) is taken as the new point ($\varepsilon H(NI), \sigma H(NI)$).

The point NI +2 on the branch curve is adjusted in a similar manner Figure A8. This is done by calling the subroutine ILABC

CALL ILABC(NI, NI +1, $\varepsilon H(NI+2), \sigma H(NI+2), \varepsilon HA, \sigma HA$)

Then ($\varepsilon HA, \sigma HA$) is taken as the new point ($\varepsilon H(NI+2), \sigma H(NI+2)$).

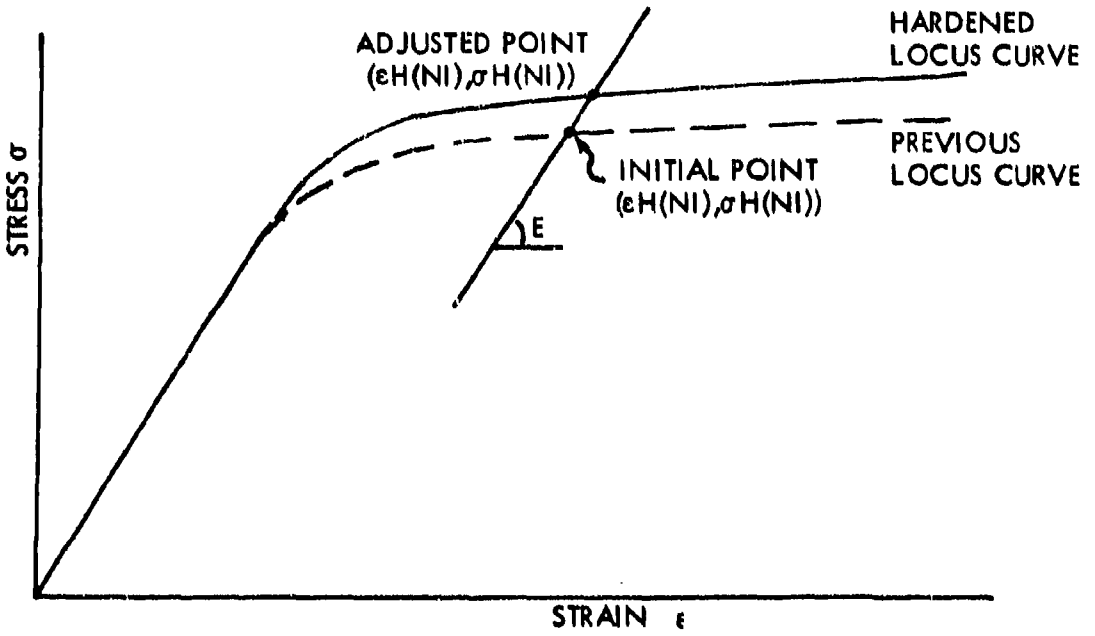

Figure A7. Adjustment of Points on the Locus Curve

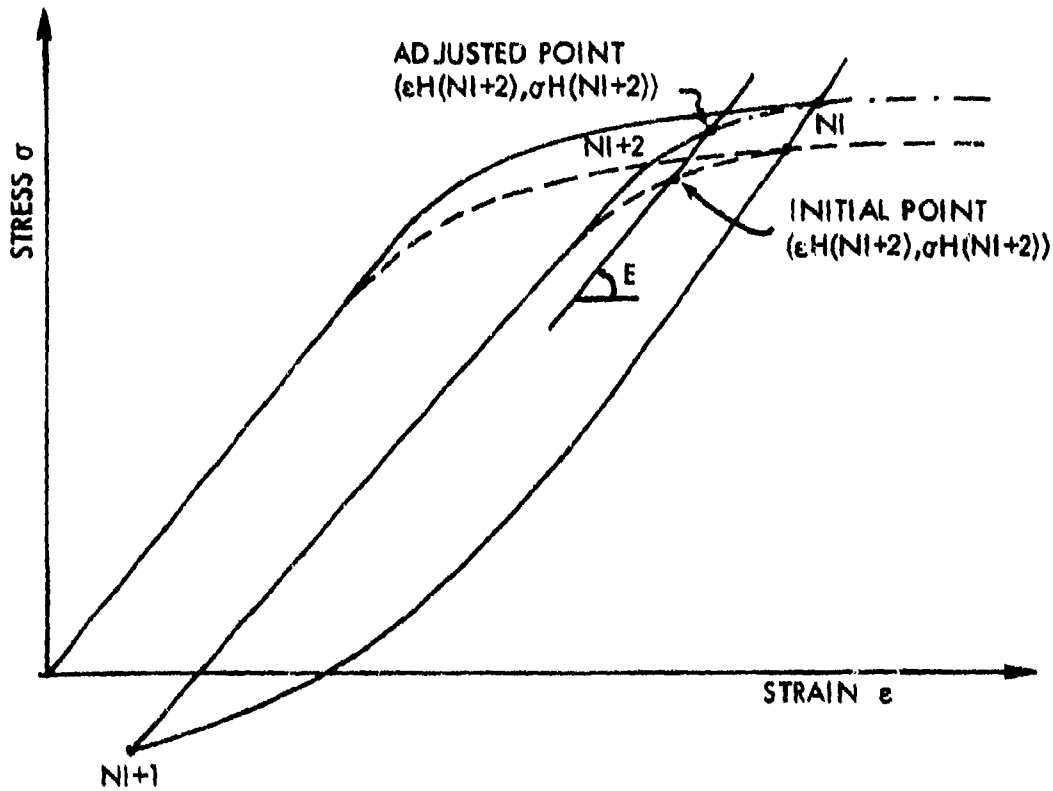

Figure A.8. Adjustment of Points on the Branch Curve

A2.5 SUBROUTINE ORIGIN (N1, N2, εBC_B, σBC_B, NPBC, εOBC, σOBC)

Purpose

This subroutine finds the origin (εOBC, σOBC) in the basic system of the branch curve defined by the NPBC points (εBC_B, σBC_B) such that it passes through the points ($\varepsilon H(N1)$, $\sigma H(N1)$) and ($\varepsilon H(N2)$, $\sigma H(N2)$).

Procedure

The algorithm considers the various locations of the branch curve in the basic system for which the points in the array (εBC_B, σBC_B) are coincident with the point ($\varepsilon H(N1)$, $\sigma H(N1)$), Figure A9. Each point defining the branch curve is considered until a location is found for which the branch curve cuts just inside the point ($\varepsilon H(N2)$, $\sigma H(N2)$). It is first necessary to develop the transformation from the basic system into the branch curve system.

The orientation of the branch curve relative to the basic system is defined by the points ($\varepsilon H(N1)$, $\sigma H(N1)$) and ($\varepsilon H(N2)$, $\sigma H(N2)$).

$$F = \frac{\varepsilon H(N2) - \varepsilon H(N1)}{|\varepsilon H(N2) - \varepsilon H(N1)|} \tag{1}$$

The origin of the branch curve in the basic system for the various locations is

$$\begin{aligned} \overline{\varepsilon OBC} &= \varepsilon H(N1) - \varepsilon BC_B(I) \times F \\ \overline{\sigma OBC} &= \sigma H(N1) - \sigma BC_B(I) \times F \end{aligned} \tag{2}$$

and the transformation from the basic system into the branch curve system is

$$\begin{aligned} \varepsilon_B &= (\varepsilon - \varepsilon OBC) \times F \\ \sigma_B &= (\sigma - \sigma OBC) \times F \end{aligned} \tag{3}$$

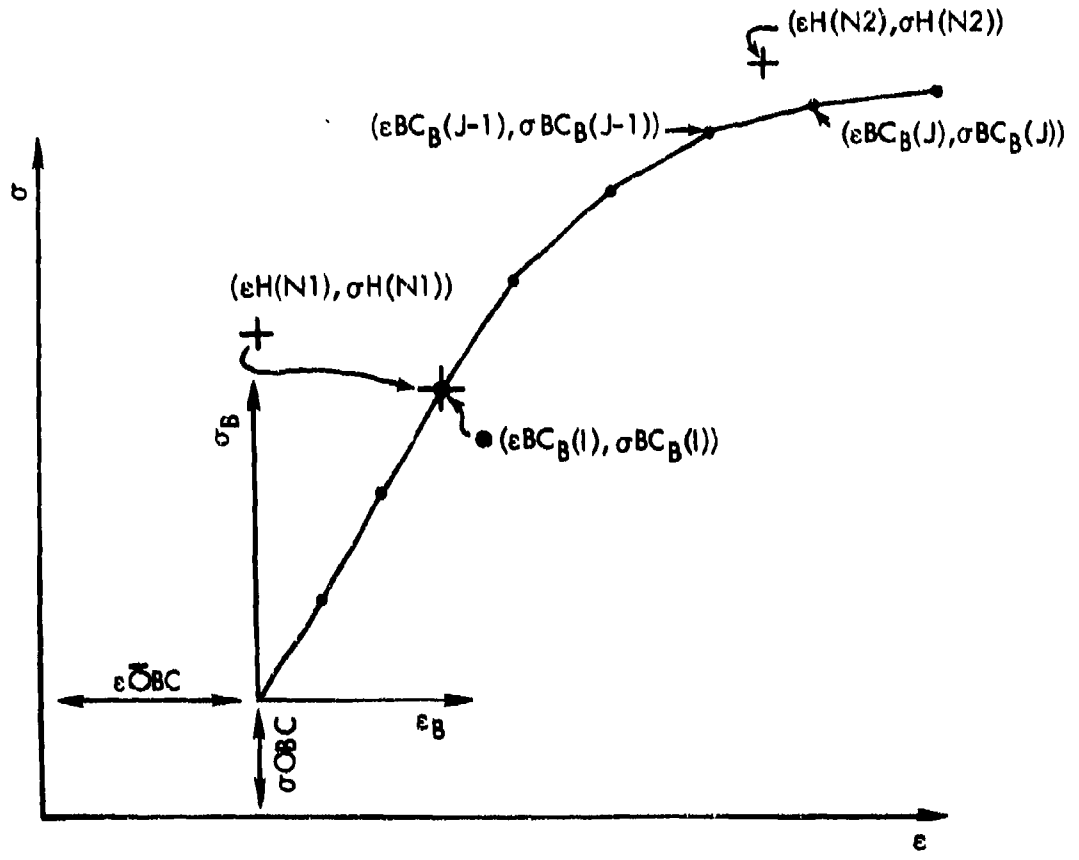

Figure A9. Initial Location of the Branch Curve

Substituting (2) into (3)

$$\varepsilon_B = (\varepsilon - H(N1))xF + \varepsilon BC_B(I)$$
$$\sigma_B = (\sigma - \sigma H(N1))xF + \sigma BC_B(I) \quad (4)$$

For the point $(\varepsilon BC_B(I), \sigma BC_B(I))$ coincident with the point $(\varepsilon H(N1), \sigma H(N1))$ it is necessary to find the points $(\varepsilon BC_B(J-1), \sigma BC_B(J-1))$ and $(\varepsilon BC_B(J), \sigma BC_B(J))$ whose strains straddle the strain for the point $(\varepsilon H(N2)), \sigma H(N2))$ i.e.

$$\varepsilon BC_B(J-1) < \varepsilon H_B(N2) \leq \varepsilon BC_B(J) \quad (5)$$

Transforming $\varepsilon H_B(N2)$ through equation (4) gives

$$\varepsilon BC_B(J-1) < (\varepsilon H(N2) - \varepsilon H(N1))xF + \varepsilon BC_B(I) \leq \varepsilon BC_B(J) \quad (6)$$

Now for the branch curve just cutting inside the point $(\varepsilon H(N2), \sigma H(N2))$

$$\sigma H_B(N2) > \sigma BC_B(J-1) + (\sigma BC_B(J) - \sigma BC_B(J-1)) \times \frac{(\varepsilon H_B(N2) - \varepsilon BC_B(J-1))}{(\varepsilon BC_B(J) - \varepsilon BC_B(J-1))} \quad (7)$$

Again transforming $\varepsilon H_B(N2)$ and $\sigma H_B(N2)$ through equation (4) gives

$$(\sigma H(N2) - \sigma H(N1)) \times F + \sigma BC_B(I) > \sigma BC_B(J-1) + (\sigma BC_B(J) - \sigma BC_B(J-1)) \times \frac{((\varepsilon H(N2) - \varepsilon H(N1)) \times F + \varepsilon BC_B(I) - \varepsilon BC_B(J-1))}{(\varepsilon BC_B(J) - \varepsilon BC_B(J-1))} \quad (8)$$

The algorithm uses equations (6) and (8) to find the point $(\varepsilon BC_B(I), \sigma BC_B(I))$ such that when it is made coincident with the point $(\varepsilon H(N1), \sigma H(N1))$ the branch curve just passes inside the point $(\varepsilon H(N2), \sigma H(N2))$. The branch curve can now be made to pass through the points $(\varepsilon H(N1), \sigma H(N1))$ and $(\varepsilon H(N2), \sigma H(N2)$ by translating

it along the line defined by the points in the basic system ($\varepsilon BC(I-1)$, $\sigma BC(I-1)$) and ($\varepsilon BC(I)$, $\sigma BC(I)$) Figure A10. The amount of translation is determined by finding the intersection between the branch curve at its current location and a line that passes through the point ($\varepsilon H(N2)$, $\sigma H(N2)$) having the same slope as the line along which the translation is to be made. The intersection εI_B, σI_B in the branch curve system is determined by making the call to the following subroutine

$$\text{CALL LPTBC}(\varepsilon H_B(N2),\ \sigma H_B(N2),\ \theta, \varepsilon I_B, \sigma I_B)$$

Where $\varepsilon H_B(N2)$, and $\sigma H_B(N2)$ are obtained by transforming the point ($\varepsilon H(N2)$, $\sigma H(N2)$) through equation (4) and θ, the slope of the line is

$$\theta = \frac{\sigma BC_B(I) - \sigma BC_B(I-1)}{\varepsilon BC_B(I) - \varepsilon BC_B(I-1)} \tag{9}$$

Then the amount of translation ($\Delta\varepsilon$,$\Delta\sigma$) is

$$\begin{aligned} \Delta\varepsilon &= \varepsilon H_B(N2) - \varepsilon I_B \\ \Delta\sigma &= \sigma H_B(N2) - \sigma I_B \end{aligned} \tag{10}$$

Transforming ($\varepsilon H_B(N2)$, $\sigma H_B(N2)$) through equation (4)

$$\begin{aligned} \Delta\varepsilon &= (\varepsilon H(N2) - \varepsilon H(N1)) \times F + \varepsilon BC_B(I) - \varepsilon I_B \\ \Delta\sigma &= (\sigma H(N2) - \sigma H(N1)) \times F + \sigma BC_B(I) - \sigma I_B \end{aligned} \tag{11}$$

Then the final origin is

$$\begin{aligned} \varepsilon OBC &= \overline{\varepsilon OBC} + \Delta\varepsilon \times F \\ \sigma OBC &= \overline{\sigma OBC} + \Delta\sigma \times F \end{aligned} \tag{12}$$

and by substituting equations (2) and (11)

$$\begin{aligned} \varepsilon OBC &= \varepsilon H(N2) - \varepsilon I_B \times F \\ \sigma OBC &= \sigma H(N2) - \sigma I_B \times F \end{aligned} \tag{13}$$

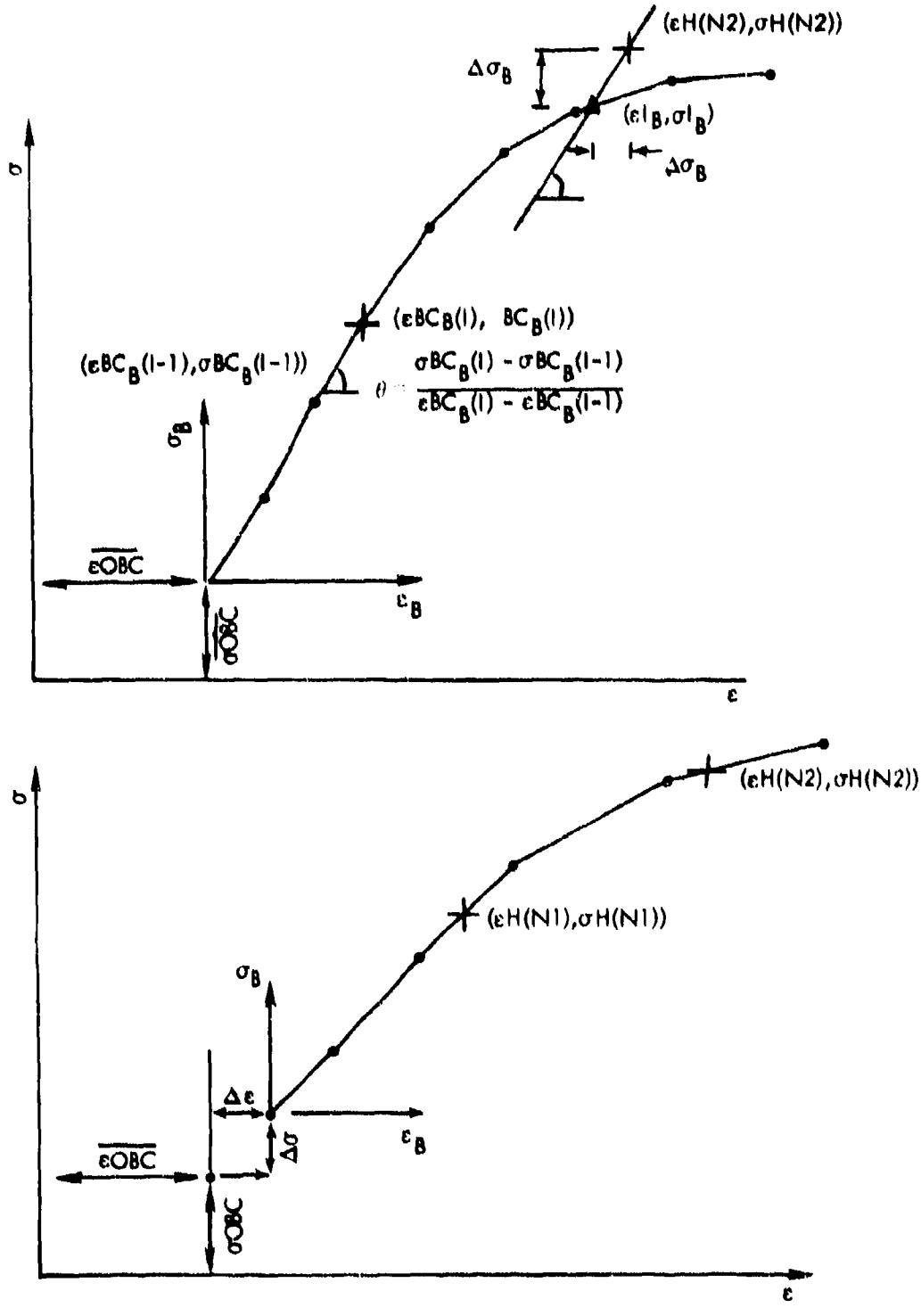

Figure A10. Translation of the Branch Curve

A2.6 SUBROUTINE MAKPLT(εPLT(1),εPLT(2),σPLT(1),σPLT(2),NFLAG)

Purpose

This subroutine is used to set up arrays εPLOT and σPLOT defining points that are to be joined together to form a curve between the two points (εPLT(1),σPLT(1) and (εPLT(2),σPLT(2)). If NFLAG > 1 the curve is represented by the branch curve and if NFLAG < 1 it is represented by the locus curve.

Procedure

The start and end points in the array are always the points (εPLT(1),σPLT(1)) and (εPLT(2),σPLT(2)). If NFLAG < 1 the remaining points in the array are the points defining the locus curve whose strains lie between εPLT(1) and εPLT(2). If NFLAG > 1 it is necessary to first locate the branch curve in the basic system such that it passes through the points (εPLT(1), σPLT(1)) and (εPLT(2), σPLT(2)). This is done by calling the subroutine ORIGIN. Subroutine origin gives the location of the origin of the branch curve in the basic system. The points on the branch curve are now transformed into the basic system and the transformed points whose strains lie between εPLT(1) and εPLT(2) are used for the plot arrays.

A2.7 SUBROUTINE INCBC(N1,N2,N,DSKT,εI,σI)

Purpose

This subroutine finds the intersection (εI,σI) between Neuber's equation, defined relative to the point (εH(N),σH(N)) by the loading increment DSKT, with a branch curve which passes through the points (εH(N1),σH(N1)) and (εH(N2),σH(N2)).

Procedure

Neuber's equation defined relative to the point (εH(N),σH(N)) by the loading increment DSKT is

$$\frac{E \times \varepsilon_N \times \sigma_N}{\left(1 - \left(\left|\frac{\varepsilon_N}{A}\right|\right)^4\right)^2} = DSKT^2 \qquad (1)$$

Consider the transformation from the basic system to a system which has an origin at (εH(N),σH(N)) Figure A11.

$$\varepsilon_N = (\varepsilon - \varepsilon H(N)) \times F$$
$$\sigma_N = (\sigma - \sigma H(N)) \times F \qquad (2)$$

where

$$F = DSKT/|DSKT| \qquad (3)$$

Substituting (2) into (1)

$$\frac{E \times (\varepsilon - \varepsilon H(N)) \times (\sigma - \sigma H(N))}{\left(1 - \left(\frac{\varepsilon - \varepsilon H(N)}{A}\right)^4\right)^2} = DSKT^2 \qquad (4)$$

Next it is necessary to find the origin (εOBC, σOBC) in the basic system of the branch curve which passes through the points (εH(N1),σH(N1)) and (εH(N2),σH(N2)). This is done by making the following call to subroutine ORIGIN

CALL ORIGIN (N1,N2,εBC,σBC,NPBC,εOBC,σOBC) (5)

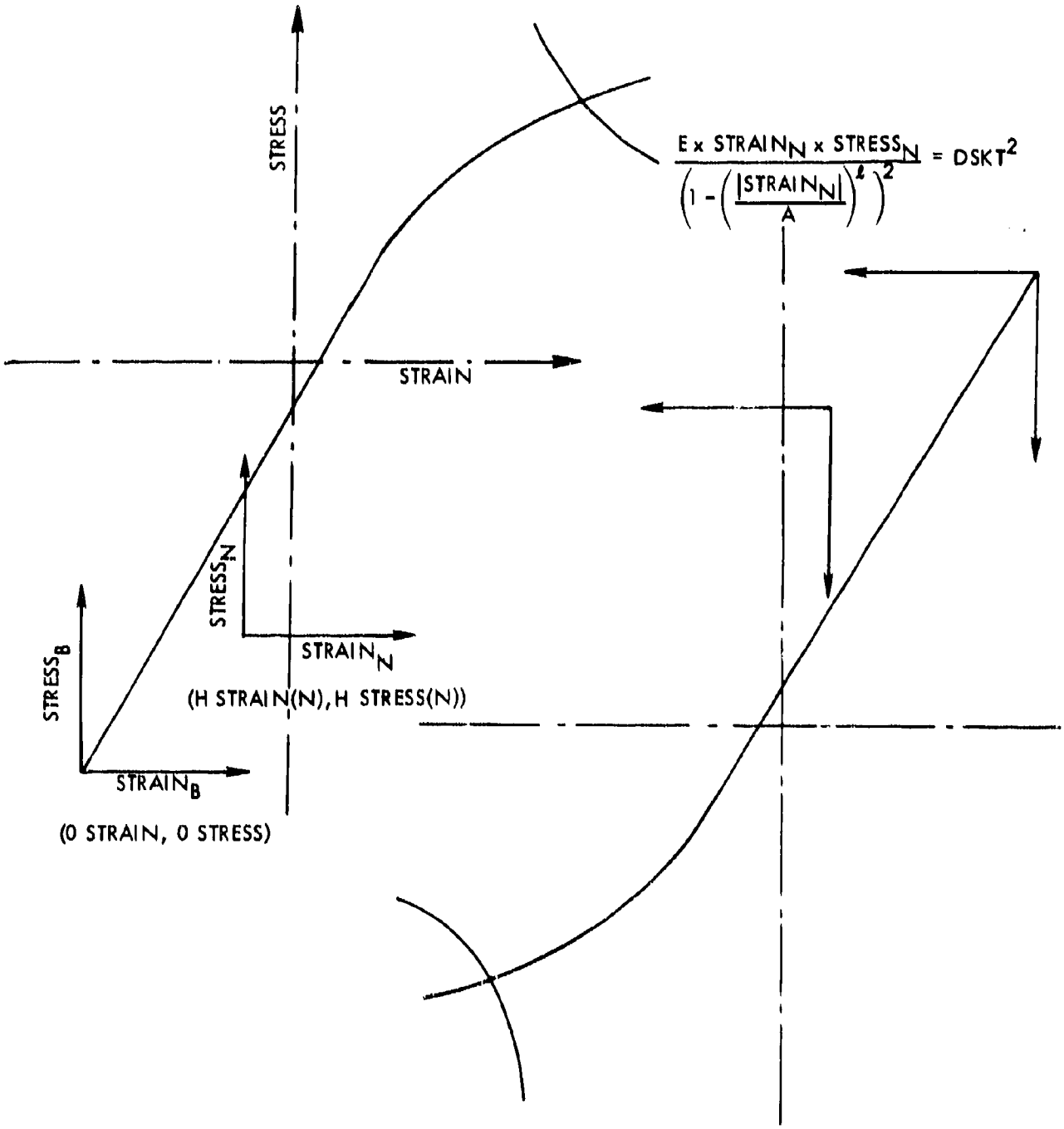

Figure A11. Transformation to a System with Its Origin at (εH(N),σH(N))

Now consider the transformation from the branch curve system ε_B, σ_B to the basic system

$$\begin{aligned} \varepsilon &= \varepsilon_B \times F + \varepsilon OBC \\ \sigma &= \sigma_B \times F + \sigma OBC \end{aligned} \tag{6}$$

Substituting (6) into (4)

$$\frac{E \times (\varepsilon_B \times F + \varepsilon OBC - \varepsilon H(N)) \times (\sigma_B \times F + \sigma OBC - \sigma H(N))}{\left(1 - \left(\left|\frac{\varepsilon_B \times F + \varepsilon OBC - \varepsilon H(N)}{A}\right|\right)^4\right)^2} = DSKT^2 \tag{7}$$

This equation is used in the following algorithm to find the intersection

- Consider the points defining the branch curve relative to its origin $(\varepsilon BC, \sigma BC)$. These points are sequentially substituted for $(\varepsilon_B, \sigma_B)$ in equation (7) until a pair $(\varepsilon BC_B(I-1), \sigma BC_B(I-1))$, $(\varepsilon BC_B(I), \sigma BC_B(I))$ are found which give solutions that straddle the value $DSKT^2$.
- The problem is now reduced to finding the intersection of a line joining the points $(\varepsilon BC_B(I-1), \sigma BC_B(I-1))$ and $(\varepsilon BC_B(I), \sigma BC_B(I))$ with Neuber's equation defined relative to the point $(\varepsilon H(N), \sigma H(N))$. This is done by making the following call to subroutine BINTS

$$\text{CALL BINTS } (\varepsilon BC_B(I-1), \varepsilon BC_B(I), \sigma BC_B(I-1), \sigma BC_B(I), N, DSKT^2, \varepsilon OBC, \sigma OBC, F, \varepsilon I_B, \sigma I_B)$$

Finally εI_B and σI_B are substituted into equations (6) to find the point of intersection $(\varepsilon I, \sigma I)$ relative to the basic system.

A2.8 SUBROUTINE ILABC(N1,N2,εP,σP,εI,σI)
COMMON/SLOPES/θ

Purpose

This subroutine finds the intersection εI,σI of the branch curve, defined by the array εBC,σBC, which passes through the points (εH(N1),σH(N1)) and (εH(N2), σH(N2)) with a line that passes through the point (εP,σP) with a slope θ.

Procedure

It is first necessary to find the origin (εOBC,σOBC) of the branch curve such that it passes through the points (εH(N1),σH(N1) and (εH(N2),σH(N2)). This is done by making the following call to the subroutine ORIGIN

$$\text{CALL ORIGIN (N1,N2,}\varepsilon BC_B,\sigma BC_B,\text{NPBC,}\varepsilon OBC,\sigma OBC)$$

Next, consider the transformation from the basic system into the branch system

$$\begin{aligned}\varepsilon_B &= (\varepsilon - \varepsilon OBC) \times F \\ \sigma_B &= (\sigma - \sigma OBC) \times F\end{aligned} \tag{1}$$

where

$$F = \frac{H(N2) - H(N1)}{|H(N2) - H(N1)|} \tag{2}$$

Find the projection $\overline{\varepsilon P}_B$ of the point (εP,σP) in the branch curve strain axis by translating along a line with slope θ, Figure A12.

$$\overline{\varepsilon P}_B = \varepsilon P_B - \sigma P_B/\theta \tag{3}$$

Substituting (1)

$$\overline{\varepsilon P}_B = ((\varepsilon - \sigma/\theta) - (\varepsilon OBC - \sigma OBC/\theta))F \tag{4}$$

Similarly translating the points (εBC_B, σBC_B) defining the branch curve into the strain axis

$$\overline{\varepsilon BC}_B = \varepsilon BC_B - \sigma BC_B/\theta \tag{5}$$

These values are scanned until a pair $\overline{\varepsilon BC}_B(J-1)$, $\overline{\varepsilon BC}_B(J)$ are found which straddle the value $\overline{\varepsilon P}_B$ i.e.

$$\overline{\varepsilon BC}_B(J-1) < \overline{\varepsilon P}_B < \overline{\varepsilon BC}_B(J) \tag{6}$$

The problem is now simply one of finding the intersection ($\varepsilon I, \sigma I$) between two lines, one which passes through the points ($\varepsilon BC_B(J-1)$, $\sigma BC_B(J-1)$) and ($\varepsilon BC_B(J)$, $\sigma BC_B(J)$), the other which passes through the point ($\varepsilon P, \sigma P$) with slope E. This is done by calling subroutine LINBR as follows

CALL LINBR($\varepsilon BC_B(J-1)$, $\varepsilon BC_B(J)$, $\sigma BC_B(J-1)$, $\sigma BC_B(J)$, εP, σP,
εOBC, σOBC, F, εI, σI)

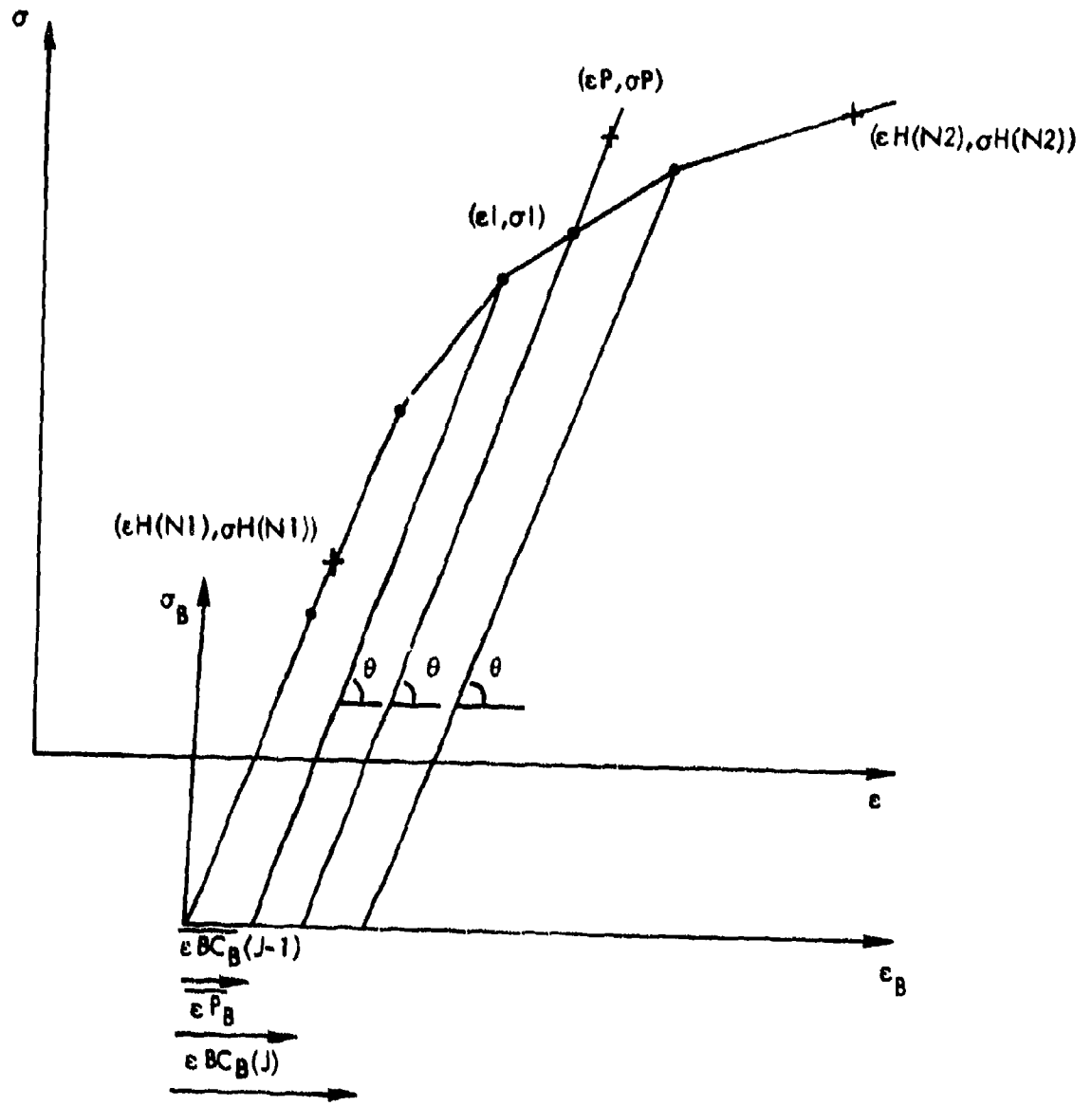

Figure A12. Projection into the Branch Curve Strain Axis

A2.9 SUBROUTINE INCLC(DSKT, N, εI, σI)

Purpose

This subroutine finds the intersection (εI, σI) between Neuber's equation, defined relative to the point (εH(N), σH(N)) by the loading increment DSKT, with the locus curve.

Procedure

Neuber's equation defined relative to the point (εH(N), σH(N)) by the loading increment DSKT is

$$\frac{E \times \varepsilon_N \times \sigma_N}{\left(1 - \left(\frac{|\varepsilon_n|}{A}\right)^{\frac{1}{2}}\right)^2} = DSKT^2 \tag{1}$$

Consider the transformation from the basic system to a system which has an origin at (εH(N), σH(N)) Figure A10.

$$\begin{aligned} \varepsilon_N &= (\varepsilon - \varepsilon H(N)) \times F \\ \sigma_N &= (\sigma - \sigma H(N)) \times F \end{aligned} \tag{2}$$

where

$$F = DSKT/|DSKT| \tag{3}$$

Substituting (2) into (1)

$$\frac{E \times (\varepsilon - \varepsilon H(N)) \times (\sigma - \sigma H(N))}{\left(1 - \left(\frac{|\varepsilon - \varepsilon H(N)|}{A}\right)^{\frac{1}{2}}\right)^2} = DSKT^2 \tag{4}$$

Now if $F > 0$ the intersection will be with the tension half of the locus curve and if $F < 0$ it will be with the compression half of the locus curve. Define the array εLC, σLC as the specific half of the locus curve being considered. This array together with equation (4) is used in the following algorithm to find the intersection.

- Sequentially substitute the points ($\varepsilon LC, \sigma LC$) into equation (4) until a pair, ($\varepsilon LC(I-1)$, $\sigma LC(I-1)$) and ($\varepsilon LC(I)$, $\sigma LC(I)$), are found which give solutions that straddle the value $DSKT^2$.

- The problem is now reduced to finding the intersection of a line joining the points ($\varepsilon LC(I-1)$, $\sigma LC(I-1)$) and ($\varepsilon LC(I)$, $\sigma LC(I)$) with Neuber's equation defined relative to the point ($\varepsilon H(N)$, $\sigma H(N)$). This is done by making the following call to subroutine DETERM

```
CALL DETERM (εLC(I-1),εLC(I), σLC(I-1), σLC(I),
    N, DSKT², εI, σI)
```

A2.10 SUBROUTINE LPTLC($\varepsilon P, \sigma P, \theta, \varepsilon I, \sigma I$)

Purpose

This subroutine finds the intersection ($\varepsilon I, \sigma I$) between the locus curve and a line that passes through the point ($\varepsilon P, \sigma P$), with a slope θ.

Procedure

Consider the projection $\overline{\varepsilon P}$ of the point ($\varepsilon P, \sigma P$) on the strain axis by translating along the line with slope θ, Figure A13.

$$\overline{\varepsilon P} = \varepsilon P - \sigma P/\theta \tag{1}$$

If $\overline{\varepsilon P} > 0$ the intersection will be with the tension half of the locus curve and if $\overline{\varepsilon P} < 0$ the intersection will be with the compression half. Define the array εLC, σLC as the specific half of the locus curve being considered. Now consider the projections $\overline{\varepsilon LC}$ of the points of this array on the strain axis by translating along the line with slope θ.

$$\overline{\varepsilon LC} = \varepsilon LC - \sigma LC/\theta \tag{2}$$

These are scanned until a pair $\overline{\varepsilon LC}(J-1)$, $\overline{\varepsilon LC}(J)$ are found which straddle the value $\overline{\varepsilon P}$ i.e.

$$\overline{\varepsilon LC}(J-1) < \overline{\varepsilon P} < \overline{\varepsilon LC}(J) \tag{3}$$

The problem is now simply one of finding the intersection of two lines, one which passes through the points ($\varepsilon LC(J-1), \sigma LC(J-1)$ and ($\varepsilon LC(J), \sigma LC(J)$), the other which intersects the strain axis at $\overline{\varepsilon P}$ with a slope θ. This is done by making the following call to subroutine LINSEC.

CALL LINSEC($\varepsilon LC(J-1), \varepsilon LC(J), \sigma LC(J-1), \sigma LC(J), \theta, \varepsilon I, \sigma I$)

COMMON LINE$|\overline{\varepsilon P}|$

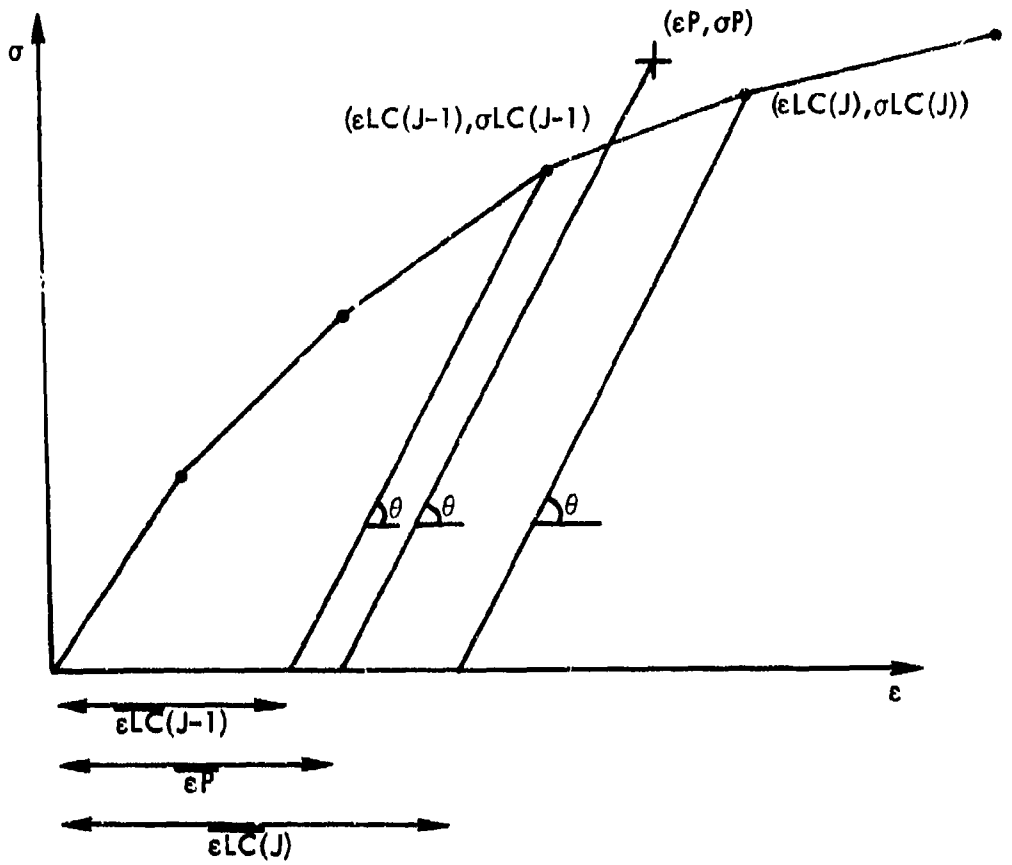

Figure A13. Projection into the Strain Axis

A2.11 SUBROUTINE LPTBC(εP_B, σP_B, θ, εI_B, σI_B)

Purpose

This subroutine finds the intersection (εI_B, σI_B) between the branch curve defined by the array (εBC_B, σBC_B) and a line which passes through the point (εP_B, σP_B) with a slope of θ.

Procedure

Consider the projection $\overline{\varepsilon BC}_B$ of the array (εBC_B, σBC_B) on the strain axis by translating along a line with slope θ, Figure A14.

$$\overline{\varepsilon BC}_B = \varepsilon BC_B - \sigma BC_B/\theta \tag{1}$$

Similarly consider the projection $\overline{\varepsilon B}$ of the point (εP_B, σP_B)

$$\overline{\varepsilon P}_B = \varepsilon P_B - \sigma P_B/\theta \tag{2}$$

The algorithm simply scans the array $\overline{\varepsilon BC}_B$ to find a pair of values $\varepsilon BC_B(J-1)$ and $\varepsilon BC_B(J)$ whose projections straddle $\overline{\varepsilon P}_B$ i.e.

$$\overline{\varepsilon BC}_B\,(J-1) \leq \overline{\varepsilon P}_B \leq \overline{\varepsilon BC}_B\,(J) \tag{3}$$

The problem is now simply one of finding the intersection of two lines, one which passes through the points ($\varepsilon BC_B(J-1)$, $\sigma BC_B(J-1)$) and ($\varepsilon BC_B(J)$, $\sigma BC_B(J)$), the other which intersects the strain axis at $\overline{\varepsilon P}_B$ with a slope θ. This is done by making the following call to subroutine LINSEC

CALL LINSEC ($\varepsilon BC_B(J-1)$, $\varepsilon BC_B(J)$, $\sigma BC_B(J-1)$, $\sigma BC_B(J)$, θ, εI_B, σI_B)

COMMON LINE| $\overline{\varepsilon P}_B$ |

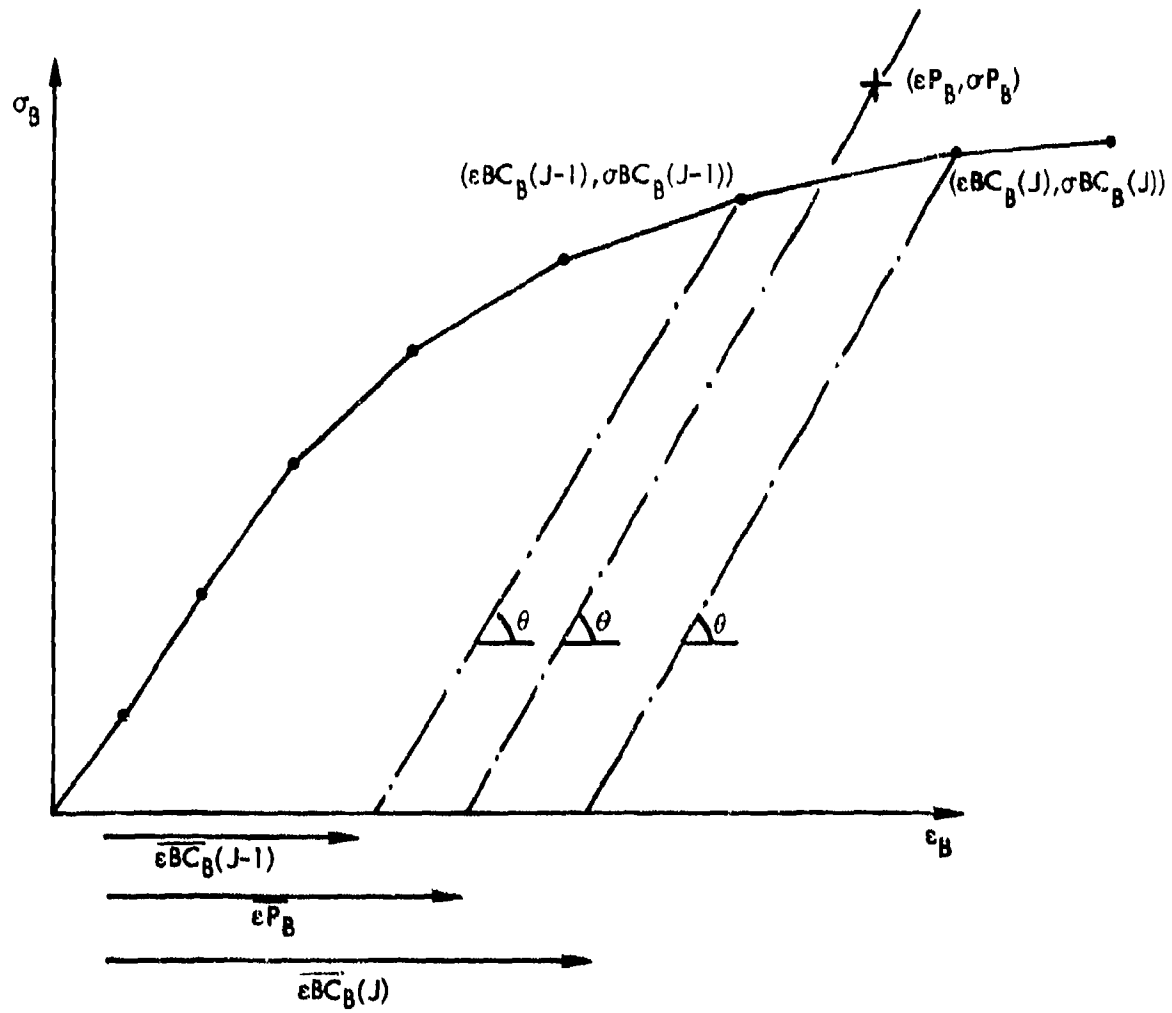

Figure A14. Projection into the Strain Axis

A2.12 SUBROUTINE RAIN (S, JMIN, JMAX)

This subroutine employs the rain flow counting method to generate the analysis spectrum from the peak spectrum S. JMIN and JMAX contain indexes for minimum peak strain or stress and maximum peak strain or stress respectively.

A2.13 SUBROUTINE SPECT (S, NS, NLOADS, S1, S2, N)

This subroutine reads block spectrum values S1, S2 and N and converts it into peak spectrum for hysteresis loop analysis.

A2.14 SUBROUTINE CRVTRP(Dε/2)

Purpose

This subroutine takes half the plastic strain increment, Dε/2, for the current loading increment and computes the hardened locus curve.

Procedure

If Dε/2 is <0 the analysis hardens the tension locus curve and if it is > 0 it hardens the compression locus curve. Consider Dε/2 > 0, the analysis uses this value to interpret the number of cycles to hardening, NTC, from the arrays, Dε, NCH, Figure A15. The sum, SNC, of the inverse if the number of cycles to hardening for all the tension cycles is then computed. This value, SNC, is then used to interpret the % hardening, PCC, of the compression locus curve from the arrays SI, PC Figure A16. The compression part of the hardened locus curve is then computed by interpreting between the monotonic compression locus curve and the cyclic locus curve using PCC i.e.

$$\sigma LCC = \sigma MCC + (\sigma CCC - \sigma MCC) + PCC$$

εMCC, εCCC, and εLCC are assumed to be equivalent

The identical procedure is used to harden the tension side of the locus curve when Dε/2 < 0.

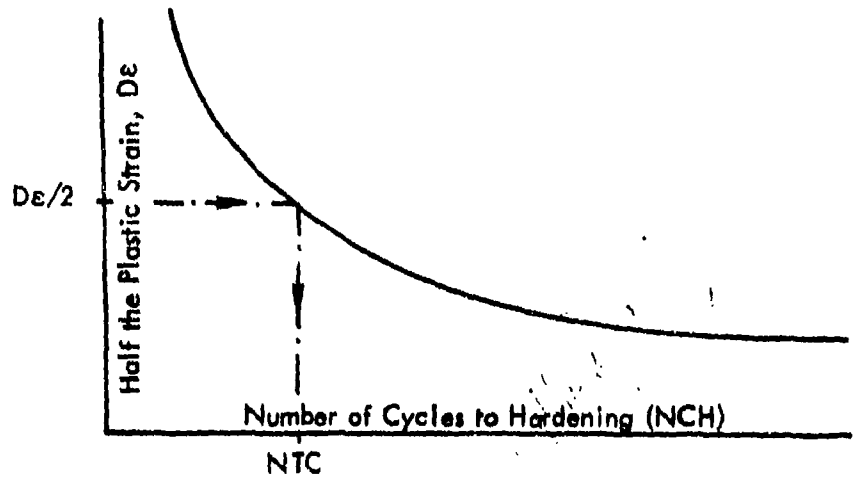

Figure 15. Interpretation of NTC

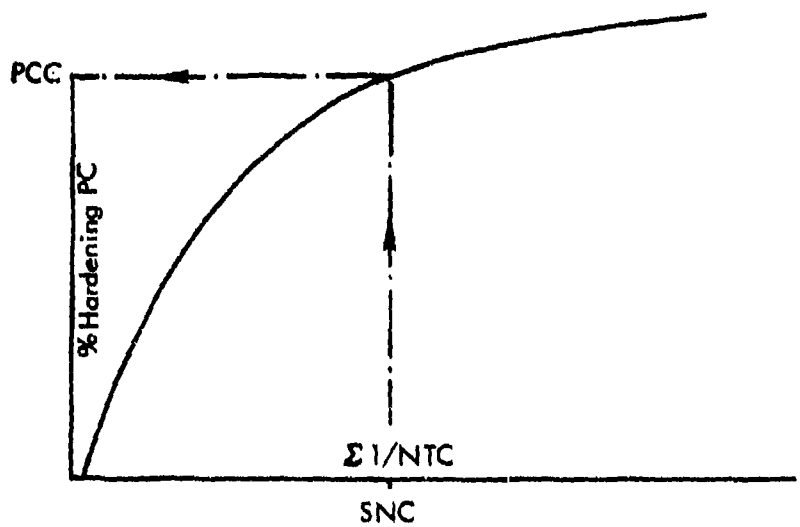

Figure 16. Interpretation of PCC

A2.15 SUBROUTINE CREEP (εH,σH,PCT,NP,T,εNP,σNP)

Purpose

This subroutine calculates the point (εNP,σNP) considering the material to have crept from the point (εH(NP),σH(NP)) over a time T. The term PCT reflects the effect of previous hold periods.

Procedure

The amount of stress relaxation σR is obtained by finding the root to the following function

$$f(\sigma R) = \sigma R + K\bar{E}\,(\sigma H(NP) - \sigma R)^{p+1}\,t^{n} \tag{1}$$

$$f'(\sigma R) = 1 + K\bar{E}\,(p+1)\,(\sigma H\,(NP) - \sigma R)^{p}\,t^{n} \tag{2}$$

Hence using the Newton's method

$$\sigma R_{i+1} = \sigma R_i - \frac{f(\sigma R)}{f'(\sigma R)} \tag{3}$$

Equation (3) is iterated until σR_{i+1} and σR_i are sufficiently close to each other. Knowing σR the creep strain εC is found from the equation

$$\varepsilon C = \sigma R/(\bar{E}\,(\sigma H(NP) - \sigma R)) \tag{4}$$

Hence

$$\begin{aligned} \varepsilon NP &= \varepsilon H(NP) - \varepsilon C \\ \sigma NP &= \sigma H(NP) - \sigma R \end{aligned} \tag{5}$$

A2.16 SUBROUTINE LINBR($\varepsilon D_B(1), \varepsilon D_B(2), \sigma D_B(1), \sigma D_B(2), \varepsilon P, \sigma P, F, \varepsilon I, \sigma I$)

Purpose

This subroutine finds the intersection ($\varepsilon I, \sigma I$) between a line defined by the points ($\varepsilon D_B(1), \sigma D_B(1)$) and ($\varepsilon D_B(2), \sigma D_B(2)$) in the branch curve system which has its origin at ($\varepsilon OBC, \sigma OBC$) in the basic system with another line which passes through the point $\varepsilon P, \sigma P$ having a slope E.

Procedure

The transformation from the basic system into the branch curve system is

$$\begin{aligned} \varepsilon_B &= (\varepsilon - \varepsilon OBC) \times F \\ \sigma_B &= (\sigma - \sigma OBC) \times F \end{aligned} \tag{1}$$

The projection of the point ($\varepsilon P, \sigma P$) in the strain axis of the branch curve system along a line whose slope is E is, Figure A17.

$$\overline{\varepsilon P}_B = \varepsilon P_B - \sigma P_B / E \tag{2}$$

Transforming through (1)

$$\overline{\varepsilon P}_B = ((\varepsilon - \sigma/E) - (\varepsilon OBC - \sigma OBC/E))F \tag{3}$$

The algorithm starts by finding the mid point ($\varepsilon I, \sigma I$) of the line defined by the two points ($\varepsilon D(1), \sigma D(1)$) and ($\varepsilon D(2), \sigma D(2)$)

$$\begin{aligned} \varepsilon I_B &= (\varepsilon D_B(1) + \varepsilon D_B(2))/2 \\ \sigma I_B &= (\sigma D_B(1) + \sigma D_B(2))/2 \end{aligned} \tag{4}$$

This point is then projected into the strain axis along a line which has a slope E

$$\varepsilon I_B = \varepsilon I_B = \sigma I_B / E \tag{5}$$

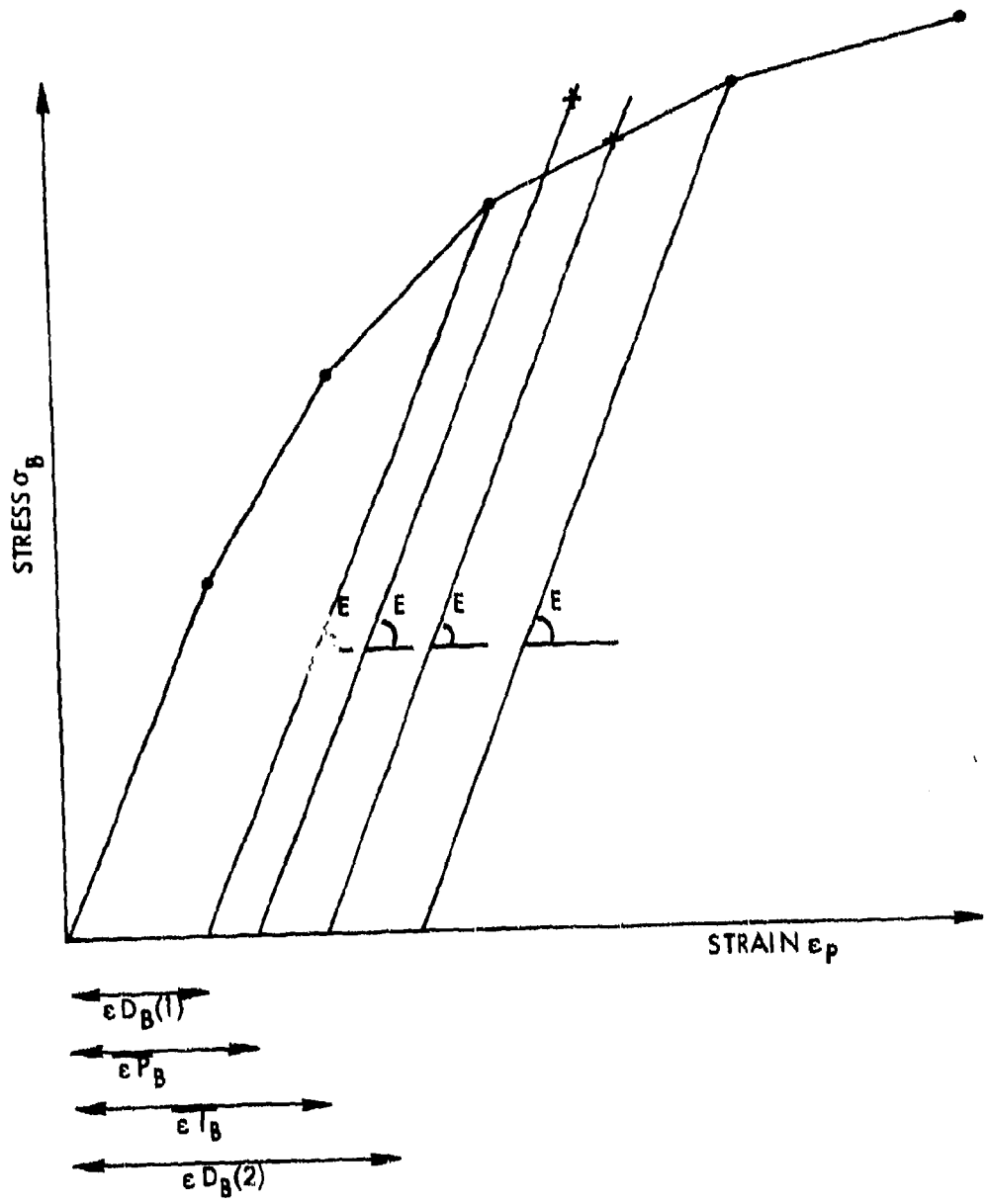

Figure A17. Projection into the Branch Curve Strain Axis

If $\overline{\varepsilon P}_B > \overline{\varepsilon I}_B$ the point $(\varepsilon D_B(2), \sigma D_B(2))$ is set equal to the point $(\varepsilon I_B, \sigma I_B)$ but if $\overline{\varepsilon P}_B < \overline{\varepsilon I}_B$ the point $(\varepsilon D_B(1), \sigma D_B(1))$ is set equal to the point $(\varepsilon I_B, \sigma I_B)$.

This is repeated until $\overline{\varepsilon I}_B$ is sufficiently close to $\overline{\varepsilon P}_B$.

Finally the point $(\overline{\varepsilon I}_B, \sigma I_B)$ is transformed into the basic system through equation (4)

$$\begin{aligned} \varepsilon I &= \overline{\varepsilon I}_B \times F + \varepsilon OBC \\ \sigma I &= \sigma I_B \times F + \sigma OBC \end{aligned} \qquad (6)$$

A2.17 SUBROUTINE BCRPLT(PLT,σPLT,NP)

Purpose

This subroutine simply takes the NP points defined by the arrays PLT,σPLT and draws straight lines between them on the CALCOMP plotter.

A2.18 SUBROUTINE FDSKT(N)

This subroutine computes DSKTS(N) for the creep analysis. CREPER calls FDSKT after the amount of creep has been calculated and the history arrays (EX,SY) have been adjusted for the computed creep.

A2.19 SUBROUTINE DAMAGE

This subroutine calculates fatigue damage using the conventional Palmgren-Miner's rule of cumulative fatigue damage. This routine is called by the RAIN subroutine.

A2.20 SUBROUTINE DETERM ($\varepsilon D(1), \varepsilon D(2), \sigma D(1), \sigma D(2), N, DSKT^2, \varepsilon I, \sigma I$)

Purpose

This subroutine finds the intersection ($\varepsilon I, \sigma I$) between a line defined by the two points ($\varepsilon D(1), \sigma D(1)$) and ($\varepsilon D(2), \sigma D(2)$) and Neuber's equation defined relative to the point ($\varepsilon H(N), \sigma H(N)$) by the term $DSKT^2$.

Procedure

From subroutine INCLC, Neuber's equation relative to the point ($\varepsilon H(N), \sigma H(N)$) is

$$\frac{E \times (\varepsilon - \varepsilon H(N)) \times (\sigma - \sigma H(N))}{\left(1 - \left(\frac{|\varepsilon - \varepsilon H(N)|}{A}\right)^{\ell}\right)^2} = DSKTS^2 \qquad (1)$$

The algorithm starts by finding the midpoint ($\varepsilon I, \sigma I$) of the line defined by the two points ($\varepsilon D(1), \sigma D(1)$) and ($\varepsilon D(2), \sigma D(2)$)

$$\begin{aligned} \varepsilon I &= (\varepsilon D(1) + \varepsilon D(2))/2 \\ \sigma I &= (\sigma D(1) + \sigma D(2))/2 \end{aligned} \qquad (2)$$

This point is then substituted into Equation (1). Then, if the solution to this equation is greater than $DSKTS^2$, the point ($\varepsilon D(2), \sigma D(2)$) is set equal to the point ($\varepsilon I, \sigma I$); and, if the solution is less than $DSKTS^2$, the point ($\varepsilon D(1), \sigma D(1)$) is set equal to the point ($\varepsilon I, \sigma I$). This procedure is repeated until the solution is sufficiently close to $DSKTS^2$.

A2.21 SUBROUTINE LINSEC(εD(1), εD(2), σD(1), σD(2), θ, εI, σI)
COMMON LINE |$\overline{\varepsilon P}$|

Purpose

This subroutine finds the intersection (εI, σI) between a line defined by the two points (εD(1), σD(1)) and (εD(2), σD(2)) and another line which intersects the strain axis at εP with a slope θ.

Procedure

The algorithm starts by finding the mid point (εI, σI) of the line defined by the two points (εD(1), σD(1)) and (εD(2), σD(2))

$$\begin{aligned} \varepsilon I &= (\varepsilon D(1) + D(2))/2 \\ \sigma I &= (\sigma D(1) + \sigma D(2))/2 \end{aligned} \tag{1}$$

This point is then projected into the strain axis along a line which has a slope of θ Figure A18.

$$\overline{\varepsilon} I = \varepsilon I - \sigma I/\theta \tag{2}$$

Then if $|\overline{\varepsilon I}| > |\varepsilon P|$ the point (εD(2), σD(2)) is set equal to the point (εI, σI) and if $|\overline{\varepsilon I}| < |\varepsilon P|$ the point (εD(1), σD(1)) is set equal to the point (εI, σI).

This procedure is repeated until $\overline{\varepsilon I}$ is sufficiently close to εP.

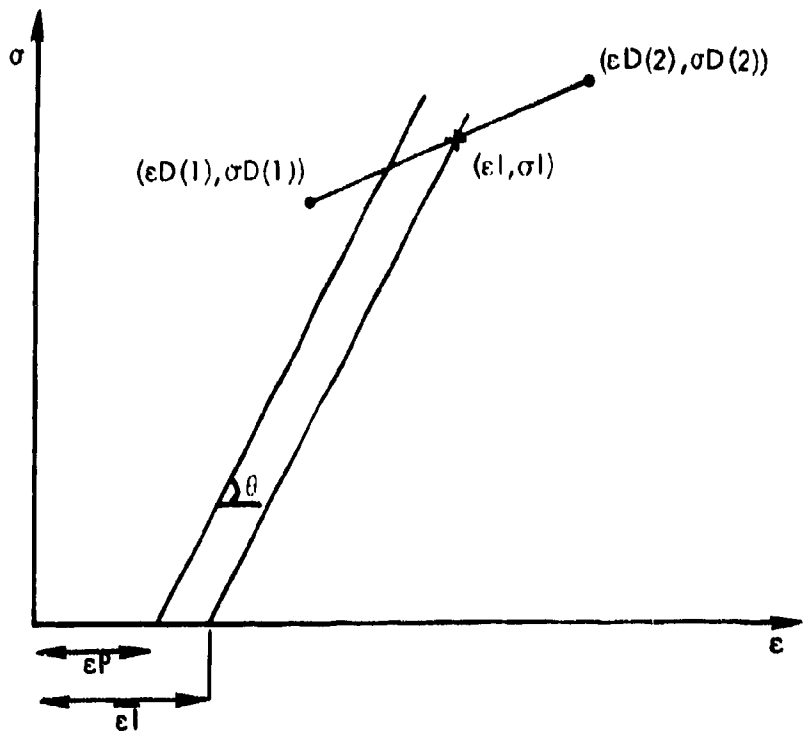

Figure A18. Projection into the Strain Axis

A2.22 SUBROUTINE BINTS($\varepsilon D_B(1), \varepsilon D_B(2), \sigma D_B(1), \sigma D_B(2), N, DSKT^2, \varepsilon OBC, \sigma OBC, F, \varepsilon I_B, \sigma I_B$)

Purpose

This subroutine puts the intersection $(\varepsilon I_B, \sigma I_B)$ in the branch curve system between Neuber's equation defined by the loading increment DSKT relative to the point $(\varepsilon H(N), \sigma H(N))$ with a line defined by the points $(\varepsilon D_B(1), \sigma D_B(1))$ and $(\varepsilon D_B(2), \sigma D_B(2))$.

Procedure

From equation (3) in the writeup for subroutine, INCBC Neuber's equation defined by DSKT relative to the point $(\varepsilon H(N), \sigma H(N))$ in terms of the branch curve coodinates that have an origin at $(\varepsilon OBC, \sigma OBC)$ is

$$\frac{E \times (\varepsilon_B \times F + \varepsilon OBC - \varepsilon H(N)) \times (\sigma_B \times F + \sigma OBC - \sigma H(N))}{\left(1 - \frac{(\varepsilon_B \times F + \varepsilon OBC - \varepsilon H(N))^{\ell}}{A}\right)^2} = DSKT^2 \qquad (1)$$

The points $(\varepsilon D_B(1), \sigma D_B(1))$ and $(\varepsilon D_B(2), \sigma D_B(2))$ are substituted in turn into the left side of equation (1) to obtain the solutions $DSKT1^2$ and $DSKT2^2$. Then

$$DSKT1^2 < DSKT^2 < DSKT2^2$$

Next, the point $(\varepsilon I_B, \sigma I_B)$ midway between $(\varepsilon D_B(1), \sigma D_B(1))$ and $(\varepsilon D_B(2), \sigma D_B(2))$ is computed

$$\begin{aligned} \varepsilon I_B &= \varepsilon D_B(1) + (\varepsilon D_B(2) - \varepsilon D_B(1))/2 \\ \sigma I_B &= \sigma D_B(1) + (\sigma D_B(2) - \sigma D_B(1))/2 \end{aligned} \qquad (2)$$

This is similarly substituted into the left side if (1) to obtain the solution $DSKTI^2$. Then if $DSKTI^2 > DSKT^2$ the point $(\varepsilon I_B, \sigma I_B)$ is substituted for the point $(\varepsilon D_B(2), \sigma D_B(2))$ but if $DSKTI^2 < DSKT^2$ it is substituted for the point $(\varepsilon D_B(1), \sigma D_B(1))$. This process is repeated until $DSKTI^2$ is sufficiently close to $DSKT^2$.

APPENDIX B

HYSTERESIS ANALYSIS USER'S GUIDE

1. INPUT DATA REQUIREMENTS

Input to the Hysteresis Loop Analysis program consists primarily of stresses with the corresponding number of applied cycles. The stress can be input as unnotched peak stresses, mean and alternate stresses, or as maximum and minimum stresses. The input stresses are converted to program units and stored in DLOAD.

Other input also comes from material properties and includes branch curves, locus curves, fully reversed cycles to harden curve and normalized hardening curve. Examples are illustrated in Figures B1 and B2. There are also two sets of material constants, one set for creep calculations and one set for the hysteresis loop analysis.

In addition to the above there are various plot option flags, print flag spectrum input option flags and a flag to compute or not compute hardening. These are all explained in the input instructions.

Sample input for an example problem is included in Appendix C.

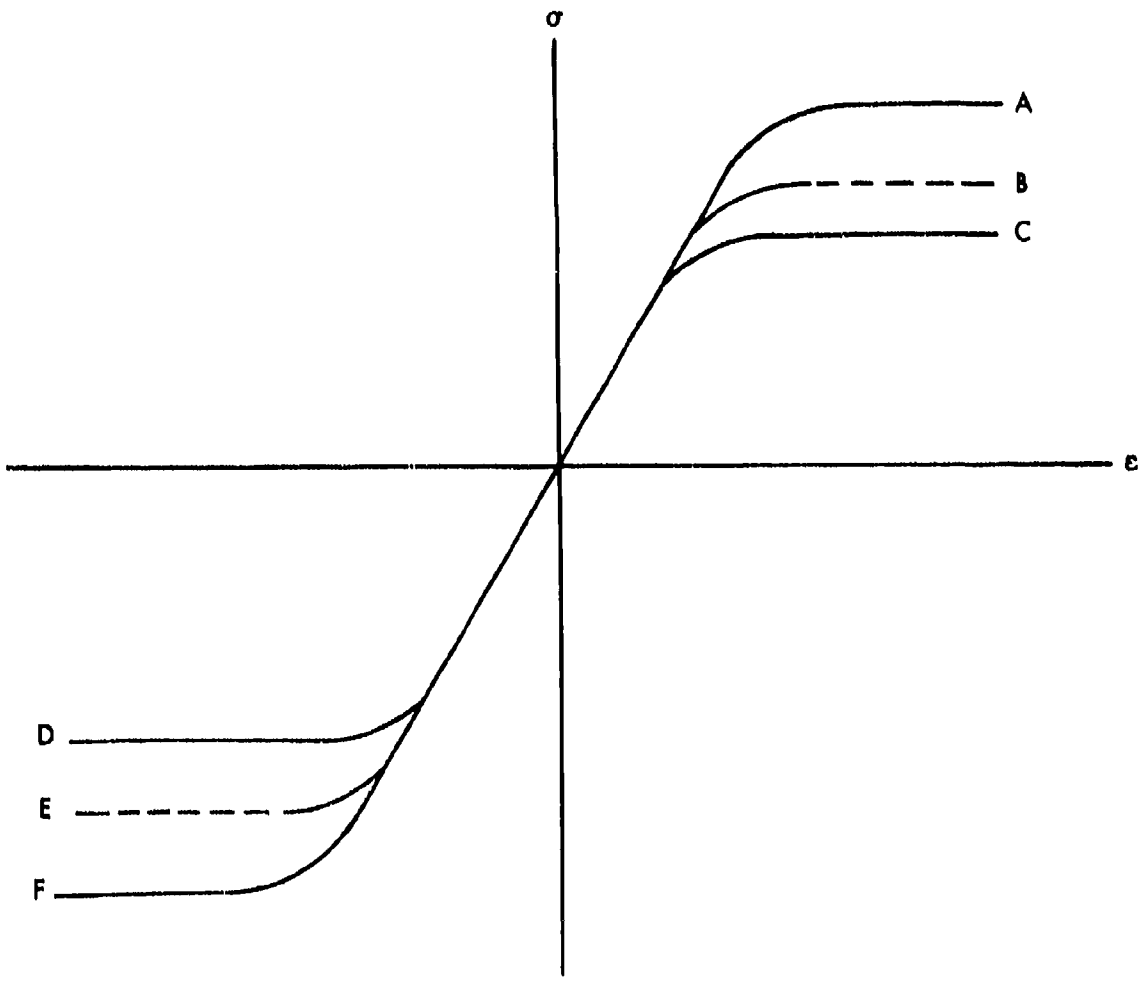

A. CYCLIC TENSION LOCUS CURVE (TLOCCE, TLOCCS)
B. PARTIALLY HARDENED LOCUS CURVE (COMPUTED)
C. MONOTONIC TENSION LOCUS CURVE (TLOCME, TLOCMS)
D. MONOTONIC COMPRESSION LOCUS CURVE (CLOCME, CLOCMS)
E. PARTIALLY HARDENED COMPRESSION LOCUS CURVE (COMPUTED)
F. CYCLIC COMPRESSION LOCUS CURVE (CLOCCE, CLOCCS)

Figure B1. Input Example of Locus Curves

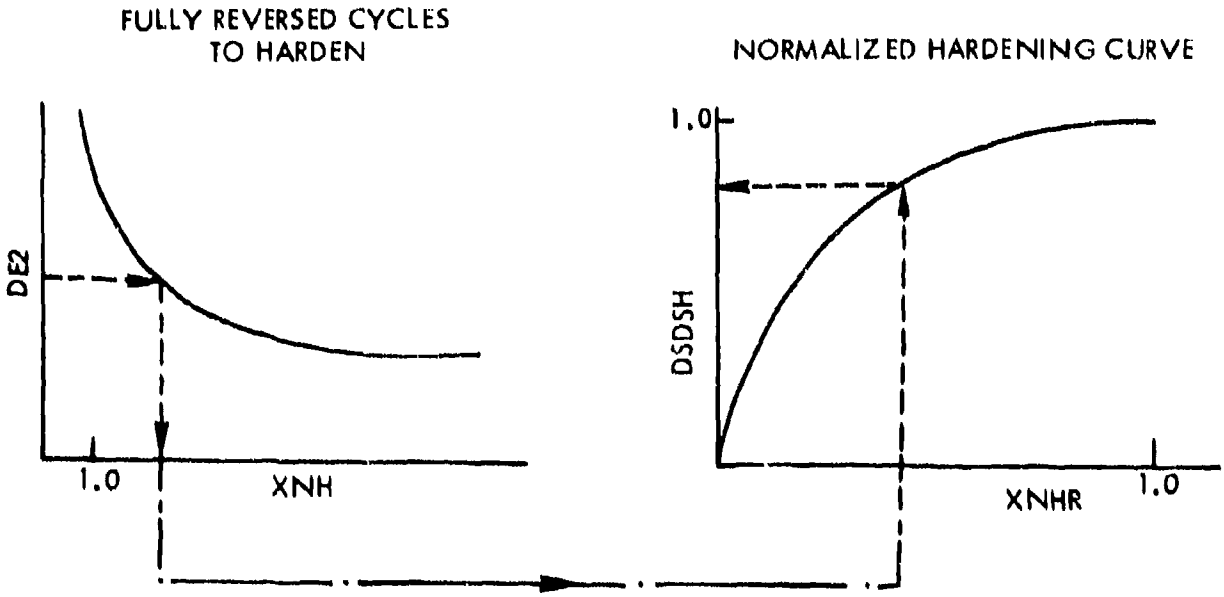

Figure B2. Example of Hardening Curves

2. INPUT INSTRUCTIONS

1. Monotonic tension and compression locus curves

READ(5,1) NLCMT,NLCMC

1 FORMAT(4I5)

NLCMT = the number of points defining the tension monotonic locus curve ≤ 25

NLCMC = the number of points defining the compression monotonic locus curve ≤ 25

READ(5,6) (TLOCME(I),I=1,NLCMT)

6 FORMAT(8F10.0)

TLOCME = the strain values for the tension monotonic locus curve

READ(5,6) (TLOCMS(I),I=1,NLCMT)

TLOCMS = the stress values for the tension monotonic locus curve

READ(5,6) (CLOCME(I),I=1,NLCMC)

CLOCME= the strain values for the compression monotonic locus curve

READ(5,6) (CLOCMS(I),I=1,NLCMC)

CLOCMS= the stress values for the compression monotonic locus curve

2. Cyclic tension and compression curves

READ(5,1) NLCCT,NLCCC

NLCCT = the number of points defining the cyclic tension locus curve ≤ 25

NLCCC = the number of points defining the cyclic compression locus curve ≤ 25

READ(5,6) (TLOCCE(I), I=1, NLCCT)

TLOCCE = the strain values for the cyclic tension locus curve

READ(5,6) (TLOCCS(I), I=1, NLCCT)

TLOCCS = the stress values for the cyclic tension locus curve

READ(5,6) (CLOCCE(I), I=1, NLCCC)

CLOCCE = the strain values for the cyclic compression locus curve

READ(5,6) (CLOCCS(I), I=1, NLCCC)

CLOCCS = the stress values for the cyclic compression locus curve

3. Upper and lower branch curves

READ(5, 1) NUBC, NLBC

NUBC = the number of values defining the upper branch curve ≤ 30

NLBC = the number of values defining the lower branch curve ≤ 30

READ(5,6) (EUBC(I), I=NUBC)

EUBC = the strain values for the upper branch curve

READ(5,6) (SUBC(I), I=NUBC)

SUBC = the stress values for the upper branch curve

READ(5,6) (ELBC(I), I=1, NLBC)

ELBC = the strain values for the lower branch curve

READ(5,6) (SLBC(I), I=1, NLBC)

SLBC = the stress values for the lower branch curve

4. Fully reversed cycles to harden curve

READ(5,1) NRP

NRP = the number of values input to define the fully reversed cycles to harden curve, ≤ 20

READ(5,6) (XNH(I), I=1, NRP)

XNH = the number of fully reversed cycles to hardening

READ(5,6) (DE2(I), I=1, NRP)

DE2 = $\Delta\epsilon/2$ (half the Δ strain)

5. Normalized hardening curve

READ(5,1) NHC

NHC = the number of values input to define the normalized hardening curve, ≤ 20

READ(5,6) (XNHR(I), I=1, NHC)

XNHR = Normalized cycles to harden

READ(5,6) (DSDSH(I), I=1, NHC)

DSDSH = Normalized $\Delta\sigma$

6. Plot, map, print and hardening flags

READ(5,1) MPLOT, IMAP, IPRINT, IHARD

MPLOT = Plot flag = 0 no plots; Plot Flag = 1 plot

IMAP = Select plot variables

= 0 plot applied loads vs. notch strain

= 1 plots notch stress vs. notch strain

IPRINT = Print flag = 0,no diagnostic print

= 1 diagnostic print

IHARD = Hardening flag

= 0 no hardening is calculated

= 1 hardening is calculated

7. Plot variables (input only if MPLOT=1)

READ(5,6) XXS,YXS,XL,XSTRT,XSCAL

XXS = X coordinate for X-axis in inches from origin (will be negative)

YXS = Y coordinate for X-axis in inches from origin (will be negative)

XL = Length of X-axis in inches

XSTRT = Starting label value on X-axis; units = in/in

XSCAL = Axis label values per inch (also used to scale X values); units = in/in

READ(5,6) XYS,YYS,YL,YSTRT,YSCAL

XYS = X coordinate for Y-axis in inches from origin (will be negative)

YYS = Y coordinate for Y-axis in inches from origin (will be negative)

YL = Length of Y-axis in inches

YSTRT = Starting label value on the Y-axis

IMAP = 1, units = ksi; IMAP = 0, units = kips

YSCAL = Y-axis label values per inch (also used to scale Y values)

IMAP = 1, units = ksi; IMAP = 0, units = kips

8. Read program options

READ(5,1) IOP1, IOP2, IOP3, IOP4

IOP1 = Spectrum input options
= 1 Block spectrum, input mean and alternate stresses
(Skip input items 11)
= 2 Block spectrum, input maximum and minimum stresses
(Skip input items 11)
= 3 Peak spectrum is input
(Skip input items 10)
= 9999 no more cases - signals end of computer run

IOP2 = Output option
= 1 writes out calculated peak spectrum
= 2 does not write out calculated peak spectrum

IOP3 = Output option
= 1 write notch strains and notch stresses
= 2 does not write notch strains and notch stresses

IOP4 = Output debug option
= 1 write stress interpolation information
= 2 do not write stress interpolation information

9. Material constants

READ(5,8) CL,A,E,K1,SLOCU,SLOCL

8 FORMAT(6F10.0)

CL = Material constant for modified Neuber's equation

A = Area material constant for modified Neuber's equation

E = Slope of the elastic portion of the locus curve (elastic modulus)

K1 = Stress concentration factor

SLOCU = last stress value on elastic portion of tension locus curve (cyclic or monotonic. Elastic portion is the same for both curves)

SLOCL = Last stress value on the elastic portion of compression locus curve (cyclic or monotonic. Elastic portion is the same for both curves)

10. Block spectrum input (IOP1=3 do not input)

READ(5,100) NPASS,NLAYER,NC

100 FORMAT(3I5)

NPASS = the number of passes to be analyzed

NLAYER = the number of layers in each pass, $\leq$ 8000

NC = the number of cycles in a block of cycles selected for hysteresis analysis

READ(5,10) S1(I),S2(I),N(I)

10 FORMAT(2F10.0,I10)

S1 = Mean stress if IOP1=1; Max. stress if IOP1=2, stress in psi

S2 = Alternate stress if IOP1=1; Min. stress if IOP1=2, stress in psi

N = Applied cycles

(Repeat NLAYER times) I=1, NLAYER

11. Peak stress input IOP1=(1 or 2 not input)

READ(5,1) NLOADS

NLOADS = the number of peak stresses (unnotched peak stress)

READ(5,101) (S(I),NS(I),T(I), I=1,NLOADS)

101 FORMAT(3F10.0)

S = Unnotched peak stress, in psi

NS = Applied cycles

T = Time in the hold condition for this peak stress, in hours

3. OUTPUT DESCRIPTION

The program output consists of three basic sections plus various options for plotting and debugging operations. The first section of the output is a printing of the material constants used in the Neuber analysis and are listed as a check of the input. Next, the strains and stresses (STRAIN and SI) are printed in eight columns across the page. Strain and stress for load cases 1 through 4 are on the first line, strain and stress for load cases 5 through 8 are on the second line, etc. through N loadings.

The third basic output consists of eleven columns of data pertaining to the damage calculations. These columns are identified by the following:

DAMG	=	the accumulative damage.
XXI	=	the damage at each load level.
TN	=	the number of accumulative applied cycles.
SIJ	=	the maximum notched stress at the corresponding load level in ksi.
SII	=	the minimum notched stress at the corresponding load level in ksi.
J	=	the index of the selected maximum load from the order of input. Example: If J=4 then this maximum stress was selected from the calculations for the fourth load that was input. This is determined from the RAIN analysis.
I	=	the index of the selected minimum load; the same as J for the maximum load.
NH	=	the number of accumulative half cycles as determined by the RAIN analysis.
NF	=	the number of accumulative whole cycles as determined by the RAIN analysis.
NS(J)	=	the applied cycles for the maximum stress from the input selected by the index J.

NS(I) = the applied cycles for the minimum stress from the input selected by the index I.

DAMAGE = the total damage for this input spectrum.

There are also four output options that can be called by input flag notes. These are:

- o MPLOT
- o IPRINT
- o IOP2
- o IOP4

MPLOT simply generates a tape for stress or load versus strain plots. The IPRINT option (IPRINT $\neq$ 0) is for program diagnostic purposes only. When this option is specified, the subroutine name is printed along with pertinent program variables (name and value are printed). When one hundred iterations (maximum allowed) are needed to solve for the intersections of curves, the program prints the number of iterations along with the variable names and values involved in the particular algorithm.

Two other options, IOP2 and IOP4, may also be selected for print-out. IOP2 will print the calculated peak stress spectrum (from input data) and will print peak and valley stresses and number of cycles. The IOP4 option is a debug option and writes the stress interpolation information from the interpolation of the S-N data used in the damage calculations.

Sample output for an example problem is included in Appendix C.

4. LIST OF COMPUTER PROGRAM SYMBOLS AND DEFINITIONS

PROGRAM SYMBOLS (MAIN)

MPLOT	Plot option - plot or no plot condition
IMAP	Selects plot variables - applied loads or notch stress vs. notch strain
XXS	X-coordinate for X-axis in inches from origin (will be negative)
YXS	Y-coordinate for X-axis in inches from origin (will be negative)
XL	Length of X-axis in inches
XSTRT	Starting label value on X-axis
XSCAL	X-axis label values per inch (also value used to scale X values)
XYS	X-coordinate for Y-axis in inches from origin (will be negative)
YYS	Y-coordinate for Y-axis in inches from origin (will be negative)
YL	Length of Y-axis in inches
YSTRT	Starting label value on Y-axis
YSCAL	Y-axis label values per inch (also value used to scale Y values)
IOP1	Spectrum input options
IOP2	Spectrum output options
IOP3	Spectrum output options
IOP4	De-bug option - gives additional print
CL	Material constant for modified Neuber's equation
A	Material constant for modified Neuber's equation
E	Elastic modulus
K1	Stress concentration factor
NPASS	Number of passes to be analyzed
NLAYER	Number of layers in each pass
NC	Number of cycles in a block of cycles selected for hysterosis analysis
S1	Mean stress if IOP1=1; Max stress if IOP1=2
S2	Alternating stress if IOP1=1; Min stress if IOP1=2
N	Number of applied cycles
NLOADS	Number of peak stresses to be input
S	Unnotched peak stress
NS	Applied cycles

LIST OF COMPUTER PROGRAM SYMBOLS AND DEFINITIONS

PROGRAM SYMBOLS (MAIN) (Continued)

NUBC	Number of points in upper branch curve
EUBC	X-axis values (stress) of upper branch curve
SUBC	Y-axis values (strain) of upper branch curve
NLBC	Number of points to define lower branch curve
ELBC	X-axis values (stress) of lower branch curve
SLBC	Y-axis values (strain) of lower branch curve
NTLC	Number of points to define tension portion of locus curve
EHTLC	X-axis values (stress) of locus curve (tension half)
SHTLC	Y-axis values (strain) of locus curve (tension half)
NCLC	Number of points to define compression portion of locus curve
EHCLC	X-axis values (stress) of locus curve (compression half)
SHCLC	Y-axis values (strain) of locus curve (compression half)
XS	Array containing computed X values (stress) used in damage calculations
YS	Array containing computed Y values (strain) used in damage calculations
NP	Pointer to current values in EX, SY arrays used in computations
SEQ	Test sequence I.D. used to identify plotted output
SAVE	Previously computed Y value (plot value)
IFLG	Flags plot routine to put new axis on for plot (Multi case computer run)
INIT	Initializes the KS index for storing stress strain history arrays XS, YS
EX	Array containing (X) computed end points of plotted curve
SY	Array containing (Y) computed end points of plotted curve
DSKTS	ΔSKT values (Neuber's term as defined in loop analysis)
DLOAD	Array containing the Δ loads (input or computed from input)
SLOCL	Last Y value on straight portion of lower locus curve
SLOCU	Last Y value on straight portion of upper locus curve
NLCCT	Number of points defining tension cyclic locus curve

LIST OF COMPUTER PROGRAM SYMBOLS AND DEFINITIONS

PROGRAM SYMBOLS (MAIN) (Continued)

NLCCC	Number of points defining compression cyclic locus curve
TLOCCE	Tension strain values for cyclic locus curve
TLOCCS	Tension stress values for cyclic locus curve
CLOCCE	Compression strain values for cyclic locus curve
CLOCCS	Compression stress values for cyclic locus curve
NLCMT	Number of points defining compression monotonic locus curve
NLCMC	Number of points defining compression monotonic locus curve
TLOCME	Tension strain values for monotonic locus curve
TLOCMS	Tension stress values for monotonic locus curve
CLOCME	Compression strain values for monotonic locus curve
CLOCMS	Compression stress values for monotonic locus curve
I	Do loop index
DAMG	Final computed damage
T	Time a given load is in hold mode
SNHT	Sumation cycles for tension hardening
SNHC	Sumation cycles for compression hardening
HARDT	Tension hardening flag
HARDC	Compression hardening flag
TCREP	Time from previous hold condition
CREP	Computed creep value
X1	Intermediate storage for X-value of end point
Y1	Intermediate storage for Y-value of end point
NHFLG	Hardening flag

PROGRAM SYMBOLS (ADJUST)

NI	Pointer used in selecting first or second values in end point arrays EX and SY
EA	Selected EX value using NI
SA	Selected SY value using NI

LIST OF COMPUTER PROGRAM SYMBOLS AND DEFINITIONS

PROGRAM SYMBOLS (ADJUST) (Continued)

NP1	One less than N1
NP2	Two less than N1

PROGRAM SYMBOLS (CRVTRP)

DS2	Half the delta strain
NCYC	The number of reversals to harden
NCYCSM	The sum of the number of reversals to harden
XNH	X value on number of fully reversed cycles to harden curve
DE2	Absolute value of DS2
XNHR	X-value on normalized hardening curve
DSDSH	Y-value on normalized hardening curve
NRP	Number of points defining number of reversals to harden curve
NHC	Number of points defining normalized hardening curve
XLOG	Log of the interpolated X value from fully reversed cycles to harden curve
XN	Anti log of XLOG
SNHC	Sumation cycles for compression hardening
I	Index for loop to bracket DS2 on number of cycles to harden curve
N1	Pointer for bracketing value on cycles to harden curve
SNH	Intermediate value of SNHC and SNHT
HARDC	Compression hardening flag
PCT	Percent hardened
SNHT	Sum of cycles to harden (tension)
HARDT	Tension hardening flag

LIST OF COMPUTER PROGRAM SYMBOLS AND DEFINITIONS

PROGRAM SYMBOLS (MAPP)

PLOTX	X values to be plotted
PLOTY	Y values to be plotted
IP	No. of points (X, Y values)
NFLG	Greater than 1 doubles the A constant in Neuber's term.
DX	Delta X difference between X values
DY	Delta Y difference between Y values
EXY	Intermediate value in converting from notch stress to applied load
F	Sets sign + or minus of Delta SKT
SAVE	Save previous point on plot

PROGRAM SYMBOLS (DRIVER)

DSKT	Input or computed delta loads
EPLT, SPLT	Intermediate points to plot
IEQ	Flag set when consecutive loads are equal
KS	Index on history array used in damage calculation
INIT	Initialization flag for first loading
NP	Index for end point arrays (EX, SY)
DSKTS	Loads array - one for each EX, SY
SLOCU	Last Y value on elastic portion of tension locus curve
SLOCL	Last Y value on elastic portion of compression locus curve
IPLT	Plot flag = 1 tension; = 2 compression
NP1	NP plus 1

PROGRAM SYMBOLS (ILABC)

N1	Pointer to a value in end points arrays EX and SY
N2	Pointer to a value in end points arrays EX and SY
EA, SA	Point defining line
E	Slope of elastic portion of locus curve

PROGRAM SYMBOLS (ILABC) (Continued)

F	Plus or minus value of 1.0 signals tension or compression
PART1	Distance from line to origin
PART2	Distance from translated line to origin
XO,YO	Translation values for branch curve
I	Index for loop on branch curve points

PROGRAM SYMBOLS (LINBR)

XB,YB	Points on the branch curve that bracket the intersection
EA,SA	Point on the line that defines the line along with slope E
XO,YO	Translation parameters for the branch curve
F	Plus or minus 1.0 that signals tension or compression
X,Y	Point on branch curve where intersection occurs
XAB,YAB	Point on branch curve above intersection
XBE,YBE	Point on branch curve below intersection
KOUNT	Count of iterations needed to find (X,Y)
PART1	Distance of line from branch curve origin
PART2	Distance of line from translated branch curve origin

PROGRAM SYMBOLS (BCRPLT)

X	X values to be plotted
Y	Y values to be plotted
IPRINT	=0 No intermediate print, >1 gives intermediate print
XX	Scaled X values
YY	Scaled Y values
NT	Pointer to proper Y title
NS	No. of words in Y title
XXS	X coordinate for X-axis in inches from origin (will be negative)
YXS	Y coordinate for X-axis in inches from origin (will be negative)
XL	Length of X-axis in inches
XSTRT	Starting label value on X-axis

PROGRAM SYMBOLS (BCRPLT) (Continued)

XSCAL	X-axis label values per inch (also value used to scale X values).
XYS	X coordinate for Y-axis in inches from origin (will be negative)
YYS	Y coordinate for Y-axis in inches from origin (will be negative)
YL	Length of Y-axis in inches
YSTRT	Starting label value on Y-axis
YSCAL	Y-axis label values per inch (also value used to scale Y values)

PROGRAM SYMBOLS (MAKPLT)

NFLG	=1 plot locus curve, >1 plot branch curve
IP	Count of points to plot
X	X-value of intersection on the appropriate curve (locus or branch)
Y	Y-value of intersection on the appropriate curve (locus or branch)
PLOTX	X-values plotted (contains end points and points between).
NS	Index used in searching input curves for intervening points, s-start
NE	Index used in searching input curves for intervening points, E-end
PLOTY	Y values plotted (from input locus and branch curve)
F	Used in effecting a sign change
NTLC	
EHTLC	
SHTLC	
NCLC	
EHCLC	
SHCLC	

PROGRAM SYMBOLS (LINSEC)

X	X-value of point half way between (XAB,YAB) and (XBE,YBE)
Y	Y-value of point half way between (XAB,YAB) and (XBE,YBE)
KOUNT	Counts the number of iterations needed to find the intersection
VALUE	Used in determining accuracy of the solution
TEST	The tolerance used in accepting a solution (epsilon)

PROGRAM SYMBOLS (LINSEC) (Continued)

XAB, YAB	Point on locus curve above intersection
XBE, YBE	Point on locus curve below intersection

PROGRAM SYMBOLS (INCLC)

DSQSKT	Neuber term squared
IP	Counter of points along locus curve
EVAL1	Value of Neuber's term last time in this routine (previous value)
EVAL2	Value of Neuber's term
EVALN	Numerator of Neuber's term
EVALD	Denominator of Neuber's term
EH	X-values on locus curve (around point of intersection of Neubers)
SH	Y-values on locus curve (curve and locus curve)
JP	Index of point below intersection on Neuber's curve

PROGRAM SYMBOLS (DETERM)

X2	X-value half way between (XAB, YAB) and (XBE, YBE)
Y2	Y-value half way between (XAB, YAB) and (XBE, YBE)
KOUNT	Count of number of times through loop to get convergence
FN	Numerator of Neuber's term
FD	Denominator of Neuber's term
FSUBI	Value of Neuber's term
ABSFI	Absolute value of difference of Neuber's term (FSUBI) and previous
	Squared value of Neuber's term passed in calling sequence

PROGRAM SYMBOLS (INCBC)

A2	2 times the material constant A
F	Sets the sign in numerator of Neuber's term by taking difference
	Of end points
N1	Pointers in EX, SY array for first point for BRCH.C. translation
N2	Pointers in EX, SY array for second point for BRCH.C. translation

PROGRAM SYMBOLS (INCBC) (Continued)

TOP	Numerator of Neuber's term
BOT	Denominator of Neuber's term
FUNCT	Value of Neuber's term
FUNCT1	Previous value of Neuber's term

PROGRAM SYMBOLS (BINTS)

X	X-value half way between (XAB and XBE)
Y	Y-value half way between (YAB and YBE)
KOUNT	Number of iterations to find intersection
A2	Two times material constant A
FN	Numerator in Neuber's term
FD	Denominator in Neuber's term
FV	Value of Neuber's term

PROGRAM SYMBOLS (ORIGIN)

YO	Y-value for origin of branch curve
F	Sets sign to flip branch curve + for upper- for lower
EUBC	X values defining branch curve
SUBC	Y values defining branch curve
ET	Slope of branch curve at current points
EA	DX translation value of branch curve
SA	DY translation value of branch curve
XO	X-value for origin of branch curve

PROGRAM SYMBOLS (SPECT)

NPASS	Number of passes to be analyzed
NLAYER	Number of layers in each pass
NC	Number of cycles in a block of cycles selected for hysteresis analysis
S1	Mean stress if IOP1=1, max. stress if IOP1=2
S2	Alt. stress if IOP1=1, min. stress if IOP1=2

PROGRAM SYMBOLS (SPECT) (Continued)

N	Applied cycles
SMAX	Maximum stress
SMIN	Minimum stress

PROGRAM SYMBOLS (DAMAGE)

DAMG	Total damage
XX1	Current incremental damage
STR	Notch root strain
TN	Total number of cycles in external spectrum
SII	Notch stress (minimum)
SIJ	Notch stress (maximum)
NH	Number of half cycles
NF	Number of full cycles
SM	Mean stress in S-N data
VS	Variable stress in S-N data
ALN	Number of allowable cycles in S-N data
AN	Interpolated number of cycles for failure for given mean and alternating stresses

PROGRAM SYMBOLS (RAIN)

JMAX	Array for maximum peak strain or stress
JMIN	Array for minimum peak strain or stress
NTOT	Total number of cycles for rain flow counting

PROGRAM SYMBOLS (LPTLC)

EA,SA	Point defining a line with slope SLP
SLP	Slope of line intersecting locus curve
X,Y	Point of intersection of a line with a locus curve
DIFF	Value that determines tension or compression locus curve
JP	Pointer in locus curve to a point below intersection

PROGRAM SYMBOL (LPTBC)

TEST	Tolerance value passed to LINSEC
DIFF	Same as TEST but used as local variable
	Both are distance to origin from line
EA, SA	Point defining line that intersects branch curve
SLP	The slope of line that intersects branch curve
I	Index on branch curve points, used in search for points that bracket intersection
J	Index on loop to find points that bracket intersection
JP	Pointer to points that bracket intersection

PROGRAM SYMBOLS (FDSKT)

FNUM	The numerator of the ΔSKT computation
FDNOM	The denominator of ΔSKT computation
DSKTS	The ΔSKT value

PROGRAM SYMBOLS (CREPER)

T	The time for this loading condition in hold, mode
PCT	The percent of creep that has occurred
TCREP	The time in the hold condition
CREP	Computed creep. Creep is only allowed where SY(NP)< SY(NP-1)
PCTN	The stress relaxation functional minus CREP
PCTD	The stress relaxation function
P	Material constant
PN	Material constant
EI, SI	Intersection of locus curve and a line
NP	The pointer to current values in history arrays EX, SY (end points)

PROGRAM SYMBOLS (CREEP)

K	Material constant used for creep calculation
EBAR	Material constant used for creep calculation

PROGRAM SYMBOLS (CREEP) (Continued)

P	Material constant used for creep calculation
PN	Material constant used for creep calculation
KOUNT	Counter for iterations needed to solve for the stress relaxation Sigma R
SIGR	The stress relaxation; current value of Sigma R (initial value = 0).
FSIGR	Function of Sigma R
FPSIGR	Derivative of FSIGR
SIGRI	Previous value of SIGR in iterative solution
CE	Creep strain

APPENDIX C

EXAMPLE PROBLEM WITH INPUT AND OUTPUT DATA LISTING

INPUT AND OUTPUT FOR A SELECTED EXAMPLE PROBLEM

To illustrate the capabilities of the hysteresis analysis program an example problem is presented here along with the input data and program output. The example problem presented here is one of the flight-by-flight spectra used in the Phase II experimental program. Spectrum 2 as discussed in Section 4.4 was used. This spectrum includes three flights, one flight with a large tension overload, plus sustained load hold periods. Typically, the spectrum can be described by,

$$50\left[(C + Hold) + 150\ (2A + B)\right] + N(2A + B)$$

where; A, B, and C are flights as defined in Figure 67.

Hold is a 1-hour sustained load hold period at -9.4 ksi after each Flight C.

N is the number of times 2A + B is repeated to produce damage at $\Sigma \frac{n}{N} = 1.0$

This example illustrates the analysis capabilities of the program for complex loading sequences as well as the creep and stress relaxation module for evaluating the time dependent effects or damage.

```
*ELT,IL   .DATAN
ELTGT7 RLIB70 02/23-08/36/19-(,0)
000001      GGO       15    17          TENSION AND COMPRESSION MONOTONIC LOCUS CURVE
000002      000     0.0         .0005     .001      .002      .004      .006      .0065     .007
000003      000     .0081       .009      .01       .012      .016      .02       .03
000004      000     0.0         5500.     11000.    22000.    44000.    66000.    70000.    72000.
000005      000     73000.      74900.    75300.    76000.    77100.    78000.    80000.
000006      000     0.0         -.0005    -.001     -.002     -.004     -.005     -.006     -.007
000007      000     -.008       -.01      -.012     -.014     -.016     -.018     -.02      -.024
000008      000     -.03
000009      000     0.0         -5500.    -11000.   -22000.   -44000.   -55000.   -61000.   -65000.
000010      000     -67000.     -71000.   -74000.   -76000.   -77500.   -78000.   -80000.   -81500.
000011      000     -84000.
000012      000       15    17          TENSION AND COMPRESSION CYCLIC LOCUSCURVE
000013      000     0.0         .0005     .001      .002      .004      .006      .0065     .007
000014      000     .0081       .009      .01       .012      .016      .02       .03
000015      000     0.0         5500.     11000.    22000.    44000.    66000.    70000.    75000.
000016      000     80000.      81900.    82300.    83000.    84100.    85000.    87000.
000017      000     0.0         -.0005    -.001     -.002     -.004     -.005     -.006     -.007
000018      000     -.008       -.01      -.012     -.014     -.016     -.018     -.02      -.024
000019      000     -.03
000020      000     0.0         -5500.    -11000.   -22000.   -44000.   -55000.   -64000.   -70500.
000021      000     -75000.     -81000.   -84000.   -86000.   -87500.   -88000.   -90000.   -91500.
000022      000     -94000.
000023      000       27    27
000024      000     0.0         .00096    .00192    .00288    .00384    .0048     .00576    .00672
000025      000     .00768      .00864    .0096     .01056    .01152    .012      .014      .016
000026      000     .018        .02       .022      .024      .027      .03       .036      .042
000027      000     .048        .054      .060
000028      000     0.0         10000.    20000.    30000.    40000.    50000.    60000.    70000.
000029      000     80000.      90000.    100000.   110000.   120000.   125000.   143000.   157000.
000030      000     168000.     175000.   180000.   183000.   186000.   188000.   191000.   192500.
000031      000     194000.     195500.   196000.
000032      000     0.0         -.00096   -.00192   -.00288   -.00384   -.0048    -.00576   -.00672
000033      000     -.00768     -.00864   -.0096    -.01056   -.01152   -.012     -.014     -.016
000034      000     .018        .02       .022      .024      .027      .03       .036      .042
000035      000     .048        .054      .060
000036      000     0.0         10000.    20000.    30000.    40000.    50000.    60000.    70000.
000037      000     80000.      90000.    100000.   110000.   120000.   125000.   143000.   157000.
000038      000     168000.     175000.   180000.   183000.   186000.   188000.   191000.   192500.
000039      000     194000.     195500.   196000.
000040      000       12                          NO. FULL REVERSED CYCLES CURVE
000041      000     4.          5.        6.        7.        10.       15.       20.       30.
000042      000     40.         50.       100.      1000.
000043      000     .0368       .0292     .024      .0212     .0158     .0130     .0118     .0108
000044      000     .0102       .01       .0092     .0088
000045      000       10                          NORMALIZED HARDENING CURVE
000046      000     .1          .2        .3        .4        .5        .6        .7        .8
000047      000     .9          1.0
000048      000     .31         .55       .72       .83       .885      .92       .94       .955
000049      000     .98         1.0
000050      000         0     1     0     1
000051      000         3     2     1     2
000052      000     1.507       .0745     11000000. 2.43      75000.    -64000.
000053      000       301
000054      000     -9400.      1.0
000055      000     17500.      1.0
000056      000     11200.      1.0
```

Figure C1. Input For Example Problem

```
000057      000     17500.      1.0
000058      000     11200.      1.0
000059      000     17500.      1.0
000060      000     11200.      1.0
000061      000     17500.      1.0
000062      000     11200.      1.0
000063      000     19100.      1.0
000064      000      9600.      1.0
000065      000     22200.      1.0
000066      000     10800.      1.0
000067      000     20600.      1.0
000068      000     12400.      1.0
000069      000     20600.      1.0
000070      000     12400.      1.0
000071      000     20600.      1.0
000072      000     12400.      1.0
000073      000     20600.      1.0
000074      000     12400.      1.0
000075      000     25200.      1.0
000076      000      5600.      1.0
000077      000     25200.      1.0
000078      000      5600.      1.0
000079      000     25200.      1.0
000080      000      5600.      1.0
000081      000     25200.      1.0
000082      000      5600.      1.0
000083      000     47300.      1.0
000084      000     -9400.      1.0      24.0
000085      000     18800.      1.0
000086      000     10100.      1.0
000087      000     18800.      1.0
000088      000     10100.      1.0
000089      000     18800.      1.0
000090      000     10100.      1.0
000091      000     18800.      1.0
000092      000     10100.      1.0
000093      000     20600.      1.0
000094      000      8400.      1.0
000095      000     21600.      1.0
000096      000      9950.      1.0
000097      000     19900.      1.0
000098      000     11700.      1.0
000099      000     19900.      1.0
000100      000     11700.      1.0
000101      000     19900.      1.0
000102      000     11700.      1.0
000103      000     19900.      1.0
000104      000     11700.      1.0
000105      000     22000.      1.0
000106      000     11900.      1.0
000107      000     22000.      1.0
000108      000     11900.      1.0
000109      000     22000.      1.0
000110      000     11900.      1.0
000111      000     22000.      1.0
000112      000     11900.      1.0
000113      000     23900.      1.0
000114      000     -9400.      1.0
```

Figure C1. Input For Example Problem (Continued)

```
000115      000     18800.      1.0
000116      000     10100.      1.0
000117      000     18800.      1.0
000118      000     10100.      1.0
000119      000     18800.      1.0
000120      000     10100.      1.0
000121      000     18800.      1.0
000122      000     10100.      1.0
000123      000     20600.      1.0
000124      000     8400.       1.0
000125      000     21600.      1.0
000126      000     9950.       1.0
000127      000     19900.      1.0
000128      000     11700.      1.0
000129      000     19900.      1.0
000130      000     11700.      1.0
000131      000     19900.      1.0
000132      000     11700.      1.0
000133      000     19900.      1.0
000134      000     11700.      1.0
000135      000     22000.      1.0
000136      000     11900.      1.0
000137      000     22000.      1.0
000138      000     11900.      1.0
000139      000     22000.      1.0
000140      000     11900.      1.0
000141      000     22000.      1.0
000142      000     11900.      1.0
000143      000     23900.      1.0
000144      000     -9400.      1.0
000145      000     17500.      1.0
000146      000     11200.      1.0
000147      000     17500.      1.0
000148      000     11200.      1.0
000149      000     17500.      1.0
000150      000     11200.      1.0
000151      000     17500.      1.0
000152      000     11200.      1.0
000153      000     19100.      1.0
000154      000     9600.       1.0
000155      000     22200.      1.0
000156      000     10800.      1.0
000157      000     20600.      1.0
000158      000     12400.      1.0
000159      000     20600.      1.0
000160      000     12400.      1.0
000161      000     20600.      1.0
000162      000     12400.      1.0
000163      000     20600.      1.0
000164      000     12400.      1.0
000165      000     25200.      1.0
000166      000     5600.       1.0
000167      000     25200.      1.0
000168      000     5600.       1.0
000169      000     25200.      1.0
000170      000     5600.       1.0
000171      000     25200.      1.0
000172      000     5600.       1.0
```

Figure C1. Input For Example Problem (Continued)

```
000173    000    27800.    1.0
000174    000    -9400.    1.0
000175    000    18800.    1.0
000176    000    10100.    1.0
000177    000    18800.    1.0
000178    000    10100.    1.0
000179    000    18800.    1.0
000180    000    10100.    1.0
000181    000    18800.    1.0
000182    000    10100.    1.0
000183    000    20600.    1.0
000184    000    8400.     1.0
000185    000    21600.    1.0
000186    000    9950.     1.0
000187    000    19900.    1.0
000188    000    11700.    1.0
000189    000    19900.    1.0
000190    000    11700.    1.0
000191    000    19900.    1.0
000192    000    11700.    1.0
000193    000    19900.    1.0
000194    000    11700.    1.0
000195    000    22000.    1.0
000196    000    11900.    1.0
000197    000    22000.    1.0
000198    000    11900.    1.0
000199    000    22000.    1.0
000200    000    11900.    1.0
000201    000    22000.    1.0
000202    000    11900.    1.0
000203    000    23900.    1.0
000204    000    -9400.    1.0
000205    000    18800.    1.0
000206    000    10100.    1.0
000207    000    18800.    1.0
000208    000    10100.    1.0
000209    000    18800.    1.0
000210    000    10100.    1.0
000211    000    18800.    1.0
000212    000    10100.    1.0
000213    000    20600.    1.0
000214    000    8400.     1.0
000215    000    21600.    1.0
000216    000    9950.     1.0
000217    000    19900.    1.0
000218    000    11700.    1.0
000219    000    19900.    1.0
000220    000    11700.    1.0
000221    000    19900.    1.0
000222    000    11700.    1.0
000223    000    19900.    1.0
000224    000    11700.    1.0
000225    000    22000.    1.0
000226    000    11900.    1.0
000227    000    22000.    1.0
000228    000    11900.    1.0
000229    000    22000.    1.0
000230    000    11900.    1.0
```


Figure C1. Input For Example Problem (Continued)

```
000231  000  22000.  1.0
000232  000  11900.  1.0
000233  000  23900.  1.0
000234  000  -9400.  1.0
000235  000  17500.  1.0
000236  000  11200.  1.0
000237  000  17500.  1.0
000238  000  11200.  1.0
000239  000  17500.  1.0
000240  000  11200.  1.0
000241  000  17500.  1.0
000242  000  11200.  1.0
000243  000  19100.  1.0
000244  000  9600.   1.0
000245  000  22200.  1.0
000246  000  10800.  1.0
000247  000  20600.  1.0
000248  000  12400.  1.0
000249  000  20600.  1.0
000250  000  12400.  1.0
000251  000  20600.  1.0
000252  000  12400.  1.0
000253  000  20600.  1.0
000254  000  12400.  1.0
000255  000  25200.  1.0
000256  000  5600.   1.0
000257  000  25200.  1.0
000258  000  5600.   1.0
000259  000  25200.  1.0
000260  000  5600.   1.0
000261  000  25200.  1.0
000262  000  5600.   1.0
000263  000  27800.  1.0
000264  000  -9400.  1.0
000265  000  18800.  1.0
000266  000  10100.  1.0
000267  000  18800.  1.0
000268  000  10100.  1.0
000269  000  18800.  1.0
000270  000  10100.  1.0
000271  000  18800.  1.0
000272  000  10100.  1.0
000273  000  20600.  1.0
000274  000  8400.   1.0
000275  000  21600.  1.0
000276  000  9950.   1.0
000277  000  19900.  1.0
000278  000  11700.  1.0
000279  000  19900.  1.0
000280  000  11700.  1.0
000281  000  19900.  1.0
000282  000  11700.  1.0
000283  000  19900.  1.0
000284  000  11700.  1.0
000285  000  22000.  1.0
000286  000  11900.  1.0
000287  000  22000.  1.0
000288  000  11900.  1.0
```

Figure C1. Input For Example Problem (Continued)

000289	000	22000.	1.0
000290	000	11900.	1.0
000291	000	22000.	1.0
000292	000	11900.	1.0
000293	000	23900.	1.0
000294	000	-9400.	1.0
000295	000	18800.	1.0
000296	000	10100.	1.0
000297	000	18800.	1.0
000298	000	10100.	1.0
000299	000	18800.	1.0
000300	000	10100.	1.0
000301	000	18800.	1.0
000302	000	10100.	1.0
000303	000	20600.	1.0
000304	000	8400.	1.0
000305	000	21600.	1.0
000306	000	9950.	1.0
000307	000	19900.	1.0
000308	000	11700.	1.0
000309	000	19900.	1.0
000310	000	11700.	1.0
000311	000	19900.	1.0
000312	000	11700.	1.0
000313	000	19900.	1.0
000314	000	11700.	1.0
000315	000	22000.	1.0
000316	000	11900.	1.0
000317	000	22000.	1.0
000318	000	11900.	1.0
000319	000	22000.	1.0
000320	000	11900.	1.0
000321	000	22000.	1.0
000322	000	11900.	1.0
000323	000	23900.	1.0
000324	000	-9400.	1.0
000325	000	17500.	1.0
000326	000	11200.	1.0
000327	000	17500.	1.0
000328	000	11200.	1.0
000329	000	17500.	1.0
000330	000	11200.	1.0
000331	000	17500.	1.0
000332	000	11200.	1.0
000333	000	19100.	1.0
000334	000	9600.	1.0
000335	000	22200.	1.0
000336	000	10800.	1.0
000337	000	20600.	1.0
000338	000	12400.	1.0
000339	000	20600.	1.0
000340	000	12400.	1.0
000341	000	20600.	1.0
000342	000	12400.	1.0
000343	000	20600.	1.0
000344	000	12400.	1.0
000345	000	25200.	1.0
000346	000	5600.	1.0

Figure C1. Input For Example Problem (Continued)

```
000347      000    25200.     1.0
000348      000    5600.      1.0
000349      000    25200.     1.0
000350      000    5600.      1.0
000351      000    25200.     1.0
000352      000    5600.      1.0
000353      000    27800.     1.0
000354      000    0.0        1.0
000355      G00    99999

END ELT.
TASK UNITS/ 0      PGM SIZE/  6144

*END
*END IGNORED - IN CONTROL MODE

*XQT      .ABS
```

Figure C1. Input For Example Problem (Concluded)

MATERIAL CONSTANTS

```
CL,A,E,K1,SLOCU,SLOCL      .150700+01     .745000-01     .110000+08     .243000+01     .750000+05     -.640000+05
 KOUNT=   101 X=   .27000-01 Y=   .18500+06 VALUE=  -.65182-J2 TEST=  -.52194-J2
```


Figure C2. Output for Example Problem

NOTCH STRESS AND STRAIN

STRAIN	SI	STRAIN	SI	STRAIN	SI	STRAIN	SI
.00000	.00000	-.20572-02	-.22739+05	.38219-02	.42041+05	.24597-02	.27057+05
.38219-02	.42041+05	.24597-02	.27057+05	.38219-02	.42041+05	.24597-02	.27057+05
.38219-02	.42041+05	.24597-02	.27057+05	.41647-02	.45812+05	.21109-02	.23220+05
.48249-02	.53074+05	.23726-02	.26098+05	.44848-02	.49333+05	.27206-02	.29927+05
.44848-02	.49333+05	.27206-02	.29927+05	.44848-02	.49333+05	.27206-02	.29927+05
.44848-02	.49333+05	.27206-02	.29927+05	.54585-02	.60043+05	.12345-02	.13580+05
.54585-02	.60043+05	.12345-02	.13580+05	.54585-02	.60043+05	.12345-02	.13580+05
.54585-02	.60043+05	.12345-02	.13580+05	.12433-01	.76394+05	.28125-03	-.48141+05
.54275-02	.23266+05	.37071-02	-.25548+03	.54275-02	.23266+05	.37071-02	-.25548+03
.54275-02	.23266+05	.37071-02	-.25548+03	.54275-02	.23266+05	.37071-02	-.25548+03
.58325-02	.27484+05	.33321-02	-.41617+04	.60575-02	.29829+05	.36771-02	-.56798+03
.56825-02	.25922+05	.40671-02	.34945+04	.56825-02	.25922+05	.40671-02	.34945+04
.56825-02	.25922+05	.40671-02	.34945+04	.56825-02	.25922+05	.40671-02	.34945+04
.61475-02	.30766+05	.41121-02	.39633+04	.61475-02	.30766+05	.41121-02	.39633+04
.61475-02	.30766+05	.41121-02	.39633+04	.61475-02	.30765+05	.41121-02	.39633+04
.65675-02	.35141+05	-.27187-02	-.49172+05	.36250-02	.16922+05	.16613-02	-.35469+04
.36250-02	.16922+05	.16613-02	-.35469+04	.36250-02	.16922+05	.16613-02	-.35469+04
.36250-02	.16922+05	.16613-02	-.35469+04	.40300-02	.21141+05	.12713-02	-.76094+04
.42550-02	.23484+05	.16163-02	-.40156+04	.38650-02	.19422+05	.20063-02	.46875+02
.38650-02	.19422+05	.20063-02	.46875+02	.38650-02	.19422+05	.20063-02	.46875+02
.38650-02	.19422+05	.20063-02	.46875+02	.43450-02	.24422+05	.20513-02	.51563+03
.43450-02	.24422+05	.20513-02	.51563+03	.43450-02	.24422+05	.20513-02	.51563+03
.43450-02	.24422+05	.20513-02	.51563+03	.47650-02	.28797+05	-.27187-02	-.49172+05
.36250-02	.16922+05	.16613-02	-.35469+04	.36250-02	.16922+05	.16613-02	-.35469+04
.36250-02	.16922+05	.16613-02	-.35469+04	.42550-02	.23484+05	.16163-02	-.40156+04
.38650-02	.19422+05	.20063-02	.46875+02	.38650-02	.19422+05	.20063-02	.46875+02
.38650-02	.19422+05	.20063-02	.46875+02	.38650-02	.19422+05	.20063-02	.46875+02
.43450-02	.24422+05	.20513-02	.51563+03	.43450-02	.24422+05	.20513-02	.51563+03
.43450-02	.24422+05	.20513-02	.51563+03	.47650-02	.28797+05	-.27187-02	-.49172+05
.36250-02	.16922+05	.16613-02	-.35469+04	.36250-02	.16922+05	.16613-02	-.35469+04
.36250-02	.16922+05	.16613-02	-.35469+04	.36250-02	.16922+05	.16613-02	-.35469+04
.42550-02	.23484+05	.16163-02	-.40156+04	.38650-02	.19422+05	.20063-02	.46875+02
.38650-02	.19422+05	.20063-02	.46875+02	.38650-02	.19422+05	.20063-02	.46875+02
.43450-02	.24422+05	.20513-02	.51563+03	.43450-02	.24422+05	.20513-02	.51563+03
.43450-02	.24422+05	.20513-02	.51563+03	.47650-02	.28797+05	-.27187-02	-.49172+05
.47650-02	.28797+05	-.27187-02	-.49172+05	.33400-02	.13953+05	.19163-02	-.89063+03
.33400-02	.13953+05	.19163-02	-.89063+03	.33400-02	.13953+05	.19163-02	-.89063+03
.33400-02	.13953+05	.19163-02	-.89063+03	.36650-02	.17547+05	.15413-02	-.47969+04
.43750-02	.24734+05	.17963-02	-.21406+04	.40150-02	.20984+05	.21563-02	.16094+04
.40150-02	.20984+05	.21563-02	.16094+04	.40150-02	.20984+05	.21563-02	.16094+04
.40150-02	.20984+05	.21563-02	.16094+04	.51350-02	.31609+05	.61125-03	-.14484+05
.51350-02	.31609+05	.61125-03	-.14484+05	.50350-02	.31609+05	.61125-03	-.14484+05
.51350-02	.31609+05	.61125-03	-.14484+05	.56230-02	.37703+05	-.27187-02	-.49172+05
.36250-02	.16922+05	.16613-02	-.35469+04	.36250-02	.16922+05	.16613-02	-.35469+04
.36250-02	.16922+05	.16613-02	-.35469+04	.36250-02	.16922+05	.16613-02	-.35469+04
.42550-02	.23484+05	.16163-02	-.40156+04	.42550-02	.23484+05	.16163-02	-.40156+04
.38650-02	.19422+05	.20063-02	.46875+02	.38650-02	.19422+05	.20063-02	.46875+02

Figure C2. Output for Example Problem (Continued)

NOTCH STRESS AND STRAIN

.38650-02	.19422+05	.20063-02	.46875+02	.38650-02	.19422+05	.20063-02	.46875+02
.43450-02	.24422+05	.20513-02	.51563+03	.43450-02	.24422+05	.20513-02	.51563+03
.43450-02	.24422+05	.20513-02	.51563+03	.43450-02	.24422+05	.20513-02	.51563+03
.47650-02	.28797+05	-.27187-02	-.49172+05	.35250-02	.16922+05	.16613-02	-.35469+04
.35250-02	.16922+05	.16613-02	-.35469+04	.35250-02	.16922+05	.16613-02	-.35469+04
.35250-02	.16922+05	.16613-02	-.35469+04	.48350-02	.21161+05	.12713-02	-.76094+04
.42550-02	.23484+05	.16163-02	-.40156+04	.38650-02	.19422+05	.20063-02	.46875+02
.38650-02	.19422+05	.20063-02	.46875+02	.38650-02	.19422+05	.20063-02	.46875+02
.38650-02	.19422+05	.20063-02	.46875+02	.43450-02	.24422+05	.20513-02	.51563+03
.43450-02	.24422+05	.20513-02	.51563+03	.43450-02	.24422+05	.20513-02	.51563+03
.43450-02	.24422+05	.20513-02	.51563+03	.47650-02	.28797+05	-.27187-02	-.49172+05
.33400-02	.13953+05	.19163-02	-.89063+03	.33400-02	.13953+05	.19163-02	-.89063+03
.33400-02	.13953+05	.19163-02	-.89063+03	.33400-02	.13953+05	.19163-02	-.89063+03
.38650-02	.17547+05	.15413-02	-.47969+04	.43750-02	.24734+05	.17963-02	-.21406+04
.40150-02	.20984+05	.21563-02	.16094+04	.40150-02	.20984+05	.21563-02	.16094+04
.40150-02	.20984+05	.21563-02	.16094+04	.43150-02	.21984+05	.21563-02	.16094+04
.50350-02	.31609+05	.61125-03	-.14484+05	.50350-02	.31609+05	.61125-03	-.14484+05
.50350-02	.31609+05	.61125-03	-.14484+05	.50350-02	.31609+05	.61125-03	-.14484+05
.56230-02	.37730+05	-.63375-03	-.27453+05				

Figure C2. Output for Example Problem (Continued)

CUMULATIVE DAMAGE

DAMG	XXI	TN	SIJ	SII	J	I	NH	NF	NS(J)	NS(I)
.000	.000	.500	.000	-22.739	1	2	1	0	1.000	1.000
.304-03	.304-03	1.000	76.394	-22.739	31	2	2	0	1.000	1.000
.304-03	.000	2.000	42.041	27.057	3	4	2	1	1.000	1.000
.304-03	.000	3.000	42.041	27.057	5	6	2	2	1.000	1.000
.304-03	.000	4.000	42.041	27.057	7	8	2	3	1.000	1.000
.304-03	.000	5.000	42.041	27.057	9	10	2	4	1.000	1.000
.304-03	.000	6.000	45.812	23.220	11	12	2	5	1.000	1.000
.314-03	.139-16	7.000	53.374	28.398	13	14	2	6	1.000	1.000
.304-03	.000	8.000	49.333	29.927	15	16	2	7	1.000	1.000
.304-03	.000	9.000	49.333	29.927	17	18	2	8	1.000	1.000
.304-03	.000	10.000	49.333	29.927	19	20	2	9	1.000	1.000
.304-03	.000	11.000	49.333	29.927	21	22	2	10	1.000	1.000
.314-03	.982-05	12.000	60.043	13.580	23	24	2	11	1.000	1.000
.323-03	.982-05	13.000	60.043	13.580	25	26	2	12	1.000	1.000
.333-03	.982-05	14.000	60.043	13.580	27	28	2	13	1.000	1.000
.343-03	.982-05	15.000	60.043	13.580	29	30	2	14	1.000	1.000
.102-02	.575-03	15.500	76.394	-49.172	31	62	3	14	1.000	1.000
.104-02	.261-04	16.500	35.141	-48.141	61	32	3	15	1.000	1.000
.104-02	.000	17.500	23.266	-.255	33	34	3	16	1.000	1.000
.104-02	.000	18.500	23.266	-.255	35	36	3	17	1.000	1.000
.104-02	.000	19.500	23.266	-.255	37	38	3	18	1.000	1.000
.104-02	.000	20.500	23.266	-.255	39	40	3	19	1.000	1.000
.104-02	.000	21.500	27.484	-4.162	41	42	3	20	1.000	1.000
.104-02	.000	22.500	29.828	-.568	43	44	3	21	1.000	1.000
.104-02	.000	23.500	25.922	3.495	45	46	3	22	1.000	1.000
.104-02	.000	24.500	25.922	3.495	47	48	3	23	1.000	1.000
.104-02	.000	25.500	25.922	3.495	49	50	3	24	1.000	1.000
.104-02	.000	26.500	25.922	3.495	51	52	3	25	1.000	1.000
.104-02	.000	27.500	30.766	3.963	53	54	3	26	1.000	1.000
.104-02	.000	28.500	30.766	3.963	55	56	3	27	1.000	1.000
.104-02	.000	29.500	30.766	3.963	57	58	3	28	1.000	1.000
.104-02	.000	30.500	30.766	3.963	59	60	3	29	1.000	1.000
.106-02	.178-04	31.000	37.703	-49.172	121	62	4	29	1.000	1.000
.106-02	.000	32.000	16.922	-3.547	63	64	4	30	1.000	1.000
.106-02	.000	33.000	16.922	-3.547	65	66	4	31	1.000	1.000
.106-02	.000	34.000	16.922	-3.547	67	68	4	32	1.000	1.000
.106-02	.000	35.000	16.922	-3.547	69	70	4	33	1.000	1.000
.106-02	.000	36.000	21.141	-7.609	71	72	4	34	1.000	1.000
.106-02	.000	37.000	23.484	-4.016	73	74	4	35	1.000	1.000
.106-02	.000	38.000	19.422	.047	75	76	4	36	1.000	1.000
.106-02	.000	39.000	19.422	.047	77	78	4	37	1.000	1.000
.106-02	.000	40.000	19.422	.047	79	80	4	38	1.000	1.000
.106-02	.000	41.000	19.422	.047	81	82	4	39	1.000	1.000
.106-02	.000	42.000	24.422	.516	83	84	4	40	1.000	1.000
.106-02	.000	43.000	24.422	.516	85	86	4	41	1.000	1.000
.106-02	.000	44.000	24.422	.516	87	88	4	42	1.000	1.000
.106-02	.000	45.000	24.422	.516	89	90	4	43	1.000	1.000
.107-02	.118-04	46.000	28.797	-49.172	91	92	4	44	1.000	1.000
.107-02	.000	47.000	13.953	-.891	93	94	4	45	1.000	1.000
.107-02	.000	48.000	13.953	-.891	95	96	4	46	1.000	1.000
.107-02	.000	49.000	13.953	-.891	97	98	4	47	1.000	1.000
.107-02	.000	50.000	13.953	-.891	99	100	4	48	1.000	1.000
.107-02	.000	51.000	17.587	-4.797	101	102	4	49	1.000	1.000
.107-02	.000	52.000	24.734	-2.141	103	104	4	50	1.000	1.000
.107-02	.000	53.000	20.984	1.609	105	106	4	51	1.000	1.000
.107-02	.000	54.000	20.984	1.609	107	108	4	52	1.000	1.000

Figure C2. Output for Example Problem (Continued)

CUMULATIVE DAMAGE

.107-02	.000	55.000	20.984	1.609	109	110	4	53	1.000	1.000
.107-02	.000	56.000	20.984	1.609	111	112	4	54	1.000	1.000
.107-02	.654-06	57.000	31.609	-14.484	113	114	4	55	1.000	1.000
.107-02	.654-06	58.000	31.609	-14.484	115	116	4	56	1.000	1.000
.108-02	.654-06	59.000	31.609	-14.484	117	118	4	57	1.000	1.000
.108-02	.654-06	60.000	31.609	-14.484	119	120	4	58	1.000	1.000
.108-02	.178-04	60.500	37.703	-49.172	121	122	5	58	1.000	1.000
.111-02	.178-04	61.000	37.703	-49.172	211	122	5	58	1.000	1.000
.111-02	.000	62.000	16.922	-3.547	123	124	5	59	1.000	1.000
.111-02	.000	63.000	16.922	-3.547	125	126	5	60	1.000	1.000
.111-02	.000	64.000	16.922	-3.547	127	128	5	61	1.000	1.000
.111-02	.000	65.000	16.922	-3.547	129	130	6	62	1.000	1.000
.111-02	.000	66.000	21.141	-7.609	131	132	6	63	1.000	1.000
.111-02	.000	67.000	23.484	-4.016	133	134	6	64	1.000	1.000
.111-02	.000	68.000	19.422	.047	135	136	6	65	1.000	1.000
.111-02	.000	69.000	19.422	.047	137	138	6	66	1.000	1.000
.111-02	.000	70.000	19.422	.047	139	140	6	67	1.000	1.000
.111-02	.000	71.000	19.422	.047	141	142	6	68	1.000	1.000
.111-02	.000	72.000	24.422	.516	143	144	6	69	1.000	1.000
.111-02	.000	73.000	24.422	.516	145	146	6	70	1.000	1.000
.111-02	.000	74.000	24.422	.516	147	148	6	71	1.000	1.000
.111-02	.000	75.000	24.422	.516	149	150	6	72	1.000	1.000
.112-02	.118-04	76.000	28.797	-49.172	151	152	6	73	1.000	1.000
.112-02	.000	77.000	16.922	-3.547	153	154	6	74	1.000	1.000
.112-02	.000	78.000	16.922	-3.547	155	156	6	75	1.000	1.000
.112-02	.000	79.000	16.922	-3.547	157	158	6	76	1.000	1.000
.112-02	.000	80.000	16.922	-3.547	159	160	6	77	1.000	1.000
.112-02	.000	81.000	21.141	-7.609	161	162	6	78	1.000	1.000
.112-02	.000	82.000	23.484	-4.016	163	164	6	79	1.000	1.000
.112-02	.000	83.000	19.422	.047	165	166	6	80	1.000	1.000
.112-02	.000	84.000	19.422	.047	167	168	6	81	1.000	1.000
.112-02	.000	85.000	19.422	.047	169	170	6	82	1.000	1.000
.112-02	.000	86.000	19.422	.047	171	172	6	83	1.000	1.000
.112-02	.000	87.000	24.422	.516	173	174	6	84	1.000	1.000
.112-02	.000	88.000	24.422	.516	175	176	6	85	1.000	1.000
.112-02	.000	89.000	24.422	.516	177	178	6	86	1.000	1.000
.112-02	.000	90.000	24.422	.516	179	180	6	87	1.000	1.000
.114-02	.118-04	91.000	28.797	-49.172	181	182	6	88	1.000	1.000
.114-02	.000	92.000	13.953	-.891	183	184	6	89	1.000	1.000
.114-02	.000	93.000	13.953	-.891	185	186	6	90	1.000	1.000
.114-02	.000	94.000	13.953	-.891	187	188	6	91	1.000	1.000
.114-02	.000	95.000	13.953	-.891	189	190	6	92	1.000	1.000
.114-02	.000	96.000	17.547	-4.797	191	192	6	93	1.000	1.000
.114-02	.000	97.000	24.734	-2.141	193	194	6	94	1.000	1.000
.114-02	.000	98.000	20.984	1.609	195	196	6	95	1.000	1.000
.114-02	.000	99.000	20.984	1.609	197	198	6	96	1.000	1.000
.114-02	.000	100.000	20.984	1.609	199	200	6	97	1.000	1.000
.114-02	.000	101.000	20.984	1.609	201	202	6	98	1.000	1.000
.114-02	.654-06	102.000	31.609	-14.484	203	204	6	99	1.000	1.000
.114-02	.654-06	103.000	31.609	-14.484	205	206	6	100	1.000	1.000
.114-02	.654-06	104.000	31.609	-14.484	207	208	6	101	1.000	1.000
.114-02	.654-06	105.000	31.609	-14.484	209	210	6	102	1.000	1.000
.116-02	.178-04	105.500	37.703	-49.172	211	212	7	102	1.000	1.000
.117-02	.178-04	106.000	37.703	-49.172	301	212	8	102	1.000	1.000
.117-02	.000	107.000	16.922	-3.547	213	214	8	103	1.000	1.000
.117-02	.000	108.000	16.922	-3.547	215	216	8	104	1.000	1.000
.117-02	.000	109.000	16.922	-3.547	217	218	8	105	1.000	1.000
.117-02	.000	110.000	16.922	-3.547	219	220	8	106	1.000	1.000

Figure C2. Output for Example Problem (Continued)

CUMULATIVE DAMAGE

.117-02	.000	111.000	21.141	-7.609	221	222	8	107	1.000	1.000
.117-02	.000	112.000	23.484	-4.016	223	224	8	108	1.000	1.000
.117-02	.000	113.000	19.422	.047	225	226	8	109	1.000	1.000
.117-02	.000	114.000	19.422	.047	227	228	8	110	1.000	1.000
.117-02	.000	115.000	19.422	.047	229	230	8	111	1.000	1.000
.117-02	.000	116.000	19.422	.047	231	232	8	112	1.000	1.000
.117-02	.000	117.000	24.422	.516	233	234	8	113	1.000	1.000
.117-02	.000	118.000	24.422	.516	235	236	8	114	1.000	1.000
.117-02	.000	119.000	24.422	.516	237	238	8	115	1.000	1.000
.117-02	.000	120.000	24.422	.516	239	240	8	116	1.000	1.000
.119-02	.118-04	121.000	28.797	-49.172	241	242	8	117	1.000	1.000
.119-02	.000	122.000	16.922	-3.547	243	244	8	118	1.000	1.000
.119-02	.000	123.000	16.922	-3.547	245	246	8	119	1.000	1.000
.119-02	.000	124.000	16.922	-3.547	247	248	8	120	1.000	1.000
.119-02	.000	125.000	16.922	-3.547	249	250	8	121	1.000	1.000
.119-02	.000	126.000	21.141	-7.609	251	252	8	122	1.000	1.000
.119-02	.000	127.000	23.484	-4.016	253	254	8	123	1.000	1.000
.119-02	.000	128.000	19.422	.047	255	256	8	124	1.000	1.000
.119-02	.000	129.000	19.422	.047	257	258	8	125	1.000	1.000
.119-02	.000	130.000	19.422	.047	259	260	8	126	1.000	1.000
.119-02	.000	131.000	19.422	.047	261	262	8	127	1.000	1.000
.119-02	.000	132.000	24.422	.516	263	264	8	128	1.000	1.000
.119-02	.000	133.000	24.422	.516	265	266	8	129	1.000	1.000
.119-02	.000	134.000	24.422	.516	267	268	8	130	1.000	1.000
.119-02	.000	135.000	24.422	.516	269	270	8	131	1.000	1.000
.120-02	.118-04	136.000	28.797	-49.172	271	272	8	132	1.000	1.000
.120-02	.000	137.000	13.953	-.891	273	274	8	133	1.000	1.000
.120-02	.000	138.000	13.953	-.891	275	276	8	134	1.000	1.000
.120-02	.000	139.000	13.953	-.891	277	278	8	135	1.000	1.000
.120-02	.000	140.000	13.953	-.891	279	280	8	136	1.000	1.000
.120-02	.000	141.000	17.547	-4.797	281	282	8	137	1.000	1.000
.120-02	.000	142.000	24.734	-2.141	283	284	8	138	1.000	1.000
.120-02	.000	143.000	23.984	1.609	285	286	8	139	1.000	1.000
.120-02	.000	144.000	20.984	1.609	287	288	8	140	1.000	1.000
.120-02	.000	145.000	20.984	1.609	289	290	8	141	1.000	1.000
.120-02	.000	146.000	20.984	1.609	291	292	8	142	1.000	1.000
.120-02	.654-06	147.000	31.609	-14.484	293	294	8	143	1.000	1.000
.120-02	.654-06	148.000	31.609	-14.484	295	296	8	144	1.000	1.000
.120-02	.654-06	149.000	31.609	-14.484	297	298	8	145	1.000	1.000
.120-02	.654-06	150.000	31.609	-14.484	299	300	8	146	1.000	1.000
.120-02	.523-05	150.500	37.703	-27.453	301	302	9	146	1.000	1.000

DAMAGE = .00120483

Figure C2. Output for Example Problem (Concluded)

REFERENCES

1. Carroll, J. R., Gilbert, G. J. and Wilkinson, R. F., "Investigation of Stress-Strain History Modeling at Stress Risers, Phase I," AFFDL-TR-76-150, June 1977.

2. Burski, M. L., "The Influence of Cyclic Loading on Residual Stress Relaxation," Thesis Presented to the School of Engineering of the Air Force Institute of Technology, Air University, December 1975.

3. McGee, W. M., Hsu, T. M., "Effects of Underloads on Fatigue Crack Growth; Technical Summary," AFFDL-TR-77-2, Vol. I, March 1977.

U.S.Government Printing Office: 1979 — 657-002/554